BEILSTEIN JOURNAL OF ORGANIC CHEMISTRY

Cobalt catalysis

Edited by Shigeki Matsunaga

Imprint

Beilstein Journal of Organic Chemistry
www.bjoc.org
ISSN 1860-5397
Email: journals-support@beilstein-institut.de

The *Beilstein Journal of Organic Chemistry* is published by the Beilstein-Institut zur Förderung der Chemischen Wissenschaften.

Beilstein-Institut zur Förderung der Chemischen Wissenschaften
Trakehner Straße 7–9
60487 Frankfurt am Main
Germany
www.beilstein-institut.de

BEILSTEIN JOURNAL OF ORGANIC CHEMISTRY

Cobalt-catalyzed directed C–H alkenylation of pivalophenone N–H imine with alkenyl phosphates

Wengang Xu and Naohiko Yoshikai*

Full Research Paper

Open Access

Address:
Division of Chemistry and Biological Chemistry, School of Physical and Mathematical Sciences, Nanyang Technological University, Singapore 637371, Singapore

Email:
Naohiko Yoshikai* - nyoshikai@ntu.edu.sg

* Corresponding author

Keywords:
alkenylation; C–C bond formation; C–H activation; cobalt; imine

Beilstein J. Org. Chem. **2018,** *14,* 709–715.
doi:10.3762/bjoc.14.60

Received: 16 January 2018
Accepted: 14 March 2018
Published: 28 March 2018

This article is part of the thematic issue "Cobalt catalysis".

Guest Editor: S. Matsunaga

Abstract

A cobalt–N-heterocyclic carbene (NHC) catalyst efficiently promotes an *ortho* C–H alkenylation reaction of pivalophenone N–H imine with an alkenyl phosphate. The reaction tolerates various substituted pivalophenone N–H imines as well as cyclic and acyclic alkenyl phosphates.

Introduction

Transition-metal-catalyzed, directing group-assisted arene C–H activation reactions have been extensively studied over the last few decades to offer a broad array of atom and step-economical methods for the synthesis of functionalized aromatic compounds [1-6]. Among various C–H transformations, the introduction of alkenyl groups into the *ortho* position of functionalized arenes has attracted significant attention because of the synthetic versatility of alkenyl groups. The C–H alkenylation has been achieved most extensively by way of the dehydrogenative Heck-type reaction of olefins [7-9]. Meanwhile, the hydroarylation of alkynes has also been explored as an alternative approach for C–H alkenylation [10]. Despite the significant progress made, each of these C–H alkenylation manifolds has some critical limitations. For example, the dehydrogenative Heck reaction is often limited to activated monosubstituted alkenes (e.g., acrylates), and is challenging with unactivated and multisubstituted alkenes [11]. The hydroarylation of alkynes does not allow for the introduction of cycloalkenyl groups because of the unavailability of the corresponding alkynes. In light of such limitations, a coupling between arene substrates and alkenyl electrophiles would offer a complementary approach for the C–H alkenylation [12]. In particular, C–H alkenylations by way of alkenyl C–O bond cleavage has attracted much attention because of the ready accessibility of the corresponding alkenyl electrophiles (e.g., acetate, phosphate) from ketones [13-17].

Over the last several years, we and others have developed a series of directed arene C–H functionalization reactions with organic electrophiles under low-valent cobalt catalysis [18-21].

In particular, our group and the Ackermann group have independently demonstrated that the combination of a cobalt–N-heterocyclic carbene (NHC) catalyst and a Grignard reagent allows for the arene C–H functionalization with organic halides and pseudohalides under the assistance of nitrogen directing groups [17,22-27]. In this connection, Ackermann developed a mild and efficient C–H alkenylation of *N*-pyrimidylindoles and pyrroles with alkenyl acetates using a cobalt–NHC catalyst (Scheme 1a) [17]. The same catalytic system also promoted the alkenylation using alkenyl carbamates, carbonates, and phosphates. More recently, we have achieved an N-arylimine-directed arene C–H alkenylation reaction with alkenyl phosphates using a different cobalt–NHC catalyst (Scheme 1b) [28]. Meanwhile, we have also demonstrated that pivaloyl N–H imine serves as a powerful directing group for cobalt-catalyzed arene C–H functionalization reactions such as the hydroarylation of alkenes and alkylation/arylation using organic halides [29,30]. These previous studies have prompted us to expand the scope of cobalt catalysis for the C–H alkenylation and thus to develop an *ortho* C–H alkenylation reaction of pivalophenone N–H imine with alkenyl phosphates using a new cobalt–NHC catalyst, which is reported herein (Scheme 1c). The present alkenylation features a mild reaction temperature and displays applicability to a variety of substituted pivalophenone N–H imines and alkenyl phosphates. It should be emphasized that pivalophenone N–H imines and related bulky N–H imines can be readily prepared from the corresponding aryl nitriles and organolithium or Grignard reagents, while analogous N-substituted imines are nontrivial to synthesize because of sluggish ketone/amine condensation. As such, the present reaction would complement the N-arylimine-directed alkenylation.

Results and Discussion

The present study commenced with screening of the reaction conditions for the coupling between pivalophenone N–H imine **1a** and cyclohexenyl phosphate **2a** (Table 1). Thus, the reaction was performed in the presence of $CoBr_2$ (10 mol %), ligand (10–20 mol %), and *t*-$BuCH_2MgBr$ (2 equiv) in THF at room temperature. While monodentate phosphines such as PPh_3 and PCy_3 were entirely ineffective (Table 1, entries 1 and 2), common bulky NHC precursors such as 1,3-bis(2,4,6-trimethylphenyl)imidazolium chloride (IMes·HCl) and 1,3-bis(2,6-diisopropylphenyl)imidazolium chloride (IPr·HCl) promoted the coupling reaction to afford the desired alkenylation product **3aa** albeit in moderate yields (Table 1, entries 3 and 4). No significant improvement was observed using the saturated analogues of IMes·HCl and IPr·HCl (Table 1, entries 5 and 6) or the 2,6-diethylphenyl analogue (IEt·HCl, Table 1, entry 7). Furthermore, the NHC precursor featuring a cyclohexane backbone and 2,6-diethylphenyl groups (**L1**·HBr), which proved to be the optimal ligand for the C–H arylation of pivalophenone N–H imine as well as for the C–H alkenylation of N-arylimine (Scheme 1a, b) [28,29], was not particularly effective for the present reaction (Table 1, entry 8). To our delight, we observed

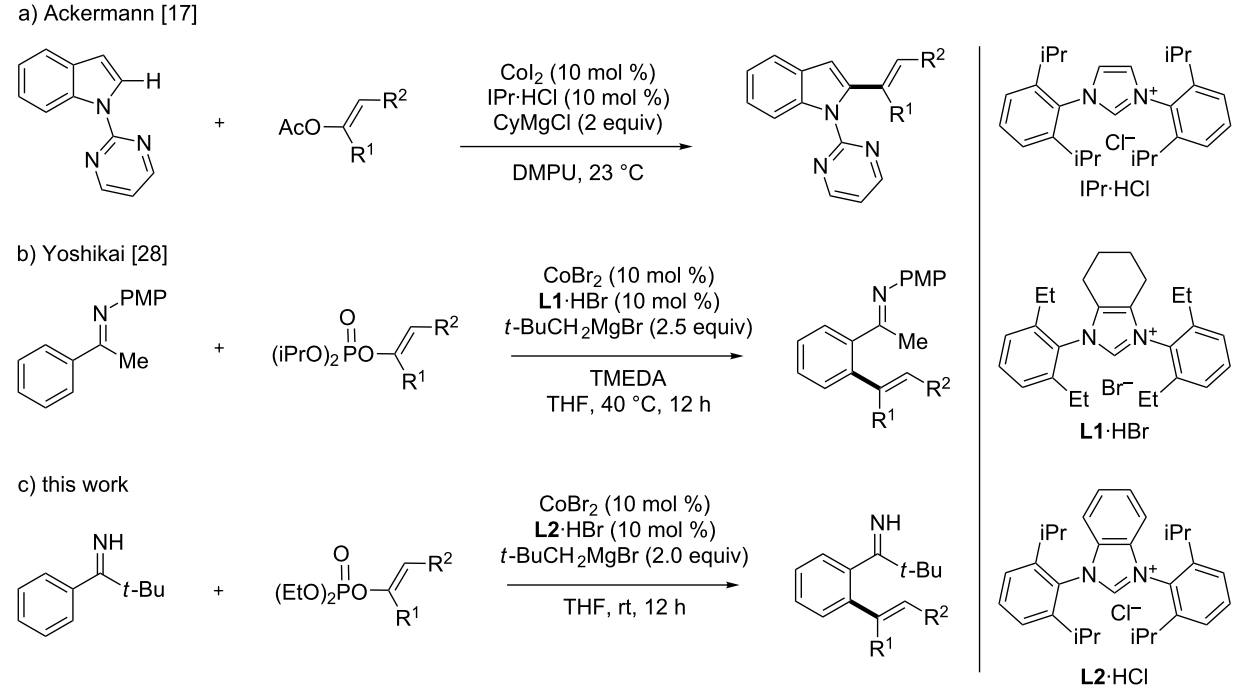

Scheme 1: Cobalt–NHC-catalyzed C–H alkenylation reactions with alkenyl electrophiles.

Table 1: Optimization of reaction conditions.[a]

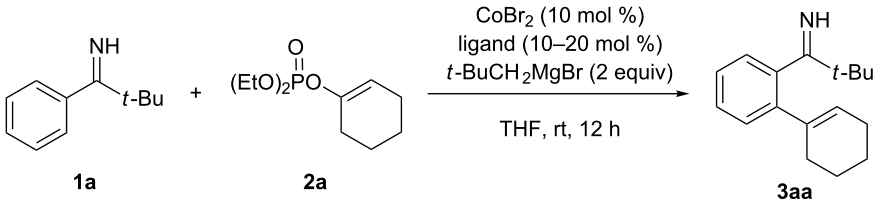

1a **2a** **3aa**

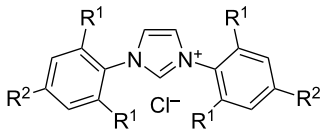

IMes·HCl (R^1 = R^2 = Me)
IPr·HCl (R^1 = iPr, R^2 = H)
IEt·HCl (R^1 = Et, R^2 = H)

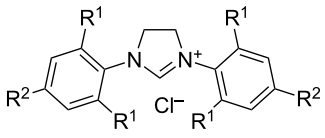

SIMes·HCl (R^1 = R^2 = Me)
SIPr·HCl (R^1 = iPr, R^2 = H)

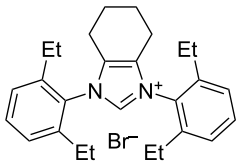

L1·HBr

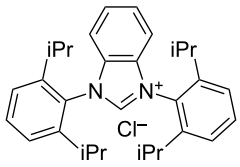

L2·HCl

entry	ligand (mol %)	yield (%)[b]
1	PPh_3 (20)	0
2	PCy_3 (20)	0
3	IMes·HCl (10)	29
4	IPr·HCl (10)	53
5	SIMes·HCl (10)	40
6	SIPr·HCl (10)	46
7	IEt·HCl (10)	38
8	**L1**·HBr (10)	37
9	**L2**·HCl (10)	88[c]

[a]The reaction was performed using 0.2 mmol of **1a** and 0.3 mmol (1.5 equiv) of **2a**. [b]Determined by GC using *n*-tridecane as an internal standard. [c]Isolated yield.

a remarkable improvement in the reaction efficiency using the benzofused analogue of IPr·HCl (**L2**·HCl), affording **3aa** in 88% yield without any trace of a dialkenylation product (Table 1, entry 9). It should be noted that, unlike the C–H arylation of pivalophenone N–H imine and the C–H alkenylation of N-arylimine (Scheme 1a, b), the addition of TMEDA was not necessary to achieve high reaction efficiency, while the reason for this remains unclear. Note also that the present reaction could employ the relatively inexpensive diethyl phosphate, whereas, in the N-arylimine-directed alkenylation, the use of diisopropyl phosphate was necessary to achieve higher and more reproducible yields (cf. Scheme 1b) [28].

With the optimized reaction conditions in hand, we explored the scope of the present alkenylation reaction. First, various substituted pivalophenone N–H imines were subjected to the reaction with **2a** (Scheme 2). Pivalophenone N–H imines bearing a series of *para*-substituents all participated in the alkenylation reaction to afford the desired products **3ba**–**ga** in good yields. The reaction of *m*-methyl-substituted imine took place preferentially at the less hindered position to afford **3ha** as the major isomer with a moderate regioselectivity of 3:1. By contrast, imines bearing *m*-methoxy, *m*-fluoro, or a 3,4-methylenedioxy group underwent exclusive alkenylation at the proximity of the functional group to afford the products **3ia**–**ka** in good yields. As was also observed in previously reported cobalt-catalyzed *ortho* C–H functionalization reactions [22,23,28,29], this regioselectivity may be ascribed to the role of the oxygen or fluorine atom as a secondary directing group to have an electrostatic interaction with the cobalt center during the C–H activation. For compound **3ja**, an increased acidity of the *ortho* position of the fluorine atom could have also contributed to the observed regioselectivity [31]. Curiously, the reaction of 2-naphthylimine resulted in the preferential alkenylation of the more hindered 1-position rather than the 3-position, with a regioselectivity of 4:1 (see **3la**).

Next, the reaction of the parent pivalophenone N–H imine **1a** with different alkenyl phosphates was explored (Scheme 3). The reaction of cyclopentenyl phosphate proceeded smoothly to

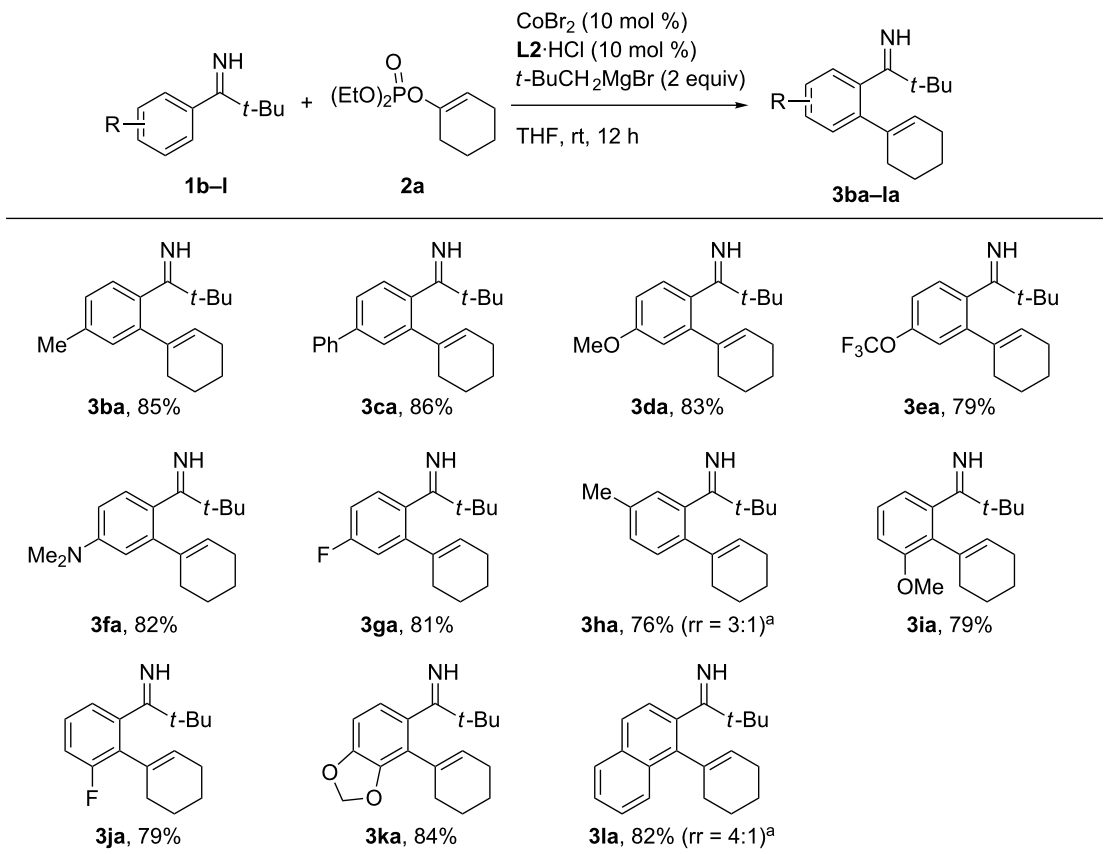

Scheme 2: Reaction of substituted pivalophenone N–H imines with **2a.** [a]The major regioisomer is shown (rr = regioisomer ratio).

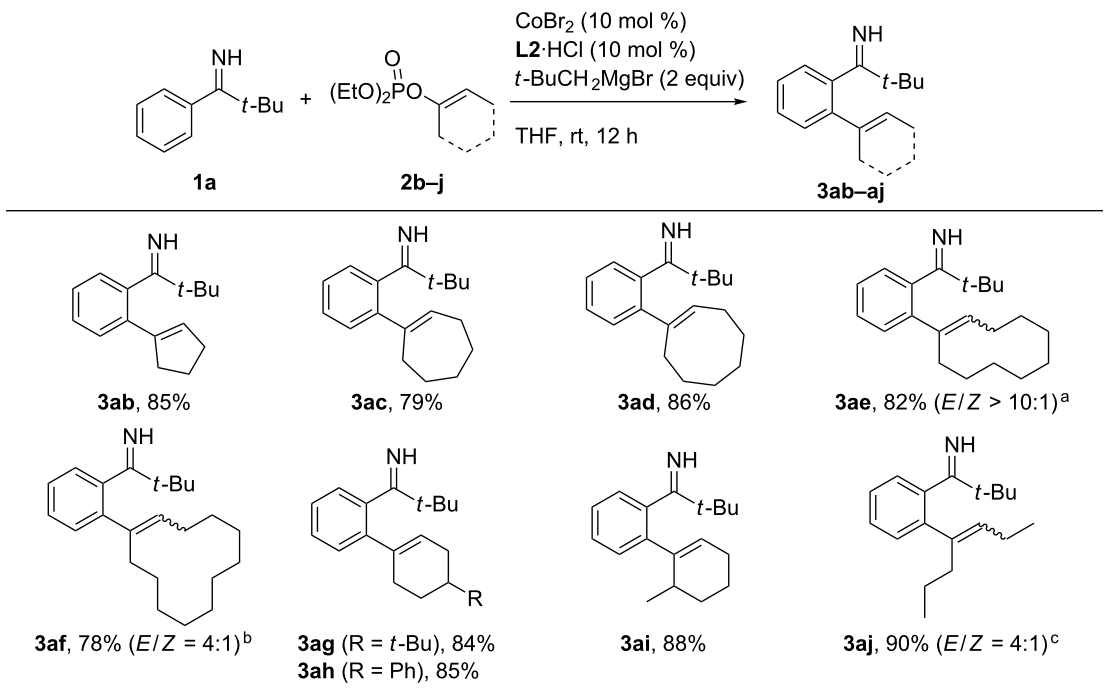

Scheme 3: Reaction of **1a** with various alkenyl phosphates. [a]A mixture of *E*- and *Z*-alkenyl phosphate (ca. 1:1) was used. [b]*Z*-rich alkenyl phosphate (*Z*/*E* = ca. 9:1) was used. [c]*E*-alkenyl phosphate was used.

afford the desired product **3ab** in a high yield of 85%. This is in a sharp contrast to the poor reactivity of the analogous diisopropyl phosphate in the N–PMP imine-directed alkenylation (12% yield). Other cycloalkenyl phosphates with larger ring sizes also efficiently underwent the C–H alkenylation to afford the respective products **3ac**–**af** in good yields. Notably, the cyclodecenylated product **3ae** was obtained in an *E*-rich form from an *E*/*Z* mixture (1:1) of the starting alkenyl phosphate, demonstrating the *E*/*Z* isomerization during the C–C-bond formation. The *E*/*Z* isomerization was also observed for the conversion of cyclododecenyl phosphate (*E*/*Z* = 9:1) to the product **3af** (*E*/*Z* = 3:1). Expectedly, 4-substituted cyclohexenyl phosphates reacted smoothly to afford the desired products **3ag** and **3ah**. Furthermore, a 6-methyl group on the cyclohexenyl phosphate did not interfere with the reaction (see **3ai**). Finally an acyclic alkenyl phosphate derived from 4-heptanone (*E* isomer) was also amenable to the alkenylation reaction, affording the product **3aj** with an *E*/*Z* ratio of 4:1.

In our previous study on the C–H alkylation and arylation of pivalophenone N–H imines, we demonstrated that the pivaloyl imine readily undergoes fragmentation into a cyano group via an iminyl radical under peroxide photolysis or copper-catalyzed aerobic conditions [29]. Under the same peroxide photolysis conditions (*t*-BuOO*t*-Bu with UV (254 nm) irradiation), the *ortho*-alkenylated imine **3aa** underwent a C–N bond-forming cyclization to afford the spirocyclic imine **4** in 81% yield (Scheme 4). The reaction likely involves the initial formation of an iminyl radical from **3aa** and a *tert*-butoxyl radical and its intramolecular addition to the cyclohexenyl group.

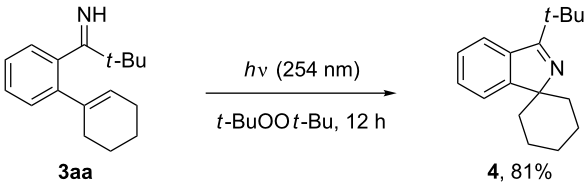

Scheme 4: The cyclization of *o*-alkenylpivalophenone N–H imine.

On the basis of our previous studies on the N-arylimine-directed C–H alkenylation and the N–H imine-directed C–H alkylation/arylation [28,29], we are tempted to propose the catalytic cycle illustrated in Scheme 5. An alkylcobalt species **A**, generated from the cobalt precatalyst and the Grignard reagent, would undergo cyclometalation of magnesium alkylidene amide **1**·MgX, generated from imine **1** and the Grignard reagent, to give a cobaltacycle species **B** while liberating an alkane R–H. The species **B** would then undergo a single-electron transfer (SET) to the alkenyl phosphate **2** to generate a pair of an oxidized cobaltacycle $\mathbf{B}^+$ and a radical anion $\mathbf{2}^{\bullet-}$. This would be followed by the elimination of a phosphate anion and imme-

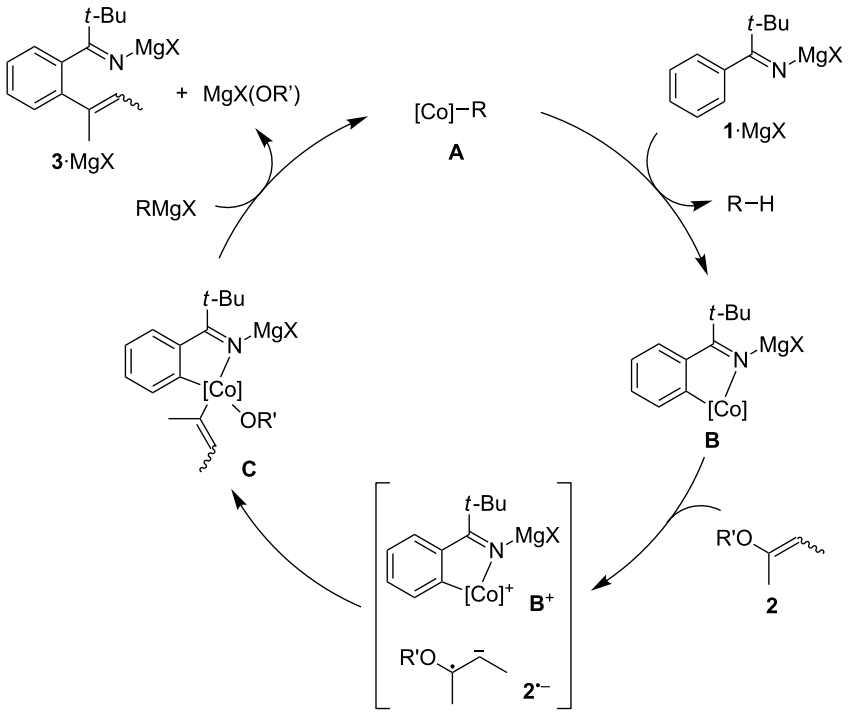

Scheme 5: Proposed catalytic cycle (R = *t*-BuCH_2, R' = P(O)$(OEt)_2$).

diate recombination of the cobalt center and the alkenyl radical to give a diorganocobalt intermediate **C**. The C–C-bond rotation of the radical anion $\mathbf{2}^{\bullet-}$ or the transiently formed alkenyl radical might be responsible for the stereochemical mutation of the C=C bond observed in some cases. The reductive elimination of **C** and subsequent transmetalation with the Grignard reagent would furnish the alkenylation product **3**·MgX and regenerate the species **A**. While the relationship between the ligand and the catalytic activity remains unclear, we speculate that a strong σ-donating ability of NHC ligands would facilitate the SET step among others.

Conclusion

In summary, we have developed an *ortho* C–H alkenylation reaction of pivalophenone N–H imines with alkenyl phosphates using a cobalt–NHC catalyst. The reaction takes place smoothly at room temperature and is applicable to a variety of substituted pivalophenone N–H imines and alkenyl phosphates. The NHC ligand architecture proved to have a significant impact on the efficiency of the present C–H/electrophile coupling. We anticipate that the elaboration of NHC ligands would also be instrumental to the improvement of other C–H activation and related transformations promoted by low-valent cobalt complexes [32-40].

Experimental

Typical procedure: Cobalt-catalyzed alkenylation of pivalophenone N–H imine **1a** with alkenyl phosphate **2a**. A 10 mL Schlenk tube equipped with a magnetic stirring bar was charged with **L2**·HCl (9.5 mg, 0.020 mmol), $CoBr_2$ (4.4 mg, 0.020 mmol), and THF (0.30 mL). The resulting solution was cooled in an ice bath, followed by the addition of *t*-$BuCH_2MgBr$ (2.0 M in THF, 0.20 mL, 0.40 mmol). After stirring for 30 min, 2,2-dimethyl-1-phenylpropan-1-imine (**1a**, 33 mg, 0.20 mmol) and cyclohex-1-en-1-yl diethyl phosphate (**2a**, 70 mg, 0.30 mmol) were added. The resulting mixture was warmed to room temperature, stirred for 12 h, and then filtered through a short silica-gel column, which was washed with ethyl acetate (5 mL). The filtrate was concentrated under reduced pressure. Silica gel chromatography (eluent: hexane/EtOAc/NEt_3 50:1:1) of the crude product afforded the desired alkenylation product as a colorless oil (43 mg, 88%).

Supporting Information

Supporting Information File 1

Experimental details and characterization data of new compounds.
[https://www.beilstein-journals.org/bjoc/content/supplementary/1860-5397-14-60-S1.pdf]

Acknowledgements

This work was supported by Ministry of Education (Singapore) and Nanyang Technological University (RG3/15, RG114/15, and MOE2016-T2-2-043).

ORCID® iDs

Naohiko Yoshikai - https://orcid.org/0000-0002-8997-3268

References

1. Colby, D. A.; Bergman, R. G.; Ellman, J. A. *Chem. Rev.* **2010,** *110,* 624–655. doi:10.1021/cr900005n
2. Ackermann, L. *Chem. Rev.* **2011,** *111,* 1315–1345. doi:10.1021/cr100412j
3. Engle, K. M.; Mei, T.-S.; Wasa, M.; Yu, J.-Q. *Acc. Chem. Res.* **2012,** *45,* 788–802. doi:10.1021/ar200185g
4. Lyons, T. W.; Sanford, M. S. *Chem. Rev.* **2010,** *110,* 1147–1169. doi:10.1021/cr900184e
5. Kakiuchi, F.; Kochi, T.; Murai, S. *Synlett* **2014,** *25,* 2390–2414. doi:10.1055/s-0034-1379210
6. De Sarkar, S.; Liu, W.; Kozhushkov, S. I.; Ackermann, L. *Adv. Synth. Catal.* **2014,** *356,* 1461–1479. doi:10.1002/adsc.201400110
7. Le Bras, J.; Muzart, J. *Chem. Rev.* **2011,** *111,* 1170–1214. doi:10.1021/cr100209d
8. Kozhushkov, S. I.; Ackermann, L. *Chem. Sci.* **2013,** *4,* 886–896. doi:10.1039/C2SC21524A
9. Zhou, L.; Lu, W. *Chem. – Eur. J.* **2014,** *20,* 634–642. doi:10.1002/chem.201303670
10. Boyarskiy, V. P.; Ryabukhin, D. S.; Bokach, N. A.; Vasilyev, A. V. *Chem. Rev.* **2016,** *116,* 5894–5986. doi:10.1021/acs.chemrev.5b00514
11. Deb, A.; Maiti, D. *Eur. J. Org. Chem.* **2017,** 1239–1252. doi:10.1002/ejoc.201601253
12. Rossi, R.; Bellina, F.; Lessi, M. *Synthesis* **2010,** 4131–4153. doi:10.1055/s-0030-1258262
13. Matsuura, Y.; Tamura, M.; Kochi, T.; Sato, M.; Chatani, N.; Kakiuchi, F. *J. Am. Chem. Soc.* **2007,** *129,* 9858–9859. doi:10.1021/ja071965m
14. Ogiwara, Y.; Tamura, M.; Kochi, T.; Matsuura, Y.; Chatani, N.; Kakiuchi, F. *Organometallics* **2014,** *33,* 402–420. doi:10.1021/om401204h
15. Meng, L.; Kamada, Y.; Muto, K.; Yamaguchi, J.; Itami, K. *Angew. Chem., Int. Ed.* **2013,** *52,* 10048–10051. doi:10.1002/anie.201304492
16. Ackermann, L.; Barfüsser, S.; Pospech, J. *Org. Lett.* **2010,** *12,* 724–726. doi:10.1021/ol9028034
17. Moselage, M.; Sauermann, N.; Richter, S. C.; Ackermann, L. *Angew. Chem., Int. Ed.* **2015,** *54,* 6352–6355. doi:10.1002/anie.201412319
18. Gao, K.; Yoshikai, N. *Acc. Chem. Res.* **2014,** *47,* 1208–1219. doi:10.1021/ar400270x
19. Yoshikai, N. *Bull. Chem. Soc. Jpn.* **2014,** *87,* 843–857. doi:10.1246/bcsj.20140149
20. Ackermann, L. *J. Org. Chem.* **2014,** *79,* 8948–8954. doi:10.1021/jo501361k
21. Moselage, M.; Li, J.; Ackermann, L. *ACS Catal.* **2016,** *6,* 498–525. doi:10.1021/acscatal.5b02344
22. Gao, K.; Lee, P.-S.; Long, C.; Yoshikai, N. *Org. Lett.* **2012,** *14,* 4234–4237. doi:10.1021/ol301934y

23. Gao, K.; Yoshikai, N. *J. Am. Chem. Soc.* **2013,** *135,* 9279–9282. doi:10.1021/ja403759x
24. Gao, K.; Yamakawa, T.; Yoshikai, N. *Synthesis* **2014,** *46,* 2024–2039. doi:10.1055/s-0033-1338658
25. Song, W.; Ackermann, L. *Angew. Chem., Int. Ed.* **2012,** *51,* 8251–8254. doi:10.1002/anie.201202466
26. Punji, B.; Song, W.; Shevchenko, G. A.; Ackermann, L. *Chem. – Eur. J.* **2013,** *19,* 10605–10610. doi:10.1002/chem.201301409
27. Mei, R.; Ackermann, L. *Adv. Synth. Catal.* **2016,** *358,* 2443–2448. doi:10.1002/adsc.201600384
28. Lee, P.-S.; Xu, W.; Yoshikai, N. *Adv. Synth. Catal.* **2017,** *359,* 4340–4347. doi:10.1002/adsc.201701105
29. Xu, W.; Yoshikai, N. *Chem. Sci.* **2017,** *8,* 5299–5304. doi:10.1039/C7SC01732D
30. Xu, W.; Yoshikai, N. *Angew. Chem., Int. Ed.* **2016,** *55,* 12731–12735. doi:10.1002/anie.201605877
31. Eisenstein, O.; Milani, J.; Perutz, R. N. *Chem. Rev.* **2017,** *117,* 8710–8753. doi:10.1021/acs.chemrev.7b00163
32. Someya, H.; Ohmiya, H.; Yorimitsu, H.; Oshima, K. *Org. Lett.* **2007,** *9,* 1565–1567. doi:10.1021/ol070392f
33. Hatakeyama, T.; Hashimoto, S.; Ishizuka, K.; Nakamura, M. *J. Am. Chem. Soc.* **2009,** *131,* 11949–11963. doi:10.1021/ja9039289
34. Kobayashi, T.; Yorimitsu, H.; Oshima, K. *Chem. – Asian J.* **2009,** *4,* 1078–1083. doi:10.1002/asia.200900111
35. Mo, Z.; Liu, Y.; Deng, L. *Angew. Chem., Int. Ed.* **2013,** *52,* 10845–10849. doi:10.1002/anie.201304596
36. Mo, Z.; Mao, J.; Gao, Y.; Deng, L. *J. Am. Chem. Soc.* **2014,** *136,* 17414–17417. doi:10.1021/ja510924v
37. Röse, P.; Hilt, G. *Synthesis* **2016,** *48,* 463–492. doi:10.1055/s-0035-1560378
38. Cahiez, G.; Moyeux, A. *Chem. Rev.* **2010,** *110,* 1435–1462. doi:10.1021/cr9000786
39. Hess, W.; Treutwein, J.; Hilt, G. *Synthesis* **2008,** 3537–3562. doi:10.1055/s-0028-1083210
40. Gosmini, C.; Bégouin, J.-M.; Moncomble, A. *Chem. Commun.* **2008,** 3221–3233. doi:10.1039/b805142a

License and Terms

BEILSTEIN JOURNAL OF ORGANIC CHEMISTRY

Three-component coupling of aryl iodides, allenes, and aldehydes catalyzed by a Co/Cr-hybrid catalyst

Kimihiro Komeyama*, Shunsuke Sakiyama, Kento Iwashita, Itaru Osaka and Ken Takaki

Full Research Paper

Open Access

Address:
Department of Applied Chemistry, Graduate School of Engineering, Hiroshima University, 1-4-1 Higashi-Hiroshima City 739-8527, Japan

Email:
Kimihiro Komeyama* - kkome@hiroshima-u.ac.jp

* Corresponding author

Keywords:
chromium; cobalt; diastereoselective; homoallyl alcohols; hybrid catalyst; three-component coupling

Beilstein J. Org. Chem. **2018,** *14,* 1413–1420.
doi:10.3762/bjoc.14.118

Received: 15 March 2018
Accepted: 22 May 2018
Published: 11 June 2018

This article is part of the thematic issue "Cobalt catalysis".

Guest Editor: S. Matsunaga

Abstract

The cobalt/chromium-catalyzed three-component coupling of aryl iodides, allenes, and aldehydes has been developed to afford multi-substituted homoallylic alcohols in a diastereoselective manner. Control experiments for understanding the reaction mechanism reveal that the cobalt catalyst is involved in the oxidative addition and carbometalation steps in the reaction, whereas the chromium salt generates highly nucleophilic allylchromium intermediates from allylcobalt species, without the loss of stereochemical information, to allow the addition to aldehydes.

Introduction

Carbon–carbon bond formation is the fundamental and central transformation of synthetic organic chemistry. The elaboration and extension of a carbon framework via a series of carbon–carbon bond-forming reactions are extremely important for medicinal chemistry and agrochemical and natural product synthesis. In these bond formations, organometallics play an essential role because they possess various reactivities depending on the central metal ions that they own. For example, carbon has strong nucleophilicity when bonded to metals with low electronegativity, as demonstrated in the reaction of organolithium, organomagnesium, organozinc, and organochromium **A**, to facilitate addition reactions of appropriate carbon electrophiles such as aldehydes (Scheme 1, top) [1]. In contrast, π-electrophilic carbon-connected late transition metals **B** facilitate the carbometalation of carbon–carbon multiple bonds, leading to multi-substituted carbon frameworks (Scheme 1, bottom) [2,3]. The nucleophilic and π-electrophilic organometallic intermediates are used properly in their favorable circumstances.

Transmetalation is one of the most vital elemental processes used to drastically change the reactivity of organometallics, involving a wide range of transition metal-catalyzed reactions. For example, transmetalation between an organonickel (or organocobalt) complex and chromium salt results in the forma-

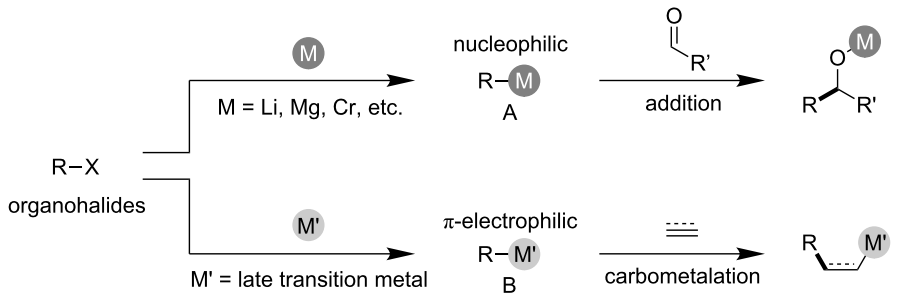

Scheme 1: Nucleophilic and π-electrophilic characters of organometallics depending on the central metals.

tion of a highly nucleophilic organochromium species, which enables efficient addition to aldehydes to give substituted secondary alcohols, as demonstrated in the Nozaki–Hiyama–Kishi (NHK) reaction (Scheme 2) [4-9]. Although the catalyst combination allows the use of organic halides as carbon nucleophiles, a multicomponent coupling reaction using a similar catalyst combination has had limited success [10-12].

We have recently demonstrated the high π-electron affinity of an organocobalt species that enabled a variety of alkyne functionalization reactions to proceed via carbocobaltation (Scheme 3) [13-15]. Furthermore, a combination of the cobalt and chromium catalyst could be applied to alkynyl iodoarene cyclization/borylation to form cyclized vinylboronic esters, in which transmetalation between the generated vinylcobalt and chromium salt was a critical step (Scheme 4) [16]. As part of our continuing work on the cobalt-catalyzed functionalization of carbon–carbon unsaturated bonds, a three-component coupling method is herein reported for the direct synthesis of highly diastereoselective multi-substituted homoallyl alcohols employing a cobalt/chromium hybrid catalyst (Scheme 5).

Results and Discussion

Initially, suitable reaction conditions were investigated for the three-component coupling reaction between iodobenzene (**1a**), 5-phenylpenta-1,2-diene (**2a**), and 4-methylbenzaldehyde (**3a**) in the presence of $CoBr_2$ (10 mol %), $CrCl_3$ (20 mol %), and manganese powder (2.0 equiv), using trimethylsilyl chloride (TMSCl, 1.2 equiv) as a trapping reagent [7]. These results are summarized in Table 1. The absence of a ligand afforded the homoallyl alcohol **4a** in 25% yield as a *syn*/*anti* (80:20) mixture of diastereomers, the ratio of which was determined by the coupling constant between the two protons at the C1- and C2-positions of **4a**; a coupling value of ^3J = ca. 5.0 Hz indicated the *syn*-form, and a coupling value of ^3J = ca. 8.0 Hz indicated the *anti*-form (Table 1, entry 1) [17]. The addition of PPh_3 (20 mol %) resulted in an increase in the product yield to 45% with a similarly diastereomer ratio (Table 1, entry 2). The use of

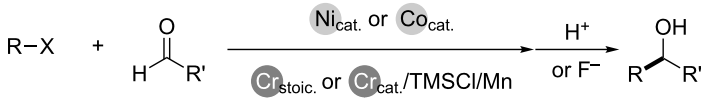

Scheme 2: Ni/Cr or Co/Cr-catalyzed NHK reaction.

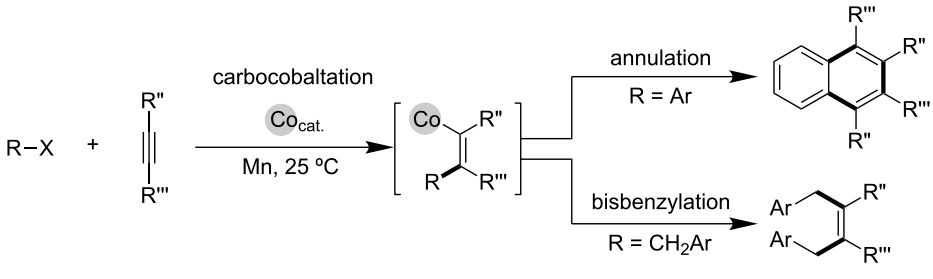

Scheme 3: Functionalization of alkynes via carbocobaltation.

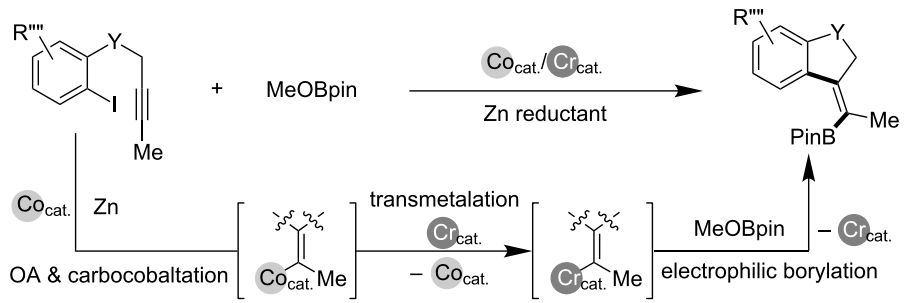

Scheme 4: Cyclization/borylation of alkynyl iodoarenes using the Co/Cr catalyst.

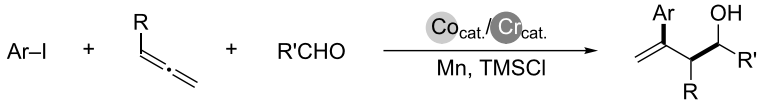

Scheme 5: Three-component coupling of aryl iodides, arenes, and aldehydes using Co/Cr catalyst (this work).

the chromium catalyst, Mn reductant, and TMSCl was crucial for the coupling (Table 1, entries 3–5). Thus, the removal of $CrCl_3$ resulted in the formation of a trace amount of **4a** with the complete consumption of allene **2a**, whereas most of iodoarene **1a** and aldehyde **3a** remained unreacted after the reaction was completed (Table 1, entry 3). Using a Zn reductant instead of Mn resulted in a negligible amount of coupling product (Table 1, entry 4), wherein **1a** was completely consumed [18]. Reaction conditions without the use of TMSCl produced **4a** in a catalytic amount (Table 1, entry 5). Other ligands were also tested (Table 1, entries 5–12), and after the screening of several phosphines and pyridine-type ligands, the latter ligands were found to be the most effective for use in the coupling reaction. Consequently, we found that iminopyridine **L3** was the best choice of ligand, and when used, it resulted in the three-component product **4a** being obtained in 69% yield with a diastereoselectivity ratio of 92:8 (Table 1, entry 13). Additionally, preformed $CoBr_2$(**L3**) gave a similar result (Table 1, entry 14). During the transformation, the chromium catalyst ligands inhibited the reaction (Table 1, entries 15–17). Also, the reaction was

Table 1: Screening of the reaction conditions.[a]

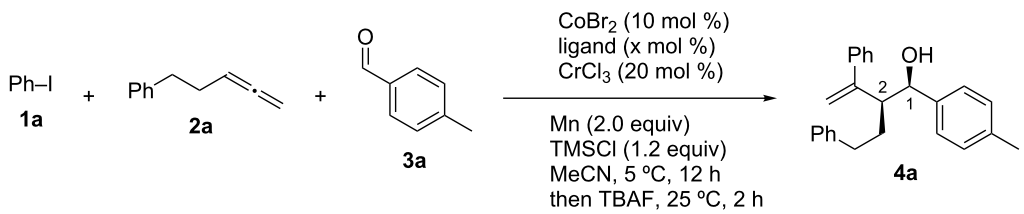

entry	ligand (x mol %)	Cr catalyst	NMR yield (%)	isomer ratio[b]
1	none	$CrCl_3$	25	80:20
2	PPh_3 (20)	$CrCl_3$	45	85:15
3	PPh_3 (20)	none	5	82:18
4[c]	PPh_3 (20)	$CrCl_3$	trace	–
5[d]	PPh_3 (20)	$CrCl_3$	18	86:14
6	dppe (10)	$CrCl_3$	8	91:9
7	dppb (10)	$CrCl_3$	trace	–
8	dppf (10)	$CrCl_3$	trace	–
9	xantphos (10)	$CrCl_3$	trace	–

Table 1: Screening of the reaction conditions.[a] (continued)

10	2,2′-bpy (10)	$CrCl_3$	45	92:8
11	**L1** (10)	$CrCl_3$	52	93:7
12	**L2** (10)	$CrCl_3$	64	91:9
13	**L3** (10)	$CrCl_3$	69	92:8
14[e]	–	$CrCl_3$	65	91:9
15	**L3** (10)	$CrCl_3$(bpy)	48	94:6
16	**L3** (10)	$CrCl_3$(**L3**)	24	92:8
17	**L3** (10)	Cr(salen)Cl	21	91:9

[a]Reaction conditions: **1a** (0.25 mmol), **2a** (0.38 mmol), and **3a** (0.25 mmol). [b]The ratio (*syn*:*anti*) was determined from the ^{1}H NMR of the crude product. [c]Zn was used instead of Mn. [d]Without the presence of TMSCl. [e]$CoBr_2$(**L3**) was used instead of $CoBr_2$.

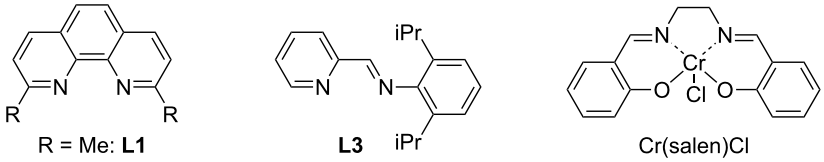

highly dependent on the solvent used; for example, dimethylformamide (DMF), tetrahydrofuran (THF), 1,4-dioxane, and toluene did not result in any formation of **4a**.

With the optimized conditions in hand, the use of aldehydes in the Co/Cr-catalyzed three-component coupling reaction was explored, as shown in Scheme 6. Electron-rich and electron-deficient aryl aldehydes, as well as 2-furylaldehyde, were well tolerated in the reaction, leading to the formation of the corresponding homoallylic alcohols with similar diastereomer ratios (**4a**–**f**). Additionally, alkyl aldehydes were also successfully used in the coupling reaction, albeit resulting in slightly lower yields (**4g**, **4g'**, **4g"** and **4h**). Next, the generality of the reaction was investigated using aryl iodides (Scheme 7) and allenes (Scheme 8). Although aryl bromides and chlorides did not participate in the coupling, a diverse set of functional groups such as methoxy (**4j**), halogens (**4k** and **4l**), trifluoromethyl (**4m**), cyano (**4n**), and ester (**4o**) substituents at the *para*-posi-

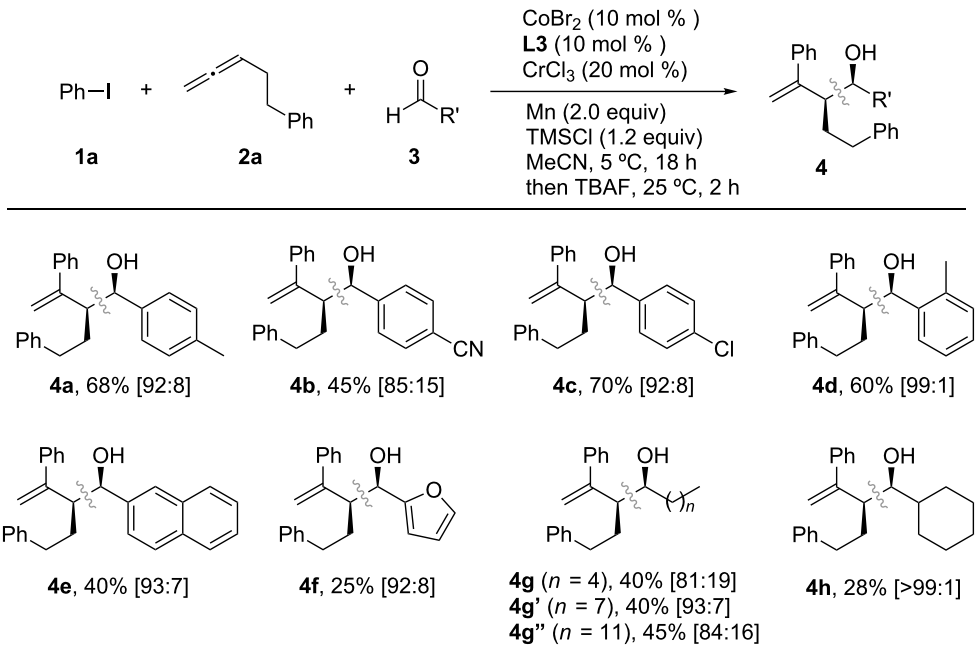

Scheme 6: Screening of aldehydes in the Co/Cr-catalyzed three-component coupling reaction. All yields are determined after isolation. The values in brackets indicate the diastereomer ratio of the *syn* and *anti* products, determined from ^{1}H NMR spectra.

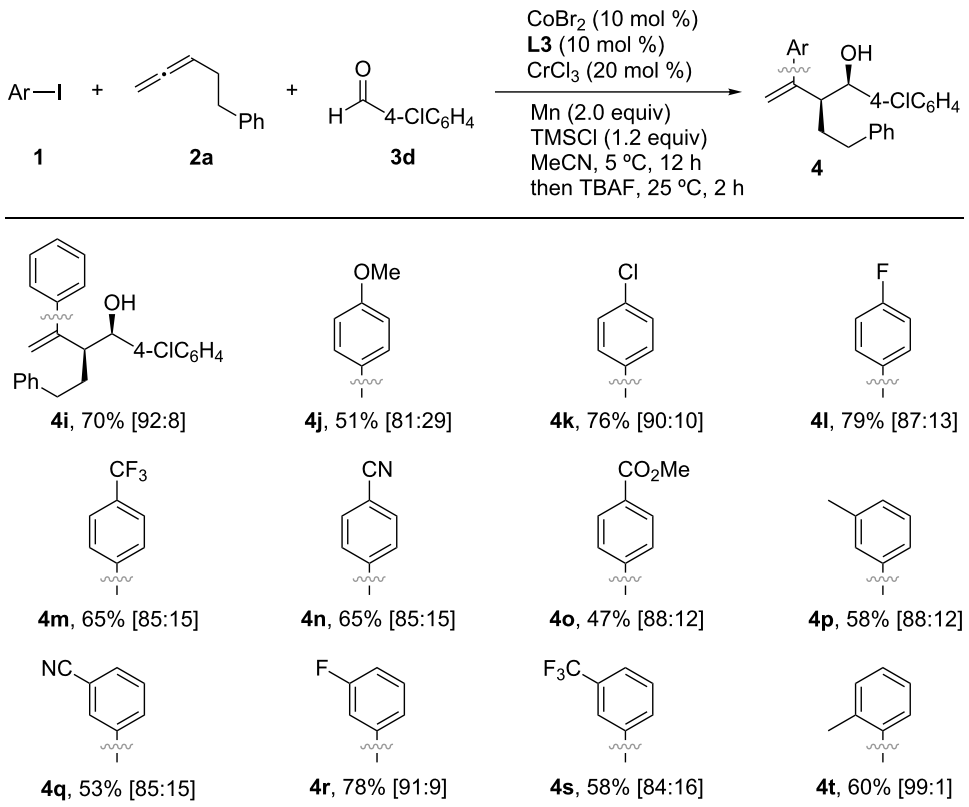

Scheme 7: Screening of aryl iodides in the Co/Cr-catalyzed three-component coupling reaction. All yields are determined after isolation. The values in brackets indicate the diastereomer ratio of the *syn* and *anti* products, determined from ^{1}H NMR spectra.

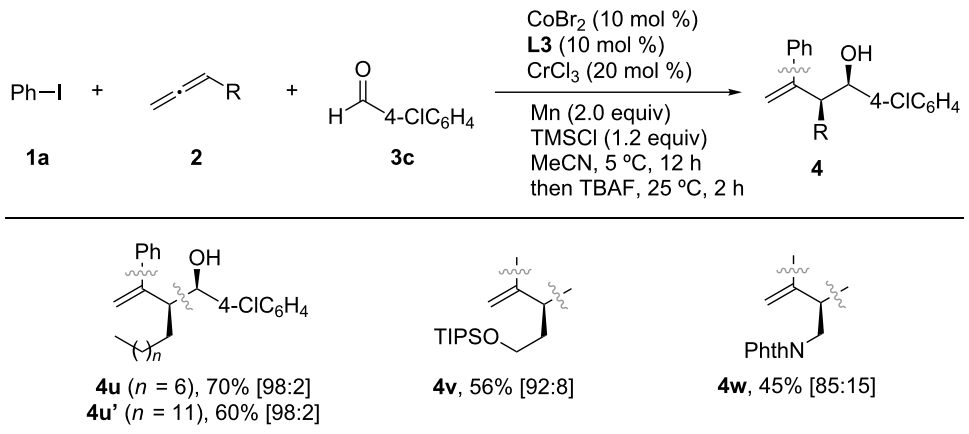

Scheme 8: Screening of allenes in the Co/Cr-catalyzed three-component coupling reaction. All yields are determined after isolation. The values in brackets indicate the diastereomer ratio of the *syn* and *anti* products, determined from ^{1}H NMR.

tion of the phenyl ring were successfully used in the reaction, giving rise to the desired coupling products in good yields (47–79%). The homoallylic alcohols **4p**–**t** were formed with a high degree of *syn*-selectivity because of *meta*- and *ortho*-substituted aryl iodides also being well tolerated in the reaction. The protocol was not only limited to the coupling of simple allenes; it was also used with heteroatom-containing functionalized allenes to afford the *syn*-homoallylic alcohols **4u**, **4u'** and **4w** in reasonably good yields (Scheme 8).

During the investigation of allenes, it was observed that, when oxygen substituents were present at the allenyl position, cou-

pling products with reversed diastereoselectivity were obtained (Scheme 9). Thus, treatment of 4-benzyloxybuta-1,2-diene (**5**) with **1** and **3a** under identical reaction conditions mainly afforded the *anti*-configured homoallylic alcohols **7**–**10** in 46–65% yield. A similar reversed diastereoselectivity was observed in the coupling reaction of silyloxy allene **6**, leading to **11** in 46% yield (*anti*/*syn* = 73:27).

A stoichiometric reaction using phenylchromium(II or III) reagents, generated from the reaction of $CrCl_2$ or $CrCl_3(thf)_2$ with phenyllithium [19,20], in the presence of allene **2a** and aldehyde **3c** provided diarylmethanes in 78–85% yields without the visible consumption of allene **2a** (Scheme 10, reaction 1). Furthermore, in the absence of the $CrCl_3$ catalyst, allene **2a** was utterly consumed, whereas most of iodide **1a** and aldehyde **3d** were recovered unreacted (Scheme 10, reaction 2). These results indicate that the arylcobalt, rather than the arylchromium intermediate, promoted the allene carbometalation. Additionally, it is thought that the vinylcobalt generated was converted to vinylchromium, which would be inactive in the oligomerization, but is a highly nucleophilic species. According to these findings, the reversed diastereoselectivity in Scheme 9 might be due to stereoelectronic effects [21,22]. Thus, the σ*(C–O) bond stabilizes the forming σ(Co–C) bond in the transition state **C** of the carbocobaltation step (Scheme 11), facilitating the further selective formation of the branched allylcobalt species **D** which could be converted into the thermodynamically more stable (*E*)-allylcobalt species **E** because of the flexible C(vinyl)–C(allyl) single bond. The generated compound **E** then undergoes transmetalation with the chromium salt to give the (*E*)-allylchromium species **F**. In contrast, the carbometalation of a simple allene produces (*Z*)-allylcobalt species **E′** and the corresponding (*Z*)-allylchromium product **F′** would be provided through a transition state such as **C′**, in which the cobalt center is connected to a less sterically hindered terminal allene carbon [23].

On the basis of these results, a plausible catalytic cycle for the cobalt/chromium-catalyzed three-component coupling reaction is shown in Scheme 12. The three-component coupling starts

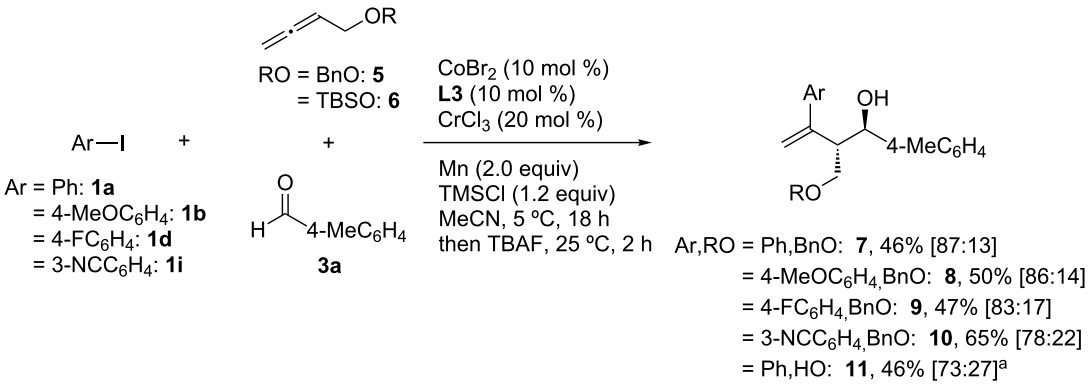

Scheme 9: Reversed diastereoselectivity using allenyl ethers **5** and **6**. [a]4-chlorobenzaldehyde was used instead of **3a**.

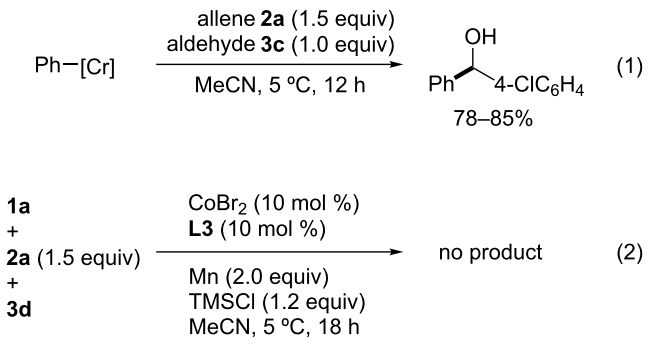

Scheme 10: Stoichiometric reaction of phenylchromium(II or III) reagents (reaction 1) and the three-component coupling without $CrCl_3$ catalyst (reaction 2).

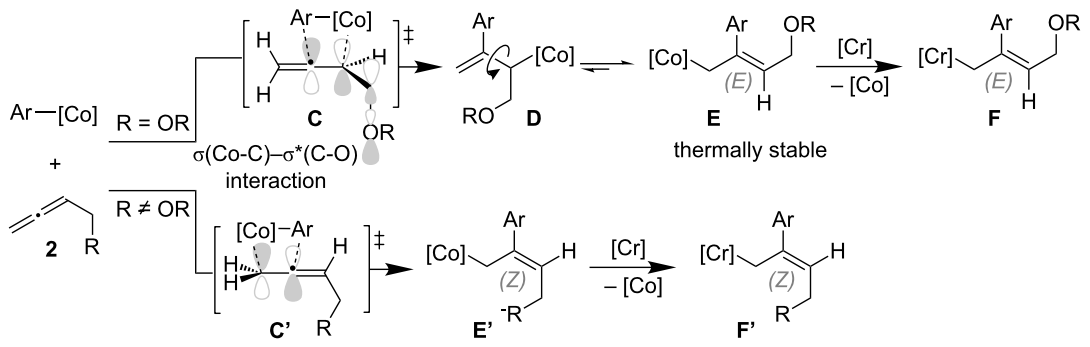

Scheme 11: The origin of the diastereoselectivity in the present three-component coupling.

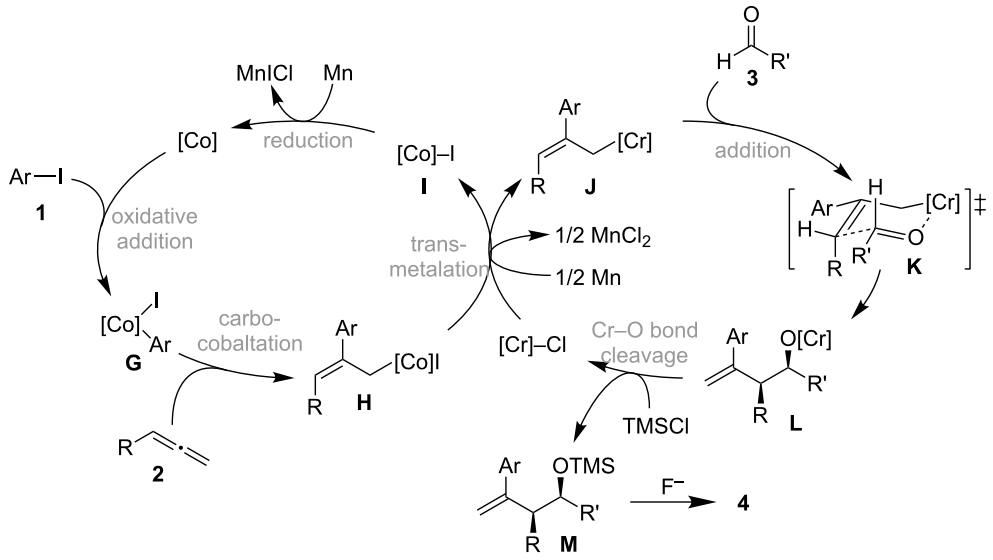

Scheme 12: Plausible reaction mechanism of the three-component coupling.

with the oxidative addition of an aryl iodide **1** to a low-valent cobalt species to form an arylcobalt species **G** that reacts with an allene **2** to stereoselectively generate an allylcobalt **H** via carbocobaltation. Rapid transmetalation between **H** and the chromium salt [8,9] triggers the transfer of the cobalt allyl group to the chromium to afford **I** and the highly nucleophilic allylchromium species **J**, which retains the same stereochemical information on the olefinic moiety as that of **H**. The allylchromium species **J** reacts with the aldehyde **3** at the γ-position of the allyl metal unit via a cyclic six-membered transition state **K** to give the chromium alkoxide **L** [24]. Finally, the Cr–O bond is cleaved by TMSCl, generating the active chromium salt for the transmetalation and the silyl ether **M**, the desilylation of which with a fluoride anion results in the formation of a homoallylic alcohol **4**.

Conclusion

The cobalt/chromium-catalyzed three-component coupling reaction of aryl iodides, allenes, and aldehydes to produce highly substituted homoallylic alcohols in a diastereoselective manner has been demonstrated. In the coupling reaction, two catalysts played individual roles; the cobalt catalyst activated aryl iodides to form arylcobalt species, which then performed allene carbocobaltation to form stereo-defined substituted (*Z*)-allylcobalt intermediates. The chromium catalyst transformed the generated allylcobalt intermediates into highly nucleophilic allylchromium species, without the isomerization of the olefinic moiety, via transmetalation between the generated allylcobalt intermediate and the chromium salt. Moreover, it was found that an oxygen atom present at the allenyl position resulted in a reversed diastereoselectivity of the homoallylic alcohol prod-

ucts; thus, the allene carbocobaltation regioselectivity could be controlled by the stereoelectronic interaction between the forming σ(C–Co) bond and a neighboring σ*(C–O) bond. Further mechanistic studies and expansion of the substrate scope, including synthetic applications of this three-component coupling, are currently in progress.

Supporting Information

Supporting Information File 1

Experimental part.
[https://www.beilstein-journals.org/bjoc/content/supplementary/1860-5397-14-118-S1.pdf]

ORCID® iDs

Kimihiro Komeyama - https://orcid.org/0000-0001-7111-2112
Itaru Osaka - https://orcid.org/0000-0002-9879-2098

References

1. Takai, K. *Bull. Chem. Soc. Jpn.* **2015,** *88,* 1511. doi:10.1246/bcsj.20150170
2. Flynn, A. B.; Ogilvie, W. W. *Chem. Rev.* **2007,** *107,* 4698. doi:10.1021/cr050051k
3. Tamaru, Y. *Modern Organonickel Chemistry;* Wiley-VCH: Weinheim, Germany, 2005.
4. Okude, Y.; Hirano, S.; Hiyama, T.; Nozaki, H. *J. Am. Chem. Soc.* **1977,** *99,* 3179. doi:10.1021/ja00451a061
5. Jin, H.; Uenishi, J.; Christ, W. J.; Kishi, Y. *J. Am. Chem. Soc.* **1986,** *108,* 5644. doi:10.1021/ja00278a057
6. Takai, K.; Tagashira, M.; Kuroda, T.; Oshima, K.; Utimoto, K.; Nozaki, H. *J. Am. Chem. Soc.* **1986,** *108,* 6048. doi:10.1021/ja00279a068
7. Fürstner, A.; Shi, N. *J. Am. Chem. Soc.* **1996,** *118,* 12349. doi:10.1021/ja9625236
8. Takai, K.; Nitta, K.; Fujimura, O.; Utimoto, K. *J. Org. Chem.* **1989,** *54,* 4732. doi:10.1021/jo00281a004
9. Usanov, D. L.; Yamamoto, H. *Angew. Chem., Int. Ed.* **2010,** *49,* 8169. doi:10.1002/anie.201002751
10. Takai, K.; Matsukawa, N.; Takahashi, A.; Fujii, T. *Angew. Chem., Int. Ed.* **1998,** *37,* 152. doi:10.1002/(SICI)1521-3773(19980202)37:1/2<152::AID-ANIE152>3.0.CO;2-8
11. Takai, K.; Toratsu, C. *J. Org. Chem.* **1998,** *63,* 6450. doi:10.1021/jo9814086
12. Xiong, Y.; Zhang, G. *J. Am. Chem. Soc.* **2018,** *140,* 2735. doi:10.1021/jacs.7b12760
13. Komeyama, K.; Kashihara, T.; Takaki, K. *Tetrahedron Lett.* **2013,** *54,* 5659. doi:10.1016/j.tetlet.2013.07.133
14. Komeyama, K.; Okamoto, Y.; Takaki, K. *Angew. Chem., Int. Ed.* **2014,** *53,* 11325. doi:10.1002/anie.201406807
15. Komeyama, K.; Asakura, R.; Fukuoka, H.; Takaki, K. *Tetrahedron Lett.* **2015,** *56,* 1735. doi:10.1016/j.tetlet.2015.02.101
16. Komeyama, K.; Kiguchi, S.; Takaki, K. *Chem. Commun.* **2016,** *52,* 7009. doi:10.1039/c6cc03086f
17. Hopkins, C. D.; Malinakova, H. C. *Org. Lett.* **2004,** *6,* 2221. doi:10.1021/ol0492795
18. Fillon, H.; Gosmini, C.; Périchon, J. *J. Am. Chem. Soc.* **2003,** *125,* 3867. doi:10.1021/ja0289494
19. Daly, J. J.; Sneeden, R. P. A.; Zeiss, H. H. *J. Am. Chem. Soc.* **1966,** *88,* 4287. doi:10.1021/ja00970a049
20. Kanno, K.-i.; Liu, Y.; Iesato, A.; Nakajima, K.; Takahashi, T. *Org. Lett.* **2005,** *7,* 5453. doi:10.1021/ol052214x
21. Ito, H.; Ito, S.; Sasaki, Y.; Matsuura, K.; Sawamura, M. *J. Am. Chem. Soc.* **2007,** *129,* 14856. doi:10.1021/ja076634o
22. Ohmiya, H.; Makida, Y.; Li, D.; Tanabe, M.; Sawamura, M. *J. Am. Chem. Soc.* **2010,** *132,* 879. doi:10.1021/ja9092264
23. Yoshida, Y.; Murakami, K.; Yorimitsu, H.; Oshima, K. *J. Am. Chem. Soc.* **2010,** *132,* 8878. doi:10.1021/ja102303s
24. Hiyama, T.; Kimura, K.; Nozaki, H. *Tetrahedron Lett.* **1981,** *22,* 1037. doi:10.1016/S0040-4039(01)82859-8

License and Terms

BEILSTEIN JOURNAL OF ORGANIC CHEMISTRY

Thiocarbonyl-enabled ferrocene C–H nitrogenation by cobalt(III) catalysis: thermal and mechanochemical

Santhivardhana Reddy Yetra‡, Zhigao Shen‡, Hui Wang and Lutz Ackermann*§

Full Research Paper

Open Access

Address:
Institut für Organische und Biomolekulare Chemie, Georg-August-Universität Göttingen, Tammannstraße 2, 37077 Göttingen, Germany

Email:
Lutz Ackermann* - Lutz.Ackermann@chemie.uni-goettingen.de

* Corresponding author ‡ Equal contributors
§ http://www.org.chemie.uni-goettingen.de/ackermann/

Keywords:
amidation; C–H activation; cobalt; ferrocene; mechanochemistry

Beilstein J. Org. Chem. **2018,** *14,* 1546–1553.
doi:10.3762/bjoc.14.131

Received: 14 May 2018
Accepted: 15 June 2018
Published: 25 June 2018

This article is part of the thematic issue "Cobalt catalysis".

Guest Editor: S. Matsunaga

Abstract

Versatile C–H amidations of synthetically useful ferrocenes were accomplished by weakly-coordinating thiocarbonyl-assisted cobalt catalysis. Thus, carboxylates enabled ferrocene C–H nitrogenations with dioxazolones, featuring ample substrate scope and robust functional group tolerance. Mechanistic studies provided strong support for a facile organometallic C–H activation manifold.

Introduction

C–H activation has surfaced as a transformative tool in molecular sciences [1-9]. While major advances have been accomplished with precious 4d transition metals, recent focus has shifted towards more sustainable base metals [10-17], with considerable progress by earth-abundant cobalt catalysts [18-22]. In this context, well-defined cyclopentadienyl-derived cobalt(III) complexes have proven instrumental for enabling a wealth of C–H transformations [23-41], prominently featuring transformative C–H nitrogenations [42,43] in an atom- and step-economical fashion [44-59]. Within our program on cobalt-catalyzed C–H activation [60-68], we have now devised C–H nitrogenations assisted by weakly-coordinating [69] thiocarbonyls [70,71], allowing the direct C–H activation on substituted ferrocenes [72-93] – key structural motifs of powerful transition metal catalyst ligands and organocatalysts (Figure 1) [94-97]. During the preparation of this article, the use of strongly-coordinating, difficult to remove directing groups has been reported [70,71]. In sharp contrast, notable features of our approach include (i) cobalt-catalyzed C–H amidations of thiocarbonylferrocenes by weak coordination, (ii) thermal and mechanochemical [98-100] cobalt-catalyzed ferrocene C–H nitrogenations, (iii) versatile access to synthetically useful

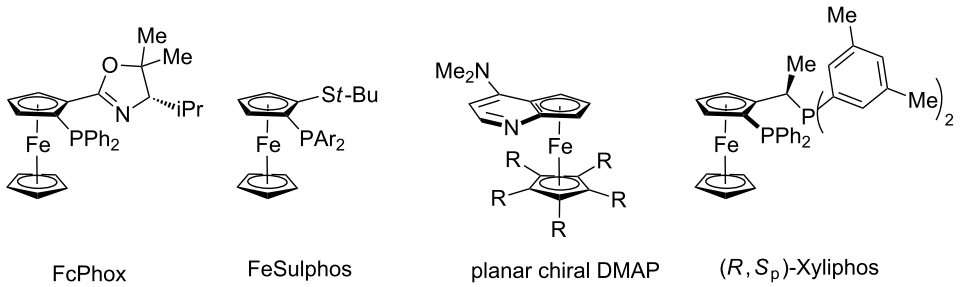

Figure 1: Selected ferrocene-based ligands and organocatalysts.

aminoketones, and (iv) key mechanistic insights on facile C–H cobaltation.

Results and Discussion

We initiated our studies by probing various reaction conditions for the envisioned C–H amidation of ferrocene **1a** (Table 1). Among a variety of ligands, N-heterocyclic carbenes and phosphines provided unsatisfactory results (Table 1, entries 1–3), while the product **3aa** was formed when using amino acid derivatives, albeit as of yet in a racemic fashion (Table 1, entries 4–7). Yet, optimal catalytic performance was realized with 1-$AdCO_2H$ (Table 1, entries 8 and 9) [101-104], particularly when using DCE as the solvent (Table 1, entries 9–12). A control experiment verified the essential nature of the cobalt catalyst (Table 1, entry 13). In contrast to the thiocarbonyl-assisted C–H amidation, the corresponding ketone failed thus

Table 1: Thiocarbonyl-assisted C−H nitrogenation of ferrocene **1a**.[a]

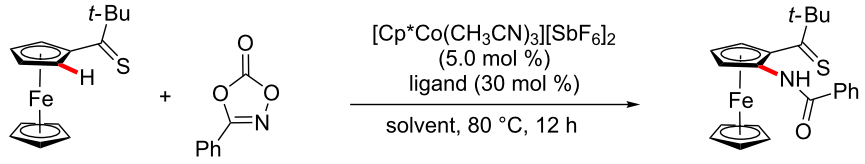

1a **2a** **3aa**

Entry	Solvent	Ligand	Yield (%)
1	DCE	–	–
2	DCE	IMes·HCl	–
3	DCE	PPh_3	–
4	DCE	Boc-Leu-OH	40
5	DCE	Boc-Val-OH	55
6	DCE	Boc-Pro-OH	30
7	DCE	Boc-Ala-OH	62
8	DCE	$MesCO_2H$	80
9	**DCE**	**1-$AdCO_2H$**	**84**
10	1,4-dioxane	1-$AdCO_2H$	75
11	toluene	1-$AdCO_2H$	79
12	GVL	1-$AdCO_2H$	35
13	DCE	1-$AdCO_2H$	–[b]

[a]Reaction conditions: **1a** (0.13 mmol), **2a** (0.15 mmol), ligand (30 mol %), [Co] (5.0 mol %), solvent (1.0 mL). [b]Reaction performed in the absence of $[Cp^*Co(CH_3CN)_3][SbF_6]_2$. Yields of isolated product.

far to deliver the desired product, under otherwise identical reaction conditions.

With the optimized reaction conditions in hand, we explored the robustness of the cobalt-catalyzed ferrocene C–H amidation with a variety of 1,4,2-dioxazol-5-ones **2** (Scheme 1). Hence, the chemoselectivity of the cobalt catalyst was reflected by fully tolerating sensitive electrophilic functional groups, including amido, chloro, bromo and nitro substituents in the *para*-, *meta*- and even the more congested *ortho*-position.

The versatile cobalt-catalyzed C–H amidation was not limited to mono-substituted ferrocenes **1** (Scheme 2). Indeed, the

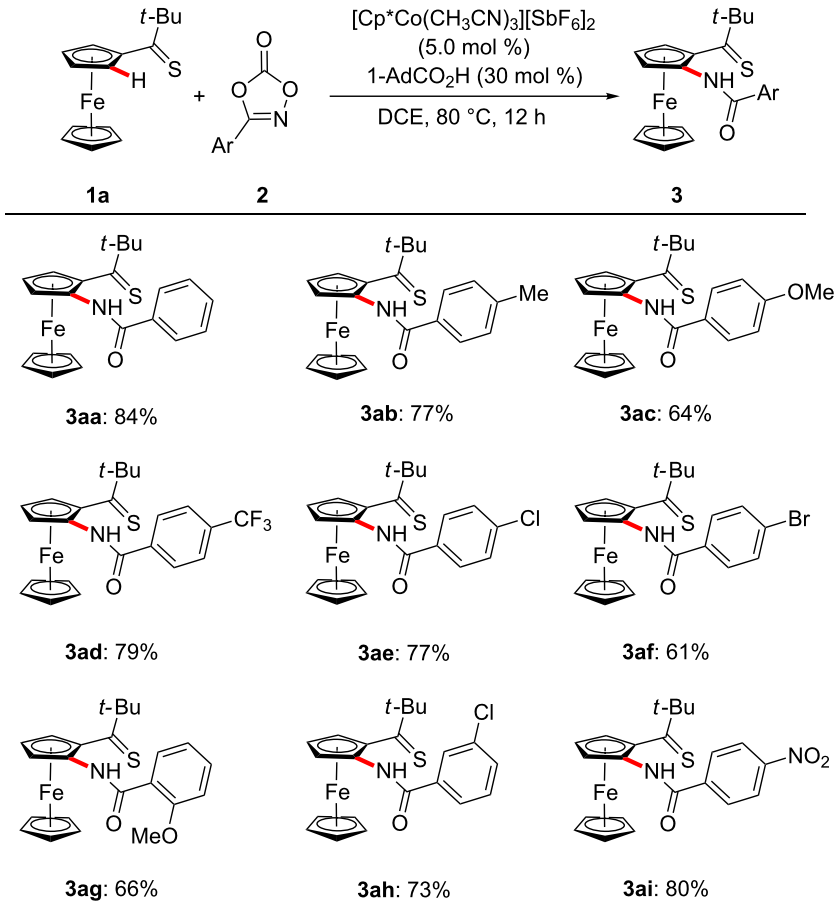

Scheme 1: Scope of substituted dioxazolones **2**.

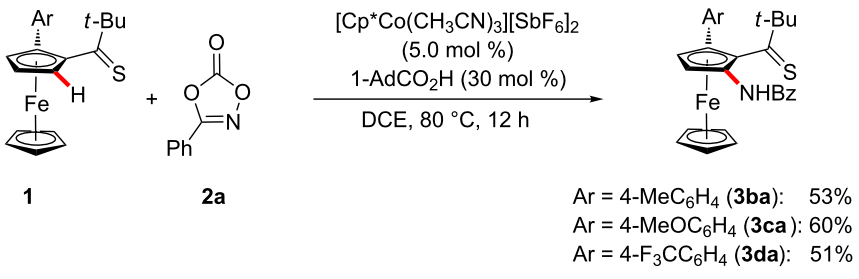

Scheme 2: C–H Amidation of arylated ferrocenes **1**.

arylated ferrocenes **1b**–**d** were identified as viable substrates likewise.

Moreover, differently substituted thiocarbonyls **1** were found to be amenable within the cobalt-catalyzed C–H amidation manifold by weak-coordination (Scheme 3).

Given the versatility of the cobalt-catalyzed C–H nitrogenation, we became intrigued to delineating its mode of action. To this end, C–H amidations in the presence of isotopically labelled co-solvents led to a significant H/D scrambling in proximity to the thiocarbonyl group. These findings are indicative of a reversible, thus facile organometallic C–H cobaltation regime (Scheme 4).

Next, intermolecular competition experiments revealed that electron-rich arylated thiocarbonylferrocene **1** reacted preferentially, which can be rationalized with a base-assisted internal electrophilic substitution (BIES) [24,105] C–H cobaltation mechanism. In addition, the electron-rich amidating reagent **2c** was found to be inherently more reactive (Scheme 5).

As to further late-stage manipulation of the thus-obtained products, the amidated thiocarbonylferrocene **3aa** could be easily transformed into the corresponding synthetically useful aminoketone **4aa** (Scheme 6), illustrating the unique synthetic utility of our strategy.

Mechanochemical molecular synthesis has attracted recent renewed attention as an attractive alternative for facilitating sustainable organic syntheses [106]. Thus, we were delighted to observe that the mechanochemical C–H nitrogenations proved likewise viable by thiocarbonyl assistance in an effective manner (Scheme 7).

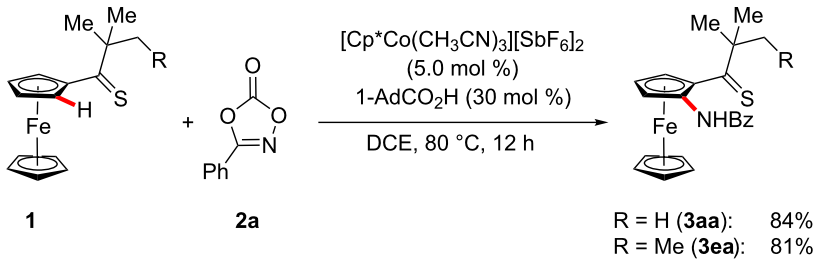

Scheme 3: Thiocarbonyl-assisted C–H amidation.

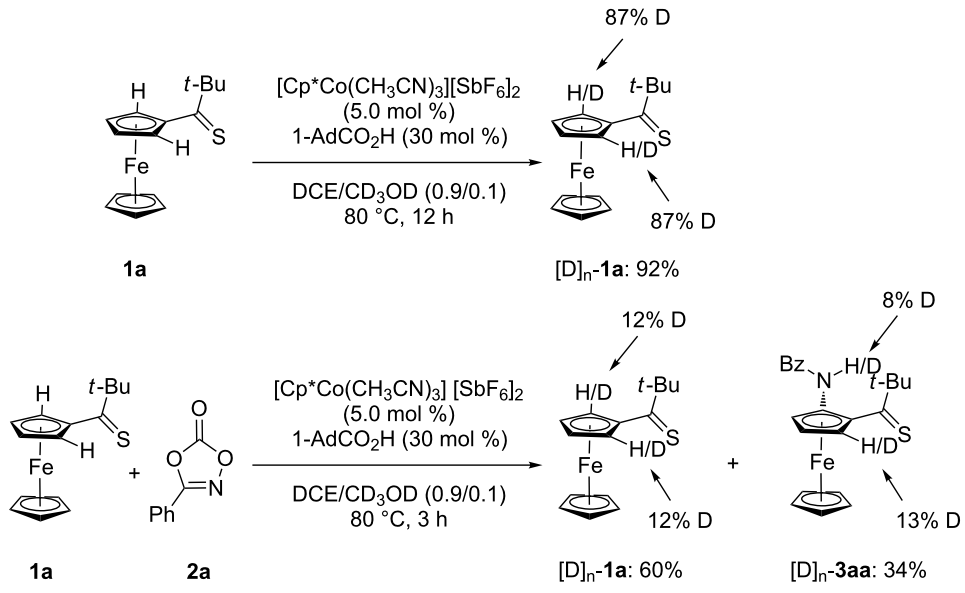

Scheme 4: H/D Exchange reactions.

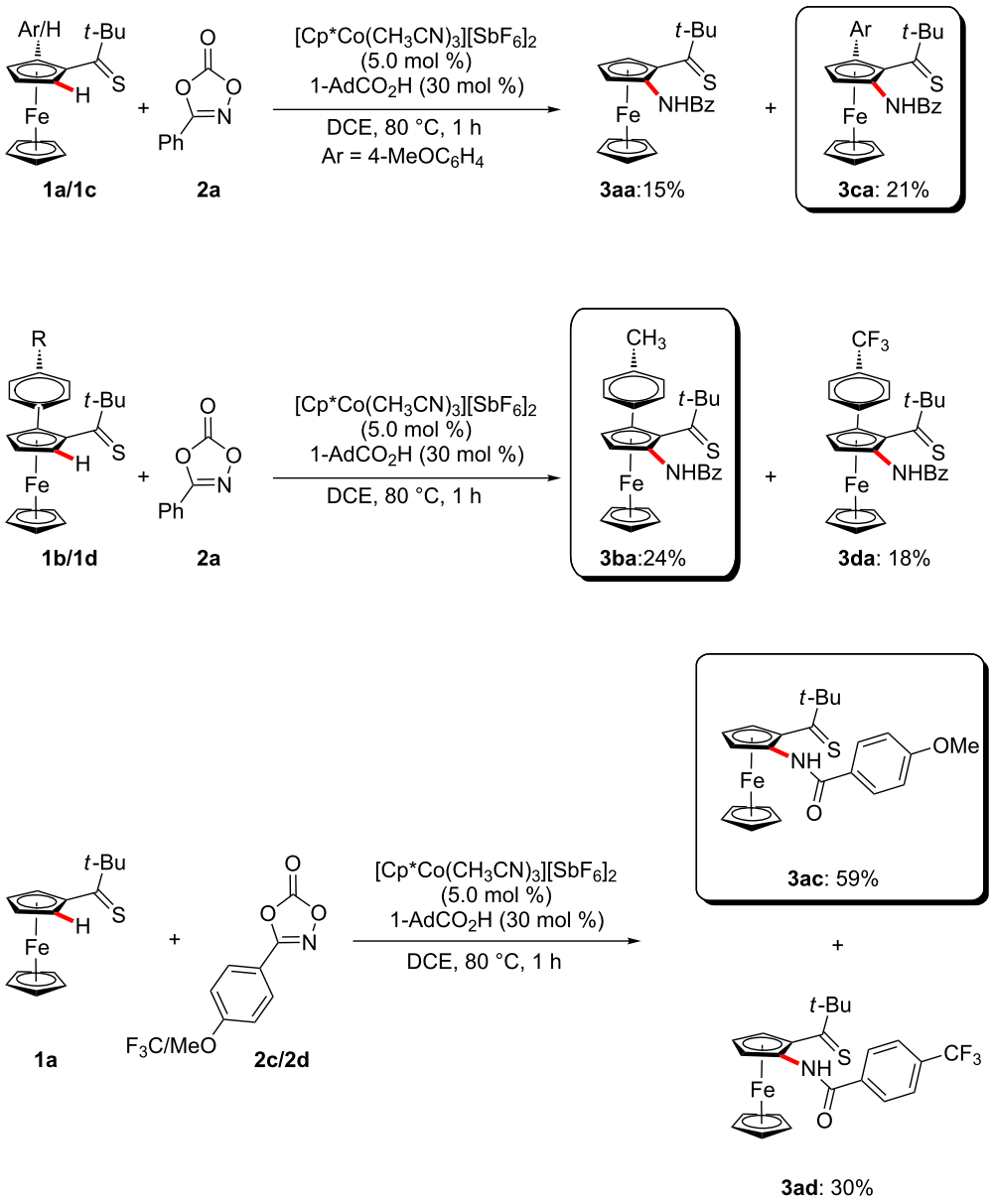

Scheme 5: Intermolecular competition experiments.

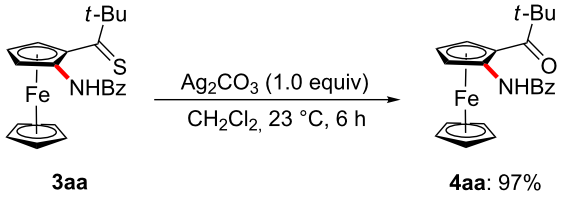

Scheme 6: Synthesis of aminoketone **4aa**.

Conclusion

In conclusion, we have reported on the unprecedented cobalt-catalyzed C–H nitrogenation of ferrocenes by weakly-coordinating thiocarbonyls. The carboxylate-assisted cobalt catalysis was characterized by high functional group tolerance and ample substrate scope. Mechanistic studies provided evidence for a facile C–H activation. The C–H amidation was achieved in a thermal fashion as well as by means of mechanochemistry, providing access to synthetically meaningful aminoketones.

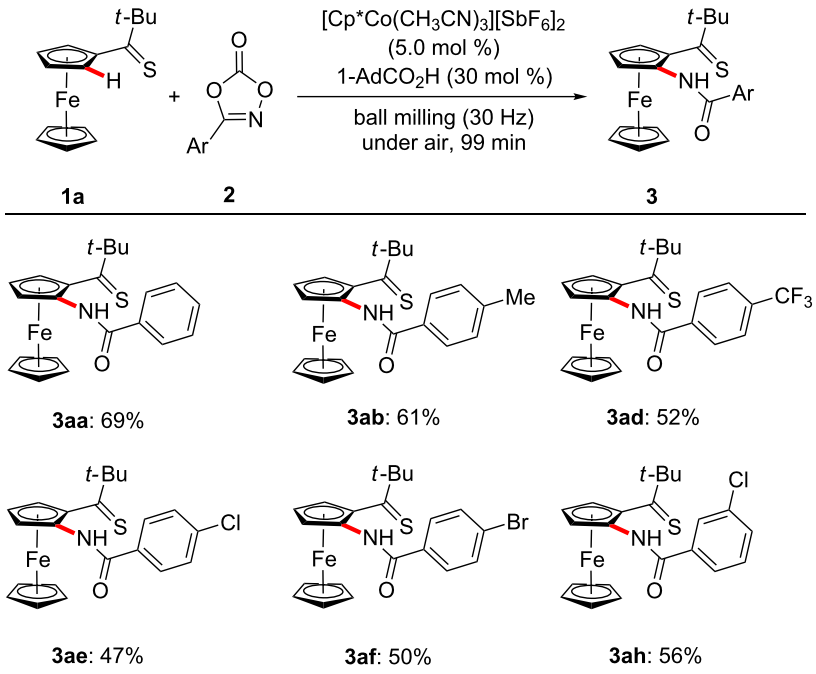

Scheme 7: Mechanochemical ferrocene C–H nitrogenation.

Supporting Information

Supporting Information File 1

Experimental procedures, characterization data, and NMR spectra for new compounds.
[https://www.beilstein-journals.org/bjoc/content/supplementary/1860-5397-14-131-S1.pdf]

Acknowledgements

Generous support by the DFG (Gottfried Wilhelm Leibniz prize), and the CSC (fellowships to Z.S. and H.W.) is gratefully acknowledged.

ORCID® iDs

Lutz Ackermann - https://orcid.org/0000-0001-7034-8772

References

1. Gandeepan, P.; Ackermann, L. *Chem* **2018,** *4,* 199–222. doi:10.1016/j.chempr.2017.11.002
2. Wei, Y.; Hu, P.; Zhang, M.; Su, W. *Chem. Rev.* **2017,** *117,* 8864–8907. doi:10.1021/acs.chemrev.6b00516
3. Ma, W.; Gandeepan, P.; Li, J.; Ackermann, L. *Org. Chem. Front.* **2017,** *4,* 1435–1467. doi:10.1039/C7QO00134G
4. He, J.; Wasa, M.; Chan, K. S. L.; Shao, Q.; Yu, J.-Q. *Chem. Rev.* **2017,** *117,* 8754–8786. doi:10.1021/acs.chemrev.6b00622
5. Zheng, Q.-Z.; Jiao, N. *Chem. Soc. Rev.* **2016,** *45,* 4590–4627. doi:10.1039/C6CS00107F
6. Borie, C.; Ackermann, L.; Nechab, M. *Chem. Soc. Rev.* **2016,** *45,* 1368–1386. doi:10.1039/C5CS00622H
7. Ye, B.; Cramer, N. *Acc. Chem. Res.* **2015,** *48,* 1308–1318. doi:10.1021/acs.accounts.5b00092
8. Satoh, T.; Miura, M. *Chem. – Eur. J.* **2010,** *16,* 11212–11222. doi:10.1002/chem.201001363
9. Ackermann, L.; Vicente, R.; Kapdi, A. R. *Angew. Chem., Int. Ed.* **2009,** *121,* 9976–10011. doi:10.1002/ange.200902996
10. Hu, Y.; Zhou, B.; Wang, C. *Acc. Chem. Res.* **2018,** *51,* 816–827. doi:10.1021/acs.accounts.8b00028
11. Liu, W.; Ackermann, L. *ACS Catal.* **2016,** *6,* 3743–3752. doi:10.1021/acscatal.6b00993
12. Cera, G.; Ackermann, L. *Top. Curr. Chem.* **2016,** *374,* 191–224. doi:10.1007/s41061-016-0059-6
13. Nakao, Y. *Chem. Rec.* **2011,** *11,* 242–251. doi:10.1002/tcr.201100023
14. Castro, L. C. M.; Chatani, N. *Chem. Lett.* **2015,** *44,* 410–421. doi:10.1246/cl.150024
15. Hirano, K.; Miura, M. *Chem. Lett.* **2015,** *44,* 868–873. doi:10.1246/cl.150354
16. Yamaguchi, J.; Muto, K.; Itami, K. *Eur. J. Org. Chem.* **2013,** 19–30. doi:10.1002/ejoc.201200914
17. Kulkarni, A. A.; Daugulis, O. *Synthesis* **2009,** 4087–4109. doi:10.1055/s-0029-1217131
18. Yoshino, T.; Matsunaga, S. *Adv. Synth. Catal.* **2017,** *359,* 1245–1262. doi:10.1002/adsc.201700042
19. Wei, D.; Zhu, X.; Niu, J.-L.; Song, M.-P. *ChemCatChem* **2016,** *8,* 1242–1263. doi:10.1002/cctc.201600040
20. Moselage, M.; Li, J.; Ackermann, L. *ACS Catal.* **2016,** *6,* 498–525. doi:10.1021/acscatal.5b02344
21. Gao, K.; Yoshikai, N. *Acc. Chem. Res.* **2014,** *47,* 1208–1219. doi:10.1021/ar400270x
22. Ackermann, L. *J. Org. Chem.* **2014,** *79,* 8948–8954. doi:10.1021/jo501361k

23. Zell, D.; Müller, V.; Dhawa, U.; Bursch, M.; Presa, R. R.; Grimme, S.; Ackermann, L. *Chem. – Eur. J.* **2017,** *23,* 12145–12148. doi:10.1002/chem.201702528
24. Zell, D.; Bursch, M.; Müller, V.; Grimme, S.; Ackermann, L. *Angew. Chem., Int. Ed.* **2017,** *56,* 10378–10382. doi:10.1002/anie.201704196
25. Ikemoto, H.; Tanaka, R.; Sakata, K.; Kanai, M.; Yoshino, T.; Matsunaga, S. *Angew. Chem., Int. Ed.* **2017,** *56,* 7156–7160. doi:10.1002/anie.201703193
26. Yan, Q.; Chen, Z.; Liu, Z.; Zhang, Y. *Org. Chem. Front.* **2016,** *3,* 678–682. doi:10.1039/C6QO00059B
27. Lu, Q.; Vásquez-Céspedes, S.; Gensch, T.; Glorius, F. *ACS Catal.* **2016,** *6,* 2352–2356. doi:10.1021/acscatal.6b00367
28. Kong, L.; Yu, S.; Zhou, X.; Li, X. *Org. Lett.* **2016,** *18,* 588–591. doi:10.1021/acs.orglett.5b03629
29. Kalsi, D.; Laskar, R. A.; Barsu, N.; Premkumar, J. R.; Sundararaju, B. *Org. Lett.* **2016,** *18,* 4198–4201. doi:10.1021/acs.orglett.6b01845
30. Bunno, Y.; Murakami, N.; Suzuki, Y.; Kanai, M.; Yoshino, T.; Matsunaga, S. *Org. Lett.* **2016,** *18,* 2216–2219. doi:10.1021/acs.orglett.6b00846
31. Boerth, J. A.; Hummel, J. R.; Ellman, J. A. *Angew. Chem., Int. Ed.* **2016,** *55,* 12650–12654. doi:10.1002/anie.201603831
32. Hummel, J. R.; Ellman, J. A. *J. Am. Chem. Soc.* **2015,** *137,* 490–498. doi:10.1021/ja5116452
33. Wang, H.; Koeller, J.; Liu, W.; Ackermann, L. *Chem. – Eur. J.* **2015,** *21,* 15525–15528. doi:10.1002/chem.201503624
34. Suzuki, Y.; Sun, B.; Sakata, K.; Yoshino, T.; Matsunaga, S.; Kanai, M. *Angew. Chem., Int. Ed.* **2015,** *54,* 9944–9947. doi:10.1002/anie.201503704
35. Sen, M.; Kalsi, D.; Sundararaju, B. *Chem. – Eur. J.* **2015,** *21,* 15529–15533. doi:10.1002/chem.201503643
36. Sauermann, N.; González, M. J.; Ackermann, L. *Org. Lett.* **2015,** *17,* 5316–5319. doi:10.1021/acs.orglett.5b02678
37. Ma, W.; Ackermann, L. *ACS Catal.* **2015,** *5,* 2822–2825. doi:10.1021/acscatal.5b00322
38. Li, J.; Ackermann, L. *Angew. Chem., Int. Ed.* **2015,** *54,* 3635–3638. doi:10.1002/anie.201409247
39. Li, J.; Ackermann, L. *Angew. Chem., Int. Ed.* **2015,** *54,* 8551–8554. doi:10.1002/anie.201501926
40. Ikemoto, H.; Yoshino, T.; Sakata, K.; Matsunaga, S.; Kanai, M. *J. Am. Chem. Soc.* **2014,** *136,* 5424–5431. doi:10.1021/ja5008432
41. Yoshino, T.; Ikemoto, H.; Matsunaga, S.; Kanai, M. *Angew. Chem., Int. Ed.* **2013,** *52,* 2207–2211. doi:10.1002/anie.201209226
42. Park, Y.; Kim, Y.; Chang, S. *Chem. Rev.* **2017,** *117,* 9247–9301. doi:10.1021/acs.chemrev.6b00644
43. Jiao, J.; Murakami, K.; Itami, K. *ACS Catal.* **2016,** *6,* 610–633. doi:10.1021/acscatal.5b02417
44. Borah, G.; Borah, P.; Patel, P. *Org. Biomol. Chem.* **2017,** *15,* 3854–3859. doi:10.1039/C7OB00540G
45. Zhang, W.; Deng, H.; Li, H. *Org. Chem. Front.* **2017,** *4,* 2202–2206. doi:10.1039/C7QO00542C
46. Xia, J.; Yang, X.; Li, Y.; Li, X. *Org. Lett.* **2017,** *19,* 3243–3246. doi:10.1021/acs.orglett.7b01356
47. Huang, J.; Huang, Y.; Wang, T.; Huang, Q.; Wang, Z.; Chen, Z. *Org. Lett.* **2017,** *19,* 1128–1131. doi:10.1021/acs.orglett.7b00120
48. Barsu, N.; Bolli, S. K.; Sundararaju, B. *Chem. Sci.* **2017,** *8,* 2431–2435. doi:10.1039/C6SC05026C
49. Wang, X.; Lerchen, A.; Glorius, F. *Org. Lett.* **2016,** *18,* 2090–2093. doi:10.1021/acs.orglett.6b00716
50. Wu, F.; Zhao, Y.; Chen, W. *Tetrahedron* **2016,** *72,* 8004–8008. doi:10.1016/j.tet.2016.10.032
51. Wang, J.; Zha, S.; Chen, K.; Zhang, F.; Song, C.; Zhu, J. *Org. Lett.* **2016,** *18,* 2062–2065. doi:10.1021/acs.orglett.6b00691
52. Wang, H.; Lorion, M. M.; Ackermann, L. *Angew. Chem., Int. Ed.* **2016,** *55,* 10386–10390. doi:10.1002/anie.201603260
53. Park, Y.; Park, K. T.; Kim, J. G.; Chang, S. *J. Am. Chem. Soc.* **2015,** *137,* 4534–4542. doi:10.1021/jacs.5b01324
54. Jeon, B.; Yeon, U.; Son, J.-Y.; Lee, P. H. *Org. Lett.* **2016,** *18,* 4610–4613. doi:10.1021/acs.orglett.6b02250
55. Park, Y.; Jee, S.; Kim, J. G.; Chang, S. *Org. Process Res. Dev.* **2015,** *19,* 1024–1029. doi:10.1021/acs.oprd.5b00164
56. Park, J.; Lee, J.; Chang, S. *Angew. Chem., Int. Ed.* **2017,** *56,* 4256–4260. doi:10.1002/anie.201701138
57. Park, J.; Chang, S. *Angew. Chem., Int. Ed.* **2015,** *54,* 14103–14107. doi:10.1002/anie.201505820
58. Mei, R.; Loup, J.; Ackermann, L. *ACS Catal.* **2016,** *6,* 793–797. doi:10.1021/acscatal.5b02661
59. Liang, Y.; Liang, Y.-F.; Tang, C.; Yuan, Y.; Jiao, N. *Chem. – Eur. J.* **2015,** *21,* 16395–16399. doi:10.1002/chem.201503533
60. Sauermann, N.; Mei, R.; Ackermann, L. *Angew. Chem., Int. Ed.* **2018,** *57,* 5090–5094. doi:10.1002/anie.201802206
61. Tian, C.; Massignan, L.; Meyer, T. H.; Ackermann, L. *Angew. Chem., Int. Ed.* **2018,** *57,* 2383–2387. doi:10.1002/anie.201712647
62. Sauermann, N.; Meyer, T. H.; Tian, C.; Ackermann, L. *J. Am. Chem. Soc.* **2017,** *139,* 18452–18455. doi:10.1021/jacs.7b11025
63. Sauermann, N.; Loup, J.; Kootz, D.; Yatham, V. R.; Berkessel, A.; Ackermann, L. *Synthesis* **2017,** *49,* 3476–3484. doi:10.1055/s-0036-1590471
64. Mei, R.; Ackermann, L. *Adv. Synth. Catal.* **2016,** *358,* 2443–2448. doi:10.1002/adsc.201600384
65. Moselage, M.; Sauermann, N.; Richter, S. C.; Ackermann, L. *Angew. Chem., Int. Ed.* **2015,** *54,* 6352–6355. doi:10.1002/anie.201412319
66. Li, J.; Ackermann, L. *Chem. – Eur. J.* **2015,** *21,* 5718–5722. doi:10.1002/chem.201500552
67. Punji, B.; Song, W.; Shevchenko, G. A.; Ackermann, L. *Chem. – Eur. J.* **2013,** *19,* 10605–10610. doi:10.1002/chem.201301409
68. Song, W.; Ackermann, L. *Angew. Chem., Int. Ed.* **2012,** *51,* 8251–8254. doi:10.1002/anie.201202466
69. Sarkar, S. D.; Liu, W.; Kozhushkov, S. I.; Ackermann, L. *Adv. Synth. Catal.* **2014,** *356,* 1461–1479. doi:10.1002/adsc.201400110
70. Cheng, H.; Hernández, J. G.; Bolm, C. *Adv. Synth. Catal.* **2018,** *360,* 1800–1804. doi:10.1002/adsc.201800161
71. Wang, S.-B.; Gu, Q.; You, S.-L. *J. Catal.* **2018,** *361,* 393–397. doi:10.1016/j.jcat.2018.03.007
72. Cai, Z.-J.; Liu, C.-X.; Gu, Q.; You, S.-L. *Angew. Chem., Int. Ed.* **2018,** *57,* 1296–1299. doi:10.1002/anie.201711451
73. Xu, J.; Liu, Y.; Zhang, J.; Xu, X.; Jin, Z. *Chem. Commun.* **2018,** *54,* 689–692. doi:10.1039/C7CC09273C
74. Gao, D.-W.; Gu, Q.; Zheng, C.; You, S.-L. *Acc. Chem. Res.* **2017,** *50,* 351–365. doi:10.1021/acs.accounts.6b00573
75. Schmiel, D.; Butenschön, H. *Eur. J. Org. Chem.* **2017,** 3041–3048. doi:10.1002/ejoc.201700358
76. Schmiel, D.; Butenschön, H. *Organometallics* **2017,** *36,* 4979–4989. doi:10.1021/acs.organomet.7b00799

77. Wang, S.-B.; Gu, Q.; You, S.-L. *J. Org. Chem.* **2017,** *82,* 11829–11835. doi:10.1021/acs.joc.7b00775
78. Wang, S.-B.; Gu, Q.; You, S.-L. *Organometallics* **2017,** *36,* 4359–4362. doi:10.1021/acs.organomet.7b00691
79. Cera, G.; Haven, T.; Ackermann, L. *Angew. Chem., Int. Ed.* **2016,** *55,* 1484–1488. doi:10.1002/anie.201509603
80. Gao, D.-W.; Gu, Q.; You, S.-L. *J. Am. Chem. Soc.* **2016,** *138,* 2544–2547. doi:10.1021/jacs.6b00127
81. Shibata, T.; Uno, N.; Sasaki, T.; Kanyiva, K. S. *J. Org. Chem.* **2016,** *81,* 6266–6272. doi:10.1021/acs.joc.6b00825
82. Urbano, A.; Hernández-Torres, G.; del Hoyo, A. M.; Martínez-Carrión, A.; Carmen Carreño, M. *Chem. Commun.* **2016,** *52,* 6419–6422. doi:10.1039/C6CC02624A
83. Wang, S.-B.; Zheng, J.; You, S.-L. *Organometallics* **2016,** *35,* 1420–1425. doi:10.1021/acs.organomet.6b00020
84. Zhu, D.-Y.; Chen, P.; Xia, J.-B. *ChemCatChem* **2016,** *8,* 68–73. doi:10.1002/cctc.201500895
85. Arae, S.; Ogasawara, M. *Tetrahedron Lett.* **2015,** *56,* 1751–1761. doi:10.1016/j.tetlet.2015.01.130
86. López, L. A.; López, E. *Dalton Trans.* **2015,** *44,* 10128–10135. doi:10.1039/C5DT01373A
87. Deng, R.; Huang, Y.; Ma, X.; Li, G.; Zhu, R.; Wang, B.; Kang, Y.-B.; Gu, Z. *J. Am. Chem. Soc.* **2014,** *136,* 4472–4475. doi:10.1021/ja500699x
88. Gao, D.-W.; Yin, Q.; Gu, Q.; You, S.-L. *J. Am. Chem. Soc.* **2014,** *136,* 4841–4844. doi:10.1021/ja500444v
89. Liu, L.; Zhang, A.-A.; Zhao, R.-J.; Li, F.; Meng, T.-J.; Ishida, N.; Murakami, M.; Zhao, W.-X. *Org. Lett.* **2014,** *16,* 5336–5338. doi:10.1021/ol502520b
90. Pi, C.; Cui, X.; Liu, X.; Guo, M.; Zhang, H.; Wu, Y. *Org. Lett.* **2014,** *16,* 5164–5167. doi:10.1021/ol502509f
91. Shibata, T.; Shizuno, T. *Angew. Chem., Int. Ed.* **2014,** *53,* 5410–5413. doi:10.1002/anie.201402518
92. Xie, W.; Li, B.; Xu, S.; Song, H.; Wang, B. *Organometallics* **2014,** *33,* 2138–2141. doi:10.1021/om5002606
93. Kornhaaß, C.; Kuper, C.; Ackermann, L. *Adv. Synth. Catal.* **2014,** *356,* 1619–1624. doi:10.1002/adsc.201301156
94. Arrayás, R. G.; Adrio, J.; Carretero, J. C. *Angew. Chem., Int. Ed.* **2006,** *45,* 7674–7715. doi:10.1002/anie.200602482
95. Fu, G. C. *Acc. Chem. Res.* **2004,** *37,* 542–547. doi:10.1021/ar030051b
96. Dai, L.-X.; Tu, T.; You, S.-L.; Deng, W.-P.; Hou, X.-L. *Acc. Chem. Res.* **2003,** *36,* 659–667. doi:10.1021/ar020153m
97. Fu, G. C. *Acc. Chem. Res.* **2000,** *33,* 412–420. doi:10.1021/ar990077w
98. Temnikov, M. N.; Anisimov, A. A.; Zhemchugov, P. V.; Kholodkov, D. N.; Goloveshkin, A. S.; Naumkin, A. V.; Chistovalov, S. M.; Katsoulis, D.; Muzafarov, A. M. *Green Chem.* **2018,** *20,* 1962–1969. doi:10.1039/C7GC03862C
99. Hermann, G. N.; Bolm, C. *ACS Catal.* **2017,** *7,* 4592–4596. doi:10.1021/acscatal.7b00582
100. Cheng, H.; Hernández, J. G.; Bolm, C. *Org. Lett.* **2017,** *19,* 6284–6287. doi:10.1021/acs.orglett.7b02973
101. Ackermann, L. *Acc. Chem. Res.* **2014,** *47,* 281–295. doi:10.1021/ar3002798
102. Ackermann, L. *Chem. Rev.* **2011,** *111,* 1315–1345. doi:10.1021/cr100412j
103. Lapointe, D.; Fagnou, K. *Chem. Lett.* **2010,** *39,* 1118–1126. doi:10.1246/cl.2010.1118
104. Ackermann, L.; Novák, P.; Vicente, R.; Hofmann, N. *Angew. Chem., Int. Ed.* **2009,** *48,* 6045–6048. doi:10.1002/anie.200902458
105. Ma, W.; Mei, R.; Tenti, G.; Ackermann, L. *Chem. – Eur. J.* **2014,** *20,* 15248–15251. doi:10.1002/chem.201404604
106. Hernández, J. G. *Chem. – Eur. J.* **2017,** *23,* 17157–17165. doi:10.1002/chem.201703605

License and Terms

BEILSTEIN JOURNAL OF ORGANIC CHEMISTRY

Cationic cobalt-catalyzed [1,3]-rearrangement of *N*-alkoxycarbonyloxyanilines

Itaru Nakamura*[1], Mao Owada[2], Takeru Jo[2] and Masahiro Terada[1,2]

Full Research Paper

Open Access

Address:
[1]Research and Analytical Center for Giant Molecule, Graduate School of Science, Tohoku University, 6-3 Aramaki Aza Aoba, Aoba-ku, Sendai 980-8578 Japan and [2]Department of Chemistry, Graduate School of Science, Tohoku University, 6-3 Aramaki Aza Aoba, Aoba-ku, Sendai 980-8578 Japan

Email:
Itaru Nakamura* - itaru-n@tohoku.ac.jp

* Corresponding author

Keywords:
anilines; cobalt catalyst; concerted reaction; N–O bond; rearrangement

Beilstein J. Org. Chem. **2018,** *14,* 1972–1979.
doi:10.3762/bjoc.14.172

Received: 15 May 2018
Accepted: 17 July 2018
Published: 31 July 2018

This article is part of the thematic issue "Cobalt catalysis".

Guest Editor: S. Matsunaga

Abstract

A cationic cobalt catalyst efficiently promoted the reaction of *N*-alkoxycarbonyloxyanilines at 30 °C, affording the corresponding *ortho*-aminophenols in good to high yields. As reported previously, our mechanistic studies including oxygen-18 labelling experiments indicate that the rearrangement of the alkoxycarbonyloxy group proceeds in [1,3]-manner. In this article, we discuss the overall picture of the cobalt-catalysed [1,3]-rearrangement reaction including details of the reaction conditions and substrate scope.

Introduction

The 2-aminophenol moiety is ubiquitously found as a core structure of biologically active compounds, such as tigecycline [1], iguratimod [2], and phosalone (Scheme 1) [3]. The scaffolds have also been frequently utilized as synthetic intermediates not only in pharmaceutical chemistry but also in materials science. Thus, it is of great importance to efficiently synthesize functionalized 2-aminophenols under mild reaction conditions in a regioselective manner. Among numerous methods, the [3,3]-rearrangement of *O*-acyl-*N*-arylhydroxylamines **1** driven by cleavage of the N–O bond is an ideal approach to selectively synthesize *O*-protected 2-aminophenols **2** while maintaining the oxidation state during the transformation (Scheme 2a) [4-11]. However, there is a significant drawback, these [3,3]-rearrangements of carboxylic acyloxy and alkoxylcarbonyloxy groups generally require long heating times at elevated reaction temperatures (>140 °C) or microwave irradiation (Scheme 2a). In contrast, *N*-sulfonyloxyanilines are known to readily undergo the [3,3]-rearrangement during the preparation of the starting material below −20 °C due to the strongly electron-withdrawing nature of the sulfonyl group (Scheme 2b) [12]. Accordingly, we envisioned that appropriate Lewis acidic metal catalysts would promote the rearrangement reaction of stable

N-acyloxyanilines to afford readily deprotectable 2-acyloxyanilines under much milder reaction conditions with high functional group tolerance. Based on this concept, we disclosed that cationic cobalt catalysts efficiently promote the reaction of O-alkoxylcarbonyl-*N*-arylhydroxylamines **1** at 30 °C, affording the corresponding 2-aminophenol derivatives **2** in good to high yields [13]. Our mechanistic studies revealed that the rearrangement of the alkoxycarbonyloxy group proceeded in an unprecedented [1,3]-manner (Scheme 2c). In this article, we describe the overall picture of the intriguing [1,3]-rearrangement reaction, particularly the detail of the reaction, which were not sufficiently discussed in our preliminary communication.

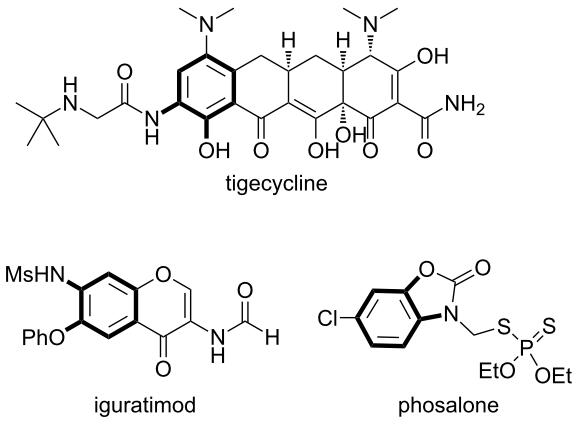

Scheme 1: *ortho*-Aminophenol derivatives.

Results and Discussion

At the beginning of this investigation, *N,O*-di(methoxycarbonyl)hydroxylaniline (**1a**) was treated with catalytic amounts of several copper salts in 1,2-dichloroethane (DCE) at 60 °C (Table 1, entries 1–7), according to our previous copper-catalysed cascade reaction involving rearrangement via N–O bond cleavage [14]. While divalent copper acetate and copper chloride did not show any catalytic activities (Table 1, entries 1 and 2), more Lewis acidic copper complexes, such as $[Cu(MeCN)_4](PF_6)_2$ and $[Cu(OTf)]_2$·toluene, afforded the corresponding 2-aminophenol derivative **2a** (Table 1, entries 3 and 4). Moreover, a cationic copper catalyst generated from $CuCl_2$ and two equivalents of $AgSbF_6$ was effective to afford **2a** in good yield (Table 1, entry 5), even at 30 °C (Table 1, entry 8). The use of a ligand, such as 1,10-phenanthroline (phen) and 1,3-bis(diphenylphosphino)propane (dppp), totally diminished the activity of cationic cobalt catalyst (Table 1, entries 6 and 7). Among metal chlorides examined, $CoCl_2$ exhibited the best catalytic activity at 30 °C, affording the corresponding **2a** in 68% yield (Table 1, entry 9), as reported previously [13]. A divalent cationic zinc catalyst also promoted the present reaction, albeit with lower chemical yield than Co(II) (Table 1, entries 10 and 11), while the use of Fe(II) and Pd(II) resulted in low chemical yield due to the formation of the *para*-isomer **3a** (Table 1, entries 12 and 13). Indeed the *para*-isomer **3a** was obtained as a major product when the reaction of **1a** was conducted using trivalent metal salts, such as $FeCl_3$ and $RuCl_3$, and tetravalent salts, such as $ZrCl_4$, as a catalyst (Table 1, entries 15–18). Although we quite recently disclosed that cationic NHC-copper

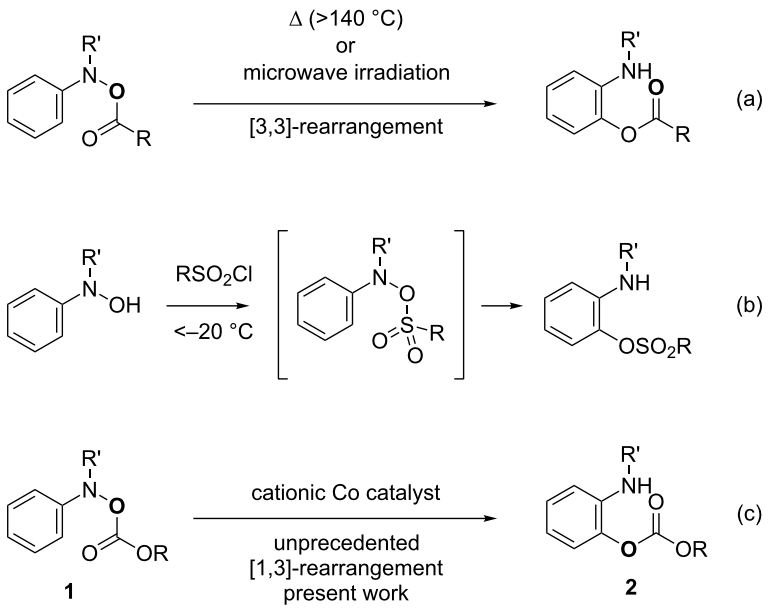

Scheme 2: Rearrangement of *N*-acyloxyanilines.

Table 1: Catalytic activity.

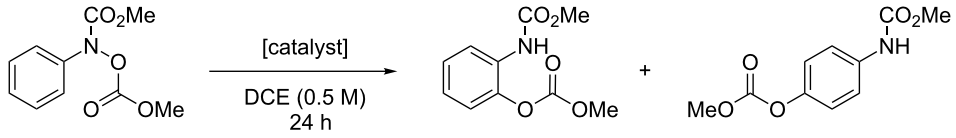

1a **2a** **3a**

entry	catalyst (mol %)	temp. (°C)	**2a** (%)[a]	**3a** (%)[a]	**1a** (%)[a]
1	$CuCl_2$ (10)	60	<1	<1	>99
2	$Cu(OAc)_2$ (10)	60	<1	<1	>99
3	$[Cu(MeCN)_4](PF_6)$ (10)	60	5	<1	75
4	$[Cu(OTf)]_2{\cdot}C_6H_5CH_3$ (10)	60	50	4	23
5	$CuCl_2$ (10), $AgSbF_6$ (20)	60	52	<1	14
6	$CuCl_2$ (10), $AgSbF_6$ (20), phen (20)	60	<1	<1	>99
7	$CuCl_2$ (10), $AgSbF_6$ (20), dppp (20)	60	<1	<1	80
8[b]	$CuCl_2$ (10), $AgSbF_6$ (20)	30	57	10	<1
9[b]	$CoCl_2$ (10), $AgSbF_6$ (20)	30	63 (68)	<3	<1
10[b]	$ZnCl_2$ (10), $AgSbF_6$ (20)	30	54	8	<1
11	$ZnCl_2$ (10), $AgSbF_6$ (10)	30	54	8	1
12[b]	$PdCl_2$ (10), $AgSbF_6$ (20)	30	24	7	<1
13[b]	$FeCl_2$ (10), $AgSbF_6$ (20)	30	32	21	1
14[b]	$FeCl_3$ (10), $AgSbF_6$ (30)	30	22	26	<1
15[b]	$RuCl_3$ (10), $AgSbF_6$ (30)	30	18	35	<1
16	$RuCl_3$ (10), $AgSbF_6$ (20)	30	21	35	<1
17	$IrCl_3$ (10), $AgSbF_6$ (30)	30	15	37	<1
18	$ZrCl_4$ (10), $AgSbF_6$ (40)	30	16	28	<1
19	IPrCuBr (10), $AgSbF_6$ (10)	30	<1	<1	12
20	$AgSbF_6$ (10)	60	53	17	7
21[b]	$AgSbF_6$ (10)	30	<3	<3	80
22[b]	$CoCl_2$ (10)	30	<1	<1	90
23	TfOH (10)	30	5	6	74
24	$(PhO)_2P(O)OH$	30	<1	<1	90
25[b]	$CoCl_2$ (10), $AgNTf_2$ (20)	30	50	1	3
26[b]	$CoCl_2$ (10), $AgPF_6$ (20)	30	<1	<1	98
27[b]	$CoCl_2$ (10), AgOTf (20)	30	<1	<1	97
28	$CoCl_2$ (10), $AgSbF_6$ (10)	30	53	3	<1
29	$CoCl_2$ (5), $AgSbF_6$ (10)	30	59	2	<1

[a]Yields were determined by ^1H NMR using CH_2Br_2 as an internal standard. Isolated yield in parenthesis. [b]Reported in the Supporting Information of our previous paper [13], except for yields of recovered **1a**.

catalysts efficiently promoted the [1,3]-alkoxy rearrangement of *N*-alkoxyaniline [15], the cationic NHC-Cu catalyst generated from IPrCuBr and $AgSbF_6$ was totally inefficient for the present reaction; **1a** was decomposed under the reaction conditions (Table 1, entry 19). Whereas $AgSbF_6$ promoted the reaction at 60 °C (Table 1, entry 20), the catalytic activity was diminished at 30 °C (Table 1, entry 21). Neutral $CoCl_2$ did not promote the present reaction (Table 1, entry 22). Brønsted acids, such as trifluoromethanesulfonic acid and diphenylphosphoric acid, were much less active (Table 1, entries 23 and 24). The kind of the counteranion significantly affected the reaction efficiency; hexafluoroantimonate and bis(trifluoromethanesulfonyl)imidate were efficient (Table 1, entries 9 and 25), while the use of hexafluorophosphate and trifluoromethanesulfonate did not promote the reaction at all (Table 1, entries 26 and 27). The use of an equal amount of $AgSbF_6$ to $CoCl_2$ resulted in slightly decreasing the chemical yield (Table 1, entry 28).

Next solvent and concentration effects were examined as summarized in Table 2. 1,2-Dichloroethane (DCE) gave the best result (Table 2, entry 1), as described previously [13]. Other halogen solvents, such as $CHCl_3$, CH_2Cl_2, and PhCl, ethereal

Table 2: Solvent and concentration effects.

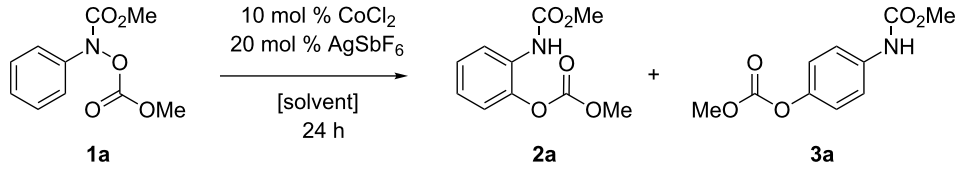

1a **2a** **3a**

entry	solvent	concentration (M)	**2a** (%)[a]	**3a** (%)[a]	**1a** (%)[a]
1[b]	DCE	0.5	63	3	<1
2[b]	$CHCl_3$	0.5	49	7	19
3[b]	CH_2Cl_2	0.5	40	2	<1
4[b]	PhCl	0.5	39	2	25
5[b]	toluene	0.5	43	1	11
6[b]	Et_2O	0.5	38	<1	1
7	MTBE	0.5	49	1	4
8	THF	0.5	<1	<1	>99
9	CH_3CN	0.5	<1	<1	98
10	DMF	0.5	<1	<1	>99
11	MeOH	0.5	4	<1	81
12	DCE	1.0	51	2	<1
13[b]	**DCE**	**0.25**	**72**	**3**	**<1**
14[b,c]	DCE	0.05	53	9	11

[a]Yields were determined by ^{1}H NMR using CH_2Br_2 as an internal standard. [b]Reported in the Supporting Information of our previous paper (ref. [13]), except for yields of recovered **1a**. [c]For 5 days.

solvent, such as Et_2O and *tert*-butyl methyl ether (MTBE), and toluene were less efficient (Table 2, entries 2–7), while the use of polar solvents, such as tetrahydrofuran (THF), acetonitrile, and *N*,*N*-dimethylformamide (DMF), resulted in quantitative recovery of the starting material **1a** (Table 2, entries 8–10). A protic solvent, such as methanol, was ineffective (Table 2, entry 11). Slight dilution of the reaction solution (0.25 M) improved the chemical yield (Table 2, entry 12).

As mentioned previously [13], carbamate-type groups, such as methoxycarbonyl, Alloc and Cbz were tolerated as a protective group on the nitrogen atom, affording the desired products **2** in good yields (Table 3, entries 1–3). The reaction of **1e** having a 2,2,2-trichloroethoxycarbonyl (Troc) group, however, resulted in decomposing **1e** (Table 3, entry 4). The use of aroyl groups gave the desired product in good yields (Table 3, entries 5–7), while the acetyl group required a prolonged reaction time (Table 3, entry 8). Substrate **1j** having a tosyl group on the nitrogen resulted in decomposition of **1j** (Table 3, entry 9). The alkoxycarbonyl groups, such as Cbz, methoxycarbonyl, and 2-chloroethoxy groups, were employed as good migrating groups (Table 3, entries 7–11), while **1m** having a Boc group on the oxygen atom did not give the desired product, due to decomposition of **1m** (Table 3, entry 12). It is noteworthy that the substrate having a highly electron-withdrawing Troc group on the oxygen atom was readily isomerized to the *ortho*-aminophenol derivative under its preparing conditions in the absence of the cationic cobalt catalyst. In sharp contrast to alkoxycarbonyloxy groups, acyloxy groups, such as the benzoyloxy group, were not migrated to the *ortho*-position, resulting in decomposing the starting material (Table 3, entry 13), as mentioned previously [13].

The reaction was applied to **1o–ab** having various substituents at the *para*-position, as summarized in Table 4. As reported previously [13], reactive functional groups, such as bromo, iodo, and alkynyl groups were tolerated, affording the desired products in good to high yields (Table 4, entries 5–7). The substrate **1v** having a methoxycarbonyl group afforded **2v** in good yield, while cyano and acetyl groups interrupted the present reaction presumably due to deactivation of the catalyst, recovering the starting materials quantitatively (Table 4, entries 9 and 10). Notably, our catalytic conditions successfully promoted the rearrangement of **1y'**, having a highly electron-deficient *p*-triflurometylphenyl group, which have not been employed in the thermal [3,3]-rearrangement reaction, when using a *p*-nitrobenzyloxycarbonyl group in place of Cbz as the migrating group (Table 4, entry 11). In addition, compatibility of the protective group on the oxygen atom was tested (Table 4, entries 12–14), since it is expected that the cationic cobalt

Table 3: Substituent effect at the hydroxylamine moiety.[a]

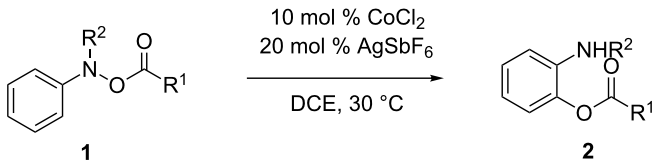

1 **2**

entry	**1**	R^1	R^2	time (h)	**2**	yield (%)[b]
1[c]	**1b**	OMe	Cbz	5	**2b**	64
2[c]	**1c**	OMe	Alloc	4	**2c**	45
3[c]	**1d**	OMe	Boc	6	**2d**	64
4	**1e**	OMe	Troc	18	–	<1
5[c]	**1f**	OMe	*p*-$MeOC_6H_4C(O)$	2	**2f**	60[d]
6[c]	**1g**	OMe	Bz	3	**2g**	75
7[c]	**1h**	OMe	*p*-$F_3CC_6H_4C(O)$	24	**2h**	61
8[c]	**1i**	OMe	Ac	120	**2i**	44
9	**1j**	OMe	Ts	11	–	<1
10[c]	**1k**	OBn	Bz	2	**2k**	82
11	**1l**	O-CH_2CH_2Cl	Bz	2	**2l**	56
12	**1m**	O-*t*Bu	Bz	10	–	<1
13[c]	**1n**	Ph	Bz	120	–	<1

[a]The reactions of **1** (0.4 mmol) were conducted in the presence of 10 mol % $CoCl_2$ and 20 mol % of $AgSbF_6$ in DCE (1.6 mL) at 30 °C. [b]Isolated yield. [c]Previously reported in [13]. [d]^{1}H NMR yield using dibromomethane as an internal standard.

Table 4: Co-catalyzed reaction of *N*-alkoxycarbonyloxyanilines **1o–ab**.[a]

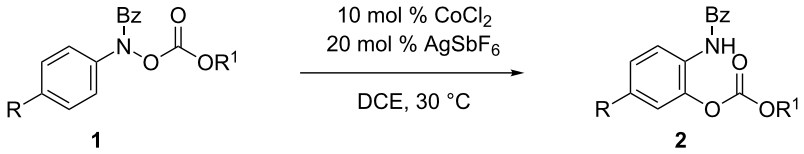

1 **2**

entry	**1**	R	R^1	time (h)	**2**	yield (%)[b]
1[c]	**1o**	Me	Bn	3	**2o**	74
2[c]	**1p**	F	Bn	11	**2p**	66[d]
3[c]	**1q**	Cl	Bn	1	**2q**	88
4[c]	**1r**	Cl	Me	3	**2r**	79
5[c]	**1s**	Br	Bn	1	**2s**	86
6[c]	**1t**	I	Bn	1	**2t**	77
7[c]	**1u**	TMSC≡C	Bn	2	**2u**	62
8[c]	**1v**	CO_2Me	Bn	15	**2v**	84[d]
9	**1w**	Ac	Bn	>120	–	<1[e]
10	**1x**	CN	Bn	>120	–	<1[e]
11[c]	**1y'**	CF_3	*p*-$O_2NC_6H_4CH_2$	48	**2y'**	76[d,f]
12	**1z**	$BzO(CH_2)_2$	Bn	72	**2z**	50[d,g]
13	**1aa**	$TBSO(CH_2)_2$	Bn	14	**2aa**	64
14	**1ab**	$MOM(CH_2)_2$	Bn	14	**2ab**	59

[a]The reactions of **1** (0.4 mmol) were conducted in the presence of 10 mol % $CoCl_2$ and 20 mol % of $AgSbF_6$ in DCE (1.6 mL) at 30 °C. [b]Isolated yield. [c]Previously reported in [13]. [d]^{1}H NMR yield using dibromomethane as an internal standard. See Supporting Information File 1 for details. [e]The starting material was quantitatively recovered. [f]Yield brsm (28% of **1y'** was recovered). [g]Isolation of **2z** was unsuccessful due to contamination by inseparable byproducts (see Supporting Information File 1).

would make the protective group labile as well as the protective group would deactivate the cationic cobalt catalyst. As results, *tert*-butyldimethylsilyl (TBS) and methoxymethyl (MOM) groups were tolerated under the cationic cobalt-catalyzed reaction conditions to afford the desired product in good yields (Table 4, entries 13 and 14). The reaction using a benzoyl group was sluggish, affording the desired product **2z** in moderate yield with formation of inseparable byproducts (Table 4, entry 12). Thus, the use of silyl- and acetal-type protective groups is suitable for the present reaction.

As reported previously [13], the fact that the present rearrangement reaction proceeds in a [1,3]-manner was confirmed by a crossover experiment and oxygen-18 labeling experiments. That is, the reaction of a 1:1 mixture of equally-reactive substrates **1h** and **1r** under the standard reaction conditions afforded only the products **2h** and **2r** derived from the starting materials (Scheme 3a). Thus, we confirmed that the present reaction proceeds in an intramolecular manner. Next, 18-oxygen-labelling experiments were conducted using substrate **1h**-^{18}O, of which the oxygen-18 content at the hydroxylamine oxygen atom was 62% [16,17]. The reaction of **1h**-^{18}O in the presence of the cationic cobalt catalyst at 30 °C followed by hydrogenative cleavage of the Cbz group afforded the phenol **4h**-^{18}O, of which the oxygen-18 content was 64% (Scheme 3b). The result clearly indicates that the rearrangement of the CbzO group in the presence of cationic cobalt catalysts proceeds in a concerted [1,3]-manner [18-24]. In addition, the reaction of **1h**-^{18}O (23% ^{18}O) in the absence of the cationic cobalt catalyst at 140 °C followed by hydrogenative deprotection afforded **4h**, of which the oxygen-18 content was less than 2% (Scheme 3c). Therefore, we concluded that the cationic cobalt catalyst not only made the reaction much milder than the thermally-induced reaction but also changed the rearrangement mode to an unprecedented [1,3]-manner. In addition, intermolecular and intramolecular competitive experiments using deuterium-labelled substrates resulted in no kinetic effect (Scheme 4). These results suggest that the C–O bond would form prior to cleavage of the C–H bond in the [1,3]-rearrangement reaction.

Due to the fact that the reaction of **1a** in the presence of tri- and tetravalent cationic metal catalysts afforded the *para*-isomer **3a** as a major product (Table 1, entries 14–18), the reaction of *ortho*-aminophenol derivative **2a** in the presence of catalytic amounts of $RuCl_3$ and $AgSbF_6$ was conducted. However, the *para*-isomer **3a** was not afforded; 73% of **2a** was recovered

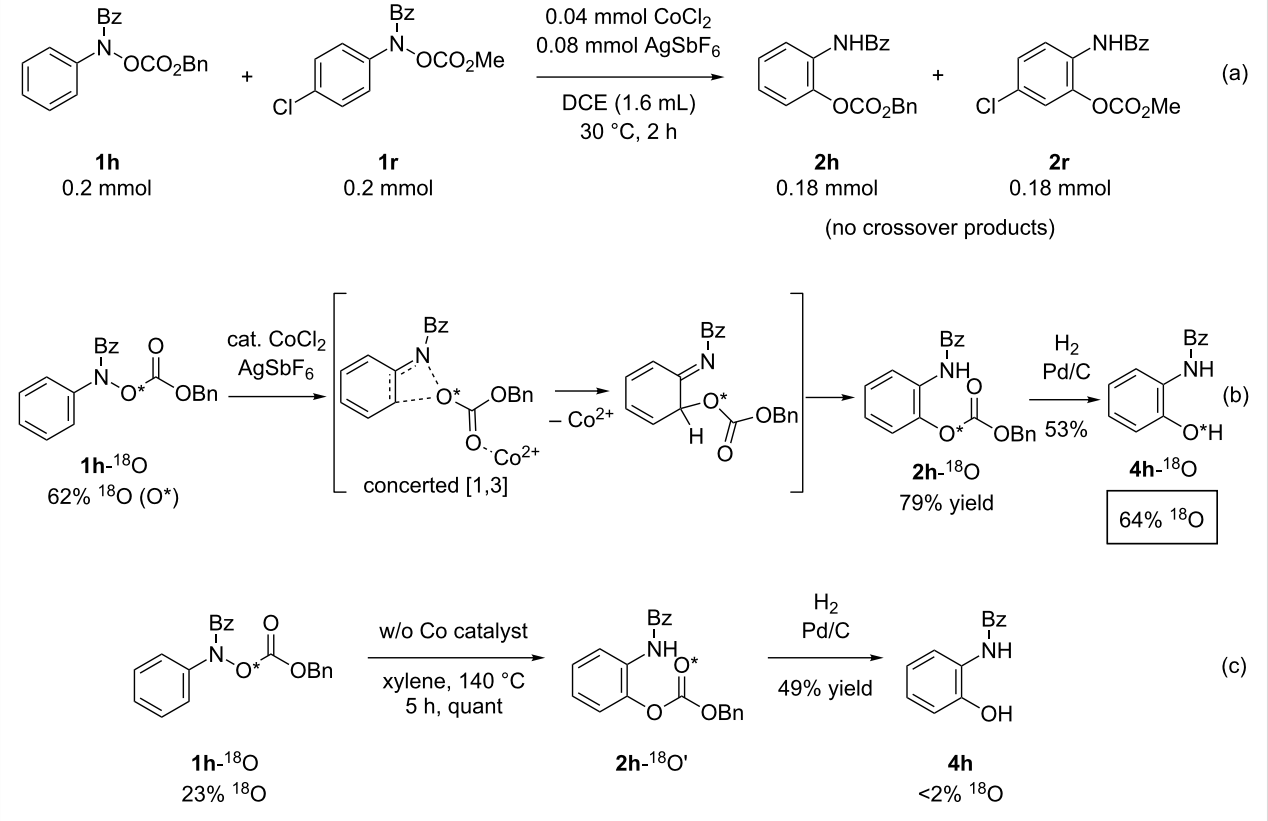

Scheme 3: Mechanistic studies, reported in [13].

(Scheme 5a). The result indicates that the *para*-isomer **3a** was not formed through the *ortho*-isomer **2a**. It is assumed that **3a** was furnished through direct C–O bond formation at the *para*-position through ionic cleavage of the N–O bond by cationic Ru(III) as a much stronger Lewis acid, while it is also possible that the second migration of the alkoxycarbonyloxy group from *ortho* to *para* occurs prior to proton transfer (Scheme 5b) [25]. Further mechanistic studies are underway in our laboratory.

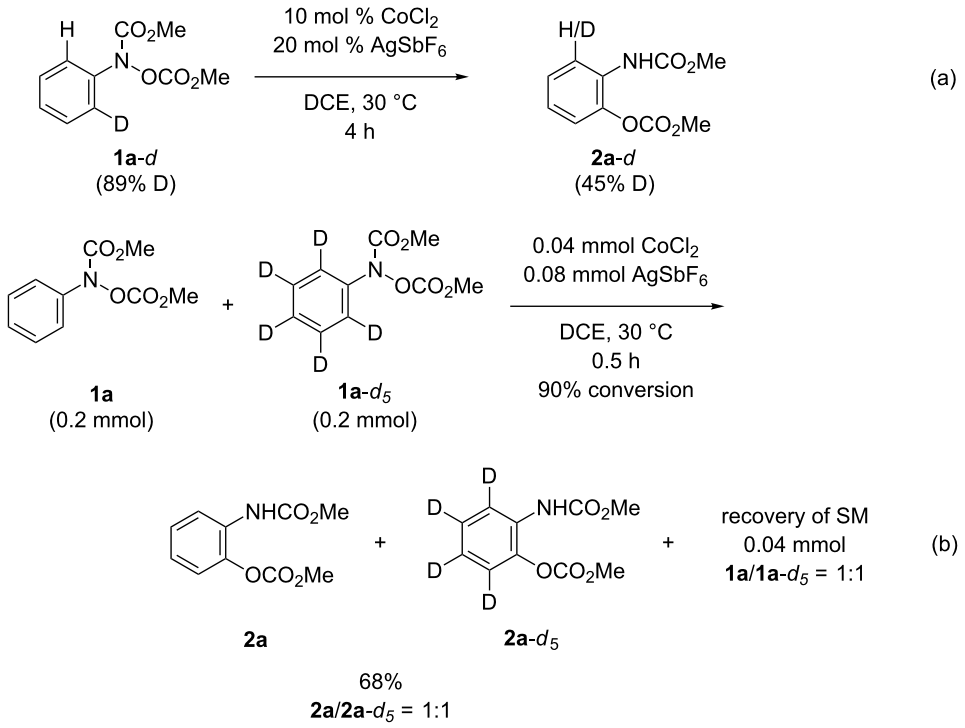

Scheme 4: Competitive experiments, reported in [13].

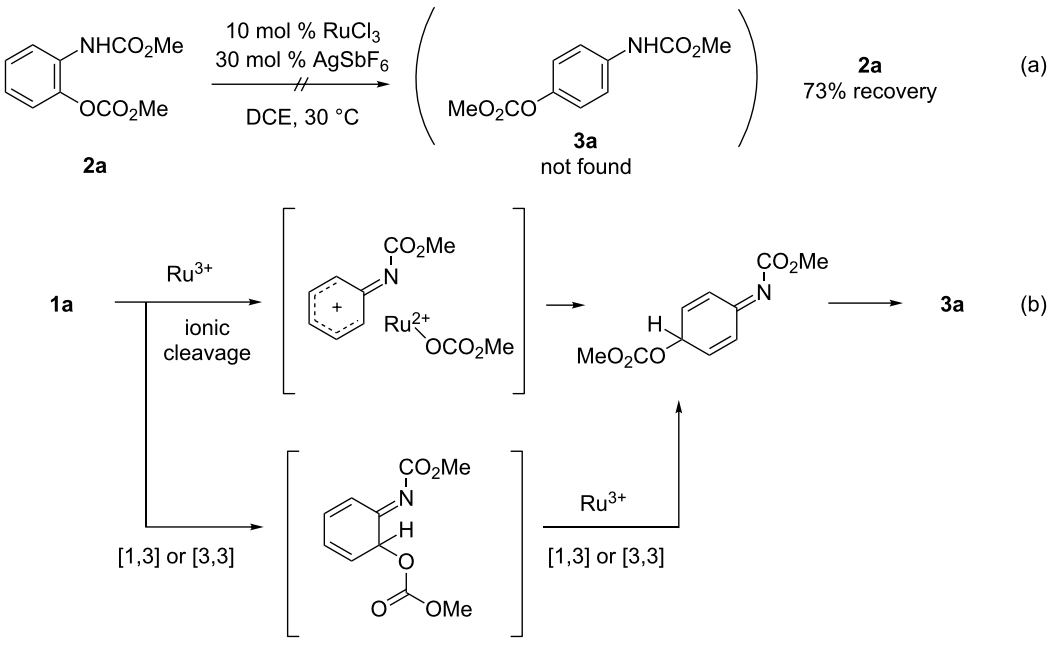

Scheme 5: Mechanism for rearrangement to the *para*-position.

Conclusion

The cationic cobalt catalysts enabled the rearrangement reaction of *N*-alkoxycarbonyloxyanilines to proceed under much milder reaction conditions, expanding the substrate scope to more electron-deficient anilines. More importantly, the cobalt catalyst changes the mode of the rearrangement to an unprecedented [1,3]-manner.

Experimental

To a mixture of **1k** (138.9 mg, 0.4 mmol), $CoCl_2$ (5.2 mg, 0.04 mmol), and $AgSbF_6$ (27.5 mg, 0.08 mmol) under an argon atmosphere in a pressure vial was added 1,2-dichloroethane (1.6 mL). Then, the mixture was stirred at 30 °C for 2 hours. After complete consumption of the starting material **1k**, the mixture was passed through a small pad of silica gel with ethyl acetate. After removing the solvents in vacuo, the residue was purified by flash silica gel column chromatography using hexane/ethyl acetate (3:1) as eluent to obtain **2k** (113.9 mg, 82%).

Supporting Information

Supporting Information File 1

General procedure and analytic data for obtained products.
[https://www.beilstein-journals.org/bjoc/content/supplementary/1860-5397-14-172-S1.pdf]

Acknowledgements

This work was supported by JSPS KAKENHI Grant Number JP16H00996 in Precisely Designed Catalysts with Customized Scaffolding.

ORCID® iDs

Itaru Nakamura - https://orcid.org/0000-0002-1452-5989
Masahiro Terada - https://orcid.org/0000-0002-0554-8652

References

1. Sum, P.-E.; Peterson, P. *Bioorg. Med. Chem. Lett.* **1999,** *9,* 1459. doi:10.1016/S0960-894X(99)00216-4
2. Aikawa, Y.; Yamamoto, M.; Yamamoto, T.; Morimoto, K.; Tanaka, K. *Inflammation Res.* **2002,** *51,* 188. doi:10.1007/PL00000291
3. Ahmad, R.; Kookana, R. S.; Alsoton, A. M.; Skjemstad, J. O. *Environ. Sci. Technol.* **2001,** *35,* 878. doi:10.1021/es001446i
4. Leffler, J. E.; Bradford Bond, W. *J. Am. Chem. Soc.* **1956,** *78,* 335. doi:10.1021/ja01583a023
5. Denney, D. B.; Denney, D. Z. *J. Am. Chem. Soc.* **1960,** *82,* 1389. doi:10.1021/ja01491a026
6. Oae, S.; Sakurai, T.; Kimura, H.; Kozuka, S. *Chem. Lett.* **1974,** *3,* 671. doi:10.1246/cl.1974.671
7. Oae, S.; Sakurai, T. *Tetrahedron* **1976,** *32,* 2289. doi:10.1016/0040-4020(76)88003-9
8. Ohta, T.; Shudo, K.; Okamoto, T. *Tetrahedron Lett.* **1978,** *19,* 1983. doi:10.1016/S0040-4039(01)94727-6
9. Porzelle, A.; Woodrow, M. D.; Tomkinson, N. C. O. *Eur. J. Org. Chem.* **2008,** 5135. doi:10.1002/ejoc.200800672
10. Porzelle, A.; Woodrow, M. D.; Tomkinson, N. C. O. *Org. Lett.* **2010,** *12,* 812. doi:10.1021/ol902885j
11. Tabolin, A. A.; Ioffe, S. L. *Chem. Rev.* **2014,** *114,* 5426. doi:10.1021/cr400196x
12. Gutschke, D.; Heesing, A.; Heuschkel, U. *Tetrahedron Lett.* **1979,** *20,* 1363–1364. doi:10.1016/S0040-4039(01)86151-7
13. Nakamura, I.; Owada, M.; Jo, T.; Terada, M. *Org. Lett.* **2017,** *19,* 2194. doi:10.1021/acs.orglett.7b00700
14. Nakamura, I.; Kudo, Y.; Terada, M. *Angew. Chem., Int. Ed.* **2013,** *52,* 7536. doi:10.1002/anie.201302751
15. Nakamura, I.; Jo, T.; Ishida, Y.; Tashiro, H.; Terada, M. *Org. Lett.* **2017,** *19,* 3059. doi:10.1021/acs.orglett.7b01110
16. The percentage of oxygen-18 content was determined by intensity of the mass spectrum.
17. Rajendran, G.; Santini, R. E.; Van Etten, R. L. *J. Am. Chem. Soc.* **1987,** *109,* 4357. doi:10.1021/ja00248a037
18. Oae, S.; Kitao, T.; Kitaoka, Y. *Tetrahedron* **1963,** *19,* 827. doi:10.1016/S0040-4020(01)99334-2
19. Nasveschuk, C. G.; Rovis, T. *Org. Biomol. Chem.* **2008,** *6,* 240. doi:10.1039/B714881J
20. Hou, S.; Li, X.; Xu, J. *J. Org. Chem.* **2012,** *77,* 10856. doi:10.1021/jo302210t
21. Wada, N.; Kaneko, K.; Ukaji, Y.; Inomata, K. *Chem. Lett.* **2011,** *40,* 440. doi:10.1246/cl.2011.440
22. Xu, J. *Curr. Org. Synth.* **2017,** *14,* 511. doi:10.2174/1570179413666161021103952
23. Hou, S.; Li, X.; Xu, J. *Org. Biomol. Chem.* **2014,** *12,* 4952. doi:10.1039/C4OB00080C
24. Yang, Z.; Hou, S.; He, W.; Cheng, B.; Jiao, P.; Xu, J. *Tetrahedron* **2016,** *72,* 2186. doi:10.1016/j.tet.2016.03.019
25. The reaction of a mixture of **1a** and **1h** in the presence of $RuCl_3$ (10 mol %) and $AgSbF_6$ (30 mol %) gave only the products **2a** and **2h** derived from the starting materials; crossover products were not detected (<3%) by HRMS. This result indicates that the rearrangement to the *para*-position proceeds in an intramolecular manner.

License and Terms

BEILSTEIN JOURNAL OF ORGANIC CHEMISTRY

Cobalt-catalyzed nucleophilic addition of the allylic C(sp^3)–H bond of simple alkenes to ketones

Tsuyoshi Mita*, Masashi Uchiyama, Kenichi Michigami and Yoshihiro Sato*

Letter

Open Access

Address:
Faculty of Pharmaceutical Sciences, Hokkaido University, Sapporo 060-0812, Japan

Email:
Tsuyoshi Mita* - tmita@pharm.hokudai.ac.jp; Yoshihiro Sato* - biyo@pharm.hokudai.ac.jp

* Corresponding author

Keywords:
alkenes; C–H activation; C(sp^3)–H bonds; cobalt; ketones

Beilstein J. Org. Chem. **2018,** *14,* 2012–2017.
doi:10.3762/bjoc.14.176

Received: 14 May 2018
Accepted: 18 July 2018
Published: 02 August 2018

This article is part of the thematic issue "Cobalt catalysis".

Guest Editor: S. Matsunaga

Abstract

We herein describe a cobalt/Xantphos-catalyzed regioselective addition of simple alkenes to acetophenone derivatives, affording branched homoallylic alcohols in high yields with perfect branch selectivities. The intermediate of the reaction would be a nucleophilic allylcobalt(I) species generated via cleavage of the low reactive allylic C(sp^3)–H bond of simple terminal alkenes.

Introduction

The cleavage of C–H bonds of unreactive hydrocarbon followed by functionalization should be an ideal method for constructing complex molecules without introduction of reactive functionality in advance [1-9]. Since terminal alkenes including α-olefins (C_xH_{2x}) are abundantly present in nature or are readily accessible, they should be appropriate starting materials for C–C bond forming reactions to create organic frameworks of value-added compounds such as natural products, drugs, and fine chemicals. There have been tremendous synthetic methods involving catalytic C–C bond construction with the double bond of terminal alkenes (e.g., Heck reaction, hydrometalation followed by functionalization, carbometalation, and olefin metathesis) [10-13]. However, direct C–C bond formation of the allylic C(sp^3)–H bond adjacent to double bonds has remained underdeveloped even though C–O bond formation of allylic C(sp^3)–H bonds was firmly established by using SeO_2 [14] or CrO_3/3,5-dimethylpyrazole [15] (ene-type allylic oxidation). Although the most prominent work on catalytic allylic functionalization studied thus far is considered to be a palladium-catalyzed C–C bond formation using a stoichiometric amount of an oxidant [16-22], the π-allylpalladium intermediate [23-25] is an electrophilic species that exclusively reacts with nucleophiles. Therefore, it would be a formidable challenge for the generation of a nucleophilic π-allylmetal complex that reacts with electrophiles, triggered by allylic C(sp^3)–H activation. To this end, Schneider [26], Kanai [27], and we [28,29] reported in 2017 catalytic allylic C(sp^3)–H activation of alkenes to react carbonyl electrophiles such as imines, ketones, and CO_2 via

nucleophilic allylmetal species (Figure 1). However, the substrates employed have been restricted to allylarenes and 1,4-enyne, and 1,4-diene derivatives and α-olefins were totally unexplored. Therefore, the next challenge would be to use less reactive α-olefins (pK_a value of 1-propene = 43). In this paper, we describe an allylic C(sp^3)–H addition of α-olefins, mainly 1-undecene and their analogues, to ketone electrophiles.

Results and Discussion

We initially conducted screening of conditions using 1 equiv of 1-undecene (**1a**) and 3 equiv of acetophenone (**2a**) as starting materials (Table 1). When the reaction was conducted at 60 °C in DMA according to our previously established catalytic conditions ($Co(acac)_2$ (10 mol %), Xantphos (20 mol %), and $AlMe_3$ (1.0 equiv)) [29], branched homoallylic alcohol **3aa** was obtained in only 23% yield with 1.6:1 diastereoselectivity (Table 1, entry 1). In constant to the C(sp^3)–H addition of allylarene to acetophenone that exhibited high linear selectivity [29], perfect branch selectivity was observed using **1a** as a substrate. When the reaction temperature was raised, the yield of **3aa** was improved to 45% yield at 90 °C (Table 1, entries 2 and 3). An increase in the amount of $AlMe_3$ to 1.5 equiv further improved the yield of **3aa** to 54% yield (Table 1, entry 4). The moderate yield was attributed to the generation of the olefin isomerization product derived from **1a** (vide infra). We then changed the equivalents of reagents **1a** and **2a**. Although the yield of **3aa** was decreased when the reaction was conducted using a 1:1 ratio of **1a** and **2a** (Table 1, entry 5), the use of an excess amount of **1a** (3 equiv) greatly improved the yield to 70% (Table 1, entry 6: optimized conditions). When 1-octadecene (**1b**) was subjected to the optimized reaction conditions without adding **2a**, internal olefins were exclusively obtained (mixture of positional and geometric isomers) in 97% yield. It was shown by ^{1}H NMR analysis that the mixture contained about 60% of 2-octadecene (*E*/*Z* mixture).

Having established the reaction conditions, we then screened the scope and limitation of substituted acetophenone derivatives using an excess amount of 1-undecene (**1a**, 3 equiv, Figure 2). Electron-neutral and electron-donating substituents such as H (**2a**), Me (**2b**), and OMe (**2c**) at the *para*-position efficiently promoted the allylic C(sp^3)–H addition, in which the reaction of **2a** could be scaled-up (1 mmol) to afford **3aa** in a slightly higher yield (78%). Electron-withdrawing substituents such as F (**2d**) and CO_2Me (**2e**) also promoted the reaction with similar levels without damaging the ester functionality. Furthermore, 2-naphtophenone (**2f**) and propiophenone (**2g**) were tolerated well, affording branched products selectively in over

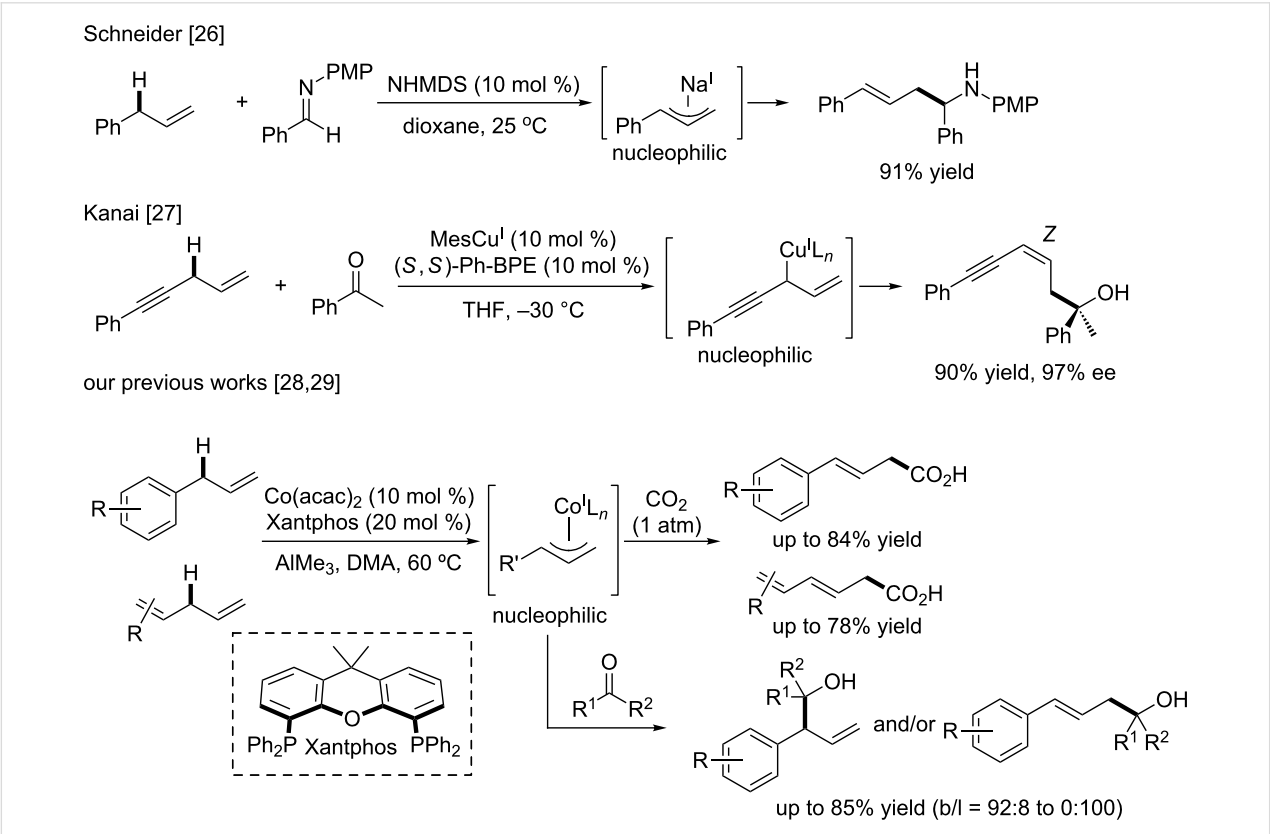

Figure 1: Precedent examples of catalytic allylic C(sp^3)–H additions to carbonyl electrophiles.

Table 1: Screening of reaction conditions.

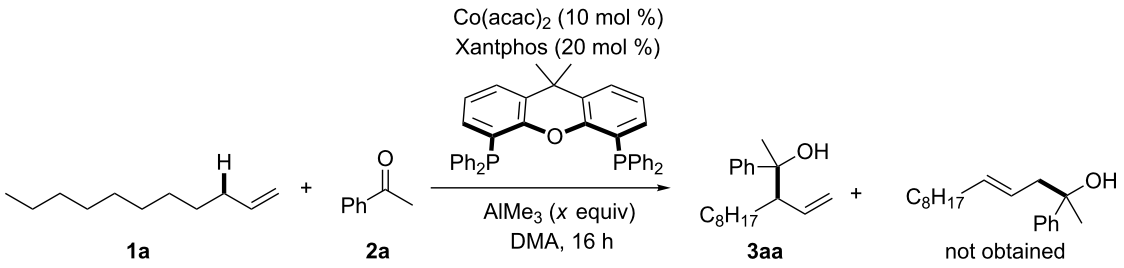

Entry	**1a**:**2a**	Temp (°C)	$AlMe_3$ (*x* equiv)	**3aa** (dr) (%)[a]
1	1:3	60	1.0	23 (1.6:1)
2	1:3	80	1.0	44 (1.3:1)
3	1:3	90	1.0	45 (1.3:1)
4[b]	1:3	90	1.5	54 (1.3:1)
5	1:1	90	1.5	46 (1.2:1)
6	3:1	90	1.5	70[c] (1.3:1)

[a]Yields were determined by ^{1}H NMR analysis using 1,1,2,2-tetrachloroethane as an internal standard. The diastereoselectivity (dr) was determined by ^{1}H NMR analysis. [b]The olefin isomerization product was obtained in 32% yield. [c]Isolated yield.

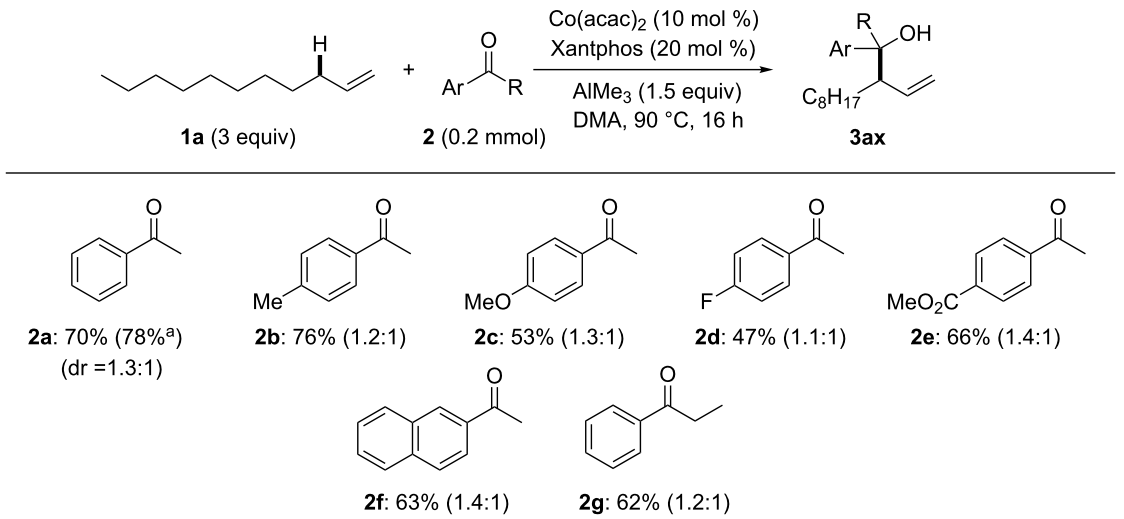

Figure 2: Substrate scope for acetophenone derivatives. [a]Preparative scale synthesis using 1 mmol of **2a**.

60% yield. However, *p*-CF_3-acetophenone (18%), acetone (14%), cyclohexanone (29%), and benzophenone (25%) were not suitable substrates for C(sp^3)–H addition of **1a** (figures not shown).

We next examined several α-olefins **1** (3 equiv) for allylic C(sp^3)–H addition to acetophenone (**2a**). Not only 1-undecene (**1a**) but also 1-octadecene (**1b**) and 6-phenyl-1-hexene (**1c**) were tolerable to afford the corresponding products in around 70% yield with perfect branch selectivity (Figure 3). Although the allylic C(sp^3)–H bond of α-olefins is weakly acidic (pK_a value of 1-propene = 43), it is noteworthy that thermal cleavage of allylic C(sp^3)–H bonds is possible without using highly basic organolithium or organomagnesium reagents (Grignard reagents) that react with ketones rather than deprotonating the allylic C(sp^3)–H bonds.

Based on the observed perfect branch selectivity, we propose the catalytic cycle of the C(sp^3)–H addition of 1-undecene (**1a**) to acetophenone (**2a**, Figure 4). First, methylcobalt(I) **I** should be generated from $Co(acac)_2$, Xantphos, and $AlMe_3$ [28,29]. Oxidative addition of the allylic C(sp^3)–H bond to **I** would

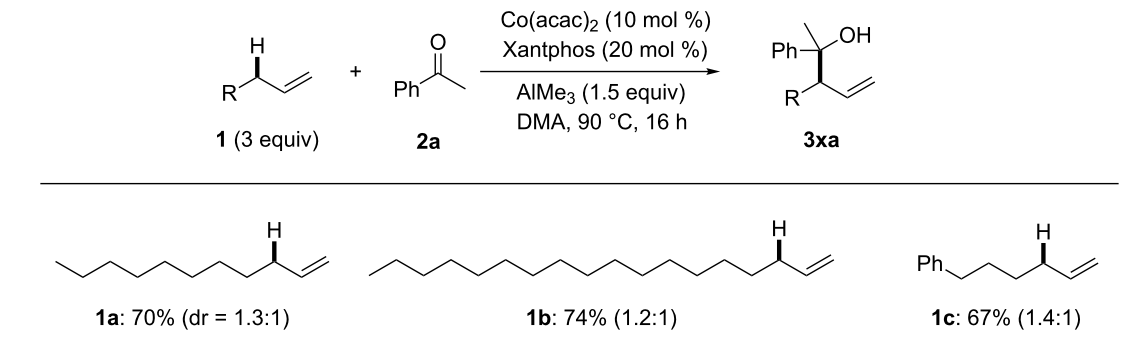

Figure 3: Substrate scope for α-olefins.

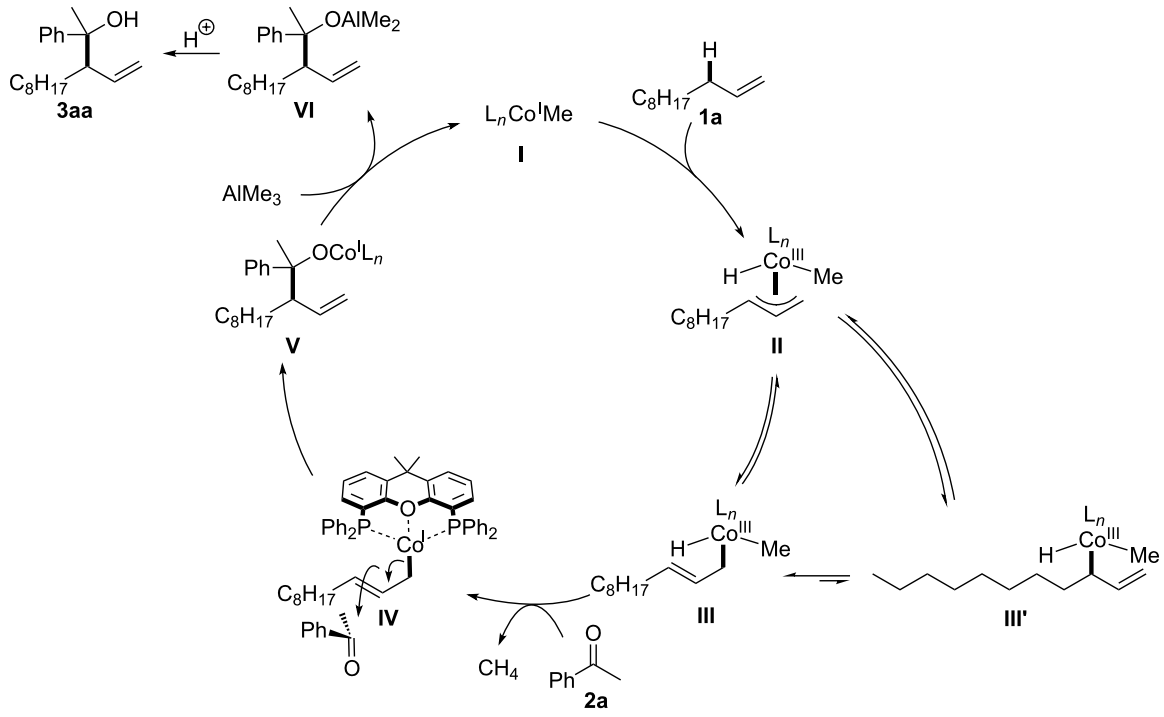

Figure 4: A possible catalytic cycle.

proceed to afford η^3-allylcobalt(III) intermediate **II**, which is tautomerized to η^1-allylcobalt(III) **III** by the assistance of the oxygen atom in the Xantphos ligand [30]. When using α-olefin as a substrate, the cobalt atom should be located at the terminal position due to the avoidance of steric repulsion between the bulky Xantphos ligand and an alkyl substitution (similar to the case of nucleophilic η^1-allylpalladium species [31-39]), whereas the cobalt atom preferred to reside at the internal position when allylarenes and 1,4-dienes were employed in our previous studies [28,29]. Subsequently, reductive elimination of methane from **III** would lead to a low-valent allylcobalt(I) species, and then C–C bond formation of **IV** with **2a** would proceed at the γ-position to produce cobalt alkoxide(I) **V** [28,29,31-39]. Transmetalation between **V** and $AlMe_3$ would furnish branched aluminium alkoxide **VI** along with the regeneration of **I**. Alkoxide **VI** is converted to homoallylic alcohol **3aa** by usual work-up.

Conclusion

In conclusion, we have successfully developed a cobalt-catalyzed nucleophilic addition of the C(sp^3)–H bond of simple alkenes to ketones. This novel transformation could realize perfect branch selectivity for all substrates. Much effort toward the development of an asymmetric variant is ongoing. We are also conducting computational analysis to explain the observed perfect regioselectivity. These results will be reported in due course.

Experimental

Representative procedure: To an oven-dried test tube was placed $Co(acac)_2$ (5.2 mg, 20 μmol, 10 mol %) and Xantphos (23.1 mg, 40 μmol, 20 mol %) in DMA (2 mL). The resulting mixture was stirred at room temperature until the materials had been completely dissolved. After the solution had been cooled to 0 ºC, it was stirred for 1 minute, and then $AlMe_3$ (2 M in toluene, 0.15 mL, 0.3 mmol, 1.5 equiv) was added. The dark green solution was stirred for another 1 minute, and then alkene **1** (0.6 mmol, 3.0 equiv) was added followed by the addition of ketone **2** (0.2 mmol, 1.0 equiv). The resulting mixture was stirred at 90 ºC for 16 h. After cooling the mixture to 0 ºC, the reaction was quenched by 1 M HCl aq and extracted with ethyl acetate (3 times). The combined organic layer was washed with brine and dried over Na_2SO_4. After the solids had been filtered off, the solvent was removed under reduced pressure and the residue was dried under vacuum to afford the crude mixture. The approximate yield of **3** was determined at this stage using 1,1,2,2-tetrachloroethane (δ = 6.1 ppm in $CDCl_3$, 2H) as an internal standard. If the ketone remained, $NaBH_4$ was added to convert it into the corresponding alcohol, which could be easily separated from **3** by silica-gel column chromatography. It was then purified by silica-gel column chromatography to afford the products **3**.

Supporting Information

Supporting Information File 1

Experimental details and characterization data.
[https://www.beilstein-journals.org/bjoc/content/supplementary/1860-5397-14-176-S1.pdf]

Acknowledgements

This work was financially supported by Grant-in-Aid for Scientific Research (C) (No. 18K05096), Grant-in-Aid for Scientific Research (B) (No. 26293001) from JSPS, and also by JST ACT-C (No. JPMJCR12YM). T.M. thanks the Naito Foundation for financial support. K.M. thanks JSPS for a fellowship (No. 14J08052).

ORCID® iDs

Tsuyoshi Mita - https://orcid.org/0000-0002-6655-3439
Kenichi Michigami - https://orcid.org/0000-0001-8025-0461
Yoshihiro Sato - https://orcid.org/0000-0003-2540-5525

References

1. Lyons, T. W.; Sanford, M. S. *Chem. Rev.* **2010,** *110,* 1147–1169. doi:10.1021/cr900184e
2. Jazzar, R.; Hitce, J.; Renaudat, A.; Sofack-Kreutzer, J.; Baudoin, O. *Chem. – Eur. J.* **2010,** *16,* 2654–2672. doi:10.1002/chem.200902374
3. Wendlandt, A. E.; Suess, A. M.; Stahl, S. S. *Angew. Chem., Int. Ed.* **2011,** *50,* 11062–11087. doi:10.1002/anie.201103945
4. Dastbaravardeh, N.; Christakakou, M.; Haider, M.; Schnürch, M. *Synthesis* **2014,** *46,* 1421–1439. doi:10.1055/s-0033-1338625
5. Guo, X.-X.; Gu, D.-W.; Wu, Z.; Zhang, W. *Chem. Rev.* **2015,** *115,* 1622–1651. doi:10.1021/cr500410y
6. Hartwig, J. F.; Larsen, M. A. *ACS Cent. Sci.* **2016,** *2,* 281–292. doi:10.1021/acscentsci.6b00032
7. Gensch, T.; Hopkinson, M. N.; Glorius, F.; Wencel-Delord, J. *Chem. Soc. Rev.* **2016,** *45,* 2900–2936. doi:10.1039/C6CS00075D
8. Yoshino, T.; Matsunaga, S. *Adv. Synth. Catal.* **2017,** *359,* 1245–1262. doi:10.1002/adsc.201700042
9. He, J.; Wasa, M.; Chan, K. S. L.; Shao, Q.; Yu, J.-Q. *Chem. Rev.* **2017,** *117,* 8754–8786. doi:10.1021/acs.chemrev.6b00622
10. Dounay, A. B.; Overman, L. E. *Chem. Rev.* **2003,** *103,* 2945–2964. doi:10.1021/cr020039h
11. Vougioukalakis, G. C.; Grubbs, R. H. *Chem. Rev.* **2010,** *110,* 1746–1787. doi:10.1021/cr9002424
12. Crossley, S. W. M.; Obradors, C.; Martinez, R. M.; Shenvi, R. A. *Chem. Rev.* **2016,** *116,* 8912–9000. doi:10.1021/acs.chemrev.6b00334
13. Shigehisa, H. *Chem. Pharm. Bull.* **2018,** *66,* 339–346. doi:10.1248/cpb.c17-01006
14. Młochowski, J.; Wójtowicz-Młochowska, H. *Molecules* **2015,** *20,* 10205–10243. doi:10.3390/molecules200610205
15. Salmond, W. G.; Barta, M. A.; Havens, J. L. *J. Org. Chem.* **1978,** *43,* 2057–2059. doi:10.1021/jo00404a049
16. Chen, M. S.; White, M. C. *J. Am. Chem. Soc.* **2004,** *126,* 1346–1347. doi:10.1021/ja039107n
17. Young, A. J.; White, M. C. *J. Am. Chem. Soc.* **2008,** *130,* 14090–14091. doi:10.1021/ja806867p
18. Kondo, H.; Yu, F.; Yamaguchi, J.; Liu, G.; Itami, K. *Org. Lett.* **2014,** *16,* 4212–4215. doi:10.1021/ol5019135
19. Ammann, S. E.; Liu, W.; White, M. C. *Angew. Chem., Int. Ed.* **2016,** *55,* 9571–9575. doi:10.1002/anie.201603576
20. Cochet, T.; Bellosta, V.; Roche, D.; Ortholand, J.-Y.; Greiner, A.; Cossy, J. *Chem. Commun.* **2012,** *48,* 10745–10747. doi:10.1039/c2cc36067e
21. Shibata, Y.; Kudo, E.; Sugiyama, H.; Uekusa, H.; Tanaka, K. *Organometallics* **2016,** *35,* 1547–1552. doi:10.1021/acs.organomet.6b00143
22. Burman, J. S.; Blakey, S. B. *Angew. Chem., Int. Ed.* **2017,** *56,* 13666–13669. doi:10.1002/anie.201707021
23. Hüttel, R.; Kratzer, J.; Bechter, M. *Chem. Ber.* **1961,** *94,* 766–780. doi:10.1002/cber.19610940329
24. Hüttel, R.; Christ, H. *Chem. Ber.* **1963,** *96,* 3101–3104. doi:10.1002/cber.19630961202
25. Trost, B. M.; Fullerton, T. J. *J. Am. Chem. Soc.* **1973,** *95,* 292–294. doi:10.1021/ja00782a080
26. Bao, W.; Kossen, H.; Schneider, U. *J. Am. Chem. Soc.* **2017,** *139,* 4362–4365. doi:10.1021/jacs.7b01542
27. Wei, X.-F.; Xie, X.-W.; Shimizu, Y.; Kanai, M. *J. Am. Chem. Soc.* **2017,** *139,* 4647–4650. doi:10.1021/jacs.7b01254
28. Michigami, K.; Mita, T.; Sato, Y. *J. Am. Chem. Soc.* **2017,** *139,* 6094–6097. doi:10.1021/jacs.7b02775
29. Mita, T.; Hanagata, S.; Michigami, K.; Sato, Y. *Org. Lett.* **2017,** *19,* 5876–5879. doi:10.1021/acs.orglett.7b02871
30. Ren, P.; Pike, S. D.; Pernik, I.; Weller, A. S.; Willis, M. C. *Organometallics* **2015,** *34,* 711–723. doi:10.1021/om500984y
31. Tamaru, Y. *J. Organomet. Chem.* **1999,** *576,* 215–231. doi:10.1016/S0022-328X(98)01060-2

32. Marshall, J. A. *Chem. Rev.* **2000,** *100,* 3163–3186. doi:10.1021/cr000003u
33. Szabó, K. J. *Chem. – Eur. J.* **2004,** *10,* 5268–5275. doi:10.1002/chem.200400261
34. Szabó, K. J. *Synlett* **2006,** 811–824. doi:10.1055/s-2006-933137
35. Zanoni, G.; Pontiroli, A.; Marchetti, A.; Vidari, G. *Eur. J. Org. Chem.* **2007,** 3599–3611. doi:10.1002/ejoc.200700054
36. Spielmann, K.; Niel, G.; de Figueiredo, R. M.; Campagne, J.-M. *Chem. Soc. Rev.* **2018,** *47,* 1159–1173. doi:10.1039/C7CS00449D
37. Mita, T.; Higuchi, Y.; Sato, Y. *Chem. – Eur. J.* **2015,** *21,* 16391–16394. doi:10.1002/chem.201503359
38. Mita, T.; Tanaka, H.; Higuchi, Y.; Sato, Y. *Org. Lett.* **2016,** *18,* 2754–2757. doi:10.1021/acs.orglett.6b01231
39. Higuchi, Y.; Mita, T.; Sato, Y. *Org. Lett.* **2017,** *19,* 2710–2713. doi:10.1021/acs.orglett.7b01055

License and Terms

BEILSTEIN JOURNAL OF ORGANIC CHEMISTRY

Cobalt-catalyzed *peri*-selective alkoxylation of 1-naphthylamine derivatives

Jiao-Na Han, Cong Du, Xinju Zhu, Zheng-Long Wang, Yue Zhu, Zhao-Yang Chu, Jun-Long Niu* and Mao-Ping Song*

Letter

Open Access

Address:
College of Chemistry and Molecular Engineering, Zhengzhou University, Zhengzhou 450001, People's Republic of China

Email:
Jun-Long Niu* - niujunlong@zzu.edu.cn; Mao-Ping Song* - mpsong@zzu.edu.cn

* Corresponding author

Keywords:
alkoxylation; C–H activation; cobalt catalysis; 1-naphthylamines; secondary alcohols

Beilstein J. Org. Chem. **2018,** *14,* 2090–2097.
doi:10.3762/bjoc.14.183

Received: 06 May 2018
Accepted: 30 July 2018
Published: 09 August 2018

This article is part of the thematic issue "Cobalt catalysis".

Guest Editor: S. Matsunaga

Abstract

A cobalt-catalyzed C(sp^2)–H alkoxylation of 1-naphthylamine derivatives has been disclosed, which represents an efficient approach to synthesize aryl ethers with broad functional group tolerance. It is noteworthy that secondary alcohols, such as hexafluoroisopropanol, isopropanol, isobutanol, and isopentanol, were well tolerated under the current catalytic system. Moreover, a series of biologically relevant fluorine-aryl ethers were easily obtained under mild reaction conditions after the removal of the directing group.

Introduction

Aryl ethers are common structural units present in many natural products, functional materials, and pharmaceuticals [1]. Consequently, a variety of strategies have emerged to access them, including Pd-catalyzed and Cu-catalyzed coupling reactions (Buchwald–Harting couplings and Ullmann reactions) [2-4]. However, these classic methods always possess some limitations such as preactivated starting materials, poor regioselectivities, and tedious steps [5]. Therefore, it is desirable to develop an effective strategy to achieve this transformation [6,7].

Over the past few decades, transition-metal-catalyzed C–H activation to form C–C or C–heteroatom bonds has attracted more attention [8-13]. In particular, the formation of C–O bonds is widely used in the syntheses of pharmaceuticals and functional materials [14-17]. The direct hydroxylation [18,19] and acetoxylation [20-22] have been developed rapidly in recent years. By contrast, alkoxylation or phenoxylation confronts great challenges because alkanols or phenols are easily converted into the corresponding aldehydes, ketones, or carboxylic acids [7,23-25]. Recently, Gooßen [26,27], Sanford [28], Song, [29,30] and others [31-42] have successfully reported alkoxylation reactions with the auxiliary of directing groups. However, the transition-metal-catalyzed C–H alkoxylation is still largely limited to palladium- [28,33-40] or copper- [26,27,29,41,42] catalyzed systems. Recently, the inexpensive cobalt catalysts have received significant attention because of their unique and

versatile activities in the C–H functionalizations [43-51]. In 2015, the cobalt-catalyzed alkoxylation of aromatic (and olefinic) carboxamides with primary alcohols was first reported by the Niu and Song group (Figure 1a) [30]. Successively, Ackermann realized the electrochemical cobalt-catalyzed alkoxylation via a similar process (Figure 1b) [32]. However, cobalt-catalyzed directed coupling of arenes with secondary alcohols has not been reported so far. Herein, we explored a simple and facile protocol for cobalt-catalyzed picolinamide-directed alkoxylation of 1-naphthylamine derivatives with alcohols (Figure 1c).

Results and Discussion

Initially, *N*-(naphthalen-1-yl)picolinamide (**1a**) and hexafluoroisopropanol (HFIP, **2a**) were chosen as the model substrates to optimize the alkoxylation reaction (Table 1, see more in Tables S1–S5 in Supporting Information File 1). To our delight, the desired product **3aa** was obtained in 66% yield when using $Co(OAc)_2{\cdot}4H_2O$ as catalyst and Ag_2CO_3 as oxidant (Table 1, entry 1). Other cobalt salts such as CoF_3 and CoF_2 were also employed as metal catalysts for C8 alkoxylation of **1a**, and CoF_2 was proved to be the optimal catalyst, affording **3aa** in 71% yield (Table 1, entries 2 and 3). Subsequently, various bases such as Na_2CO_3, K_2CO_3, and Cs_2CO_3 were screened (Table 1, entries 4–6), which indicated that Cs_2CO_3 was most effective and the alkoxylated product **3aa** could be isolated in 82% yield. Next, the effect of oxidants on the reactivity was investigated, and Ag_2CO_3 showed a superior result compared with alternative oxidants (Table 1, entries 6–8). Moreover, DCE and HFIP as co-solvents demonstrated higher reactivity, resulting in a slightly increased yield in 84% (Table 1, entries 9–11). Finally, variation of the reaction temperature did not promote the reaction efficiency.

With the established alkoxylated protocol in hand, the substrate scope of 1-naphthylamine derivatives was explored as shown in Scheme 1. Halogenated naphthylamines could afford the target products in 86–88% yields (**3ba**–**3ca**). Nitro- (**1d**) and benzenesulfonyl- (**1e**) substituted naphthylamines were found to proceed smoothly via this strategy (61–64%). In addition, a disubstituted naphthylamine provided the alkoxylated product in 47% yield (**3fa**). Moreover, a *Boc* amino group at C5 of the substrate **1g** was also compatible with the transformation (33%). When a methoxy group was located at the C7 site of the naphthylamine, sterically hindered product **3ha** was obtained in 81%. Besides, some benzylamine derivatives (*N*-(1-phenylethyl)picolinamide and *N*-benzhydrylpicolinamide) were attempted. However, no desired product could be detected.

Next, the substrate scope of alcohols was investigated. As shown in Scheme 2, both primary and secondary alcohols were compatible with the slightly modified optimized conditions. A

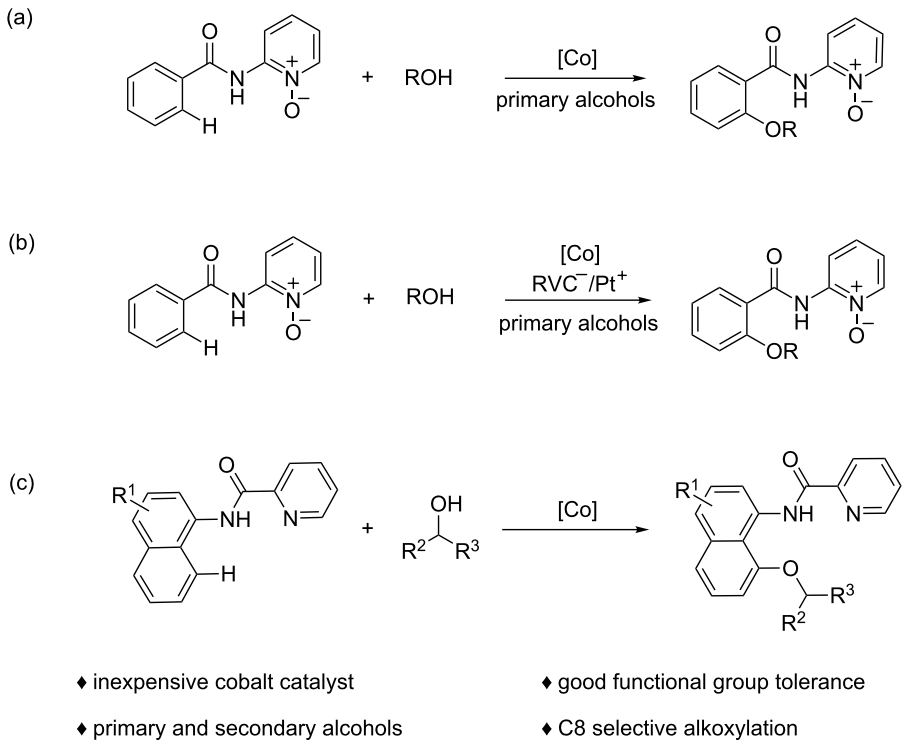

Figure 1: Strategies for cobalt-catalyzed alkoxylation.

Table 1: Optimization of the reaction conditions.[a]

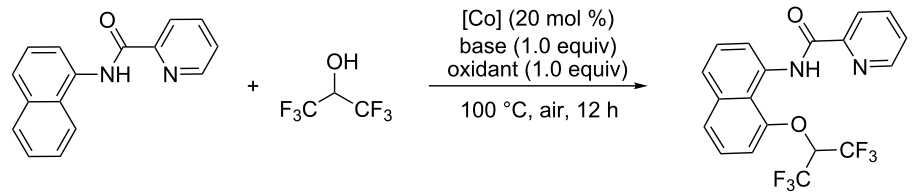

1a **2a** **3aa**

entry	catalyst	base	oxidant	yield (%)
1	$Co(OAc)_2·4H_2O$	*t*-AmONa	Ag_2CO_3	66
2	CoF_3	*t*-AmONa	Ag_2CO_3	60
3	CoF_2	*t*-AmONa	Ag_2CO_3	71
4	CoF_2	Na_2CO_3	Ag_2CO_3	58
5	CoF_2	K_2CO_3	Ag_2CO_3	67
6	CoF_2	Cs_2CO_3	Ag_2CO_3	82
7	CoF_2	Cs_2CO_3	$AgNO_3$	11
8	CoF_2	Cs_2CO_3	Ag_2O	32
9[b]	CoF_2	Cs_2CO_3	Ag_2CO_3	84
10[c]	CoF_2	Cs_2CO_3	Ag_2CO_3	80
11[d]	CoF_2	Cs_2CO_3	Ag_2CO_3	77

[a]Reaction conditions: **1a** (0.2 mmol), **2a** (1.0 mL), Co-catalyst (20 mol %), oxidant (1.0 equiv), base (1.0 equiv), 100 °C, air, 12 h. [b]DCE (1.0 mL) as co-solvent. [c]$PhCF_3$ (1.0 mL) as co-solvent. [d]PhF (1.0 mL) as co-solvent. DCE = 1,2-dichloroethane.

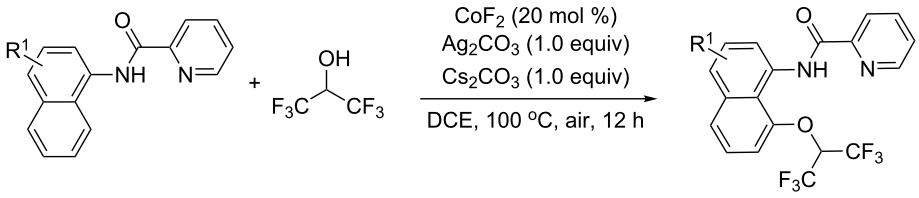

1a–h **2a** **3**

3ba, 88% **3ca**, 86% **3da**, 64% **3ea**, 61%

3fa, 47% **3ga**, 33% **3ha**, 81%

Scheme 1: Reaction scope with respect to *N*-(naphthalen-1-yl)picolinamide derivatives. Reaction conditions: **1** (0.2 mmol), **2a** (1.0 mL), CoF_2 (20 mol %), Ag_2CO_3 (1.0 equiv), Cs_2CO_3 (1.0 equiv), DCE (1.0 mL), 100 °C, air, 12 h.

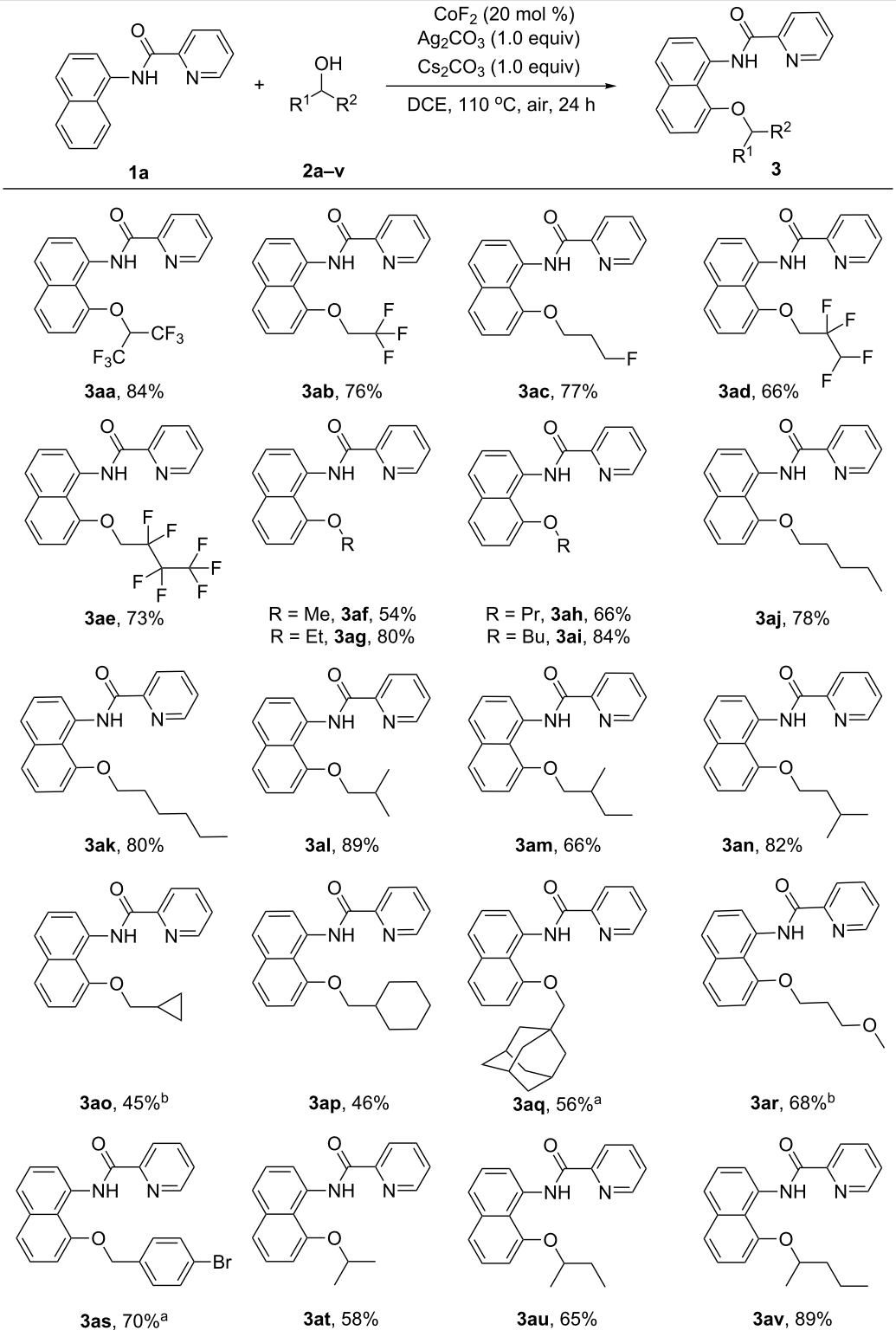

Scheme 2: Reaction scope with respect to alcohols. Reaction conditions: **1a** (0.2 mmol), **2** (1.0 mL), CoF_2 (20 mol %), Ag_2CO_3 (1.0 equiv), Cs_2CO_3 (1.0 equiv), DCE (1.0 mL), 110 °C, air, 24 h. [a]**2q** or **2s** (5.0 equiv). [b]48 h.

variety of fluoro-substituted alcohols **2a**–**e** proceeded smoothly to afford the corresponding products in moderate to good yields (66–84%). Simple primary alkyl alcohols were well tolerated to provide the desired products in 54–84% yields (**3af**–**ak**). Also, the branched alcohols **2l**, **2m**, and **2n** were employed to afford the corresponding products in 66–89% yields. Cyclopropyl-

methanol (**2o**), cyclohexylmethanol (**2p**), and adamantanemethanol (**2q**) were compatible with the transformation (45–56%). Moreover, an aliphatic ether and benzyl alcohol were proved to be effective coupling partners to provide **3ar** and **3as** in 68% and 70% yields, respectively. Compared with Co-catalyzed alkoxylation of arenes with primary alcohols [30,31], HFIP (**2a**), isopropanol (**2t**), isobutanol (**2u**), and isopentanol (**2v**) could all proceed smoothly to deliver the alkoxylated products in 58–89% yields. Furthermore, we attempted some tertiary alcohols (*tert*-butanol and 2-methyl-2-butanol). However, no desired product could be detected.

In order to study the reaction mechanism, a series of control experiments were carried out (Scheme 3, see more details in Supporting Information File 1). In the absence of cobalt salt, no product was obtained under the standard reaction conditions. Under an argon atmosphere and without Ag_2CO_3, the product was isolated in 12% yield when a stoichiometric amount of CoF_3 was introduced, whereas no product was obtained in the presence of CoF_2 (Scheme 3, reaction 1). These results imply that the reaction should initiates from a Co^{III} species. The addition of a radical quencher, benzoquinone (BQ), suppressed the formation of product **3aa**. When 2,2,6,6-tetramethyl-1-piperidinyloxyl (TEMPO) or 2,6-di-*tert*-butyl-4-methylphenol (BHT) was added under the standard reaction conditions, a significantly reduced yield (39% or 23%) was obtained (Scheme 3, reaction 2). These facts suggest that a radical approach may be involved in the reaction. Moreover, in the parallel experiments, a KIE value of 1.1 was observed between **1a** or [D_1]-**1a** with **2a**, which indicates that Co-catalyzed C–H bond cleavage should not be the rate determining step (Scheme 3, reaction 3).

On the basis of the above studies and previous literature [30,31,46,47], a plausible reaction mechanism for cobalt-catalyzed alkoxylation was proposed. As shown in Scheme 4, initially, $Co^{II}X_2$ could be oxidized to $Co^{III}X_2OR$ in the presence of a silver salt and an alcohol. Based on the experiments and the density functional theory calculations (DFT) [30,31],

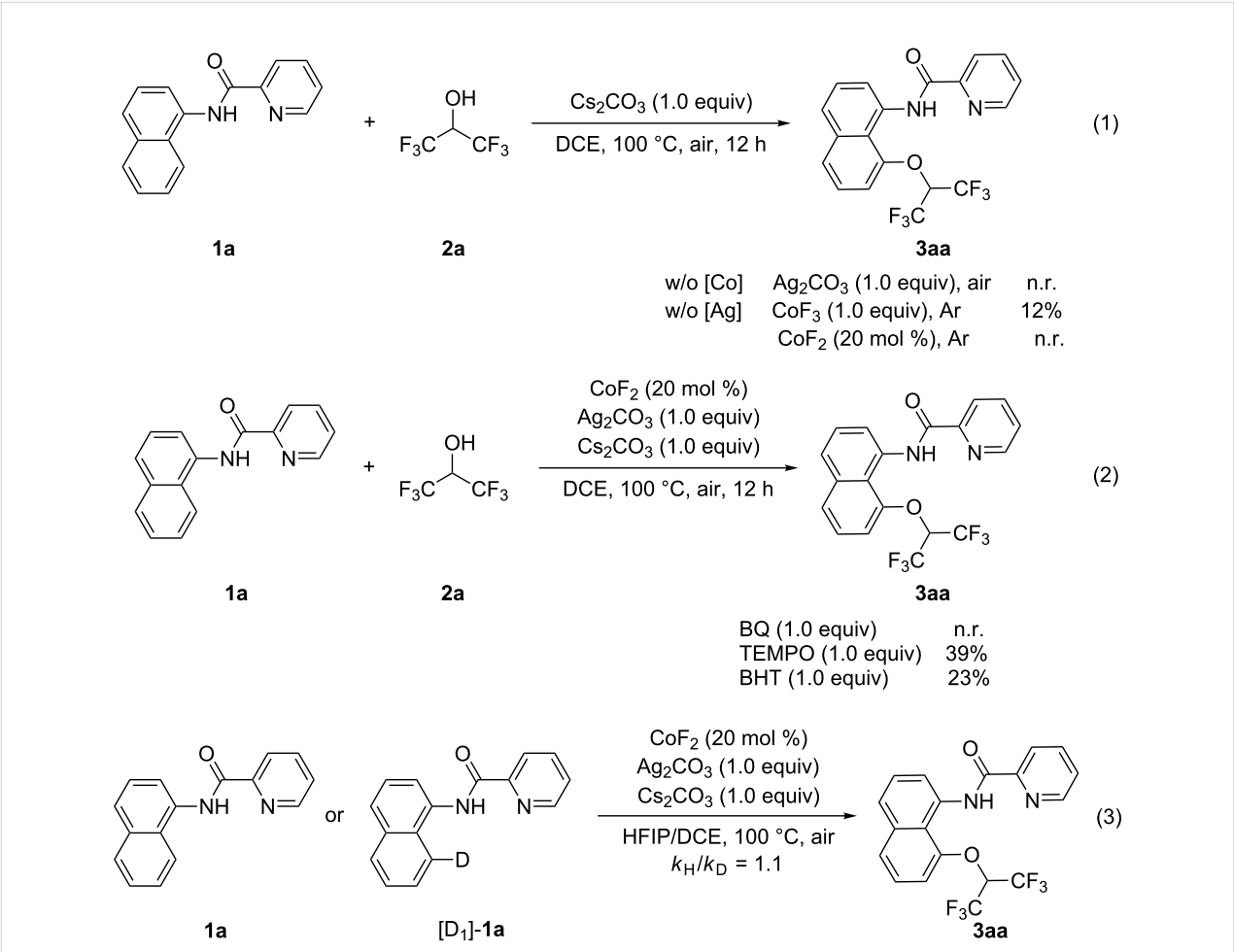

Scheme 3: Control experiments and mechanistic studies.

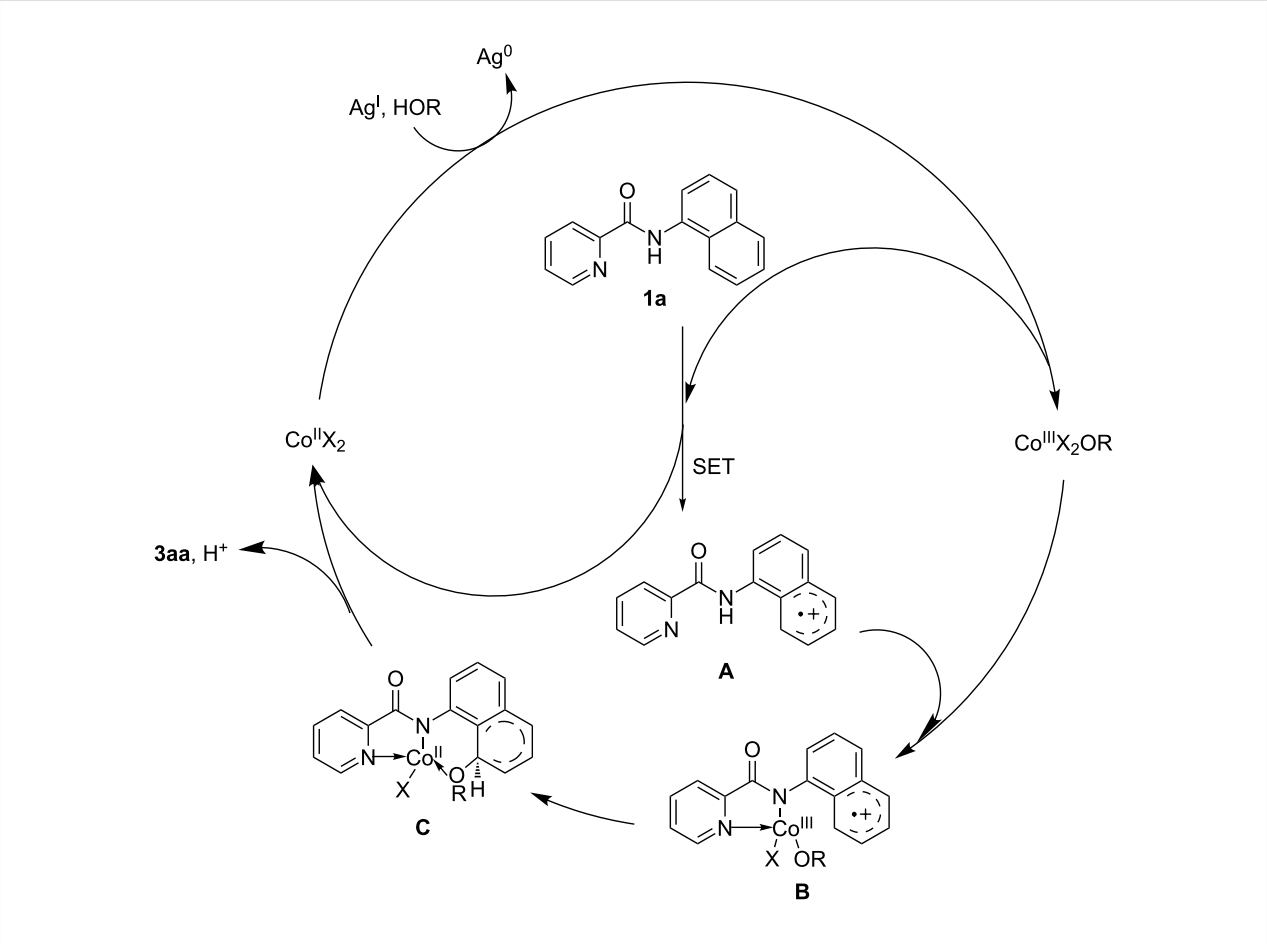

Scheme 4: Proposed reaction mechanism.

the C–H activation most possibly proceeded via a single-electron transfer (SET) path compared to a concerted metalation-deprotonation (CMD) path. Followed by an intermolecular SET process, the cation-radical intermediate **A** was generated, which coordinates with a Co^{III} species to provide the intermediate **B**. Subsequently, the transfer of ligand OR from the coordinated Co^{III} to the naphthalene ring led to the formation of intermediate **C**. Finally, the alkoxylated product **3aa** was released accompanied with the deprotonation and the Co^{II} species was transformed into the Co^{III} species by re-oxidization.

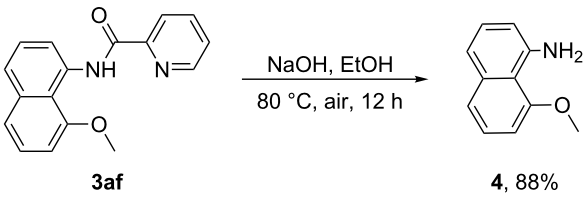

Scheme 5: Removal of the directing group.

The current alkoxylation methodology also exhibited potential applications. When treated with NaOH at 80 °C, the picolinic acid directing group could be easily removed, and the corresponding **4** was obtained in 88% yield (Scheme 5).

Conclusion

In summary, a cobalt-catalyzed C8 alkoxylation of naphthylamine derivatives with both primary and secondary alcohols was developed. This protocol is characterized by mild reaction conditions, broad substrate scope, and good functional group tolerance. Moreover, the excellent compatibility of fluorine-substituted alcohols (for instance, HFIP, trifluoroethanol, and 3-fluoropropanol etc.) shows that this strategy is highly valuable for the syntheses of biologically relevant fluorine-aryl ethers after the removal of the directing group. The above studies of the mechanism indicate that this reaction undergoes a SET process and cobalt salt is the actual catalyst. Overall, this protocol provides a new insight into the cobalt-catalyzed alkoxylation of naphthylamine derivatives. Further exploration of this strategy to aliphatic substrates is currently in progress.

Supporting Information

Supporting Information File 1

Experimental details and characterization data of new compounds, and X-ray crystal structure details for **3aa**.
[https://www.beilstein-journals.org/bjoc/content/supplementary/1860-5397-14-183-S1.pdf]

Supporting Information File 2

Crystallographic information file for compound **3aa**.
[https://www.beilstein-journals.org/bjoc/content/supplementary/1860-5397-14-183-S2.cif]

Acknowledgements

The work was supported by the National Natural Science Foundation of China (Nos. 21772179, 21502173, 21672192), Outstanding Young Talent Research Fund of Zhengzhou University (No. 1521316002).

ORCID® iDs

Jun-Long Niu - https://orcid.org/0000-0001-8012-4676
Mao-Ping Song - https://orcid.org/0000-0003-3883-2622

References

1. Enthaler, S.; Company, A. *Chem. Soc. Rev.* **2011,** *40,* 4912–4924. doi:10.1039/c1cs15085e
2. Altman, R. A.; Shafir, A.; Choi, A.; Lichtor, P. A.; Buchwald, S. L. *J. Org. Chem.* **2008,** *73,* 284–286. doi:10.1021/jo702024p
3. Hartwig, J. F. *Nature* **2008,** *455,* 314–322. doi:10.1038/nature07369
4. Monnier, F.; Taillefer, M. *Angew. Chem., Int. Ed.* **2009,** *48,* 6954–6971. doi:10.1002/anie.200804497
5. Bruice, T. C. *J. Am. Chem. Soc.* **1957,** *79,* 702–705. doi:10.1021/ja01560a055
6. Beccalli, E. M.; Broggini, G.; Martinelli, M.; Sottocornola, S. *Chem. Rev.* **2007,** *107,* 5318–5365. doi:10.1021/cr068006f
7. Chen, X.; Hao, X.-S.; Goodhue, C. E.; Yu, J.-Q. *J. Am. Chem. Soc.* **2006,** *128,* 6790–6791. doi:10.1021/ja061715q
8. Colby, D. A.; Bergman, R. G.; Ellman, J. A. *Chem. Rev.* **2010,** *110,* 624–655. doi:10.1021/cr900005n
9. Xiao, B.; Gong, T.-J.; Liu, Z.-J.; Liu, J.-H.; Luo, D.-F.; Xu, J.; Liu, L. *J. Am. Chem. Soc.* **2011,** *133,* 9250–9253. doi:10.1021/ja203335u
10. Wei, Y.; Yoshikai, N. *Org. Lett.* **2011,** *13,* 5504–5507. doi:10.1021/ol202229w
11. John, A.; Nicholas, K. M. *J. Org. Chem.* **2011,** *76,* 4158–4162. doi:10.1021/jo200409h
12. Zhao, J.; Wang, Y.; He, Y.; Liu, L.; Zhu, Q. *Org. Lett.* **2012,** *14,* 1078–1081. doi:10.1021/ol203442a
13. Zhang, C.; Feng, P.; Jiao, N. *J. Am. Chem. Soc.* **2013,** *135,* 15257–15262. doi:10.1021/ja4085463
14. Huang, R.; Huang, Y.; Lin, X.; Rong, M.; Weng, Z. *Angew. Chem., Int. Ed.* **2015,** *54,* 5736–5739. doi:10.1002/anie.201501257
15. Shan, G.; Yang, X.; Zong, Y.; Rao, Y. *Angew. Chem., Int. Ed.* **2013,** *52,* 13606–13610. doi:10.1002/anie.201307090
16. Yan, Y.; Feng, P.; Zheng, Q.-Z.; Liang, Y.-F.; Lu, J.-F.; Cui, Y.; Jiao, N. *Angew. Chem., Int. Ed.* **2013,** *52,* 5827–5831. doi:10.1002/anie.201300957
17. Krylov, I. B.; Vil', V. A.; Terent'ev, A. O. *Beilstein J. Org. Chem.* **2015,** *11,* 92–146. doi:10.3762/bjoc.11.13
18. Zhang, Y.-H.; Yu, J.-Q. *J. Am. Chem. Soc.* **2009,** *131,* 14654–14655. doi:10.1021/ja907198n
19. Li, X.; Liu, Y.-H.; Gu, W.-J.; Li, B.; Chen, F.-J.; Shi, B.-F. *Org. Lett.* **2014,** *16,* 3904–3907. doi:10.1021/ol5016064
20. Dick, A. R.; Hull, K. L.; Sanford, M. S. *J. Am. Chem. Soc.* **2004,** *126,* 2300–2301. doi:10.1021/ja031543m
21. Cheng, X.-F.; Li, Y.; Su, Y.-M.; Yin, F.; Wang, J.-Y.; Sheng, J.; Vora, H. U.; Wang, X.-S.; Yu, J.-Q. *J. Am. Chem. Soc.* **2013,** *135,* 1236–1239. doi:10.1021/ja311259x
22. Emmert, M. H.; Cook, A. K.; Xie, Y. J.; Sanford, M. S. *Angew. Chem., Int. Ed.* **2011,** *50,* 9409–9412. doi:10.1002/anie.201103327
23. Hoover, J. M.; Ryland, B. L.; Stahl, S. S. *J. Am. Chem. Soc.* **2013,** *135,* 2357–2367. doi:10.1021/ja3117203
24. Kumpulainen, E. T. T.; Koskinen, A. M. P. *Chem. – Eur. J.* **2009,** *15,* 10901–10911. doi:10.1002/chem.200901245
25. Okada, T.; Asawa, T.; Sugiyama, Y.; Kirihara, M.; Iwai, T.; Kimura, Y. *Synlett* **2014,** *25,* 596–598. doi:10.1055/s-0033-1340483
26. Bhadra, S.; Dzik, W. I.; Gooßen, L. J. *Angew. Chem., Int. Ed.* **2013,** *52,* 2959–2962. doi:10.1002/anie.201208755
27. Bhadra, S.; Matheis, C.; Katayev, D.; Gooßen, L. J. *Angew. Chem., Int. Ed.* **2013,** *52,* 9279–9283. doi:10.1002/anie.201303702
28. Desai, L. V.; Malik, H. A.; Sanford, M. S. *Org. Lett.* **2006,** *8,* 1141–1144. doi:10.1021/ol0530272
29. Zhang, L.-B.; Hao, X.-Q.; Zhang, S.-K.; Liu, K.; Ren, B.; Gong, J.-F.; Niu, J.-L.; Song, M.-P. *J. Org. Chem.* **2014,** *79,* 10399–10409. doi:10.1021/jo502005j
30. Zhang, L.-B.; Hao, X.-Q.; Zhang, S.-K.; Liu, Z.-J.; Zheng, X.-X.; Gong, J.-F.; Niu, J.-L.; Song, M.-P. *Angew. Chem., Int. Ed.* **2015,** *54,* 272–275. doi:10.1002/anie.201409751
31. Guo, X.-K.; Zhang, L.-B.; Wei, D.; Niu, J.-L. *Chem. Sci.* **2015,** *6,* 7059–7071. doi:10.1039/C5SC01807B
32. Sauermann, N.; Meyer, T. H.; Tian, C.; Ackermann, L. *J. Am. Chem. Soc.* **2017,** *139,* 18452–18455. doi:10.1021/jacs.7b11025
33. Wang, G.-W.; Yuan, T.-T. *J. Org. Chem.* **2010,** *75,* 476–479. doi:10.1021/jo902139b
34. Jiang, T.-S.; Wang, G.-W. *J. Org. Chem.* **2012,** *77,* 9504–9509. doi:10.1021/jo301964m
35. Li, W.; Sun, P. *J. Org. Chem.* **2012,** *77,* 8362–8366. doi:10.1021/jo301384r
36. Kolle, S.; Batra, S. *Org. Biomol. Chem.* **2015,** *13,* 10376–10385. doi:10.1039/C5OB01500F
37. Zheng, Y.-W.; Ye, P.; Chen, B.; Meng, Q.-Y.; Feng, K.; Wang, W.; Wu, L.-Z.; Tung, C.-H. *Org. Lett.* **2017,** *19,* 2206–2209. doi:10.1021/acs.orglett.7b00463
38. Yin, Z.; Jiang, X.; Sun, P. *J. Org. Chem.* **2013,** *78,* 10002–10007. doi:10.1021/jo401623j
39. Shi, S.; Kuang, C. *J. Org. Chem.* **2014,** *79,* 6105–6112. doi:10.1021/jo5008306
40. Li, S.; Zhu, W.; Gao, F.; Li, C.; Wang, J.; Liu, H. *J. Org. Chem.* **2017,** *82,* 126–134. doi:10.1021/acs.joc.6b02257
41. Yin, X.-S.; Li, Y.-C.; Yuan, J.; Gu, W.-J.; Shi, B.-F. *Org. Chem. Front.* **2015,** *2,* 119–123. doi:10.1039/C4QO00276H

42. Lu, W.; Xu, H.; Shen, Z. *Org. Biomol. Chem.* **2017,** *15,* 1261–1267. doi:10.1039/C6OB02582J
43. Yoshikai, N. *Bull. Chem. Soc. Jpn.* **2014,** *87,* 843–857. doi:10.1246/bcsj.20140149
44. Fallon, B. J.; Derat, E.; Amatore, M.; Aubert, C.; Chemla, F.; Ferreira, F.; Perez-Luna, A.; Petit, M. *J. Am. Chem. Soc.* **2015,** *137,* 2448–2451. doi:10.1021/ja512728f
45. Moselage, M.; Li, J.; Ackermann, L. *ACS Catal.* **2016,** *6,* 498–525. doi:10.1021/acscatal.5b02344
46. Wei, D.; Zhu, X.; Niu, J.-L.; Song, M.-P. *ChemCatChem* **2016,** *8,* 1242–1263. doi:10.1002/cctc.201600040
47. Tan, G.; He, S.; Huang, X.; Liao, X.; Cheng, Y.; You, J. *Angew. Chem., Int. Ed.* **2016,** *55,* 10414–10418. doi:10.1002/anie.201604580
48. Kalsi, D.; Barsu, N.; Sundararaju, B. *Chem. – Eur. J.* **2018,** *24,* 2360–2364. doi:10.1002/chem.201705710
49. Du, C.; Li, P.-X.; Zhu, X.; Suo, J.-F.; Niu, J.-L.; Song, M.-P. *Angew. Chem., Int. Ed.* **2016,** *55,* 13571–13575. doi:10.1002/anie.201607719
50. Zhang, J.; Chen, H.; Lin, C.; Liu, Z.; Wang, C.; Zhang, Y. *J. Am. Chem. Soc.* **2015,** *137,* 12990–12996. doi:10.1021/jacs.5b07424
51. Wang, Y.; Du, C.; Wang, Y.; Guo, X.; Fang, L.; Song, M.-P.; Niu, J.-L.; Wei, D. *Adv. Synth. Catal.* **2018,** *360,* 2668–2677. doi:10.1002/adsc.201800036

License and Terms

BEILSTEIN JOURNAL OF ORGANIC CHEMISTRY

Cobalt bis(acetylacetonate)–*tert*-butyl hydroperoxide–triethylsilane: a general reagent combination for the Markovnikov-selective hydrofunctionalization of alkenes by hydrogen atom transfer

Xiaoshen Ma[1] and Seth B. Herzon[*1,2]

Full Research Paper

Open Access

Address:
[1]Department of Chemistry, Yale University, New Haven, Connecticut 06520, United States and [2]Department of Pharmacology, Yale School of Medicine, New Haven, Connecticut 06520, United States

Email:
Seth B. Herzon[*] - seth.herzon@yale.edu

* Corresponding author

Keywords:
HAT; hydrogen atom transfer; hydrofunctionalization

Beilstein J. Org. Chem. **2018,** *14,* 2259–2265.
doi:10.3762/bjoc.14.201

Received: 22 May 2018
Accepted: 19 July 2018
Published: 28 August 2018

This article is part of the thematic issue "Cobalt catalysis".

Guest Editor: S. Matsunaga

Abstract

We show that cobalt bis(acetylacetonate) [$Co(acac)_2$], *tert*-butyl hydroperoxide (TBHP), and triethylsilane (Et_3SiH) constitute an inexpensive, general, and practical reagent combination to initiate a broad range of Markovnikov-selective alkene hydrofunctionalization reactions. These transformations are believed to proceed by cobalt-mediated hydrogen atom transfer (HAT) to the alkene substrate, followed by interception of the resulting alkyl radical intermediate with a SOMOphile. In addition, we report the first reductive couplings of unactivated alkenes and aryldiazonium salts by an HAT pathway. The simplicity and generality of the $Co(acac)_2$–TBHP–Et_3SiH reagent combination suggests it as a useful starting point to develop HAT reactions in complex settings.

Introduction

Many powerful methods to effect alkene hydrogenation [1-4] and Markovnikov-selective hydroheterofunctionalization (H–X addition, X = O [5-9], I [3], Br [3], Se [3], S [8-10], Cl [8,11], F [12,13], and N [8,14-17]) by metal-mediated hydrogen atom transfer (HAT) [18-21] are now known. Additionally, methods to achieve carbon–carbon bond formation to alkenes by HAT have been developed (e.g., reductive coupling [22-28], formal hydromethylation [29], cycloisomerization [8,30,31], hydrooximation [32], hydroheteroarylation [28,33-35], hydroarylation [36-38], and cross-coupling [37]). Many of these transformations have found applications in synthesis [6,39-47]. Although mechanistically-complex [28] the outcome of these reactions can be rationalized as initiating by HAT to the alkene, to form the kinetically- and thermodynamically-favored alkyl radical intermediate, which may be in equilibrium with the corresponding metal alkyl complex. This radical then undergoes addition

to a second reagent (SOMOphile) to form the functionalized product (Scheme 1).

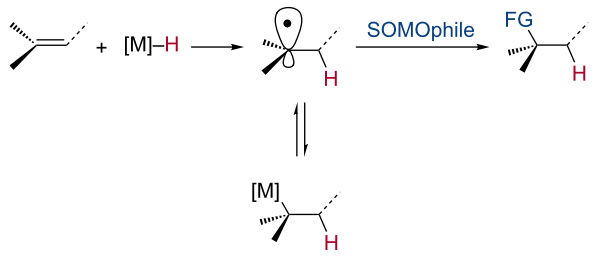

Scheme 1: General mechanism of alkene hydrofunctionalization via HAT.

A wide range of manganese, cobalt, or iron-based complexes containing diverse supporting ligands have found use in these reactions. To the best of our knowledge, the iron oxalate–sodium borohydride system, introduced by Boger and co-workers [8], is the only reagent combination shown to accommodate a broad range of SOMOphiles. However, the cobalt–salen complexes that are commonly employed [10,11,13,15,16,30-32,36,37,48] contain many different ligand architectures [21], and often need to be prepared by multistep sequences. Here we report a uniform set of reaction conditions to achieve a broad range of HAT hydrofunctionalization reactions using the simple reagents cobalt acetoacetonate [$Co(acac)_2$], *tert*-butyl hydroperoxide (TBHP), and triethylsilane (Et_3SiH). The practicality and generality of this system should motivate its application in synthesis.

Results and Discussion

In 2014, we reported the reduction of alkenyl halides (e.g., **1**, Scheme 2) utilizing $Co(acac)_2$, TBHP, and two reductants, triethylsilane and 1,4-dihydrobenzene (DHB) [2]. Mechanistic studies showed that Et_3SiH participates in the formation of a cobalt hydride intermediate that delivers a hydrogen atom to the less-substituted position of the alkene. The resulting alkyl radical is believed to abstract a second hydrogen atom from DHB to generate the reduced product [2]. This mechanism separates the alkyl radical formation and functionalization steps by employing two different reagents. Accordingly, we investigated the application of this system in other HAT reactions. In these studies, methallyl *p*-methoxybenzoate (**3a**) was used as substrate (Table 1).

Under our standard reduction conditions, alkene **3a** was transformed to isobutyl *p*-methoxybenzoate (**4a**) in 86% yield (entry 1, Table 1). Inspired by the methods of Boger [12] and Hiroya [13], a number of fluorination reagents were examined to achieve hydrofluorination. Although no product was observed using SelectFluor®, diethylaminosulfur trifluoride (DAST), or tosyl fluoride (see Supporting Information File 1, Table S1, entries 2–4), *N*-fluorobenzenesulfonimide (NFSI) provided the desired hydrofluorination product **4b** in 36% yield (Table 1, entry 2). Carreira and co-workers reported the first hydrochlorination reaction via a cobalt-catalyzed HAT process [11]. By utilizing *p*-toluenesulfonyl chloride (TsCl) and *p*-toluenesulfonyl bromide (TsBr) under our conditions, the desired hydrochlorination and hydrobromination products **4c** and **4d** were obtained in 92% and 95% yields, respectively [3] (Table 1, entries 3 and 4). To our knowledge, the formation of **4d** represents the first Markovnikov-selective alkene hydrobromination by an HAT pathway. Attempts to extend this reaction to hydroiodination using related reagents, *p*-toluenesulfonyl iodide, *N*-iodosuccinimide, or molecular iodine failed to provide the expected product (see Supporting Information File 1, Table S1, entries 9–11) [3]. Surprisingly, diiodomethane, possessed the desired reactivity and the hydroiodination product **4e** was isolated in 89% yield (Table 1, entry 5) [3]. Ethyl iodoacetate, iodoacetonitrile, and 1,2-diiodoethane were also effective, but the yields of **4e** and conversion of **3a** were lower (see Supporting Information File 1, Table S1, entries 13–15). Mukaiyama and co-workers' pioneering Markonikov-selective alkene hydration reaction [5,49-54] proceeds using dioxygen as the oxygen atom source. Exposure of the alkene **3a** to similar conditions provided the tertiary alcohol **4f** in 69% yield (Table 1, entry 6). Inspired by Girijavallabhan and co-workers' report [10], we were able to trap the tertiary alkyl radical with *S*-phenyl benzene thiosulfonate ($PhSO_2SPh$, Table 1, entry 7) and *Se*-phenyl 4-methylbenzenesulfonoselenoate (TsSePh, Table 1, entry 8) [3] to afford the corresponding products **4g** and **4h** in 96% and 89% yields, respectively. Carreira and co-workers reported the hydroazidation of alkenes using cobalt–salen complexes as hydrogen atom transfer agents and *para*-toluenesulfonyl azide as an azide source [16,48,55]. After

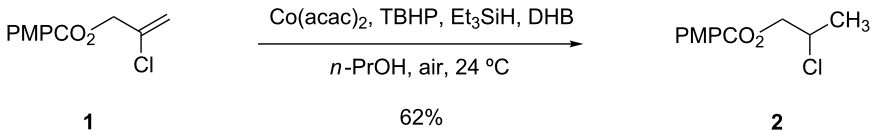

1 **2**

Scheme 2: Reduction of the alkenyl chloride **1** by HAT.

Table 1: Markovnikov Hydrofunctionalization of **3a**.[a]

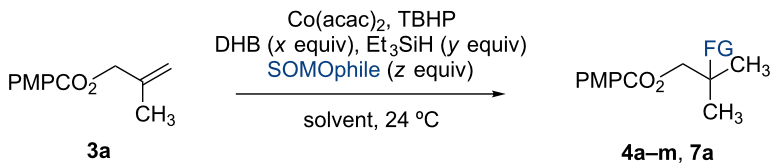

3a **4a–m**, **7a**

entry	x	y	SOMOphile	z	solvent	product	yield[b]
1	5.00	5.00	–	–	*n*-propanol	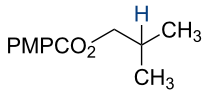 **4a**	86%
2	2.50	10.0	NFSI	2.50	CH_2Cl_2	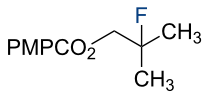 **4b**	36%
3	2.50	10.0	TsCl	2.50	*n*-propanol	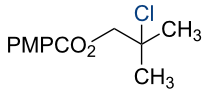 **4c**	92%
4	3.75	10.0	TsBr	2.50	*n*-propanol	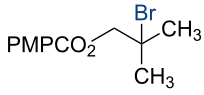 **4d**	95%
5	3.75	10.0	CH_2I_2	15.0	CH_2Cl_2	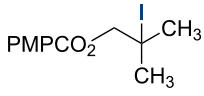 **4e**	89%
6	10.0	10.0	O_2	–	*n*-propanol	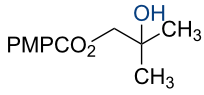 **4f**	69%
7	2.50	10.0	$PhSO_2SPh$	2.50	*n*-propanol	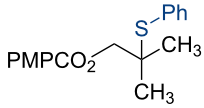 **4g**	96%
8	2.50	10.0	TsSePh	2.50	*n*-propanol	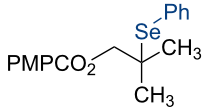 **4h**	89%
9	1.00	10.0	*p*-ABSA	5.00	CH_3CN	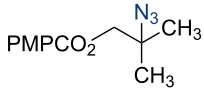 **4i**	79%
10	0	6.25	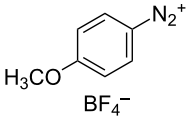 **5a**	1.50	CH_2Cl_2	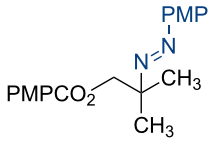 **7a**	92%

Table 1: Markovnikov Hydrofunctionalization of **3a**.[a] (continued)

11	3.75	10.0	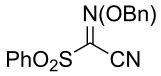 **6a**	2.50	*n*-propanol	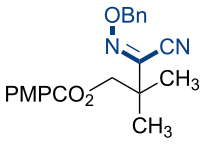 **4j**	60%
12	3.75	10.0	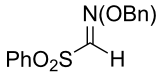 **6b**	2.50	*n*-propanol	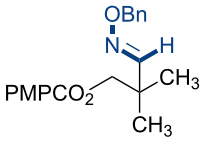 **4k**	48%
13	0	5.00	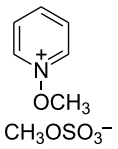 **6c**	5.00	CH_2Cl_2	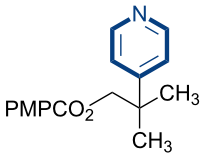 **4l**	66% 4.7:1 rr[b]
14	0	5.00	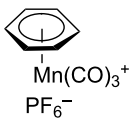 **6d**	1.00	CH_3CN	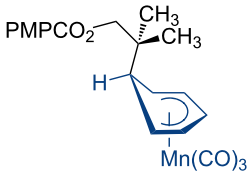 **4m**	50%

[a]For detailed reaction conditions, see Supporting Information File 1. [b]Isolated yields after purification by flash-column chromatography. [b]rr = ratio of regioisomers.

careful optimization of the azidation reagent (*p*-acetamidobenzenesulfonyl azide (*p*-ABSA)) and additive equivalents (see Supporting Information File 1, Table S1, entries 19–28), the tertiary alkyl azide **4i** was obtained in 79% yield (Table 1, entry 9).

To broaden the scope of C–N coupling process via HAT, we investigated other nitrogen-containing SOMOphiles in the HAT reaction. Employing 4-methoxyphenyldiazonium tetrafluoroborate (**5a**) in our HAT conditions, the alkyl aryl azo product **7a** was obtained in 92% yield (Table 1, entry 10). Due to the importance of azo compounds in synthetic organic chemistry, industrial dyes, and medicinal chemistry [56,57], we investigated the scope of this transformation (Scheme 3). By varying the alkene substitution pattern, we determined that the coupling of tertiary radicals is more efficient than secondary radicals. For example, methallyl *p*-methoxybenzoate (**3a**) and prenyl *p*-methoxybenzoate (**3c**, not shown) afforded the azo compounds **7a** and **7c** in 92% and 91% yields, respectively. By comparison the yield of the azo product using allyl *p*-methoxybenzoate (**3b**, now shown) as substrate was somewhat lower (77%). Diazonium salts bearing substituents with different steric and electronic properties were examined. These experiments revealed that this coupling is compatible with a broad range of functional groups and aryl substitution patterns (**7d–j**, 52–97%). The naphthylazo derivative **7k** was obtained in 69% yield using 1-naphthyldiazonium tetrafluoroborate. However, aryldiazonium salts bearing nitro substituents were not compatible with this HAT coupling. For example, the use of *p*-nitrobenzendiazonium tetrafluoroborate failed to provide the expected coupling product **7l**. This may be due to alternative reaction pathways involving reduction of the nitro substituent [17].

Additional carbon–carbon bond formation strategies were also examined using the $Co(acac)_2$ HAT system. Sulfonyl oximes **6a** and **6b** [32] afforded the carbon–carbon coupled products **4j** and **4k** in 60% and 48% yields, respectively (Table 1, entries 11 and 12, respectively). Recently, our laboratory reported a formal intermolecular hydroheteroarylation using *N*-methoxy heteroarenium salts by $Co(acac)_2$-mediated HAT [33,34]. In the original reports, 36 discrete unactivated alkenes were coupled with 38 different heteroarenium salts under mild conditions [33,34]. A representative example comprises the coupling of methallyl *p*-methoxybenzoate (**3a**) with *N*-methoxypyridinium

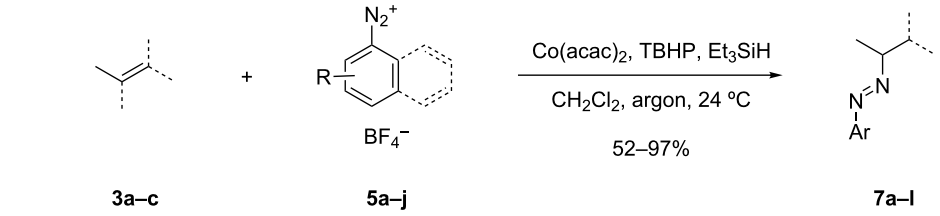

3a–c **5a–j** **7a–l**

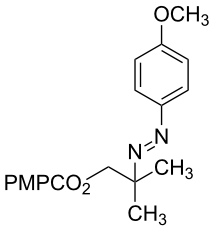

7a, 92%[a]

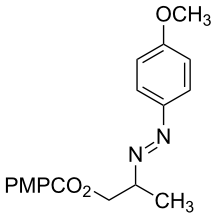

7b, 77%

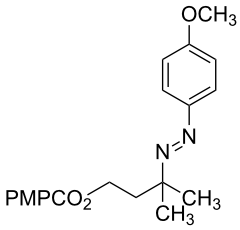

7c, 91%

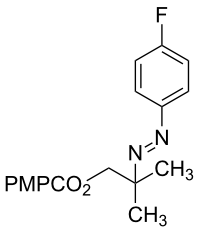

7d, 82%

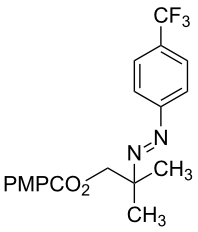

7e, 71%

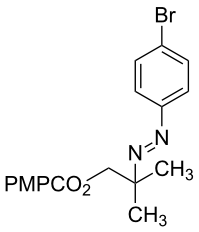

7f, 65%

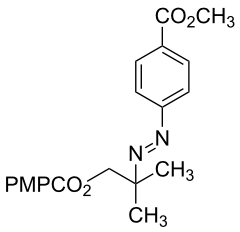

7g, 52%

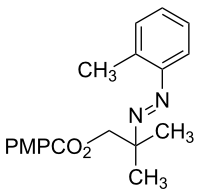

7h, 97%

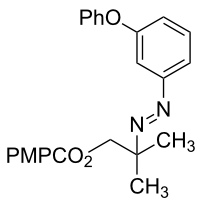

7i, 77%

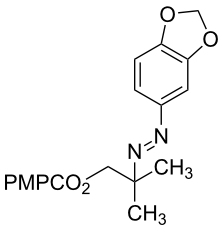

7j, 81%

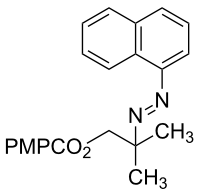

7k, 69%

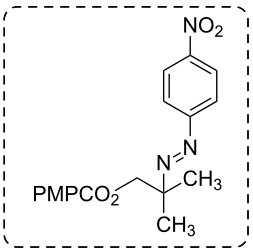

7l, 0%

Scheme 3: Substrate scope of alkyl-aryl azo compound synthesis via HAT. Conditions: alkene (0.250 mmol), diazonium salt (1.50 equiv), $Co(acac)_2$ (1.00 equiv), TBHP (1.00 equiv), Et_3SiH (6.25 equiv), CH_2Cl_2 (0.2 M), argon, 15–120 min. All yields are isolated yields after flash-column chromatography. [a]Reaction conducted on 1.00 mmol scale.

methyl sulfate (**6c**) to form the hydropyridylation product **4l** in 66% yield and as a 4.7:1 ratio of regioisomers (Table 1, entry 13). We also demonstrated that the alkyl radical generated from the HAT process can be trapped by (η^6-benzene)manganese tricarbonyl hexafluorophosphate (**6d**) to provide the reductive coupling product **4m** in 50% yield (Table 1, entry 14).

Conclusion

In summary, we have demonstrated that under a consistent set of conditions, the $Co(acac)_2$–TBHP–Et_3SiH system effects a diverse array of Markovnikov-selective hydrofunctionalization reactions of unactivated alkenes (H–X addition, X = H, F, Cl, Br, I, O, S, Se, N, and C). We have also reported the first reductive coupling reactions of alkenes and aryldiazonium salts under HAT conditions. These transformations proceed in high regioselectivity and efficiency. Further efforts will focus on expanding the alkene scope and exploring the site-selectivity in polyene substrates.

Supporting Information

Supporting Information File 1

Detailed experimental procedures and characterization data for all new compounds.
[https://www.beilstein-journals.org/bjoc/content/supplementary/1860-5397-14-201-S1.pdf]

Acknowledgements

Financial support from the National Science Foundation (CHE-1151563) is gratefully acknowledged.

ORCID® iDs

Xiaoshen Ma - https://orcid.org/0000-0002-0713-2896
Seth B. Herzon - https://orcid.org/0000-0001-5940-9853

References

1. Iwasaki, K.; Wan, K. K.; Oppedisano, A.; Crossley, S. W. M.; Shenvi, R. A. *J. Am. Chem. Soc.* **2014,** *136,* 1300–1303. doi:10.1021/ja412342g
2. King, S. M.; Ma, X.; Herzon, S. B. *J. Am. Chem. Soc.* **2014,** *136,* 6884–6887. doi:10.1021/ja502885c
3. Ma, X.; Herzon, S. B. *Chem. Sci.* **2015,** *6,* 6250–6255. doi:10.1039/C5SC02476E
4. Obradors, C.; Martinez, R. M.; Shenvi, R. A. *J. Am. Chem. Soc.* **2016,** *138,* 4962–4971. doi:10.1021/jacs.6b02032
5. Isayama, S.; Mukaiyama, T. *Chem. Lett.* **1989,** *18,* 573–576. doi:10.1246/cl.1989.573
6. Ishikawa, H.; Colby, D. A.; Boger, D. L. *J. Am. Chem. Soc.* **2008,** *130,* 420–421. doi:10.1021/ja078192m
7. Ishikawa, H.; Colby, D. A.; Seto, S.; Va, P.; Tam, A.; Kakei, H.; Rayl, T. J.; Hwang, I.; Boger, D. L. *J. Am. Chem. Soc.* **2009,** *131,* 4904–4916. doi:10.1021/ja809842b
8. Leggans, E. K.; Barker, T. J.; Duncan, K. K.; Boger, D. L. *Org. Lett.* **2012,** *14,* 1428–1431. doi:10.1021/ol300173v
9. Ma, X.; Herzon, S. B. *J. Org. Chem.* **2016,** *81,* 8673–8695. doi:10.1021/acs.joc.6b01709
10. Girijavallabhan, V.; Alvarez, C.; Njoroge, F. G. *J. Org. Chem.* **2011,** *76,* 6442–6446. doi:10.1021/jo201016z
11. Gaspar, B.; Carreira, E. M. *Angew. Chem., Int. Ed.* **2008,** *47,* 5758–5760. doi:10.1002/anie.200801760
12. Barker, T. J.; Boger, D. L. *J. Am. Chem. Soc.* **2012,** *134,* 13588–13591. doi:10.1021/ja3063716
13. Shigehisa, H.; Nishi, E.; Fujisawa, M.; Hiroya, K. *Org. Lett.* **2013,** *15,* 5158–5161. doi:10.1021/ol402696h
14. Kato, K.; Mukaiyama, T. *Chem. Lett.* **1992,** *21,* 1137–1140. doi:10.1246/cl.1992.1137
15. Waser, J.; Carreira, E. M. *J. Am. Chem. Soc.* **2004,** *126,* 5676–5677. doi:10.1021/ja048698u
16. Waser, J.; Nambu, H.; Carreira, E. M. *J. Am. Chem. Soc.* **2005,** *127,* 8294–8295. doi:10.1021/ja052164r
17. Gui, J.; Pan, C.-M.; Jin, Y.; Qin, T.; Lo, J. C.; Lee, B. J.; Spergel, S. H.; Mertzman, M. E.; Pitts, W. J.; La Cruz, T. E.; Schmidt, M. A.; Darvatkar, N.; Natarajan, S. R.; Baran, P. S. *Science* **2015,** *348,* 886–891. doi:10.1126/science.aab0245
18. Eisenberg, D. C.; Norton, J. R. *Isr. J. Chem.* **1991,** *31,* 55–66. doi:10.1002/ijch.199100006
19. Gansäuer, A.; Shi, L.; Otte, M.; Huth, I.; Rosales, A.; Sancho-Sanz, I.; Padial, N. M.; Oltra, J. E. *Hydrogen Atom Donors: Recent Developments*. In *Radicals in Synthesis III;* Heinrich, M.; Gansäuer, A., Eds.; Topics in Current Chemistry; Springer: Berlin Heidelberg, 2012. doi:10.1007/128_2011_124
20. Hoffmann, R. W. *Chem. Soc. Rev.* **2016,** *45,* 577–583. doi:10.1039/C5CS00423C
21. Crossley, S. W. M.; Obradors, C.; Martinez, R. M.; Shenvi, R. A. *Chem. Rev.* **2016,** *116,* 8912–9000. doi:10.1021/acs.chemrev.6b00334
22. Choi, J.; Tang, L.; Norton, J. R. *J. Am. Chem. Soc.* **2007,** *129,* 234–240. doi:10.1021/ja066325i
23. Choi, J.; Pulling, M. E.; Smith, D. M.; Norton, J. R. *J. Am. Chem. Soc.* **2008,** *130,* 4250–4252. doi:10.1021/ja710455c
24. Li, G.; Han, A.; Pulling, M. E.; Estes, D. P.; Norton, J. R. *J. Am. Chem. Soc.* **2012,** *134,* 14662–14665. doi:10.1021/ja306037w
25. Lo, J. C.; Yabe, Y.; Baran, P. S. *J. Am. Chem. Soc.* **2014,** *136,* 1304–1307. doi:10.1021/ja4117632
26. Lo, J. C.; Gui, J.; Yabe, Y.; Pan, C.-M.; Baran, P. S. *Nature* **2014,** *516,* 343–348. doi:10.1038/nature14006
27. Kuo, J. L.; Hartung, J.; Han, A.; Norton, J. R. *J. Am. Chem. Soc.* **2015,** *137,* 1036–1039. doi:10.1021/ja511883b
28. Lo, J. C.; Kim, D.; Pan, C.-M.; Edwards, J. T.; Yabe, Y.; Gui, J.; Qin, T.; Gutiérrez, S.; Giacoboni, J.; Smith, M. W.; Holland, P. L.; Baran, P. S. *J. Am. Chem. Soc.* **2017,** *139,* 2484–2503. doi:10.1021/jacs.6b13155
29. Dao, H. T.; Li, C.; Michaudel, Q.; Maxwell, B. D.; Baran, P. S. *J. Am. Chem. Soc.* **2015,** *137,* 8046–8049. doi:10.1021/jacs.5b05144
30. Crossley, S. W. M.; Barabé, F.; Shenvi, R. A. *J. Am. Chem. Soc.* **2014,** *136,* 16788–16791. doi:10.1021/ja5105602
31. Gaspar, B.; Carreira, E. M. *Angew. Chem., Int. Ed.* **2007,** *46,* 4519–4522. doi:10.1002/anie.200700575
32. Gaspar, B.; Carreira, E. M. *J. Am. Chem. Soc.* **2009,** *131,* 13214–13215. doi:10.1021/ja904856k

33. Ma, X.; Herzon, S. B. *J. Am. Chem. Soc.* **2016,** *138,* 8718–8721. doi:10.1021/jacs.6b05271
34. Ma, X.; Dang, H.; Rose, J. A.; Rablen, P.; Herzon, S. B. *J. Am. Chem. Soc.* **2017,** *139,* 5998–6007. doi:10.1021/jacs.7b02388
35. Bordi, S.; Starr, J. T. *Org. Lett.* **2017,** *19,* 2290–2293. doi:10.1021/acs.orglett.7b00833
36. Crossley, S. W. M.; Martinez, R. M.; Guevara-Zuluaga, S.; Shenvi, R. A. *Org. Lett.* **2016,** *18,* 2620–2623. doi:10.1021/acs.orglett.6b01047
37. Green, S. A.; Matos, J. L. M.; Yagi, A.; Shenvi, R. A. *J. Am. Chem. Soc.* **2016,** *138,* 12779–12782. doi:10.1021/jacs.6b08507
38. Green, S. A.; Vásquez-Céspedes, S.; Shenvi, R. A. *J. Am. Chem. Soc.* **2018**. doi:10.1021/jacs.8b05868
39. Shenvi, R. A.; Guerrero, C. A.; Shi, J.; Li, C.-C.; Baran, P. S. *J. Am. Chem. Soc.* **2008,** *130,* 7241–7243. doi:10.1021/ja8023466
40. Schindler, C. S.; Stephenson, C. R. J.; Carreira, E. M. *Angew. Chem., Int. Ed.* **2008,** *47,* 8852–8855. doi:10.1002/anie.200803655
41. Jeker, O. F.; Carreira, E. M. *Angew. Chem., Int. Ed.* **2012,** *51,* 3474–3477. doi:10.1002/anie.201109175
42. Barker, T. J.; Duncan, K. K.; Otrubova, K.; Boger, D. L. *ACS Med. Chem. Lett.* **2013,** *4,* 985–988. doi:10.1021/ml400281w
43. Leggans, E. K.; Duncan, K. K.; Barker, T. J.; Schleicher, K. D.; Boger, D. L. *J. Med. Chem.* **2013,** *56,* 628–639. doi:10.1021/jm3015684
44. Shigehisa, H.; Suwa, Y.; Furiya, N.; Nakaya, Y.; Fukushima, M.; Ichihashi, Y.; Hiroya, K. *Angew. Chem., Int. Ed.* **2013,** *52,* 3646–3649. doi:10.1002/anie.201210099
45. George, D. T.; Kuenstner, E. J.; Pronin, S. V. *J. Am. Chem. Soc.* **2015,** *137,* 15410–15413. doi:10.1021/jacs.5b11129
46. Ruider, S. A.; Sandmeier, T.; Carreira, E. M. *Angew. Chem., Int. Ed.* **2015,** *54,* 2378–2382. doi:10.1002/anie.201410419
47. Allemann, O.; Brutsch, M.; Lukesh, J. C.; Brody, D. M.; Boger, D. L. *J. Am. Chem. Soc.* **2016,** *138,* 8376–8379. doi:10.1021/jacs.6b04330
48. Waser, J.; Gaspar, B.; Nambu, H.; Carreira, E. M. *J. Am. Chem. Soc.* **2006,** *128,* 11693–11712. doi:10.1021/ja062355+
49. Mukaiyama, T.; Isayama, S.; Inoki, S.; Kato, K.; Yamada, T.; Takai, T. *Chem. Lett.* **1989,** *18,* 449–452. doi:10.1246/cl.1989.449
50. Inoki, S.; Kato, K.; Takai, T.; Isayama, S.; Yamada, T.; Mukaiyama, T. *Chem. Lett.* **1989,** *18,* 515–518. doi:10.1246/cl.1989.515
51. Isayama, S.; Mukaiyama, T. *Chem. Lett.* **1989,** *18,* 569–572. doi:10.1246/cl.1989.569
52. Isayama, S.; Mukaiyama, T. *Chem. Lett.* **1989,** *18,* 1071–1074. doi:10.1246/cl.1989.1071
53. Kato, K.; Yamada, T.; Takai, T.; Inoki, S.; Isayama, S. *Bull. Chem. Soc. Jpn.* **1990,** *63,* 179–186. doi:10.1246/bcsj.63.179
54. Isayama, S. *Bull. Chem. Soc. Jpn.* **1990,** *63,* 1305–1310. doi:10.1246/bcsj.63.1305
55. Gaspar, B.; Waser, J.; Carreira, E. M. *Synthesis* **2007,** 3839–3845. doi:10.1055/s-2007-1000817
56. Hunger, K.; Mischke, P.; Rieper, W.; Zhang, S. Azo Dyes. *Ullmann's Encyclopedia of Industrial Chemistr;* Wiley-VCH Verlag GmbH & Co. KGaA, 2000. doi:10.1002/14356007.o03_o07.pub2
57. Acton, Q. A. *Azo Compounds—Advances in Research and Application: 2013 Edition: ScholarlyBrief;* ScholarlyEditions: Atlanta, GA, 2013.

License and Terms

BEILSTEIN JOURNAL OF ORGANIC CHEMISTRY

Hydroarylations by cobalt-catalyzed C–H activation

Rajagopal Santhoshkumar and Chien-Hong Cheng*

Review

Open Access

Address:
Department of Chemistry, National Tsing Hua University, Taiwan

Email:
Chien-Hong Cheng* - chcheng@mx.nthu.edu.tw

* Corresponding author

Keywords:
catalysis; C−C formation; C–H activation; cobalt; hydroarylation

Beilstein J. Org. Chem. **2018,** *14,* 2266–2288.
doi:10.3762/bjoc.14.202

Received: 28 May 2018
Accepted: 02 August 2018
Published: 29 August 2018

This article is part of the thematic issue "Cobalt catalysis".

Guest Editor: S. Matsunaga

Abstract

As an earth-abundant first-row transition metal, cobalt catalysts offer a broad range of economical methods for organic transformations via C–H activation. One of the transformations is the addition of C–H to C–X multiple bonds to afford alkylation, alkenation, amidation, and cyclization products using low- or high-valent cobalt catalysts. This hydroarylation is an efficient approach to build new C–C bonds in a 100% atom-economical manner. In this review, the recent developments of Co-catalyzed hydroarylation reactions and their mechanistic studies are summarized.

Introduction

For the last three decades, atom-economical synthetic approaches have played a substantial role in organic synthesis owing to the necessity of green chemistry for the modern universe [1-3]. In this context, catalytic C–H functionalization has been acknowledged as an atom- and step-economical process [4-6]. A wide range of transition metal-catalyzed non-directed or directing group assisted C–H activation methodologies have been developed to build new C–X (X = carbon or heteroatom) bonds [7-10] and they offer efficient routes to the synthesis of natural products, materials, agrochemicals, polymers, and pharmaceuticals [11-15]. Specifically, the first-row transition metal catalysts, which are less expensive and more environmentally benign, have attracted significant attention in recent years [16-27]. As a member of the first-row transition metals, cobalt complexes are known to be extensively involved in homogeneous catalysis, in particular, C–H activation.

In 1941, Kharasch and Fields applied a cobalt salt as the catalyst for the homocoupling of Grignard reagents [28]. After 15 years, Murahashi discovered a cobalt-catalyzed chelation-assisted *ortho* C–H carbonylation of azobenzene and imines as the preliminary example of directing group assisted C–H activation reactions (Scheme 1) [29,30]. Following to these pioneering works, the groups of Kochi [31], Kisch [32], Klein [33,34], and Brookhart [35] have made their crucial contributions in the cobalt-mediated/catalyzed C–H functionalization. In recent years, Yoshikai [36], Kanai/Matsunaga [37], and

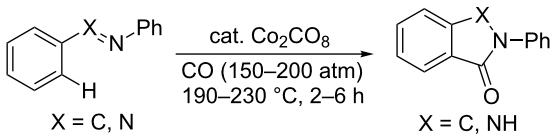

Scheme 1: Cobalt-catalyzed C–H carbonylation.

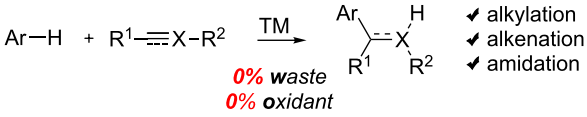

Scheme 2: Hydroarylation by C–H activation.

Daugulis [38] introduced different cobalt systems, which played a significant portion in C–H activation by its unique reactivity as an alternative to third-row noble metal catalysts [16,17,20-25]. Nakamura [39], Ackermann [40], and Glorius [41] also involved in cobalt-catalyzed C–H functionalization. Of these reactions, alkylation, alkenation, amidation, and cyclization of arenes with the relevant coupling partners are an economical and straightforward approach for the synthesis of diverse alkyls, alkenes, amides and cyclic compounds.

A simple addition of a "inert" C–H bond to multiple bonds (hydroarylation) is a 100% atom economical process to build fundamental alkyls and alkenes (Scheme 2) [42-45]. It is an efficient alternative to C–H alkylation reactions with alkyl halides where one equivalent of salt waste was released, and dehydrogenative Heck coupling with alkenes for the synthesis of alkenes, which required a stoichiometric amount of oxidant. Herein, we wish to review the cobalt-catalyzed hydroarylation of alkynes, alkenes, allenes, enynes, imines, and isocyanates.

These reactions usually proceed via either an oxidative addition of Ar–H to a low-valent cobalt to form **A1** intermediate or a C–H activation with high-valent cobalt to give **A2** via deprotonation, followed by migratory insertion and reductive elimination or protonation (Scheme 3). We believe that this review will be helpful to the researchers for their future research on hydroarylation using earth-abundant metal catalysts.

Review

1. Hydroarylation of alkynes

1.1 Low-valent cobalt-catalyzed hydroarylation of alkynes

Hydroarylation of alkynes is an efficient method to synthesize aromatic alkenes in a highly atom-economical way [44]. In 1994, Kisch and co-workers developed the first cobalt-catalyzed hydroarylation of alkynes with azobenzenes **1** to synthesize dialkenated products **2** (Scheme 4) [32]. The reaction resulted in an *anti*-addition of the C–H bond with alkynes using the cobalt(I) catalysts $CoH(N_2)(PPh_3)_3$ or $CoH_3(PPh_3)_3$ under neat reaction conditions.

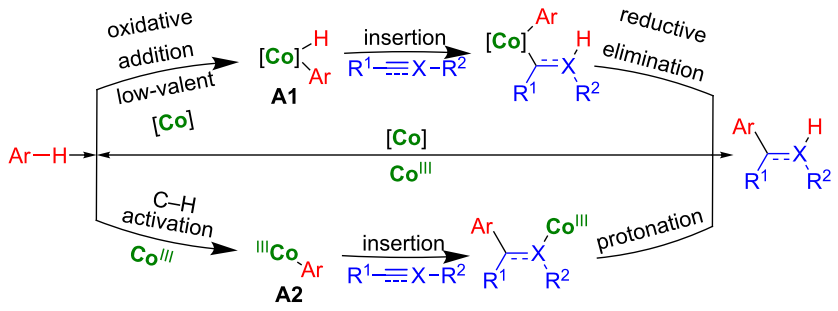

Scheme 3: Pathways for cobalt-catalyzed hydroarylations.

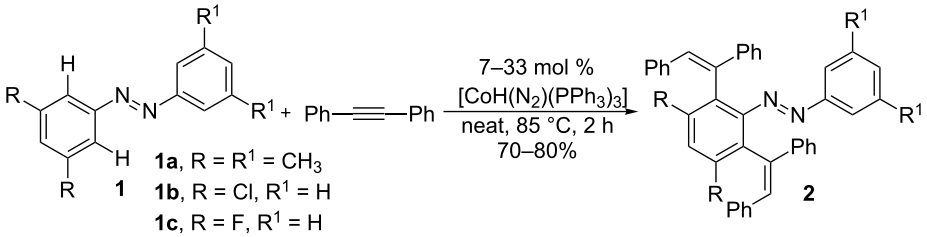

Scheme 4: Co-catalyzed hydroarylation of alkynes with azobenzenes.

After fifteen years, Yoshikai and co-workers developed a low-valent cobalt system for C–H functionalization [16,36]. Thus, the reaction of 2-aryl pyridines **3** with internal alkynes in the presence of 10 mol % $CoBr_2$, 20 mol % $PMePh_2$, and 1 equiv of MeMgCl as a reductant yielded *ortho* alkenated products **4** with high regio- and stereoselectivities (Scheme 5) [36]. The found intermolecular kinetic isotope effect (KIE) of k_H/k_D = 2.1 and H/D crossover studies strongly suggest that the reaction proceeds through an oxidative addition of a C–H bond to low-valent cobalt followed by alkyne insertion and reductive elimination. Furthermore, the new C–C bond formation occurred at the less-hindered carbon of the unsymmetrical alkynes, which causes the high regioselectivity.

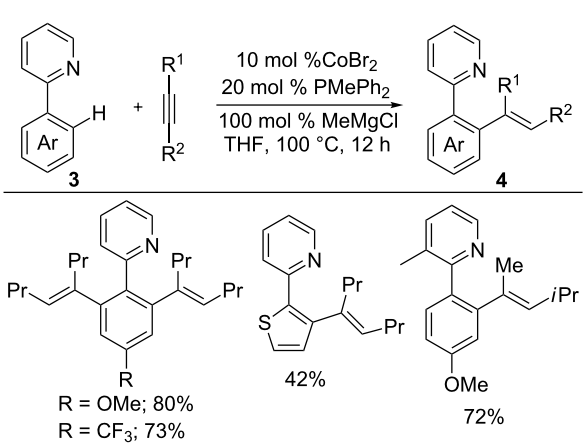

Scheme 5: Co-catalyzed hydroarylation of alkynes with 2-arylpyridines.

Later, they proved that the hydroarylation reaction was also feasible with benzoxazoles **5** to form alkenated products **6** using $CoBr_2$, bis[(2-diphenylphosphino)phenyl] ether (DPEphos), Grignard reagent, and pyridine as an additive (Scheme 6) [46]. Similarly, benzothiazoles also efficiently underwent hydroheteroarylation by using suitable ligands [47]. The reaction was successfully extended to indoles and benzimidazoles **7** bearing a removable 2-pyrimidyl (2-pym) directing group with alkynes at ambient temperature (Scheme 7) [48]. These reactions resemble the Ni(0)-catalyzed hydroheteroarylation reaction [49].

In addition, imines **9** and **11** bearing a *p*-methoxyphenyl (PMP) group were also treated with internal alkynes in the presence of

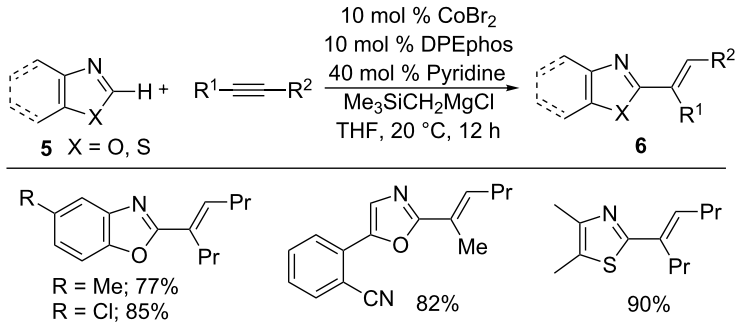

Scheme 6: Co-catalyzed addition of azoles to alkynes.

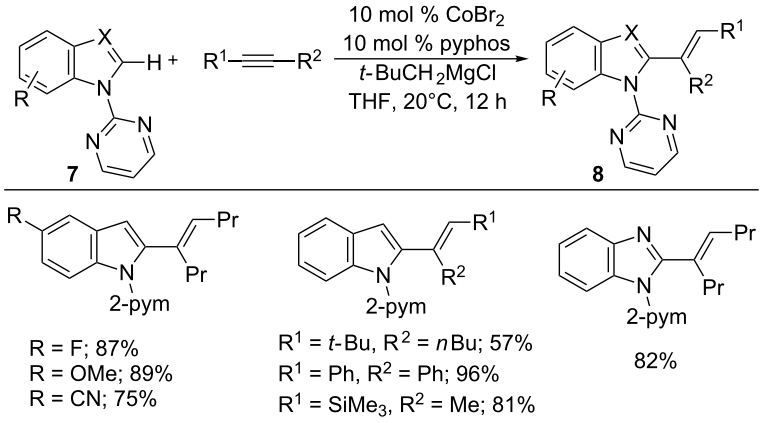

Scheme 7: Co-catalyzed addition of indoles to alkynes.

a cobalt catalyst generated from $CoBr_2$, P(3-$ClC_6H_4)_3$, and *t*-$BuCH_2MgBr$ at room temperature to give trisubstituted alkenes **10** and **12** in good yields (Scheme 8) [50,51]. The reaction featured a broad scope of alkynes and imines. The *ortho* alkenated imines could be further transformed into useful products, such as aminoindanols and benzofulvenes under hydrolysis conditions. Based on the mechanistic studies, a possible reaction mechanism for the hydroarylation reaction was proposed in Scheme 9. The reaction begins with the generation of an ambiguous low-valent cobalt catalyst from the reaction of $CoBr_2$, ligand and Grignard reagent, which gives the alkane and MgX_2 as the by-products. Then, coordination of the alkyne with the cobalt catalyst afforded **B1** and the oxidative addition of C–H gave the cobalt complex **B2**. Intramolecular insertion of the Co–H bond into the alkyne and subsequent reductive elimination of the less-hindered alkenyl carbon with aryl group in **B3** provides the desired alkene **10** and regenerates the active cobalt catalyst for the next cycle.

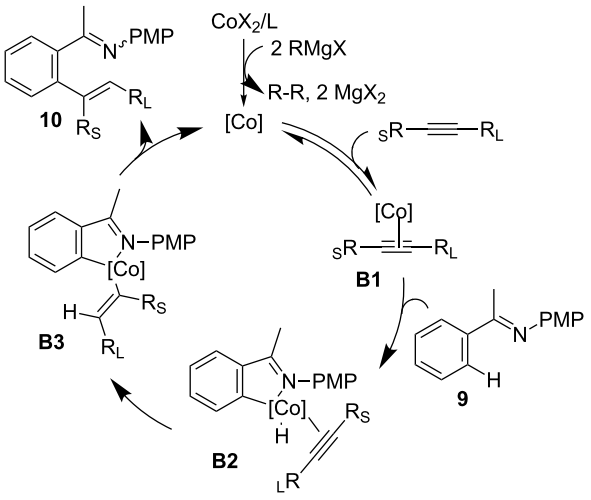

Scheme 9: A plausible pathway for Co-catalyzed hydroarylation of alkynes.

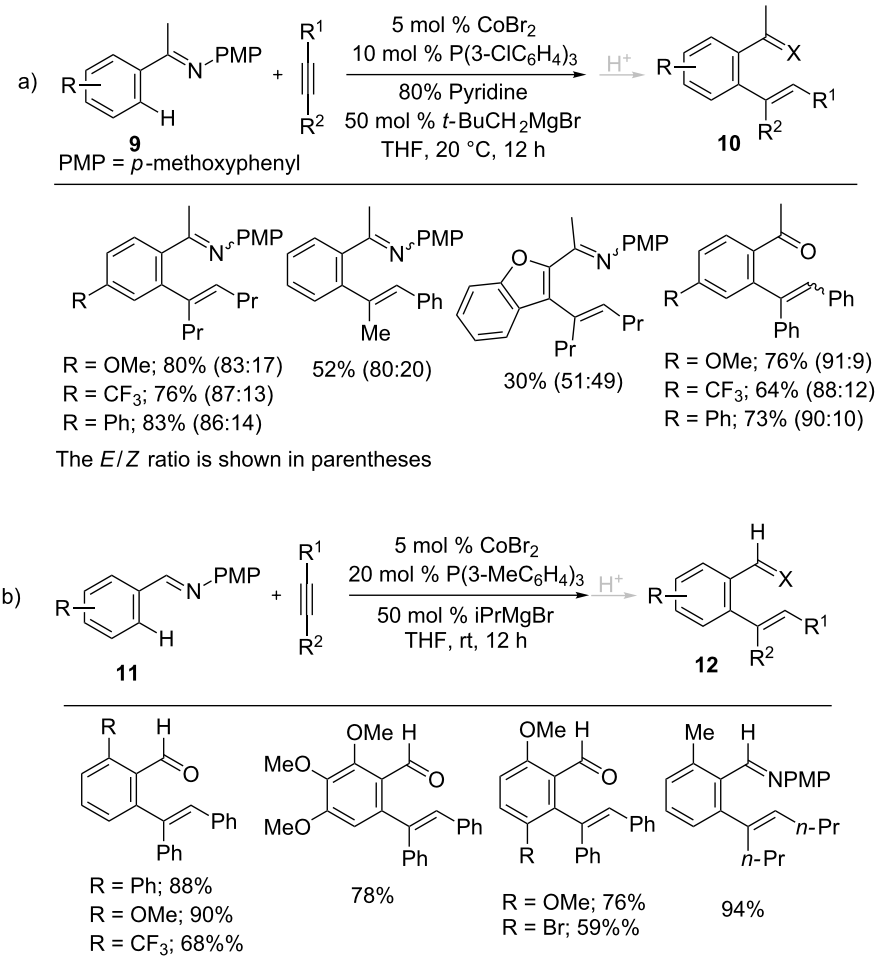

Scheme 8: Co-catalyzed hydroarylation of alkynes with imines.

In 2015, Petit's group developed a hydroarylation reaction of internal alkynes with imines using a low-valent cobalt catalyst without reductant or additives (Scheme 10) [52]. The reaction afforded alkenes **13** in excellent yields with *anti*-selectivity. The alkene product originally should be *syn*-**13**, but it rearranged to *anti*-**13** at the high reaction temperature likely catalyzed by the cobalt complex. Moreover, the found intermolecular KIE of 1.4 and density functional theory (DFT) calculations strongly suggest that the reaction proceeds through concerted hydrogen transfer by an oxidative pathway, reductive elimination, and subsequent isomerization.

1.2 Co(III)-catalyzed hydroarylation of alkynes

In 2013, Kanai/Matsunaga and co-workers developed an air-stable Co(III)Cp* catalyst as an economical alternative to Cp*Rh(III) for C–H functionalization [37]. The Co(III) catalyst was applied for the hydroarylation of alkynes with indoles **14** to form alkenes **15** with linear selectivity (Scheme 11) [53]. The reaction features a broad substrate scope including a variety of indoles, terminal and internal alkynes, mild reaction conditions and inexpensive catalyst. The reaction proceeds through an amide-assisted C–H metalation followed by alkyne insertion and protonation [54]. The reaction also acknowledged that the Co(III) species possess unique nucleophilic reactivity compared with the Rh(III) species for the annulation reaction. The hydroarylation reaction further extended to pyrroles for selective monoalkenylation using $[Cp^*Co(CH_3CN)_3](SbF_6)_2$ as the catalyst [55].

In contrast, branched-selective hydroarylation of terminal alkynes was achieved by Li et al. The addition of arenes **7** to propargyl alcohols, protected propargyl amines, and silyl alkynes in the presence of $CoCp^*(CO)I_2$ catalyst gave uncommon branched-selective products **16** in good yields with reasonable selectivity (Scheme 12) [56]. DFT calculations indicated that the regioselectivity of silyl alkynes was controlled by its steric effect in the protonolysis step, whereas the electronic nature of propargyl alcohols and amines played a key role in the selectivity control during the insertion. Moreover, the control experiments and DFT calculations show that HOPiv played a crucial role in both the C−H activation and the protonolysis step.

In 2016, Yu and co-workers developed a hydroarylation of alkynes with different arenes including phenylpyridines, pyrazole, and 6-arylpurines **17** using 5 mol % $Cp^*Co(CO)I_2$,

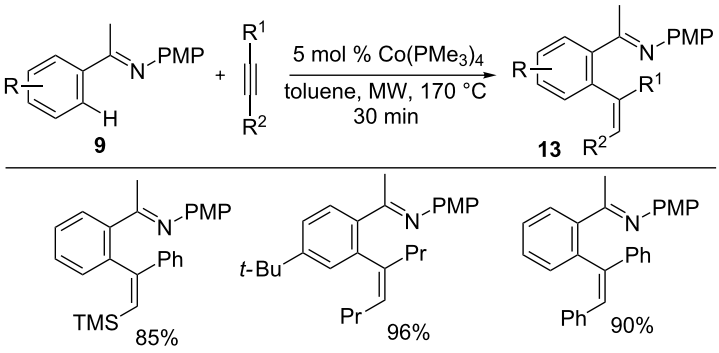

Scheme 10: Co-catalyzed *anti*-selective C–H addition to alkynes.

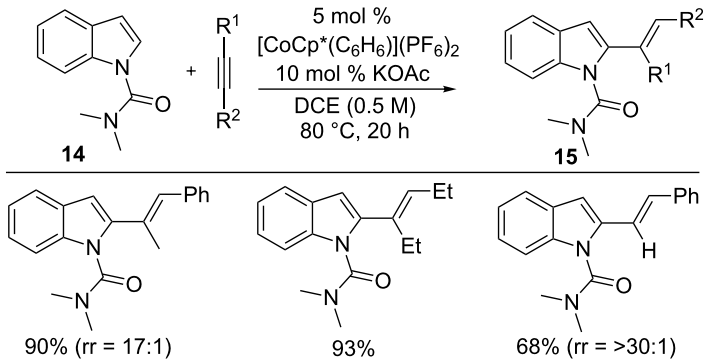

Scheme 11: Co(III)-catalyzed hydroarylation of alkynes with indoles.

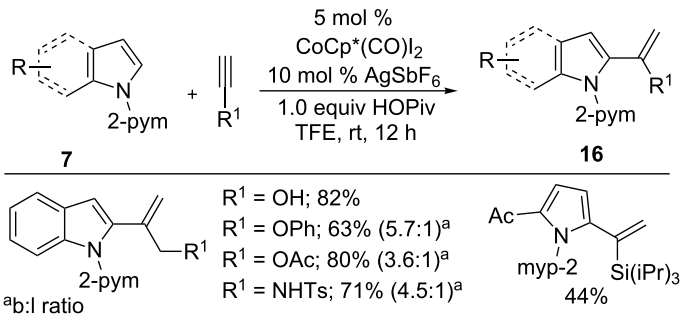

Scheme 12: Co(III)-catalyzed branch-selective hydroarylation of alkynes.

10 mol % $AgSbF_6$, and 0.5 equiv PivOH in DCE (Scheme 13) [57]. The reaction proceeded efficiently with various alkynes to give alkenes **18**, however, the reaction was limited to terminal alkynes. Additionally, they applied this methodology to design a mitochondria-targeted imaging dye from electron-withdrawing formyl-substituted indoles and alkynes.

Later, Maji's group reported an *N*-*tert*-butyl amide-directed mono- and di-alkenylation reactions using a cobalt catalyst (Scheme 14) [58]. The reaction was also applied for the preparation of π-conjugated alkenes by four-fold C–H activation, which was found to be fluorescence active. The KIE studies provided k_H/k_D of 2.8 and 2.6 through intermolecular and intra-

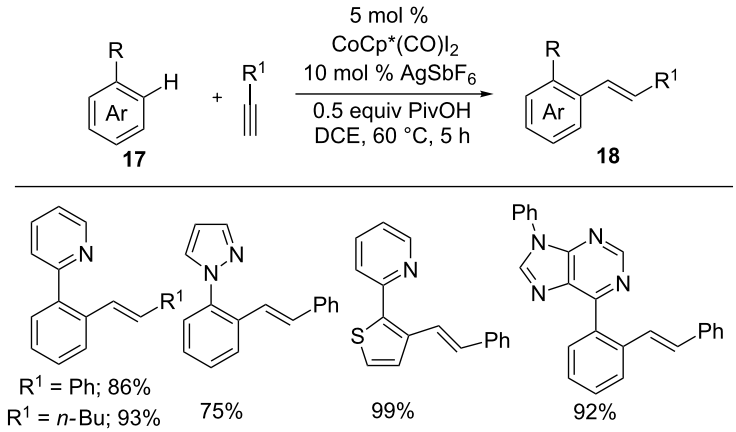

Scheme 13: Co(III)-catalyzed hydroarylation of terminal alkynes with arenes.

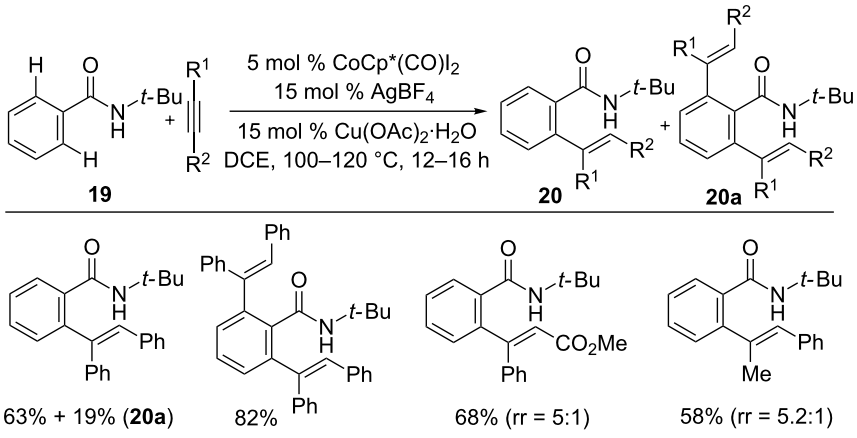

Scheme 14: Co(III)-catalyzed hydroarylation of alkynes with amides.

molecular experiments, respectively. These results strongly suggest that the C–H activation may be involved in the rate-limiting step. It is noteworthy that the reaction is limited to internal alkynes.

Recently, Sundararaju and co-workers developed a Co-catalyzed hydroarylation reaction of alkynes with phenylpyrazoles **21** (Scheme 15) [59]. The reaction exhibited tolerance toward a variety of functionalities on arenes as well as alkynes. The isolated cationic cobalt intermediate (**C3**) and the mechanistic studies strongly indicate that the reaction proceeds through C–H activation via concerted metallation-deprotonation (CMD) to form cobaltacycle **C1.** Subsequently, alkyne coordination (**C2**) and migratory insertion of alkyne provide alkenyl intermediate **C3**. Finally, protonolysis gives the desired alkene product **22** and regenerates the active cobalt(III) catalyst for the next cycle.

2. Hydroarylation of alkenes

2.1 Low-valent cobalt-catalyzed hydroarylation of alkenes

As alkynes efficiently participated in low-valent cobalt-catalyzed hydroarylations (section 1.1), Nakamura and co-workers developed an analogous hydroarylation reaction of alkenes [39]. Thus, the reaction of amides **23** with alkenes in the presence of 10 mol % $Co(acac)_3$, 1.5 equiv CyMgCl, and 6.0 equiv DMPU provided C–H alkylated products **24** in good yields with high linear selectivity (Scheme 16).

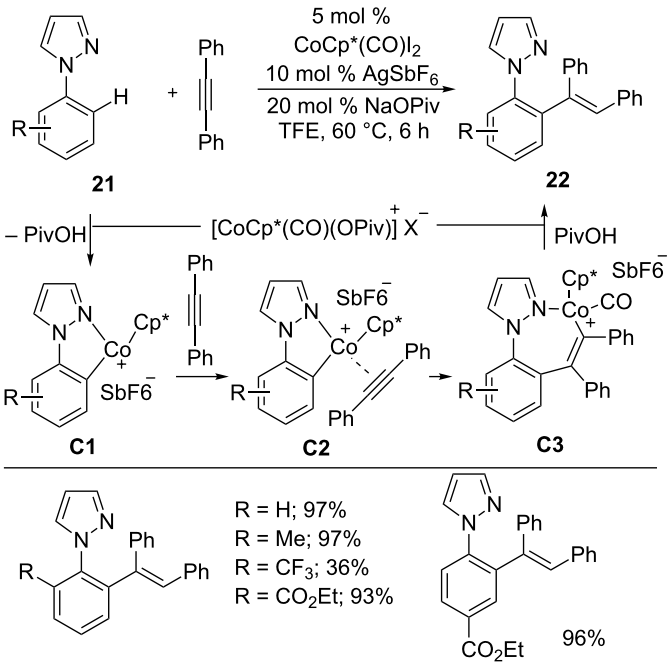

Scheme 15: Co(III)-catalyzed C–H alkenylation of arenes.

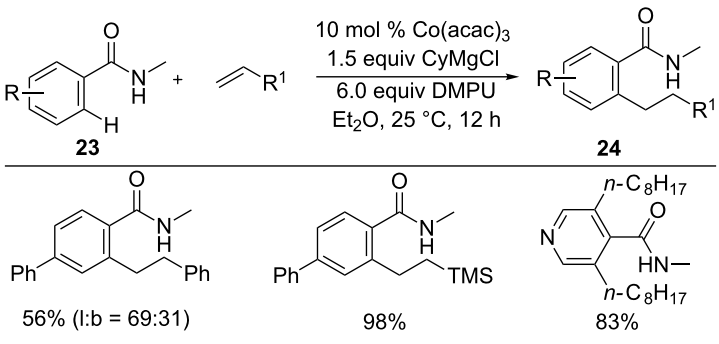

Scheme 16: Co-catalyzed alkylation of substituted benzamides with alkenes.

Later, Yoshikai's group reported a ligand-controlled hydroarylation of styrenes with 2-phenylpyridines **3** in the presence of $CoBr_2$-IMes and $CoBr_2$-PCy_3 catalysts to synthesize linear and branched selective products **25** and **26**, respectively, in good yields with high selectivity control (Scheme 17) [60]. It is noteworthy that the electronic nature of the substrates also controlled the addition selectivity; electron-withdrawing group (CF_3 and F) substituted arenes **3** favored branched addition product **26** in both catalytic systems.

Similarly, imines **9** were employed for the hydroarylation reaction to form linear or branched addition products by tuning ligands and additives. Thus, the reaction of imines **9** with vinylsilanes as well as alkyl alkenes gave linear addition products **27a,b** under mild reaction conditions (Scheme 18a,b) [61]. The addition of indoles to vinylsilanes also succeeded in a similar manner [62]. When styrenes were employed for the hydroarylation with imines **9**, the reaction required 4.0 equiv of 2-methoxypyridine as the additive in the presence of $CoBr_2$, [bis(2,4-dimethoxyphenyl)(phenyl)phosphine] and CyMgBr to afford linear-selective products **27c** (Scheme 18c) [63].

Recently, N–H imines **9d** has also become an efficient directing group for the hydroarylation reaction. The addition of N–H imines **9d** to vinylsilanes or alkyl alkenes was achieved using a low-valent cobalt catalyst to form alkylated products **27d** (Scheme 19) [64]. The N–H imines overcame substrate scope limitation from previous reports with *N*-aryl and *N*-alkylimines. Moreover, multiple C–H alkylation was also succeeded with benzophenone imines in high yields with linear selectivity under the mild reaction conditions.

In contrast, the addition of ketimines **9** to styrenes gave branched selective alkylation products **28** in the presence of the catalyst system $CoBr_2$/P(4-FC_6H_4)$_3$ and CyMgBr (Scheme 20a) [65]. In a similar manner, aldimines **9** also reacted with styrenes to give branched-selective alkyls **28a** under modified reaction conditions (Scheme 20b) [66]. Moreover, the Co-catalyzed hydroarylation of styrene with ketimine or aldimine proceeded without Grignard reagent using Mg metal as the reductant [67]. Recently, N–H imines **9d** were also employed for the hydroarylation reaction with styrenes, giving a branched-selective hydroarylation product in good yields [68].

Based on the mechanistic studies and DFT calculations [69], a plausible mechanism for the cobalt-catalyzed ligand-controlled hydroarylation of alkenes was proposed in Scheme 21. The reaction begins with the generation of low-valent cobalt from $CoBr_2$, ligand, and Grignard reagent. Then, imine **9** assisted an *ortho* C–H metallation by oxidative addition and provides Co–H intermediate **D1**. Coordination of alkene with **D1** and insertion of the alkene to Co–H gives intermediate **D3** or **D3'**, which is converted into product **27** or **28** and low-valent cobalt by reductive elimination.

Indoles also efficiently participated in intra- and intermolecular hydroarylation reactions to access useful organic skeletons [70-73]. Thus, the reaction of indole bearing an aldimine and homoallyl group **29** in the presence of $CoBr_2$, SIMes·HCl and Me_3SiCH_2MgCl gave dihydropyrroloindoles **30**, whereas the IPr·HCl ligand provided tetrahydropyridoindoles **31** in reasonable regioselectivity (Scheme 22) [70]. Remarkably, the regioselectivity of the reaction is not only controlled by the steric effect of NHC ligand, but also depends on the olefin tether in **29**. Recently, Petit and co-workers also developed an intra- and intermolecular hydroarylation of indoles using $Co(PMe_3)_4$ as the catalyst under Grignard-free conditions [72].

In 2015, an asymmetric hydroarylation of styrenes with indoles was reported by Yoshikai and co-workers (Scheme 23) [73].

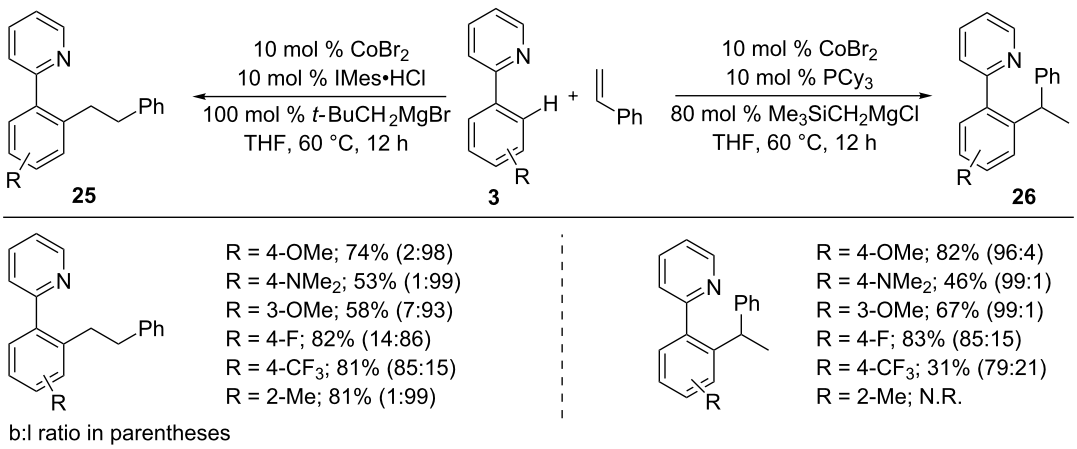

Scheme 17: Co-catalyzed switchable hydroarylation of styrenes with 2-aryl pyridines.

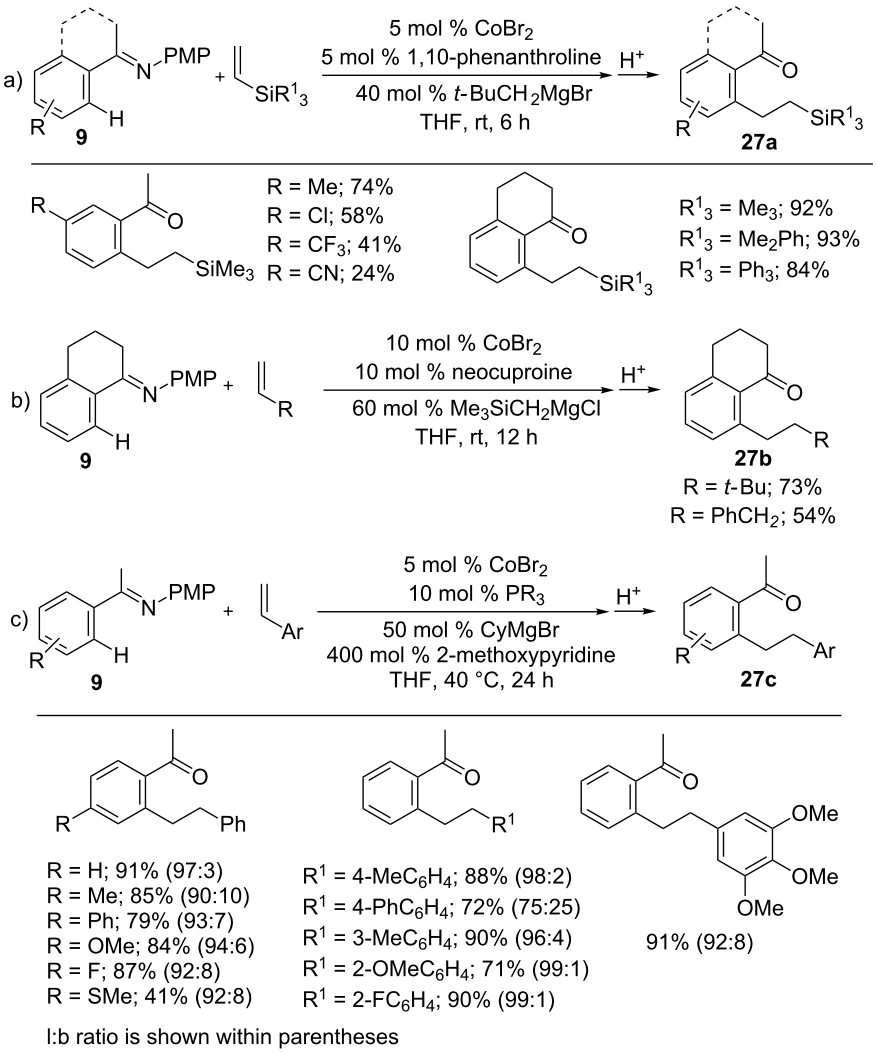

Scheme 18: Co-catalyzed linear-selective hydroarylation of alkenes with imines.

Among varies *N*-protected indoles, *N*-Boc indoles **32** in the presence of $Co(acac)_3$ and phosphoramidite ligand **L** afforded alkylated products **33** in high yields and enantioselectivity. A wide range of indoles and styrenes were well tolerated to form the corresponding alkyl products **33** in a branched selective manner.

In addition to the directing group strategies, remote C4-selective alkylation of pyridines [74] was also feasible with alkenes as Kanai et al. reported (Scheme 24a) [75]. The addition of pyridine (**34**) to alkenes in the presence of 1 mol % $CoBr_2$, 20 mol % BEt_3, and $LiBEt_3H$ as a hydride source provided branched-selective products **35a** with styrenes, while alkylalkenes resulted in linear-selective products **35b**. Similarly, quinolines **34a** also underwent hydroarylation reaction with styrene to give C4-selective alkylated products **36** in good regioselectivity (Scheme 24b) [76].

2.2 Co(III)-catalyzed hydroarylation of alkenes

In 2013, Kanai/Matsunaga and co-workers reported a hydroarylation reaction of activated alkenes with phenyl pyridines **3** in the presence of the air-stable $[Co(III)Cp^*(benzene)](PF_6)_2$ catalyst, giving hydroarylation products **37** in good yields (Scheme 25) [37]. The reaction proceeds through directed *ortho* C–H metallation to form five-membered cobaltacycle **E1** and alkene insertion to give complex **E2**. Protonation then provides product **37** and an active Co(III) catalyst for the next cycle.

Terminal alkenes were also applied in hydroarylation reaction as Sundararaju and co-workers demonstrated (Scheme 26a) [77]. Likewise, Whiteoak's group reported a cobalt-catalyzed hydroarylation of terminal alkenes with amides **39** [78]. The reaction of vinyl ketones with amides provided alkylated product **40**, whereas acrolein resulted in biologically useful azepinones in good yields (Scheme 26b).

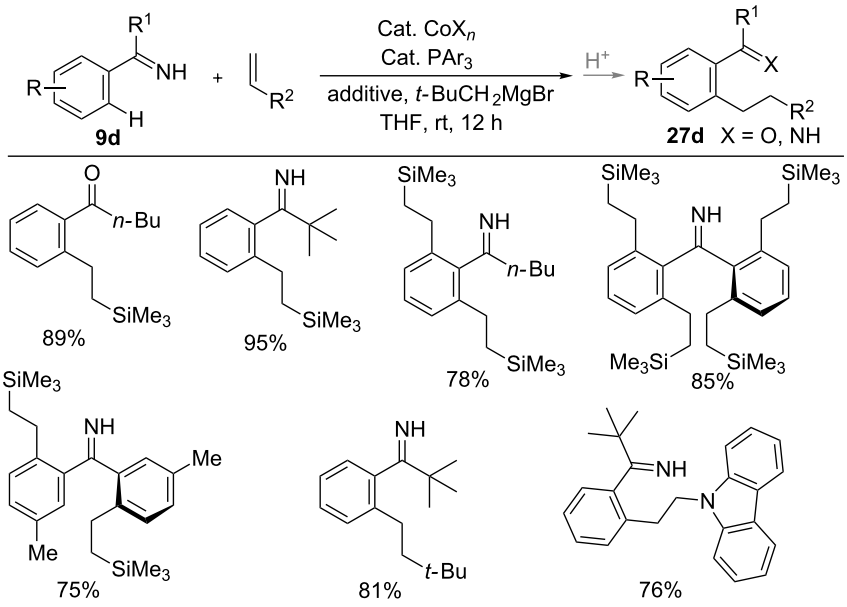

Scheme 19: Co-catalyzed linearly-selective hydroarylation of alkenes with N–H imines.

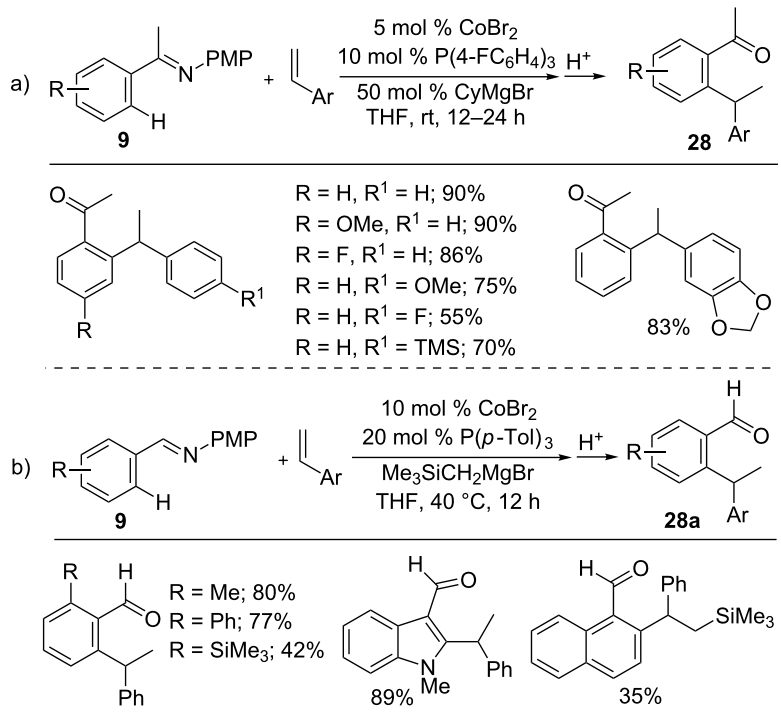

Scheme 20: Co-catalyzed branched-selective hydroarylation of alkenes with imines.

N-Pyrimidylindole is a highly reactive arene in cobalt-catalyzed C–H functionalizations. In this context, Li and co-workers developed an addition reaction of indoles **7** with activated alkenes using a cobalt(III) catalyst (Scheme 27) [79]. The reaction tolerated a wide range of alkenes including vinyl aldehyde, ketones, and divinyl ketones and a variety of arenes to give C2-alkylation products **41** in good yields.

Similarly, alkylalkenes were subjected to hydroarylation with indoles by Ackermann et al. [80]. The addition of indoles **42**

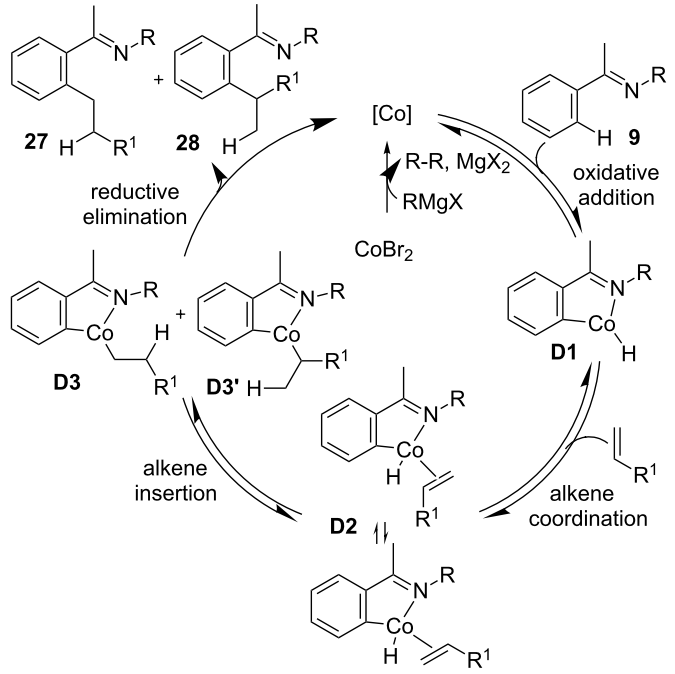

Scheme 21: Mechanism of Co-catalyzed hydroarylation of alkenes.

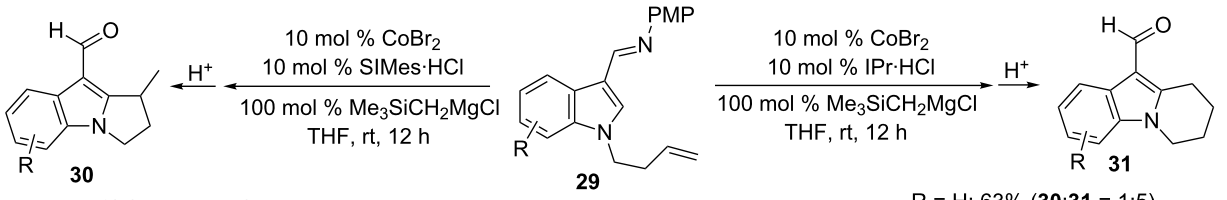

R = H; 84% (**30**:**31** = 8:1)
R = 5-OMe; 56% (**30**:**31** = 5.2:1)
R = 6-F; 82% (**30**:**31** = 9:1)
R = 7-Me; 62% (**30**:**31** = 4.1:1)

R = H; 63% (**30**:**31** = 1:5)
R = 5-OMe; 45% (**30**:**31** = 1:2.2)
R = 6-F; 71% (**30**:**31** = 1:2.5)
R = 7-Me; 59% (**30**:**31** = 1:2.3)

Scheme 22: Co-catalyzed intramolecular hydroarylation of indoles.

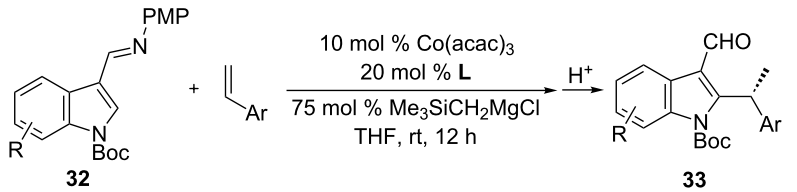

R^1 = OMe; 88% (86% ee)
R^1 = F; 63% (80% ee)

R = F; 72% (87% ee)
R = Cl; 45% (83% ee)

Scheme 23: Co-catalyzed asymmetric hydroarylation of alkenes with indoles.

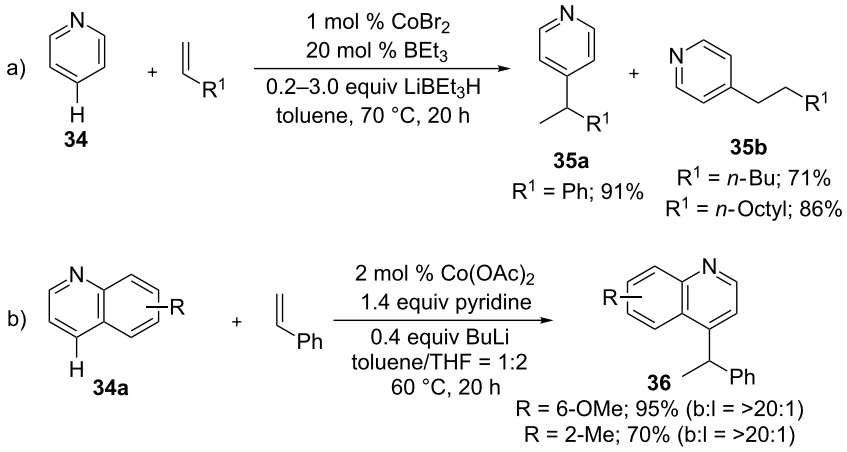

Scheme 24: Co-catalyzed hydroarylation of alkenes with heteroarenes.

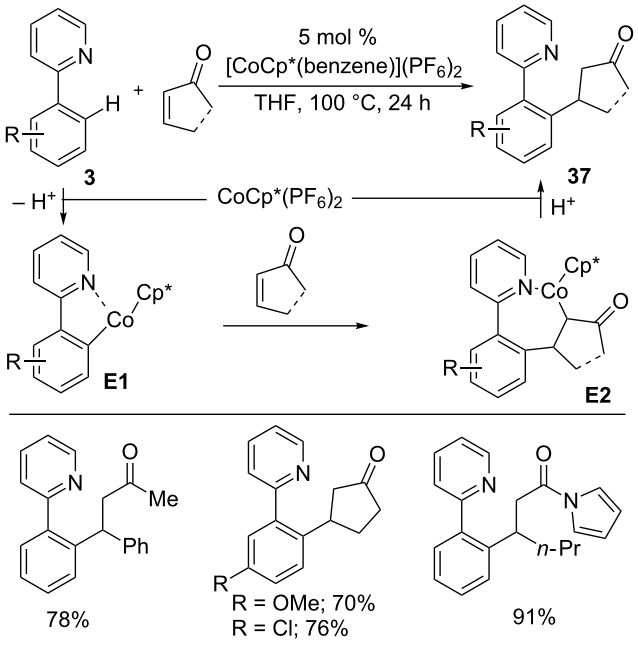

Scheme 25: Co(III)-catalyzed hydroarylation of activated alkenes with 2-phenyl pyridines.

into alkylalkenes in the presence of 10 mol % $CoCp^*(CO)I_2$, 20 mol % $AgSbF_6$ at 120 °C gave linear-selective products **43**, whereas additional 1.0 equiv 1-$AdCO_2H$ at 50 °C resulted in predominantly branched-selective products **44** (Scheme 28). The reaction features switchable regioselectivity, a broad scope, and an inexpensive catalyst. Moreover, DFT calculations and mechanistic studies revealed that the switchable regioselectivity was driven by a change in mechanism from linear ligand-to-ligand hydrogen transfer to branched base-assisted internal electrophilic-type substitution.

In addition to activated and unactivated alkylalkenes, vinylcyclopropanes also underwent hydroarylation reactions with indoles **42** via C–H/C–C activation (Scheme 29a) [81]. The reaction afforded allylated products **45** in high stereoselectivities. DFT calculations and mechanistic studies strongly indicate that the reaction proceeds through the generation of complex **F1** by pyridine-directed C–H activation. Subsequently, alkene insertion with **F1** and C–C activation of **F2** give intermediate **F3**. Finally, protonolysis provides the desired product **45** and an active Co(III)Cp*. Due to the low activation energy, the

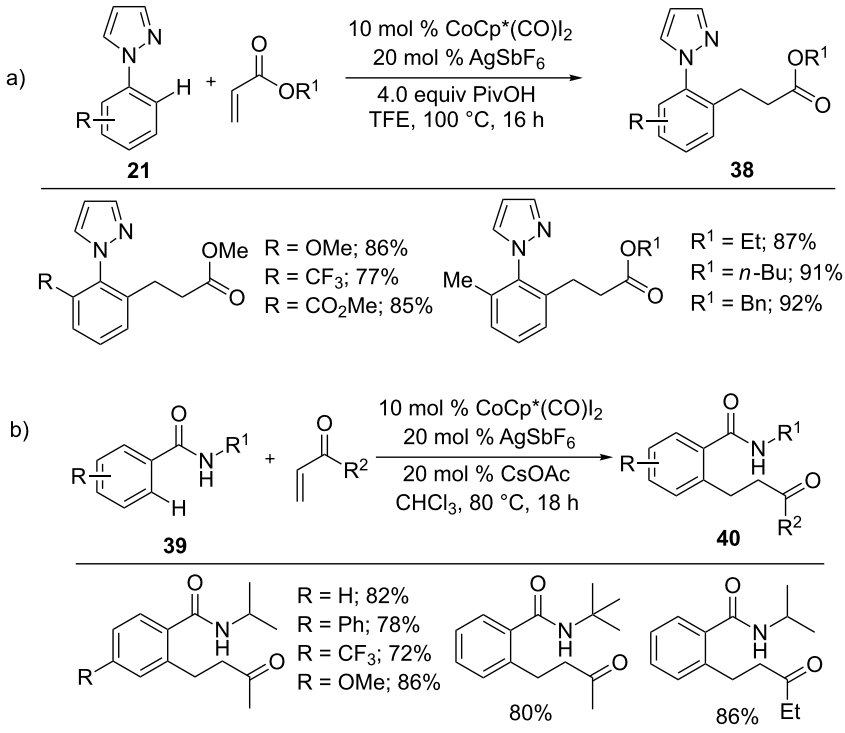

Scheme 26: Co(III)-catalyzed C–H alkylation of arenes.

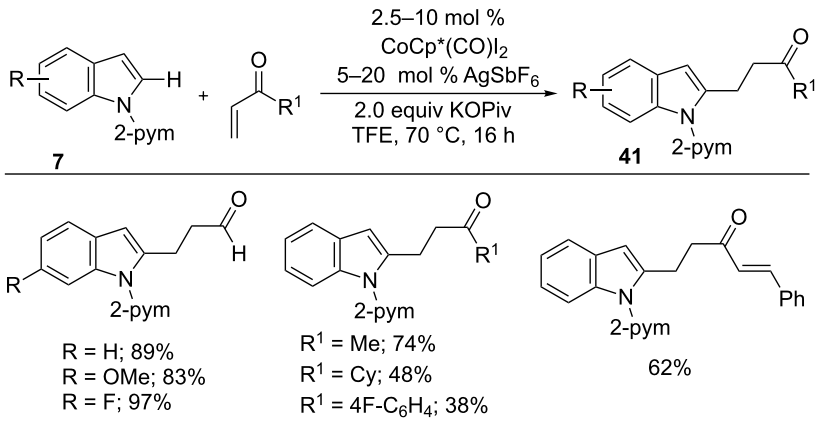

Scheme 27: Co(III)-catalyzed C2-alkylation of indoles.

thermodynamically less stable *Z* diastereomer is preferred in the reaction, which is in contrast to the rhodium(III)-catalyzed reaction [82]. Later, Li and co-workers developed a cobalt-catalyzed hydroarylation of 2-vinyloxiranes with indoles **7** to form C2-allylated products **46**, albeit in low stereoselectivity (Scheme 29b) [83]. Similarly, Cheng et al. reported a hydroarylation reaction of arenes **7** with a bicyclic alkene to form ring-opening products **47** via C–H/C–O activation (Scheme 29c) [84]. The product **47** was further converted into the C–H naphthylation product in the presence of an acid.

Maleimides turned out to be an efficient coupling partner in C–H functionalization to synthesize biologically useful succinimides in highly atom-economical manner. Thus, Li et al. developed a cobalt-catalyzed hydroarylation of maleimides and maleate esters with arenes **48** (Scheme 30) [85]. A variety of arenes including indoles, 2-arylpyridines, 6-arylpurine, and vinyl pyridines were employed to give alkylated products **49** in good to moderate yields. As well, Prabhu and co-workers also reported a Co-catalyzed hydroarylation reaction of maleimides with indoles [86].

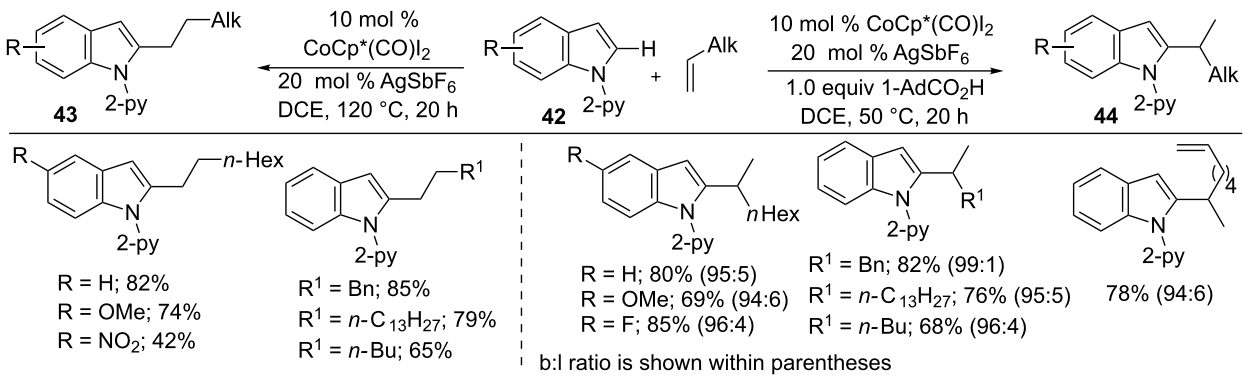

Scheme 28: Co(III)-catalyzed switchable hydroarylation of alkyl alkenes with indoles.

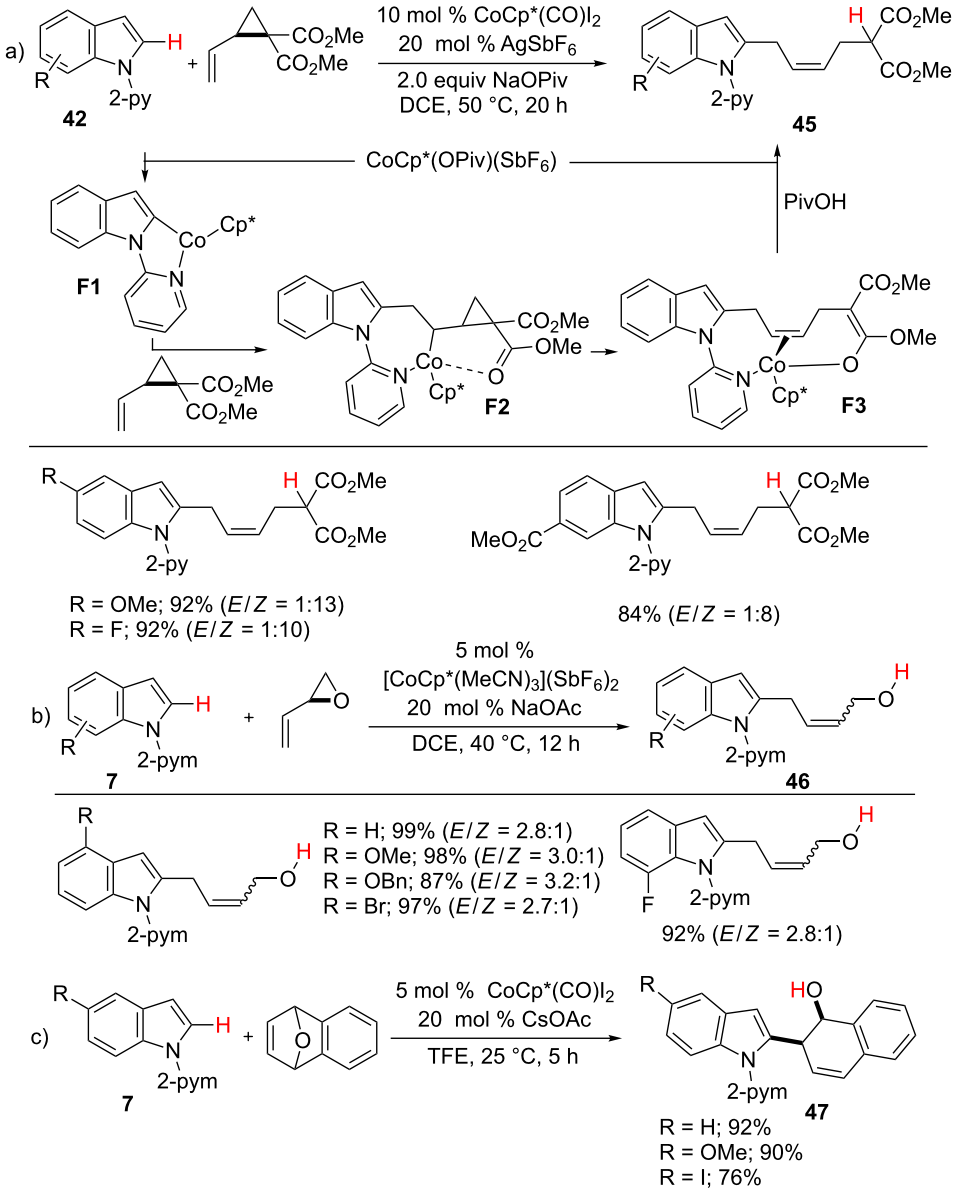

Scheme 29: Co(III)-catalyzed C2-allylation of indoles.

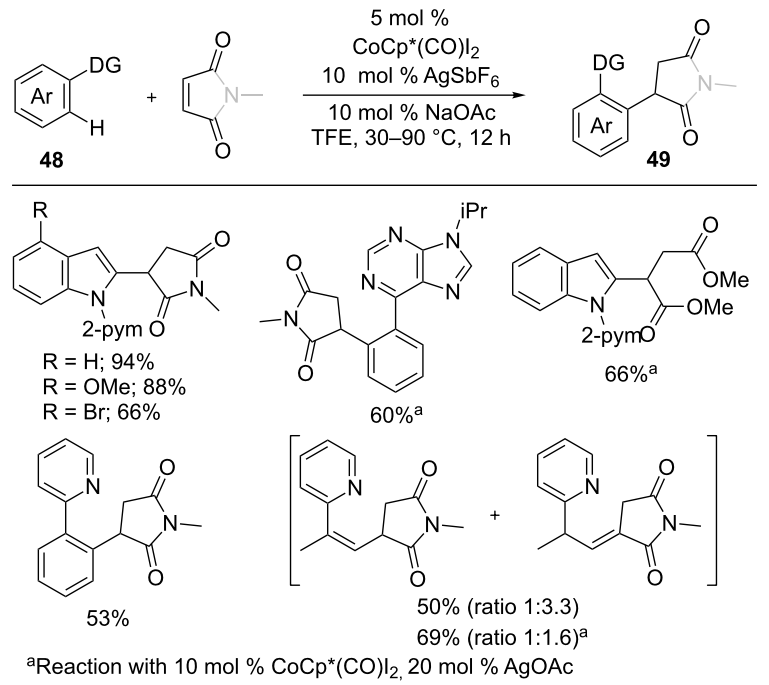

Scheme 30: Co(III)-catalyzed *ortho* C–H alkylation of arenes with maleimides.

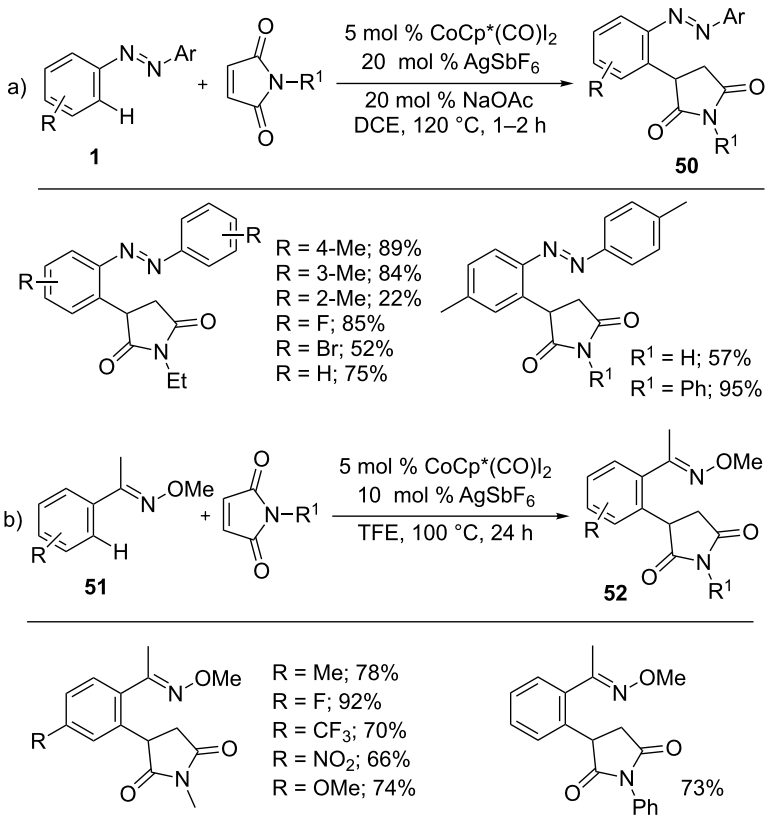

Scheme 31: Co(III)-catalyzed hydroarylation of maleimides with arenes.

The hydroarylation of maleimides was further demonstrated with different arenes (Scheme 31). Thus, azobenzenes **1** were subjected to alkylation reaction with maleimides to form a variety of succinimides **50** in good yields (Scheme 31a) [87]. Likewise, oximes **51** [88] were also efficient participated in the hydroarylation of maleimides (Scheme 31b).

3. Hydroarylation of allenes

An allene is an exceptional functional group in organic synthesis due to its cumulative double bonds [89,90]. In this context, Ackermann and co-workers developed a coupling reaction of arenes **53** with allenes to give hydroarylation products **54** (Scheme 32) [91]. The merits of the reaction are broad scope including a variety of arenes and allenes, and high atom economy. Based on the mechanistic studies and DFT calculations, a plausible mechanism was proposed. The reaction starts with the generation of the active cobalt(III) species **G1** from [Cp*CoI_2(CO)], $AgSbF_6$, and arene **53**. Subsequently, C–H metallation of **G1** by ligand-to-ligand hydrogen transfer provides cobaltacycle **G2** and an allene insertion gives intermediate **G3**. Protonation and isomerization generate cobalt complex **G4**, which is converted into alkenated product **54** by ligand exchange.

4. Hydroarylation of enynes

Catalytic cyclization of 1,*n*-enynes has become as an attractive tool for the preparation of cyclic adducts with a variety of functionalities in a one-pot process [92]. As the cyclization of 1,*n*-enynes with organometallics is well-known, the addition of an inert C–H bond to 1,*n*-enynes further enhances the economy of cyclization process. Thus, Cheng and co-workers reported a cobalt-catalyzed hydroarylative cyclization of 1,*n*-enynes with carbonyl compounds **55** to form a wide range of functionalized dihydrofurans and pyrrolidines **56** in good yields (Scheme 33a)

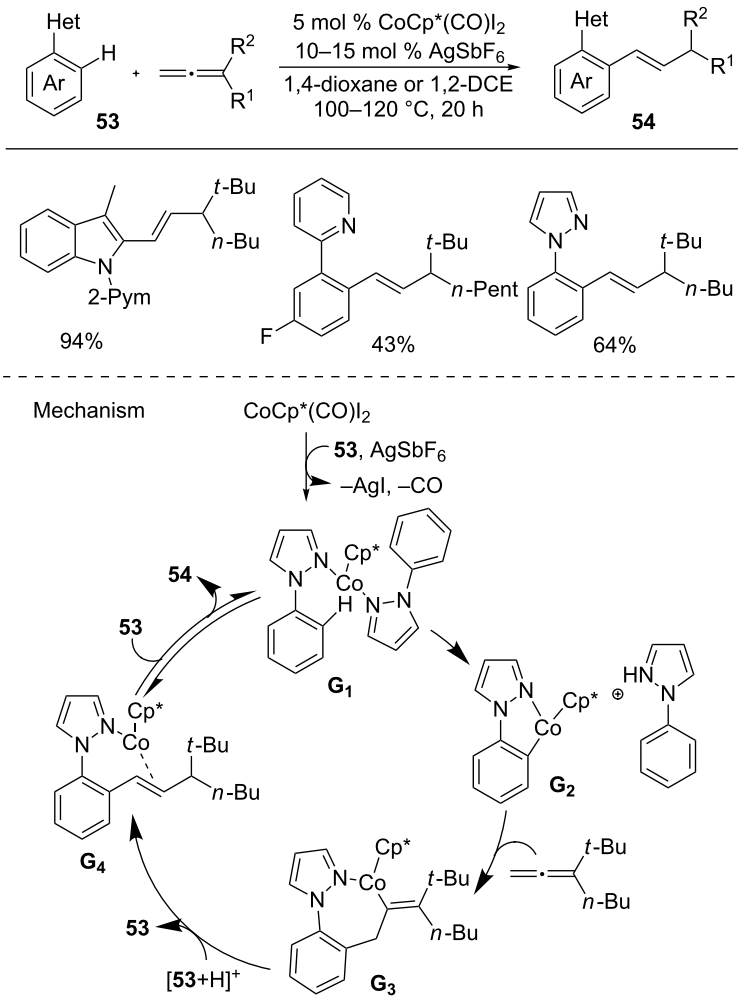

Scheme 32: Co(III)-catalyzed hydroarylation of allenes with arenes.

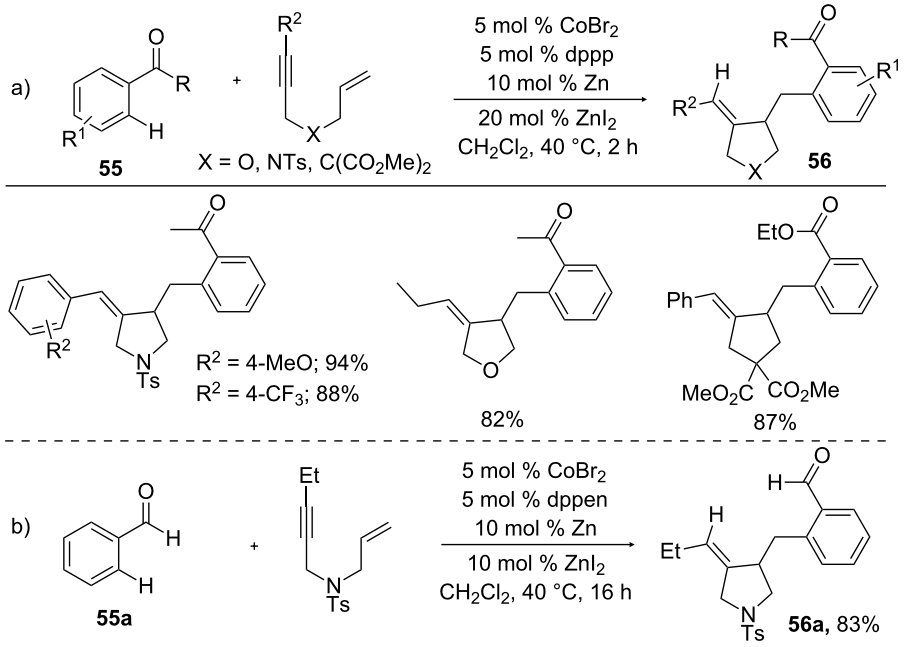

Scheme 33: Co-catalyzed hydroarylative cyclization of enynes with carbonyl compounds.

[93]. By tuning the diphosphine ligands, the reaction was extended to aromatic aldehyde **55a**, where slightly electron-deficient ethylene diphosphine ligand delivered hydroarylation product **56a**, but a mild electron-rich ligand resulted in hydroacylation product (Scheme 33b) [94].

A plausible mechanism for the hydroarylative cyclization of enynes was shown in Scheme 34. The reaction begins with the reduction of Co(II) to Co(I) by Zn dust. The enyne compound underwent oxidative addition with Co(I) to form bicyclic cobaltacycle **H1**. After the reversible coordination of arene **55** with **H1** to generate intermediate **H2**, *ortho* C–H cobaltation provides complex **H3**, which changed into product **56** and Co(I) catalyst by reductive elimination of **H3**.

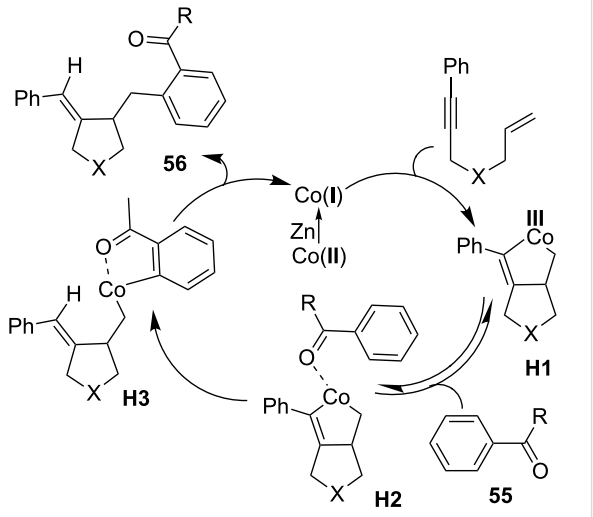

Scheme 34: Mechanism for the Co-catalyzed hydroarylative cyclization of enynes with carbonyl compounds.

5. Hydroarylation of C=X (X = N, O) bonds

5.1 Low-valent cobalt-catalyzed hydroarylation of C=X bonds

Transition-metal-catalyzed addition of C–H bond to polar π bonds such as imines, isocyanates and carbonyls is one of the efficient methods to incorporate heteroatoms in organic molecules [45]. Yoshikai et al. developed an addition reaction of arylpyridines **3** to imines using low-valent cobalt catalyst generated from $CoCl_2$, IPr·HCl, and *t*-BuMgBr (Scheme 35) [95]. The reaction tolerated a wide range of arylpyridines and aldimines, giving diarylmethylamines **57** in good yields. The reaction possibly proceeds through the formation of neopentylcobalt ([Co]-R), which undergoes oxidative addition with arylpyridine to generate **I1**. Then, elimination of neopentane (R–H) by reductive elimination gives cobaltacycle **I2**. Nucleophilic addition of **I2** to imines, followed by transmetallation with a Grignard reagent and protonation provide the desired hydroarylation product **57**.

In addition to imines, aziridines were also amenable to the cobalt-catalyzed hydroarylation reaction (Scheme 36) [96]. Treatment of 2-phenylpyridines **3** with varies aryl-substituted

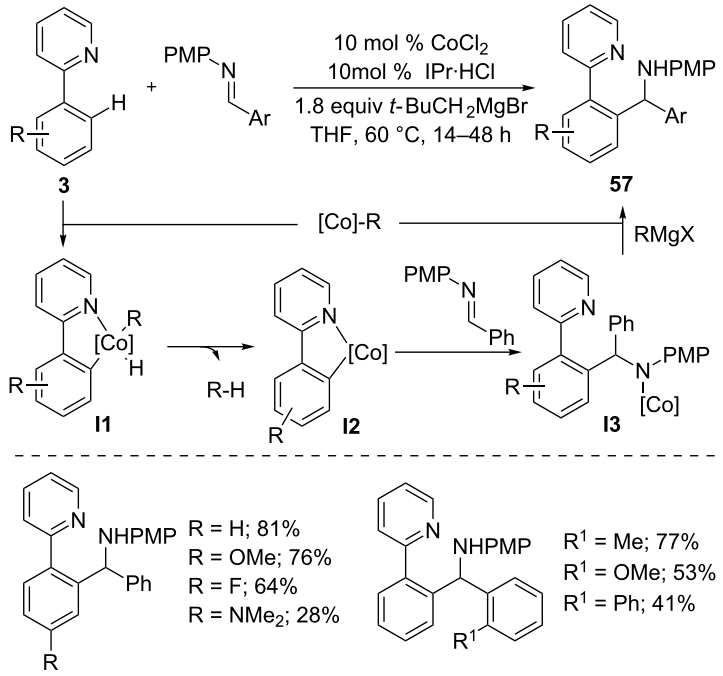

Scheme 35: Co-catalyzed addition of 2-arylpyridines to aromatic aldimines.

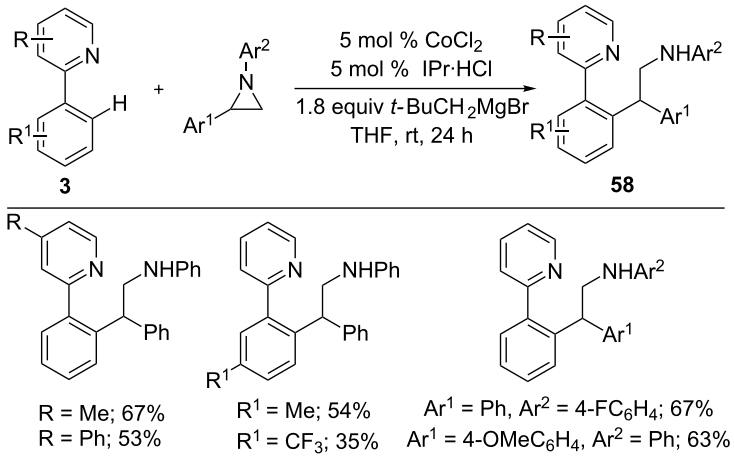

Scheme 36: Co-catalyzed addition of 2-arylpyridines to aziridines.

aziridines gave 1,1-diarylethane derivatives **58** in a highly regioselective manner. It is noteworthy that nucleophilic addition took place selectively at the more hindered C-2 position of aziridines, which results in high regioselectivity.

5.2 Cobalt(III)-catalyzed hydroarylation of C=X bonds

As the Co(III)Cp* catalyst acts an efficient air-stable catalyst for hydroarylation of the C=C bond, it would also provide a user-friendly method for C=X bonds. Thus, imines were employed for hydroarylation reaction with 2-phenylpyridines **3** in the presence of [CoCp*(benzene)]$(PF_6)_2$ catalyst by Kanai/Matsunaga and co-workers (Scheme 37a) [37]. The reaction afforded diarylmethylamines **59** in good to moderate yields, however, the imines used was limited to aldimines. Similarly, indoles **7** also efficiently underwent the hydroarylation reaction with various substituted aldimines to provide C-2 alkylated indoles **60** (Scheme 37b) [97].

In 2016, Wang's group demonstrated that ketenimines participated in hydroarylation reaction with arenes **7** in the presence of $CoCp^*(CO)I_2$ and $AgNTf_2$ (Scheme 38) [98]. The reaction

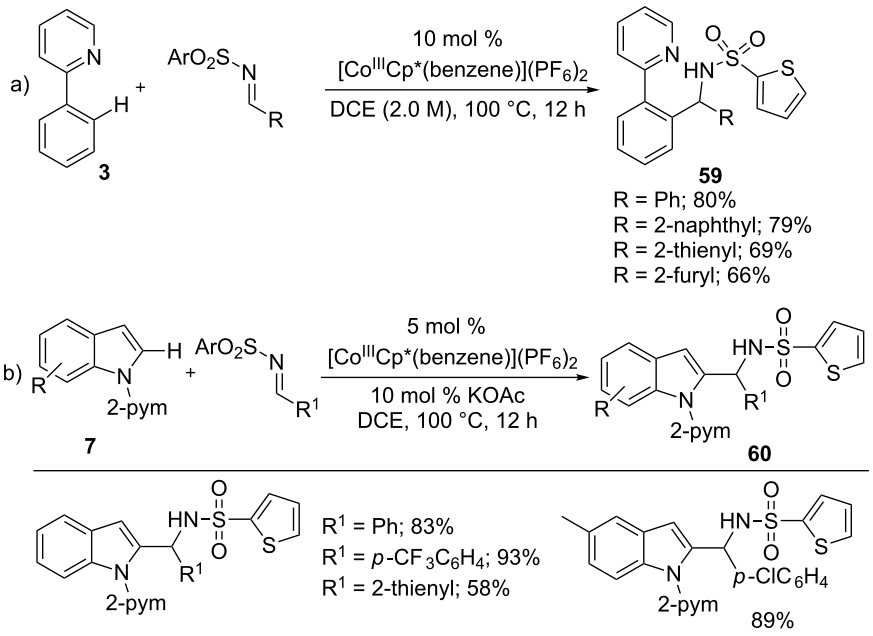

Scheme 37: Co(III)-catalyzed hydroarylation of imines with arenes.

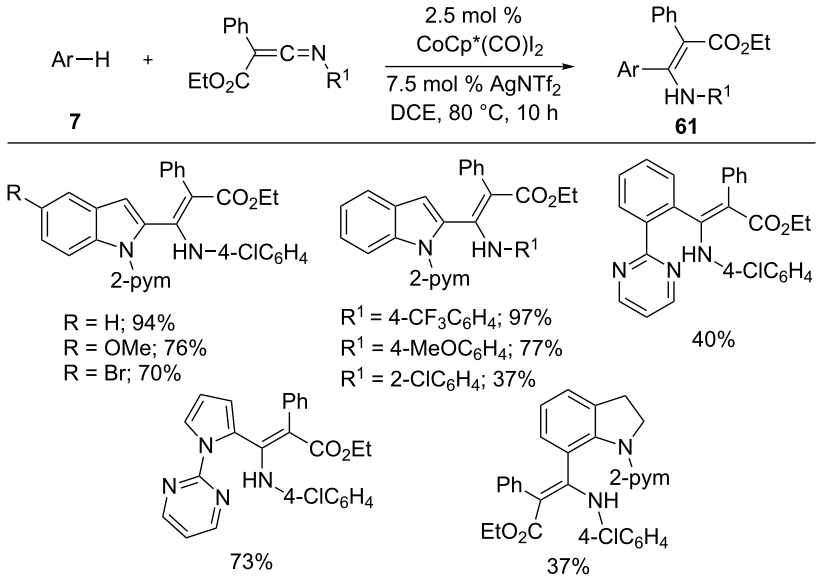

Scheme 38: Co(III)-catalyzed addition of arenes to ketenimines.

tolerated various pyrimidine containing arenes, such as indole, phenyl, and pyrrole with different ketenimines to form enaminylation products **61**. Subsequently, the hydroarylation products **61** were further converted into bioactive pyrrolo[1,2-*a*]indoles by sodium ethoxide-promoted cyclization.

The three-component coupling also becomes viable through a Co(III)-catalyzed hydroarylation strategy as Ellman and co-workers demonstrated (Scheme 39) [99]. The reaction of arene **21** with vinyl ketones and aldehydes in the presence of $[CoCp^*(C_6H_6)][B(C_6F_5)_4]_2$ and LiOAc gave alcohol products **62** with high diastereoselectivity at ambient reaction conditions. The unique nature of cobalt was well presented by its superior reactivity and diastereoselectivity and it outmatched the rhodium catalyst. Different pyrazole derivatives with a wide range of aldehydes or imines were participated well in the reaction, affording the addition products **62** in good yields. The catalytic cycle starts with the coordination of active cobalt catalyst

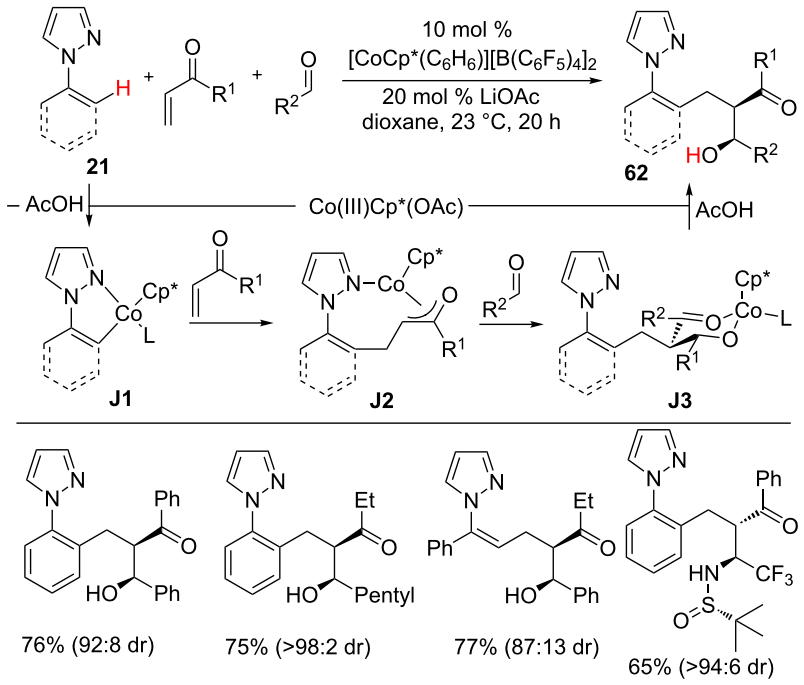

Scheme 39: Co(III)-catalyzed three-component coupling.

with arene **21** followed by C–H activation to give five-membered cobaltacycle **J1**. Insertion of the alkene with **J1** forms cobalt enolate **J2**, which converts into **J3** by the addition of aldehyde via a chair transition state in a diastereoselective manner. Finally, protonolysis affords product **62** and regenerates the active Co(III)Cp* catalyst for the next cycle. Later, Li et al. reported a Co(III)-catalyzed hydroarylation of glyoxylate with pyrimidine containing indoles and pyrroles **7** to provide products **63** with high productivity (Scheme 40) [79].

Similar to the imine, isocyanate is also an efficient electrophile for hydroarylation of C=N bond. It provides a high atom- and step-economical method for the preparation of aromatic, vinyl, and heterocyclic amides. Thus, Ackermann and co-workers developed an inexpensive cobalt-catalyzed hydroarylation of isocyanates with (hetero)arenes **64** (Scheme 41) [100]. The reaction can tolerate a broad range of arenes and isocyanates, providing amide products **65** with notable site selectivity. The found inter- and intramolecular KIEs (k_H/k_D) of 1.4 shows that the C−H activation may not be the rate the determining step. Moreover, competition experiments indicate that the reaction favors electron-rich arenes **64** and electron-deficient isocyanates. Ellman's group also reported a similar C–H amidation reaction of aryl pyrazoles **64** with isocyanates in the presence of $[CoCp^*(C_6H_6)](PF_6)_2$ and KOAc [101].

Conclusion

Hydroarylation is an emerging methodology in organic synthesis, because it is a highly atom-, step-, and redox-economical and simple reaction compared to traditional synthetic methods

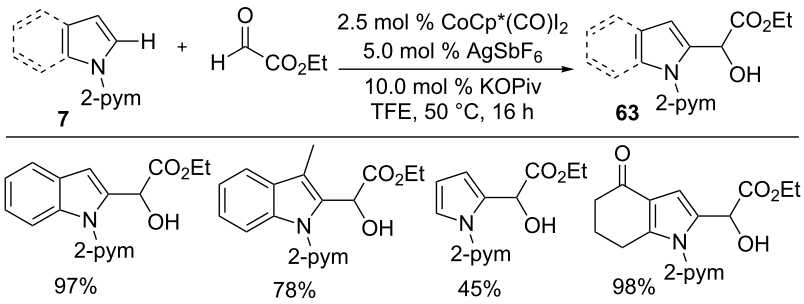

Scheme 40: Co(III)-catalyzed hydroarylation of aldehydes.

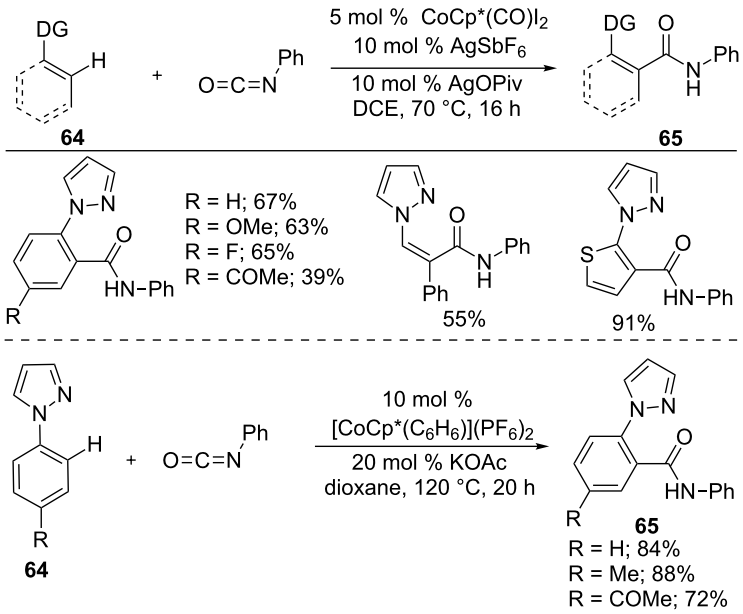

Scheme 41: Co(III)-catalyzed addition of arenes to isocyanates.

to construct new C−C bonds. Among the first-row transition metals, both low- and high-valent cobalt catalysts have played a substantial role in these hydroarylation reactions providing an economical alternative to the precious metal-catalyzed reactions and also showed distinct selectivity in some cases. Switchable regioselective hydroarylation of styrene using low-valent cobalt catalyst and Co(III)-catalyzed hydroarylation of alkylalkenes with indoles are remarkable examples in this manner. A wide range of C−H bonds has been successfully added to alkynes, alkenes, imines etc. to build alkyls, alkenes, alcohols, amides, and cyclic skeletons with excellent efficacy. Considering the importance of green processes for the ever-growing universe, economical and waste-free hydroarylation strategy will continue to draw great attention in the field of organic synthesis.

Acknowledgements

We thank the Ministry of Science and Technology of the Republic of China (MOST-105-2633-M-007-003) for the support of these studies.

ORCID® iDs

Rajagopal Santhoshkumar - https://orcid.org/0000-0002-4357-4026

References

1. Cathcart, C. *Chem. Ind.* **1990,** *5,* 684–687.
2. Anastas, P. T.; Williamson, T. C. Green Chemistry: An Overview. *Green Chemistry;* ACS Symposium Series, Vol. 626; American Chemical Society: Washington, DC, U.S.A., 1996; pp 1–17. doi:10.1021/bk-1996-0626.ch001
3. Anastas, P. T. *Chem. Rev.* **2007,** *107,* 2167–2168. doi:10.1021/cr0783784
4. Trost, B. M. *Science* **1991,** *254,* 1471–1477. doi:10.1126/science.1962206
5. Trost, B. M. *Angew. Chem., Int. Ed. Engl.* **1995,** *34,* 259–281. doi:10.1002/anie.199502591
6. Trost, B. M. *Acc. Chem. Res.* **2002,** *35,* 695–705. doi:10.1021/ar010068z
7. Shang, X.; Liu, Z.-Q. *Chem. Soc. Rev.* **2013,** *42,* 3253–3260. doi:10.1039/c2cs35445d
8. De Sarkar, S.; Liu, W.; Kozhushkov, S. I.; Ackermann, L. *Adv. Synth. Catal.* **2014,** *356,* 1461–1479. doi:10.1002/adsc.201400110
9. Gensch, T.; Hopkinson, M. N.; Glorius, F.; Wencel-Delord, J. *Chem. Soc. Rev.* **2016,** *45,* 2900–2936. doi:10.1039/C6CS00075D
10. He, J.; Wasa, M.; Chan, K. S. L.; Shao, Q.; Yu, J.-Q. *Chem. Rev.* **2017,** *117,* 8754–8786. doi:10.1021/acs.chemrev.6b00622
11. Gutekunst, W. R.; Baran, P. S. *Chem. Soc. Rev.* **2011,** *40,* 1976. doi:10.1039/c0cs00182a
12. Chen, D. Y.-K.; Youn, S. W. *Chem. – Eur. J.* **2012,** *18,* 9452–9474. doi:10.1002/chem.201201329
13. Yamaguchi, J.; Yamaguchi, A. D.; Itami, K. *Angew. Chem., Int. Ed.* **2012,** *51,* 8960–9009. doi:10.1002/anie.201201666
14. Tao, P.; Jia, Y. *Sci. China: Chem.* **2016,** *59,* 1109–1125. doi:10.1007/s11426-016-0058-7
15. Wencel-Delord, J.; Glorius, F. *Nat. Chem.* **2013,** *5,* 369–375. doi:10.1038/nchem.1607
16. Gao, K.; Yoshikai, N. *Acc. Chem. Res.* **2014,** *47,* 1208–1219. doi:10.1021/ar400270x
17. Ackermann, L. *J. Org. Chem.* **2014,** *79,* 8948–8954. doi:10.1021/jo501361k
18. Liu, W.; Ackermann, L. *ACS Catal.* **2016,** *6,* 3743–3752. doi:10.1021/acscatal.6b00993
19. Castro, L. C. M.; Chatani, N. *Chem. Lett.* **2015,** *44,* 410–421. doi:10.1246/cl.150024

20. Wei, D.; Zhu, X.; Niu, J.-L.; Song, M.-P. *ChemCatChem* **2016,** *8,* 1242–1263. doi:10.1002/cctc.201600040
21. Moselage, M.; Li, J.; Ackermann, L. *ACS Catal.* **2016,** *6,* 498–525. doi:10.1021/acscatal.5b02344
22. Yoshino, T.; Matsunaga, S. *Adv. Synth. Catal.* **2017,** *359,* 1245–1262. doi:10.1002/adsc.201700042
23. Usman, M.; Ren, Z.-H.; Wang, Y.-Y.; Guan, Z.-H. *Synthesis* **2017,** 1419–1443. doi:10.1055/s-0036-1589478
24. Wang, S.; Chen, S.-Y.; Yu, X.-Q. *Chem. Commun.* **2017,** *53,* 3165–3180. doi:10.1039/C6CC09651D
25. Prakash, S.; Kuppusamy, R.; Cheng, C.-H. *ChemCatChem* **2018,** *10,* 683–705. doi:10.1002/cctc.201701559
26. Wendlandt, A. E.; Suess, A. M.; Stahl, S. S. *Angew. Chem., Int. Ed.* **2011,** *50,* 11062–11087. doi:10.1002/anie.201103945
27. Shang, R.; Ilies, L.; Nakamura, E. *Chem. Rev.* **2017,** *117,* 9086–9139. doi:10.1021/acs.chemrev.6b00772
28. Kharasch, M. S.; Fields, E. K. *J. Am. Chem. Soc.* **1941,** *63,* 2316–2320. doi:10.1021/ja01854a006
29. Murahashi, S. *J. Am. Chem. Soc.* **1955,** *77,* 6403–6404. doi:10.1021/ja01628a120
30. Murahashi, S.; Horiie, S. *J. Am. Chem. Soc.* **1956,** *78,* 4816–4817. doi:10.1021/ja01599a079
31. Kochi, J. K.; Tang, R. T.; Bernath, T. *J. Am. Chem. Soc.* **1973,** *95,* 7114–7123. doi:10.1021/ja00802a036
32. Halbritter, G.; Knoch, F.; Wolski, A.; Kisch, H. *Angew. Chem., Int. Ed. Engl.* **1994,** *33,* 1603–1605. doi:10.1002/anie.199416031
33. Klein, H.-F.; Helwig, M.; Koch, U.; Flörke, U.; Haupt, H.-J. *Z. Naturforsch., B: J. Chem. Sci.* **1993,** *48,* 778–784. doi:10.1515/znb-1993-0612
34. Klein, H.-F.; Camadanli, S.; Beck, R.; Leukel, D.; Flörke, U. *Angew. Chem., Int. Ed.* **2005,** *44,* 975–977. doi:10.1002/anie.200460978
35. Lenges, C. P.; Brookhart, M. *J. Am. Chem. Soc.* **1997,** *119,* 3165–3166. doi:10.1021/ja9639776
36. Gao, K.; Lee, P.-S.; Fujita, T.; Yoshikai, N. *J. Am. Chem. Soc.* **2010,** *132,* 12249–12251. doi:10.1021/ja106814p
37. Yoshino, T.; Ikemoto, H.; Matsunaga, S.; Kanai, M. *Angew. Chem., Int. Ed.* **2013,** *52,* 2207–2211. doi:10.1002/anie.201209226
38. Grigorjeva, L.; Daugulis, O. *Angew. Chem., Int. Ed.* **2014,** *53,* 10209–10212. doi:10.1002/anie.201404579
39. Ilies, L.; Chen, Q.; Zeng, X.; Nakamura, E. *J. Am. Chem. Soc.* **2011,** *133,* 5221–5223. doi:10.1021/ja200645w
40. Song, W.; Ackermann, L. *Angew. Chem., Int. Ed.* **2012,** *51,* 8251–8254. doi:10.1002/anie.201202466
41. Yu, D.-G.; Gensch, T.; de Azambuja, F.; Vásquez-Céspedes, S.; Glorius, F. *J. Am. Chem. Soc.* **2014,** *136,* 17722–17725. doi:10.1021/ja511011m
42. Yoshikai, N. Hydroarylation of Alkynes and Alkenes using Group 7-9 First-Row Transition Metal Catalysts. *Catalytic Hydroarylation of Carbon-Carbon Multiple Bonds;* Wiley-VCH Verlag GmbH: Weinheim, Germany, 2017; pp 193–216. doi:10.1002/9783527697649.ch6
43. Dong, Z.; Ren, Z.; Thompson, S. J.; Xu, Y.; Dong, G. *Chem. Rev.* **2017,** *117,* 9333–9403. doi:10.1021/acs.chemrev.6b00574
44. Kitamura, T. *Eur. J. Org. Chem.* **2009,** 1111–1125. doi:10.1002/ejoc.200801054
45. Hummel, J. R.; Boerth, J. A.; Ellman, J. A. *Chem. Rev.* **2017,** *117,* 9163–9227. doi:10.1021/acs.chemrev.6b00661
46. Ding, Z.; Yoshikai, N. *Org. Lett.* **2010,** *12,* 4180–4183. doi:10.1021/ol101777x
47. Ding, Z.; Yoshikai, N. *Synthesis* **2011,** 2561–2566. doi:10.1055/s-0030-1260077
48. Ding, Z.; Yoshikai, N. *Angew. Chem., Int. Ed.* **2012,** *51,* 4698–4701. doi:10.1002/anie.201200019
49. Nakao, Y.; Kanyiva, K. S.; Oda, S.; Hiyama, T. *J. Am. Chem. Soc.* **2006,** *128,* 8146–8147. doi:10.1021/ja0623459
50. Lee, P.-S.; Fujita, T.; Yoshikai, N. *J. Am. Chem. Soc.* **2011,** *133,* 17283–17295. doi:10.1021/ja2047073
51. Yamakawa, T.; Yoshikai, N. *Tetrahedron* **2013,** *69,* 4459–4465. doi:10.1016/j.tet.2013.02.092
52. Fallon, B. J.; Derat, E.; Amatore, M.; Aubert, C.; Chemla, F.; Ferreira, F.; Perez-Luna, A.; Petit, M. *J. Am. Chem. Soc.* **2015,** *137,* 2448–2451. doi:10.1021/ja512728f
53. Ikemoto, H.; Yoshino, T.; Sakata, K.; Matsunaga, S.; Kanai, M. *J. Am. Chem. Soc.* **2014,** *136,* 5424–5431. doi:10.1021/ja5008432
54. Sakata, K.; Eda, M.; Kitaoka, Y.; Yoshino, T.; Matsunaga, S. *J. Org. Chem.* **2017,** *82,* 7379–7387. doi:10.1021/acs.joc.7b01047
55. Tanaka, R.; Ikemoto, H.; Kanai, M.; Yoshino, T.; Matsunaga, S. *Org. Lett.* **2016,** *18,* 5732–5735. doi:10.1021/acs.orglett.6b02997
56. Zhou, X.; Luo, Y.; Kong, L.; Xu, Y.; Zheng, G.; Lan, Y.; Li, X. *ACS Catal.* **2017,** *7,* 7296–7304. doi:10.1021/acscatal.7b02248
57. Wang, S.; Hou, J.-T.; Feng, M.-L.; Zhang, X.-Z.; Chen, S.-Y.; Yu, X.-Q. *Chem. Commun.* **2016,** *52,* 2709–2712. doi:10.1039/C5CC09707J
58. Bera, S. S.; Debbarma, S.; Ghosh, A. K.; Chand, S.; Maji, M. S. *J. Org. Chem.* **2017,** *82,* 420–430. doi:10.1021/acs.joc.6b02516
59. Sen, M.; Rajesh, N.; Emayavaramban, B.; Premkumar, J. R.; Sundararaju, B. *Chem. – Eur. J.* **2018,** *24,* 342–346. doi:10.1002/chem.201705183
60. Gao, K.; Yoshikai, N. *J. Am. Chem. Soc.* **2011,** *133,* 400–402. doi:10.1021/ja108809u
61. Gao, K.; Yoshikai, N. *Angew. Chem., Int. Ed.* **2011,** *50,* 6888–6892. doi:10.1002/anie.201101823
62. Ding, Z.; Yoshikai, N. *Beilstein J. Org. Chem.* **2012,** *8,* 1536–1542. doi:10.3762/bjoc.8.174
63. Xu, W.; Yoshikai, N. *Angew. Chem., Int. Ed.* **2014,** *53,* 14166–14170. doi:10.1002/anie.201408028
64. Xu, W.; Yoshikai, N. *Angew. Chem., Int. Ed.* **2016,** *55,* 12731–12735. doi:10.1002/anie.201605877
65. Dong, J.; Lee, P.-S.; Yoshikai, N. *Chem. Lett.* **2013,** *42,* 1140–1142. doi:10.1246/cl.130508
66. Lee, P.-S.; Yoshikai, N. *Angew. Chem., Int. Ed.* **2013,** *52,* 1240–1244. doi:10.1002/anie.201207958
67. Xu, W.; Pek, J. H.; Yoshikai, N. *Adv. Synth. Catal.* **2016,** *358,* 2564–2568. doi:10.1002/adsc.201600403
68. Xu, W.; Yoshikai, N. *Org. Lett.* **2018,** *20,* 1392–1395. doi:10.1021/acs.orglett.8b00164
69. Yang, Z.; Yu, H.; Fu, Y. *Chem. – Eur. J.* **2013,** *19,* 12093–12103. doi:10.1002/chem.201203666
70. Ding, Z.; Yoshikai, N. *Angew. Chem., Int. Ed.* **2013,** *52,* 8574–8578. doi:10.1002/anie.201305151
71. Yamakawa, T.; Yoshikai, N. *Chem. – Asian J.* **2014,** *9,* 1242–1246. doi:10.1002/asia.201400135
72. Fallon, B. J.; Derat, E.; Amatore, M.; Aubert, C.; Chemla, F.; Ferreira, F.; Perez-Luna, A.; Petit, M. *Org. Lett.* **2016,** *18,* 2292–2295. doi:10.1021/acs.orglett.6b00939
73. Lee, P.-S.; Yoshikai, N. *Org. Lett.* **2015,** *17,* 22–25. doi:10.1021/ol503119z

74. Nakao, Y.; Yamada, Y.; Kashihara, N.; Hiyama, T. *J. Am. Chem. Soc.* **2010,** *132,* 13666–13668. doi:10.1021/ja106514b
75. Andou, T.; Saga, Y.; Komai, H.; Matsunaga, S.; Kanai, M. *Angew. Chem., Int. Ed.* **2013,** *52,* 3213–3216. doi:10.1002/anie.201208666
76. Yamamoto, S.; Saga, Y.; Andou, T.; Matsunaga, S.; Kanai, M. *Adv. Synth. Catal.* **2014,** *356,* 401–405. doi:10.1002/adsc.201300991
77. Barsu, N.; Emayavaramban, B.; Sundararaju, B. *Eur. J. Org. Chem.* **2017,** 4370–4374. doi:10.1002/ejoc.201700696
78. Chirila, P. G.; Adams, J.; Dirjal, A.; Hamilton, A.; Whiteoak, C. J. *Chem. – Eur. J.* **2018,** *24,* 3584–3589. doi:10.1002/chem.201705785
79. Li, J.; Zhang, Z.; Ma, W.; Tang, M.; Wang, D.; Zou, L.-H. *Adv. Synth. Catal.* **2017,** *359,* 1717–1724. doi:10.1002/adsc.201700097
80. Zell, D.; Bursch, M.; Müller, V.; Grimme, S.; Ackermann, L. *Angew. Chem., Int. Ed.* **2017,** *56,* 10378–10382. doi:10.1002/anie.201704196
81. Zell, D.; Bu, Q.; Feldt, M.; Ackermann, L. *Angew. Chem., Int. Ed.* **2016,** *55,* 7408–7412. doi:10.1002/anie.201601778
82. Wu, J.-Q.; Qiu, Z.-P.; Zhang, S.-S.; Liu, J.-G.; Lao, Y.-X.; Gu, L.-Q.; Huang, Z.-S.; Li, J.; Wang, H. *Chem. Commun.* **2015,** *51,* 77–80. doi:10.1039/C4CC07839J
83. Kong, L.; Yu, S.; Tang, G.; Wang, H.; Zhou, X.; Li, X. *Org. Lett.* **2016,** *18,* 3802–3805. doi:10.1021/acs.orglett.6b01806
84. Muralirajan, K.; Prakash, S.; Cheng, C.-H. *Adv. Synth. Catal.* **2017,** *359,* 513–518. doi:10.1002/adsc.201601026
85. Zhang, Z.; Han, S.; Tang, M.; Ackermann, L.; Li, J. *Org. Lett.* **2017,** *19,* 3315–3318. doi:10.1021/acs.orglett.7b01480
86. Muniraj, N.; Prabhu, K. R. *ACS Omega* **2017,** *2,* 4470–4479. doi:10.1021/acsomega.7b00870
87. Muniraj, N.; Prabhu, K. R. *J. Org. Chem.* **2017,** *82,* 6913–6921. doi:10.1021/acs.joc.7b01094
88. Chen, X.; Ren, J.; Xie, H.; Sun, W.; Sun, M.; Wu, B. *Org. Chem. Front.* **2018,** *5,* 184–188. doi:10.1039/C7QO00687J
89. Ma, S. *Chem. Rev.* **2005,** *105,* 2829–2872. doi:10.1021/cr020024j
90. Santhoshkumar, R.; Cheng, C.-H. *Asian J. Org. Chem.* **2018,** *7,* 1151–1163. doi:10.1002/ajoc.201800133
91. Nakanowatari, S.; Mei, R.; Feldt, M.; Ackermann, L. *ACS Catal.* **2017,** *7,* 2511–2515. doi:10.1021/acscatal.7b00207
92. Aubert, C.; Buisine, O.; Malacria, M. *Chem. Rev.* **2002,** *102,* 813–834. doi:10.1021/cr980054f
93. Santhoshkumar, R.; Mannathan, S.; Cheng, C.-H. *Org. Lett.* **2014,** *16,* 4208–4211. doi:10.1021/ol501904e
94. Santhoshkumar, R.; Mannathan, S.; Cheng, C.-H. *J. Am. Chem. Soc.* **2015,** *137,* 16116–16120. doi:10.1021/jacs.5b10447
95. Gao, K.; Yoshikai, N. *Chem. Commun.* **2012,** *48,* 4305–4307. doi:10.1039/c2cc31114c
96. Gao, K.; Paira, R.; Yoshikai, N. *Adv. Synth. Catal.* **2014,** *356,* 1486–1490. doi:10.1002/adsc.201400049
97. Yoshino, T.; Ikemoto, H.; Matsunaga, S.; Kanai, M. *Chem. – Eur. J.* **2013,** *19,* 9142–9146. doi:10.1002/chem.201301505
98. Zhou, X.; Fan, Z.; Zhang, Z.; Lu, P.; Wang, Y. *Org. Lett.* **2016,** *18,* 4706–4709. doi:10.1021/acs.orglett.6b02353
99. Boerth, J. A.; Hummel, J. R.; Ellman, J. A. *Angew. Chem., Int. Ed.* **2016,** *55,* 12650–12654. doi:10.1002/anie.201603831
100. Li, J.; Ackermann, L. *Angew. Chem., Int. Ed.* **2015,** *54,* 8551–8554. doi:10.1002/anie.201501926
101. Hummel, J. R.; Ellman, J. A. *Org. Lett.* **2015,** *17,* 2400–2403. doi:10.1021/acs.orglett.5b00910

License and Terms

BEILSTEIN JOURNAL OF ORGANIC CHEMISTRY

A challenging redox neutral Cp*Co(III)-catalysed alkylation of acetanilides with 3-buten-2-one: synthesis and key insights into the mechanism through DFT calculations

Andrew Kenny, Alba Pisarello, Arron Bird, Paula G. Chirila, Alex Hamilton* and Christopher J. Whiteoak*

Full Research Paper

Open Access

Address:
Department of Biosciences and Chemistry, Sheffield Hallam University, Sheffield, S1 1WB, United Kingdom

Email:
Alex Hamilton* - a.hamilton@shu.ac.uk; Christopher J. Whiteoak* - c.whiteoak@shu.ac.uk

* Corresponding author

Keywords:
acetanilides; alkylation; C–H activation; cobalt catalysis; DFT studies

Beilstein J. Org. Chem. **2018,** *14,* 2366–2374.
doi:10.3762/bjoc.14.212

Received: 25 June 2018
Accepted: 23 August 2018
Published: 10 September 2018

This article is part of the thematic issue "Cobalt catalysis".

Guest Editor: S. Matsunaga

Abstract

Traditional, established palladium cross-coupling procedures are widely applied in complex molecule synthesis; however, there is a significant disadvantage in the requirement for pre-functionalised substrates (commonly halides/triflates). Direct C–H activation protocols provide the opportunity for a novel approach to synthesis, although this field is still in its relative infancy and often transferability between substrate classes remains unresolved and limitations not fully understood. This study focuses on the translation of an established Cp*Co(III)-catalysed alkylation of benzamides to related acetanilides using 3-buten-2-one as coupling partner. The developed procedure provides a wide substrate scope in terms of substituted acetanilides, although the optimised conditions were found to be more forcing than those for the corresponding benzamide substrates. Interestingly, density functional theory (DFT) studies reveal that the major impediment in the mechanism is not the C–H activation step, but instead and unexpectedly, effective competition with more stable compounds (resting states) not involved in the catalytic cycle.

Introduction

Controlled functionalisation of ubiquitous C–H bonds has been identified as one of the key challenges in modern day chemical research [1-3], providing the potential to access complex chemical structures more efficiently. In this context, transition metal catalysis is seen as a potential solution, building on the traditional and well-established palladium-catalysed cross-coupling protocols [4]. Whilst second and third row transition metals are well applied in cross-coupling protocols through C–H activation under mild conditions [5], the drive to use first row metals continues to provide an exciting challenge [6]. The interest in

the application of these first-row transition metals stems from their low cost, ready availability and often wider reactivity profiles. One particular example which is currently attracting significant interest is cobalt, a metal which has found many applications in C–H functionalisation through exploitation of its diverse mechanisms [7]. Since 2013, the cobalt pre-catalysts, $[Cp^*Co(C_6H_6)](PF_6)_2$ and $[Cp^*Co(CO)I_2]$, have been successfully applied in a number of diverse C–H functionalisation protocols [8-12]. Whilst many of these protocols are very elegant, few examples are able to be applied to the full range of substrates and this presents one of the limitations to date compared with traditional palladium cross-coupling which is diversely applicable. Of interest to us are the readily available benzamide substrates, which are an interesting class of compounds as the amide moiety has been exploited as a common directing group [13] and countless pharmaceutical and agrochemical compounds contain these moieties. If the amide is reversed in the benzamide, the resulting compounds are acetanilides, which have been utilised far less as substrates in C–H functionalisation protocols [13], although a few examples do exist using the $[Cp^*Co(CO)I_2]$ pre-catalyst [14-17]. Cp*Co(III)-catalysed C–H alkylation of unactivated aromatic C–H bonds with α,β-unsaturated ketones has been previously reported by ourselves (Scheme 1a) [18] and others [19,20]. Given our example focusing on the functionalisation of benzamides we wondered if the previously developed protocol could be directly transferred successfully to acetanilides, therefore further expanding the applicability of the developed methodology. The expected product from this reaction has previously been obtained through a C–H functionalisation approach in 43% yield from the Cp*Rh(III)-catalysed coupling of allylic alcohols with acetanilide through a redox-active mechanism (Scheme 1b) [21], thus requiring stoichiometric oxidant ($Cu(OAc)_2$), whereas the new protocol described in this report is intended to provide a more attractive redox-neutral alternative, obviating the requirement for addition of terminal oxidant (Scheme 1c). Herein, our results from this study will be reported and the difficulties of this translation will be explained

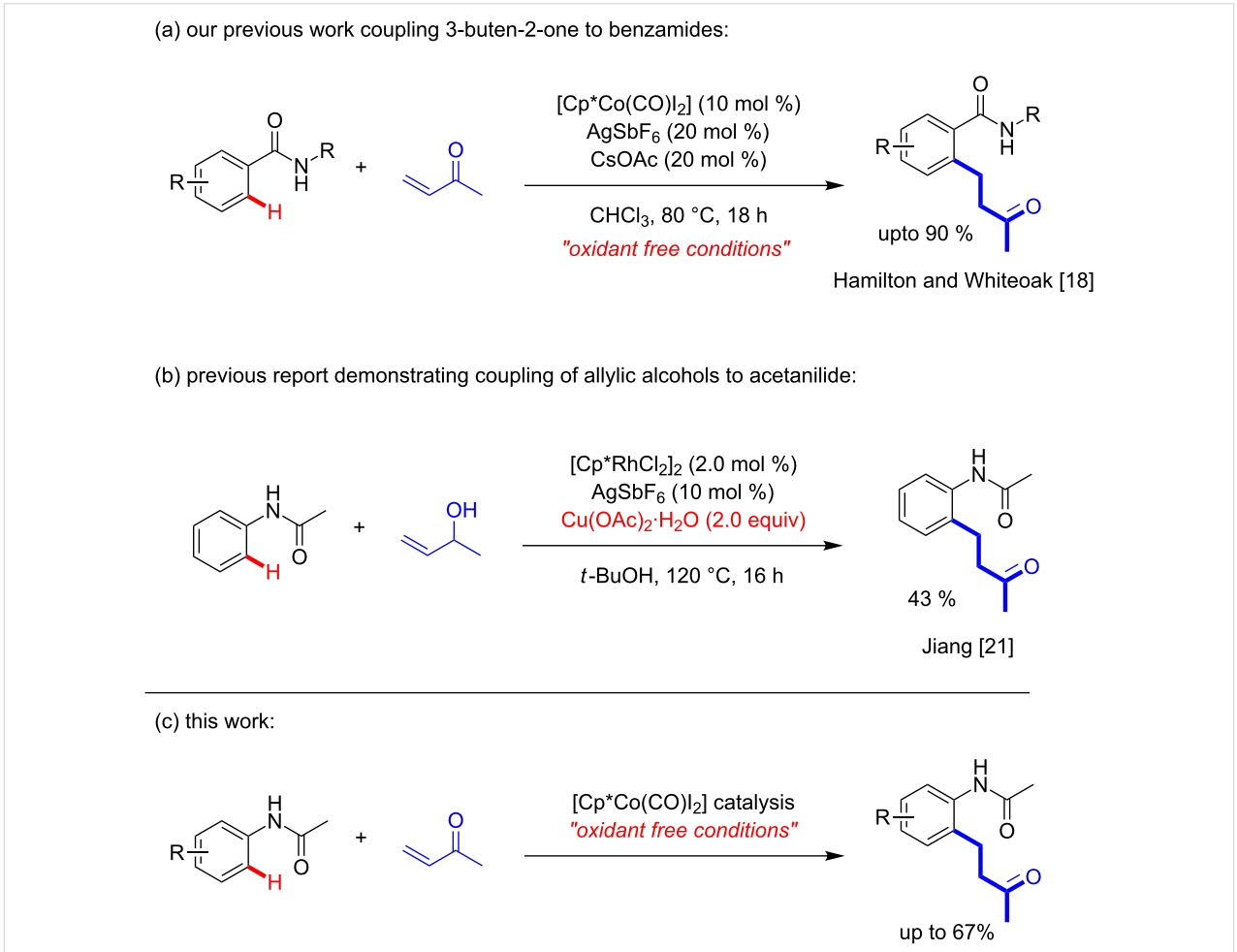

Scheme 1: (a) Our previously reported Cp*Co(III) redox-neutral coupling of 3-buten-2-one to benzamides, (b) previous oxidative alkylation of acetanilide through the coupling of allylic alcohols under Cp*Rh(III) catalysis, and (c) the Cp*Co(III) redox-neutral coupling described in this work.

through a DFT study of the mechanism, which will also be directly compared with the use of benzamides as substrates.

Results and Discussion

Initial investigations into the Cp*Co(III)-catalysed coupling of acetanilide (**1a**) with 3-buten-2-one, using the optimised conditions for the same coupling previously reported with benzamides, provided poor yields (18%; Scheme 2a). Subsequent reaction condition optimisation led to the inclusion of an increased catalyst loading (20 mol %) and change of solvent/base, which resulted in a synthetically useful yield of the coupling product **2a** (58%; Scheme 2b). This need for increased catalyst loading was also previously reported by Kanai and Matsunaga for the alkenylation of acetanilide with ethyl acrylate under Cp*Co(III) catalysis [14]. To the best of our knowledge, this is the first time that 3-buten-2-one has been successfully coupled to acetanilide through metal-mediated C–H functionalisation and provides a redox-neutral alternative, with enhanced yield, to the Cp*Rh(III)-catalysed coupling of allylic alcohols reported by Jiang and co-workers which requires the inclusion of 2.0 equivalents of $Cu(OAc)_2$ for the same products [21].

With the optimised conditions in hand, the potential scope/limitations of the catalytic protocol were studied (Scheme 3). Pleasingly, acetanilides with both electron-donating (**1b**–**d**) and electron-withdrawing substituents (**1e**–**g**) could be converted in yields of between 39-67%. The lower yields of some of these conversions highlight the challenging nature of this coupling. Thereafter, regioselectivity was studied by the inclusion of a range of *meta*-substituted acetanilides (**1h**–**m**). In most cases the products were obtained in a regioselective manner with substitution at the least hindered C–H bond. This regioselectivity has been observed previously in Cp*Co(III)-catalysis using benzamides as substrates by ourselves and others [14,18,22-24]. There are, however, two notable examples which should be commented upon; as we and others have previously observed, the *meta*-fluoro substituted compound favours functionalisation at the most hindered C–H bond, furnishing **2l**. Whilst the *meta*-methoxy-substituted acetanilide provided an unexpected inseparable mixture of the products derived from functionalisation of the least/most hindered C–H bond (**2ma** and **2mb**; combined yield of 44%) and a isolable amount (18%) of doubly functionalised product (functionalisation of least and most hindered C–H bonds), **2mc**. Neither acetanilides with either methyl or fluoro substituents in the *ortho*-position (**1n** and **1o**, respectively) could be successfully converted under the optimised conditions, with only traces of the products observed in the crude reaction mixtures. Increasing the steric bulk on the carbonyl from methyl to *tert*-butyl did not affect the obtained yield (**2p**).

In an effort to further understand the reaction mechanism involved in the C–H functionalisation of acetanilide substrates with 3-buten-2-one, we employed DFT calculations (Figure 1) using M06 level of theory which has been previously success-

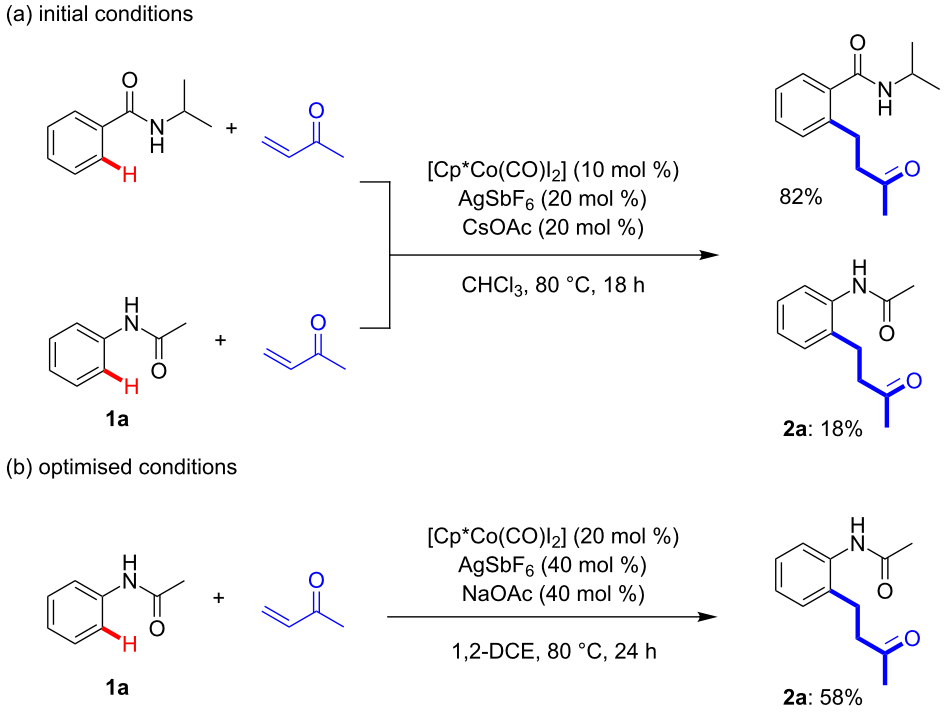

Scheme 2: Summary of reaction conditions optimisation.

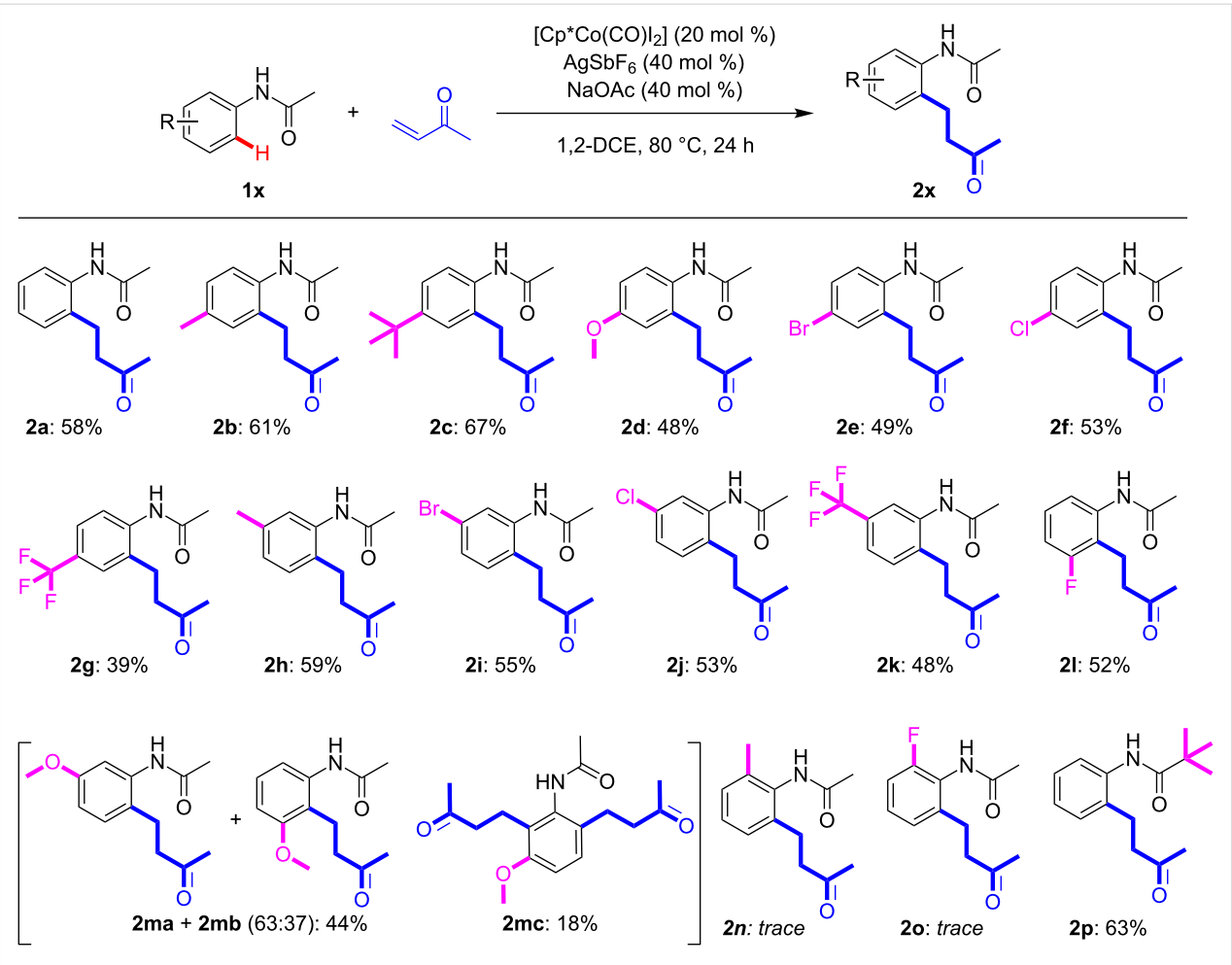

Scheme 3: Substrate scope of Cp*Co(III)-catalysed coupling of 3-buten-2-one with functionalised acetanilides. All reactions carried out on a 1.0 mmol scale with isolated yields reported.

fully applied for cobalt-catalysed C–H functionalisation reactions [25,26]. Previous studies from our group have already discussed the O- vs N-binding of benzamide substrates to the $[Cp^*Co(III)OAc]^+$ catalyst [18]. In line with this benzamide functionalisation mechanism, the acetanilide coordinates to the cobalt centre through the ketone oxygen to form **Int 1**. This allows for reasonably close proximity of the C_{sp^2}-H proton for internal abstraction by the acetate group. The C–H activation step has an energy span barrier of 17.8 kcal mol^{-1}, leading to the formation of the 6-membered organometallic cobaltacycle (**Int 2$_{AcOH}$**) with an associated acetic acid. This barrier is approximately 3.5 kcal mol^{-1} lower in energy than the related benzamide C–H activation step, this in itself is an interesting result as it might logically be thought that C–H activation at the δ-position would be less favourable compared to the γ-position. Substitution of the acetic acid for 3-buten-2-one is energetically unfavourable (≈9 kcal mol^{-1}), which differs significantly from the benzamide functionalisation example, where the substitution if favoured (Figure 2). The carbon–carbon bond formation step, functionalisation of the aromatic ring, proceeds with a low barrier (3.4 kcal mol^{-1}) leading to an 8-membered cobaltacycle. As with the previous study the tautomerization to the metallo–enol structure is an important step in the reaction, interestingly the 8- to 10-membered ring tautomerization is energetically less hindered than the 7- to 9-membered benzamide equivalent. This energy difference could be influenced by the ordering of the reaction steps, with the addition of an acetic acid group to either the keto or enol form (benzamide or acetanilide respectively). Addition of the acetic acid group to the acetanilide keto intermediate (**Int 3$_{ketone}$**) was calculated but proved to be less favourable than the initial tautomerization. Protonation of the unsaturated β-carbon position formed the highly stable **Int 5**, which dissociates to form the observed product and regenerate the cationic active catalyst species $[Cp^*Co(III)OAc]^+$. The less than 0.5 kcal mol^{-1} energy difference between the C–H activation and C–C bond formation steps makes identification of the rate limiting step difficult by DFT calculations alone, however, parallel kinetic isotope effect

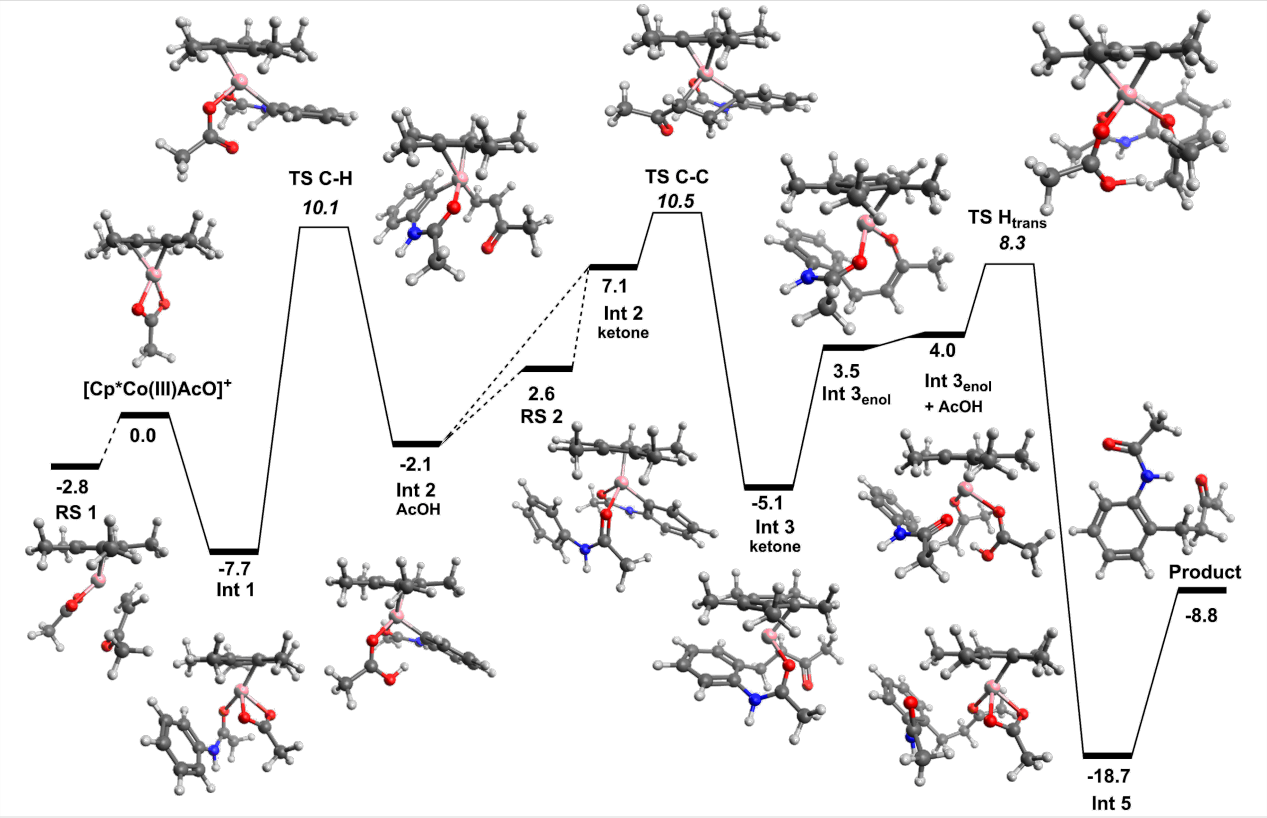

Figure 1: Mechanistic pathway for Cp*Co(III)-catalysed alkylation of acetanilide with 3-buten-2-one obtained from DFT studies; **Int A** is the direct interaction between the cationic [Cp*Co(III)AcO]$^+$ species and the 3-buten-2-one coupling partner.

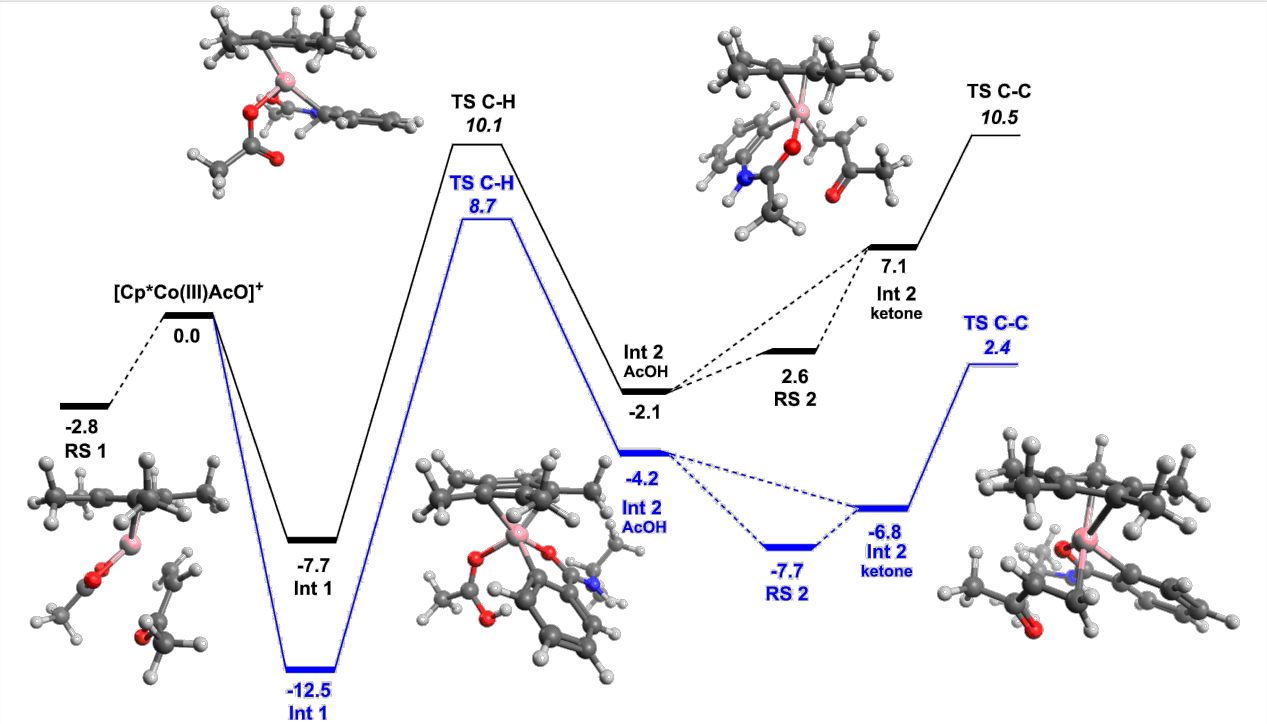

Figure 2: Comparison between energies during the Cp*Co(III)-catalysed coupling of 3-buten-2-one with acetanilide (black line) and benzamide (blue line); **RS 1** is the direct interaction between the cationic [Cp*Co(III)AcO]$^+$ species and the 3-buten-2-one coupling partner and **RS 2** is the interaction of the metallocycle intermediate with a second acetanilide.

(KIE) experiments do suggest that the C–H activation step is not rate limiting (KIE = 1.3), which is not inconsistent with the calculated mechanism.

As demonstrated in this work, experimentally functionalisation of the acetanilide with 3-buten-2-one requires significantly harsher reaction conditions compared to the equivalent benzamide functionalisation. From initial comparison of the two free energy surfaces these results are difficult to interpret. Although the barriers for the acetanilide reaction are greater, no one barrier is significantly large enough to account for harsher conditions. One interesting difference between the two mechanisms is the different energy requirements for the addition of the ketone group and the 3-buten-2-one (Figure 2). The endergonic ligand exchange between acetic acid and ketone, for the acetanilide reaction, is clearly a differentiating step in the reaction. Coupled with a more energetically favourable resting state (**RS2**), resulting from addition of another substrate molecule to the initial metallocycle, the conversion is more challenging and therefore requires harsher reaction conditions. This competitive binding (**Int 2$_{substrate}$** vs **RS 2**) is similar to that proposed by Bergman and Ellman for Cp*Rh(III)-catalysed arylation of imines [27]. Additionally **RS 1**, resulting from binding of the 3-buten-2-one to the active catalyst, for the acetanilide reaction is energetically more competitive compared to the benzamide reaction where both the ketone and substrate binding are preferable. The inclusion of a number of competitive intermediates/resting states on the potential energy surface goes some way to account for the observed differential experimental conditions for the two, different, yet related classes of substrate. This reactant limitation from **RS 1** is not observed in the benzamide reaction due to the exergonic nature of the ligand exchange (Figure 2). Although **RS 2** is energetically more favourable, compared to **Int 2$_{ketone}$**, the energy difference of only 0.9 kcal mol^{-1} would lead to facile ligand exchange. Structurally the main difference between the acetanilide and benzamide intermediates is the 6- vs 5-membered cobaltacycle ring. Understanding the influence this difference has on the binding strength of the functionalising group (3-buten-2-one in this example) is an important step in understanding why some reactions catalysed by [Cp*Co(III)OAc]$^{+}$ are more successful than others. To probe this phenomenon in more detail we performed quantum theory of atoms in molecules (QTAIM) analysis using Multiwfn software [28] of the two intermediate structures, identifying the relevant parameters at the bond critical points (*bcp*) of interest. QTAIM analysis has been used previously in the field of transition metal organometallic complexes to understand ligand binding [29-31].

Analysis of the relative structural parameters for the two complexes (Table 1 and Figure 3) highlights an increase in bond lengths for the ketone substrate bound to the cobalt with the acetanilide ligand. The implied stronger cobalt to ketone interaction with the benzamide ligand is also confirmed with the QTAIM *bcp* parameters (Co·C$_\alpha$ and Co·C$_\beta$); the increased electron density (ρ) and the greater negative terms for H(r) and V(r) all suggest a stronger bonding interaction. The decreased electron density at the C$_\alpha$·C$_\beta$ *bcp* suggests greater donation of electron density to the cobalt, this is confirmed by the increase in electron density at the three centred *bcp* (Co·C$_\alpha$=C$_\beta$). The slight

Table 1: QTAIM and structural parameters for **Int 2$_{ketone}$** with the acetanilide and benzamide substrates.

	QTAIM properties				
acetanilide	ρ	$\nabla^2\rho$	H(r)	V(r)	bond (Å)
Co·C$_\alpha$	0.0777	0.1924	−0.0225	−0.0931	2.13
Co·C$_\beta$	0.0792	0.1851	−0.0241	−0.0945	2.10
C$_\alpha$·C$_\beta$	0.3038	−0.8028	−0.3106	−0.4205	1.40
Co·C$_\alpha$=C$_\beta$	0.0769	0.2423	−0.0199	−0.1003	2.00
Co·O	0.0859	0.4713	−0.0167	−0.1512	1.95
Co·C$_{lig}$	0.1147	0.1385	−0.0504	−0.1355	1.97
benzamide	ρ	$\nabla^2\rho$	H(r)	V(r)	bond (Å)
Co·C$_\alpha$	0.0829	0.1950	−0.0261	−0.1001	2.09
Co·C$_\beta$	0.0839	0.1906	−0.0271	−0.1018	2.08
C$_\alpha$·C$_\beta$	0.3012	−0.7910	−0.3061	−0.4145	1.41
Co·C$_\alpha$=C$_\beta$	0.0815	0.2600	−0.0221	−0.1092	1.96
Co·O	0.0853	0.4346	−0.0185	−0.1458	1.96
Co·C$_{lig}$	0.1222	0.1489	−0.0565	−0.1502	1.94

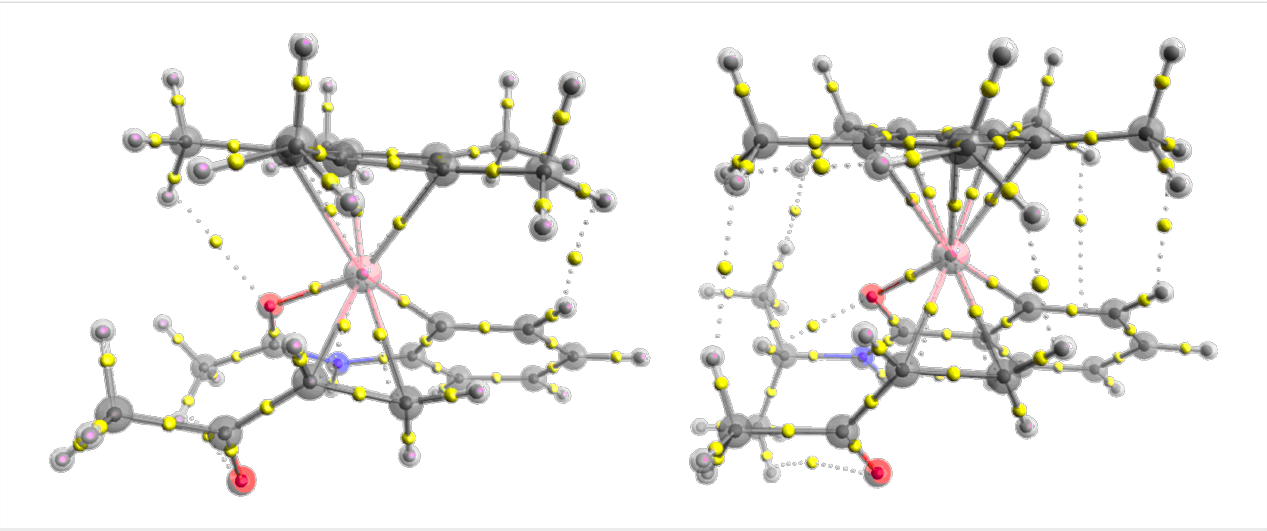

Figure 3: Comparative visualisation of *bcp* for **Int 2$_{ketone}$** with the acetanilide (left) and benzamide substrates (right).

asymmetric binding of the ketone is highlighted with shorter bond lengths and greater ρ and H(r) and V(r) parameters for Co·C$_β$, this asymmetry is more pronounced for the acetanilide complex. The reason for the stronger binding of the ketone substrate to the Co-benzamide complex can be explained by the significant differences observed for the cobaltacycle ligand binding. The 5-membered cobaltacycle (with benzamide as the ligand) shows a significantly stronger cobalt–carbon interaction (Co·C$_{lig}$) coupled with a decrease in the ionic nature of the Co·O interaction (positive $\nabla^2\rho$ term) suggesting better orbital overlap for the 5-membered ring. The stronger binding to the benzamide ligand makes the cobalt centre more electron deficient, facilitating greater alkene π-electron donation and therefore a stronger interaction with the substrate. The combination of these two stabilising interactions reduces the relative energy of the benzamide complex with respect to the acetanilide complex.

In order to experimentally exemplify the preference in reactivity between the acetanilide and benzamide substrates, the acetanilide containing two aromatic moieties (**1q**) was subjected to the optimised reaction conditions (Scheme 4). The DFT studies suggested that selectivity should be observed between the two aromatic rings, in favour of the benzamide-type C–H functionalisation. In agreement with this proposal the reaction outcome demonstrates that the acetanilide environment is more challenging to convert than the corresponding benzamide environment. Indeed, the purified reaction product predominantly contains the benzamide substituted product **3q**, with traces of impurity which is proposed to be the acetanilide product (for the spectra see Supporting Information File 1). The exact regioselectivity of the major product was confirmed through the correlation between the carbonyl C atom and the single *ortho*-hydrogen atom on the newly substituted aromatic ring (see Supporting Information File 1 for all correlation spectra).

Conclusion

In summary, the translation to acetanilides of a previously successful Cp*Co(III)-catalysed alkylation of benzamides with 3-buten-2-one has been attempted. It has been found that this reaction is extremely challenging under these original conditions and that in order to obtain synthetically useful yields a significant increase in catalyst loading (20 mol %) is required. The optimised protocol is able to successfully provide coupling

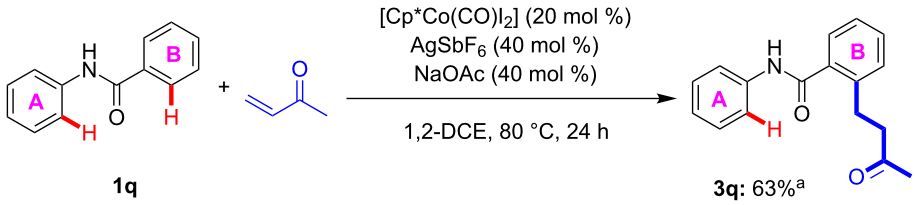

Scheme 4: Competitive experiment between coupling to acetanilide (ring A) or benzamide (ring B). [a]Major product **3q** obtained after purification with inseparable traces of proposed acetanilide coupling product.

products starting from a range of substituted acetanilides. The DFT studies on the mechanism demonstrate that in comparison to the previously reported benzamide example, the key step of co-ordination of the unsaturated coupling partner to the organometallic intermediate is significantly less favourable, thus a number of resting states of the catalyst become energetically more accessible, providing the reason for the requirement of more forcing conditions. Overall, this study provides an example of the challenges that need to be overcome when attempting to directly transfer an established protocol to even a related substrate class.

Experimental

Typical reaction protocol for alkylation: The experimental alkylation procedure is similar to that as described in [18]. A screw top vial, under air, was charged with acetanilide substrate (1.0 mmol), [Cp*Co(CO)I_2] (20 mol %, 0.20 mmol, 95.2 mg), $AgSbF_6$ (40 mol %, 0.4 mmol, 137.4 mg), NaOAc (40 mol %, 0.4 mmol, 16.4 mg), 3-buten-2-one (1.5 equiv, 1.5 mmol, 105 mg) and 1,2-DCE (8.0 mL). The vial was sealed, and the reaction mixture heated to 80 °C with stirring for 24 hours. After this period, the solvent was removed under reduced pressure and the crude product purified by column chromatography (ethyl acetate/petroleum ether; 80:20 in most cases). For full characterisation data of all products obtained, see Supporting Information File 1.

Computational details: All DFT calculations undertaken using the ORCA 3.03 computational software [32]. Optimisations were performed at the BP86-D3BJ/def2-TZVP level of theory [33-39] and final single point energies and solvation corrections calculated at M06/def2-TZVP [38-41]. Frequencies calculations approximated the ZPE correction and entropic contributions to the free energy term as well as confirming all intermediate were true with no imaginary modes and all transition states had the correct critical frequency of decomposition (imaginary mode). Solvation correction was implemented with the COSMO [42] model for CH_2Cl_2. Graphical visualisation using Gabedit 2.4.8 [43] and Avogadro 1.2.0 [44] programs. For full computational details see Supporting Information File 1. QTAIM analysis was performed with Multiwfn software [28].

Supporting Information

Supporting Information File 1

Experimental details and analytical data of new compounds including their original ^1H and ^{13}C and COSY spectra and data for all structures obtained from the DFT study.
[https://www.beilstein-journals.org/bjoc/content/supplementary/1860-5397-14-212-S1.pdf]

Acknowledgements

The authors would like to thank the Department of Biosciences and Chemistry at Sheffield Hallam University for funding. CJW and PGC would also like to thank COST Action CA15106 (CHAOS: C–H Activation in Organic Synthesis) for funding and providing a fruitful platform for discussion. The authors would also like to thank Dr. Daniel Allwood for his input in assisting the assignment of NMR spectra.

ORCID® iDs

Christopher J. Whiteoak - https://orcid.org/0000-0003-1501-5582

References

1. Hartwig, J. F.; Larsen, M. A. *ACS Cent. Sci.* **2016,** *2,* 281–292. doi:10.1021/acscentsci.6b00032
2. Davies, H. M. L.; Morton, D. *ACS Cent. Sci.* **2017,** *3,* 936–943. doi:10.1021/acscentsci.7b00329
3. Labinger, J. A.; Bercaw, J. E. *Nature* **2002,** *417,* 507–514. doi:10.1038/417507a
4. Johansson Seechurn, C. C. C.; Kitching, M. O.; Colacot, T. J.; Snieckus, V. *Angew. Chem., Int. Ed.* **2012,** *51,* 5062–5085. doi:10.1002/anie.201107017
5. Gensch, T.; Hopkinson, M. N.; Glorius, F.; Wencel-Delord, J. *Chem. Soc. Rev.* **2016,** *45,* 2900–2936. doi:10.1039/C6CS00075D
6. Pototschnig, G.; Maulide, N.; Schnürch, M. *Chem. – Eur. J.* **2017,** *23,* 9206–9232. doi:10.1002/chem.201605657
7. Planas, O.; Chirila, P. G.; Whiteoak, C. J.; Ribas, X. *Adv. Organomet. Chem.* **2018,** *69,* 209–282. doi:10.1016/bs.adomc.2018.02.002
8. Moselage, M.; Li, J.; Ackermann, L. *ACS Catal.* **2016,** *6,* 498–525. doi:10.1021/acscatal.5b02344
9. Wei, D.; Zhu, X.; Niu, J.-L.; Song, M.-P. *ChemCatChem* **2016,** *8,* 1242–1263. doi:10.1002/cctc.201600040
10. Yoshino, T.; Matsunaga, S. *Adv. Synth. Catal.* **2017,** *359,* 1245–1262. doi:10.1002/adsc.201700042
11. Wang, S.; Chen, S.-Y.; Yu, X.-Q. *Chem. Commun.* **2017,** *53,* 3165–3180. doi:10.1039/C6CC09651D
12. Chirila, P. G.; Whiteoak, C. J. *Dalton Trans.* **2017,** *46,* 9721–9739. doi:10.1039/C7DT01980G
13. Das, R.; Kumar, G. S.; Kapur, M. *Eur. J. Org. Chem.* **2017,** 5439–5459. doi:10.1002/ejoc.201700546
14. Suzuki, Y.; Sun, B.; Yoshino, T.; Kanai, M.; Matsunaga, S. *Tetrahedron* **2015,** *71,* 4552–4556. doi:10.1016/j.tet.2015.02.032
15. Park, J.; Chang, S. *Angew. Chem., Int. Ed.* **2015,** *54,* 14103–14107. doi:10.1002/anie.201505820
16. Yan, Q.; Chen, Z.; Liu, Z.; Zhang, Y. *Org. Chem. Front.* **2016,** *3,* 678–682. doi:10.1039/C6QO00059B
17. Kuppusamy, R.; Santhoshkumar, R.; Boobalan, R.; Wu, H.-R.; Cheng, C.-H. *ACS Catal.* **2018,** *8,* 1880–1883. doi:10.1021/acscatal.7b04087
18. Chirila, P. G.; Adams, J.; Dirjal, A.; Hamilton, A.; Whiteoak, C. J. *Chem. – Eur. J.* **2018,** *24,* 3584–3589. doi:10.1002/chem.201705785
19. Yoshino, T.; Ikemoto, H.; Matsunaga, S.; Kanai, M. *Angew. Chem., Int. Ed.* **2013,** *52,* 2207–2211. doi:10.1002/anie.201209226

20. Li, J.; Zhang, Z.; Ma, W.; Tang, M.; Wang, D.; Zou, L.-H. *Adv. Synth. Catal.* **2017,** *359,* 1717–1724. doi:10.1002/adsc.201700097
21. Huang, L.; Wang, Q.; Qi, J.; Wu, X.; Huang, K.; Jiang, H. *Chem. Sci.* **2013,** *4,* 2665–2669. doi:10.1039/c3sc50630d
22. Gensch, T.; Vàsquez-Céspedes, S.; Yu, D.-G.; Glorius, F. *Org. Lett.* **2015,** *17,* 3714–3717. doi:10.1021/acs.orglett.5b01701
23. Bunno, Y.; Murakami, N.; Suzuki, Y.; Kanai, M.; Yoshino, T.; Matsunaga, S. *Org. Lett.* **2016,** *18,* 2216–2219. doi:10.1021/acs.orglett.6b00846
24. Chirila, P. G.; Skibinski, L.; Miller, K.; Hamilton, A.; Whiteoak, C. J. *Adv. Synth. Catal.* **2018,** *360,* 2324–2332. doi:10.1002/adsc.201800133
25. Guo, X.-K.; Zhang, L.-B.; Wei, D.; Niu, J.-L. *Chem. Sci.* **2015,** *6,* 7059–7071. doi:10.1039/C5SC01807B
26. Wang, Y.; Du, C.; Wang, Y.; Guo, X.; Fang, L.; Song, M.-P.; Niu, J.-L.; Wei, D. *Adv. Synth. Catal.* **2018,** *360,* 2668–2677. doi:10.1002/adsc.201800036
27. Tauchert, M. E.; Incarvito, C. D.; Rheingold, A. L.; Bergman, R. G.; Ellman, J. A. *J. Am. Chem. Soc.* **2012,** *134,* 1482–1485. doi:10.1021/ja211110h
28. Lu, T.; Chen, F. *J. Comput. Chem.* **2012,** *33,* 580–592. doi:10.1002/jcc.22885
29. Cortés-Guzmán, F.; Bader, R. F. W. *Coord. Chem. Rev.* **2005,** *249,* 633–662. doi:10.1016/j.ccr.2004.08.022
30. Farrugia, L. J.; Evans, C.; Lentz, D.; Roemer, M. *J. Am. Chem. Soc.* **2009,** *131,* 1251–1268. doi:10.1021/ja808303j
31. Yan, J.; Liu, C.; Zhang, D. *Org. Biomol. Chem.* **2018,** *16,* 5321–5331. doi:10.1039/C8OB00996A
32. Neese, F. *Wiley Interdiscip. Rev.: Comput. Mol. Sci.* **2012,** *2,* 73–78. doi:10.1002/wcms.81
33. Neese, F. *J. Comput. Chem.* **2003,** *24,* 1740–1747. doi:10.1002/jcc.10318
34. Becke, A. D. *Phys. Rev. A* **1988,** *38,* 3098–3100. doi:10.1103/PhysRevA.38.3098
35. Perdew, J. P. *Phys. Rev. B* **1986,** *33,* 8822–8824. doi:10.1103/PhysRevB.33.8822
36. Perdew, J. P. *Phys. Rev. B* **1986,** *34,* 7406. doi:10.1103/PhysRevB.34.7406
37. Grimme, S.; Ehrlich, S.; Goerigk, L. *J. Comput. Chem.* **2011,** *32,* 1456–1465. doi:10.1002/jcc.21759
38. Weigend, F.; Ahlrichs, R. *Phys. Chem. Chem. Phys.* **2005,** *7,* 3297–3305. doi:10.1039/b508541a
39. Schäfer, A.; Horn, H.; Ahlrichs, R. *J. Chem. Phys.* **1992,** *97,* 2571–2577. doi:10.1063/1.463096
40. Neese, F.; Wennmohs, F.; Hanson, A.; Becker, U. *Chem. Phys.* **2009,** *356,* 98–109. doi:10.1016/j.chemphys.2008.10.036
41. Zhao, Y.; Truhlar, D. G. *Theor. Chem. Acc.* **2008,** *120,* 215–241. doi:10.1007/s00214-007-0310-x
42. Sinnecker, S.; Rajendran, A.; Klamt, A.; Diedenhofen, M.; Neese, F. *J. Phys. Chem. A* **2006,** *110,* 2235–2245. doi:10.1021/jp056016z
43. Allouche, A.-R. *J. Comput. Chem.* **2011,** *32,* 174–182. doi:10.1002/jcc.21600
44. Hanwell, M. D.; Curtis, D. E.; Lonie, D. C.; Vandermeersch, T.; Zurek, E.; Hutchison, G. R. *J. Cheminf.* **2012,** *4,* No. 17. doi:10.1186/1758-2946-4-17

License and Terms

BEILSTEIN JOURNAL OF ORGANIC CHEMISTRY

Cobalt- and rhodium-catalyzed carboxylation using carbon dioxide as the C1 source

Tetsuaki Fujihara* and Yasushi Tsuji*

Review

Open Access

Address:
Department of Energy and Hydrocarbon Chemistry, Graduate School of Engineering, Kyoto University, Nishikyo-ku, Kyoto 615-8510, Japan

Email:
Tetsuaki Fujihara* - tfuji@scl.kyoto-u.ac.jp; Yasushi Tsuji* - ytsuji@scl.kyoto-u.ac.jp

* Corresponding author

Keywords:
carbon dioxide; carboxylation; cobalt; homogeneous catalysts; rhodium

Beilstein J. Org. Chem. **2018,** *14,* 2435–2460.
doi:10.3762/bjoc.14.221

Received: 18 June 2018
Accepted: 28 August 2018
Published: 19 September 2018

This article is part of the thematic issue "Cobalt catalysis".

Guest Editor: S. Matsunaga

Abstract

Carbon dioxide (CO_2) is one of the most important materials as renewable chemical feedstock. In this review, the Co- and Rh-catalyzed transformation of CO_2 via carbon–carbon bond-forming reactions is summarized. Combinations of metals (cobalt or rhodium), substrates, and reducing agents realize efficient carboxylation reactions using CO_2. The carboxylation of propargyl acetates and alkenyl triflates using cobalt complexes as well as the cobalt-catalyzed reductive carboxylation of α,β-unsaturated nitriles and carboxyamides in the presence of Et_2Zn proceed. A Co complex has been demonstrated to act as an efficient catalyst in the carboxylation of allylic C(sp^3)–H bonds. Employing zinc as the reductant, carboxyzincation and the four-component coupling reaction between alkyne, acrylates, CO_2, and zinc occur efficiently. Rh complexes also catalyze the carboxylation of arylboronic esters, C(sp^2)–H carboxylation of aromatic compounds, and hydrocarboxylation of styrene derivatives. The Rh-catalyzed [2 + 2 + 2] cycloaddition of diynes and CO_2 proceeds to afford pyrones.

Introduction

Carbon dioxide (CO_2) is one of the most important materials as renewable feedstock [1-4]. However, the thermodynamic and kinetic stability of CO_2 sometimes limits its utility. Classically, harsh reaction conditions such as high temperature and high pressure of CO_2 were required. To overcome these problems, the use of transition-metal catalysts has been considered as a fundamental and reliable method. In the last decade, considerable attention has been focused on the development of the catalytic fixation of CO_2 via carbon–carbon (C–C) bond formation using a variety of organic compounds as starting materials [5-20]. A key factor for the successful catalytic fixation of CO_2 is the carbon–metal bond formation when transition metals are used as the catalyst. In addition, the choice of suitable reducing agents is also crucial for realizing effective carboxylation reactions.

In this review, the Co- and Rh-catalyzed transformations of CO_2 via C–C bond-forming reactions are summarized. First, we

describe Co-catalyzed carboxylation reactions, including the carboxylation of propargyl acetates and alkenyl triflates. Then, the Co-catalyzed reductive carboxylation of α,β-unsaturated nitriles and carboxyamides is addressed. In addition, a Co catalyst can catalyze the allylic C(sp^3)–H carboxylation of allylarenes when a suitable ligand is used. In the presence of zinc powder, the Co-catalyzed carboxyzincation of alkynes and the four-component coupling reaction between alkyne, acrylates, CO_2, and zinc proceed in an efficient manner. Visible-light-driven hydrocarboxylation reactions are shown. We also summarize carboxylation reactions catalyzed by rhodium that is a homologous element of cobalt. Carboxylations of arylboronic esters are described. Rh complexes are also effective catalysts in C(sp^2)–H carboxylation reactions. Employing Et_2Zn or visible light, the Rh-catalyzed hydrocarboxylation of styrene derivatives has been achieved. Furthermore, the formation of pyrones from diynes and CO_2 can be effectively catalyzed by Rh complexes.

Review

Cobalt catalysts

Carboxylation of propargyl acetates

Allyl and propargyl electrophiles, such as halides and esters, are well known as efficient reagents in transition-metal-catalyzed C–C bond-forming reactions [21-23]. In particular, the carboxylation of allyl esters with CO_2 has been catalyzed by Pd or Ni under electrochemical reaction conditions [24,25]. For catalytic reactions using reducing agents, Martin reported Ni-catalyzed regiodivergent carboxylation of allyl acetates in the presence of Mn as the reductant [26]. Mita and Sato found that Pd-catalyzed carboxylation of allylic alcohols proceeded using Et_2Zn as the reducing agent [27]. The carboxylation of propargyl chloride was reported as one of the examples concerning the Ni-catalyzed carboxylation of benzyl chlorides [28].

We have found that Co complexes can catalyze the carboxylation of propargyl acetates with CO_2 using Mn powder as the reducing agent [29]. Thus, the carboxylation of a propargyl acetate **1a** was performed in the presence of CoI_2(phen) (phen = 1,10-phenanthroline) and Mn powder (3.0 equiv) in *N*,*N*-dimethylacetamide (DMA) under an atmospheric pressure of CO_2 at room temperature (Scheme 1). Under optimized reaction conditions, the carboxylated product **2a-Me** was obtained in 83% yield after derivatization to the corresponding methyl ester. In the absence of the Co catalyst, **2a-Me** was not obtained. Moreover, Mn powder proved to be essential for the carboxylation to proceed. Using CoI_2(bpy) (bpy = 2,2′-bipyridine) as the catalyst afforded **2a-Me** in 76% yield, whereas $CoI_2(PPh_3)_2$ and CoI_2(dppe) (dppe = 1,2-bis(diphenylphosphino)ethane) suppressed the carboxylation.

The carboxylation of various propargyl acetates containing the trimethylsilyl (TMS) group as the R^1 group proceeded under the optimal reaction conditions, affording the corresponding carboxylic acids **2b**–**e** in good-to-high yields (Scheme 2). Notably, the ester and chloro functionalities in **2b** and **2c**, respectively, were compatible with the reaction conditions. For the carboxylation of tertiary-alcohol-derived acetates to the corresponding carboxylic acids **2d**,**e**, CoI_2(bpy) was found to be an effective catalyst. The yields of product **2** decreased when less bulky substituents (R^1) were used. Thus, **1f** (R^1 = *tert*-butyldimethylsilyl) afforded the corresponding product **2f** in 88% yield, whereas **1g** (R^1 = *t*-Bu) and **1h** (R^1 = Cy) afforded **2g** and **2h** in 57% and 26% yields, respectively.

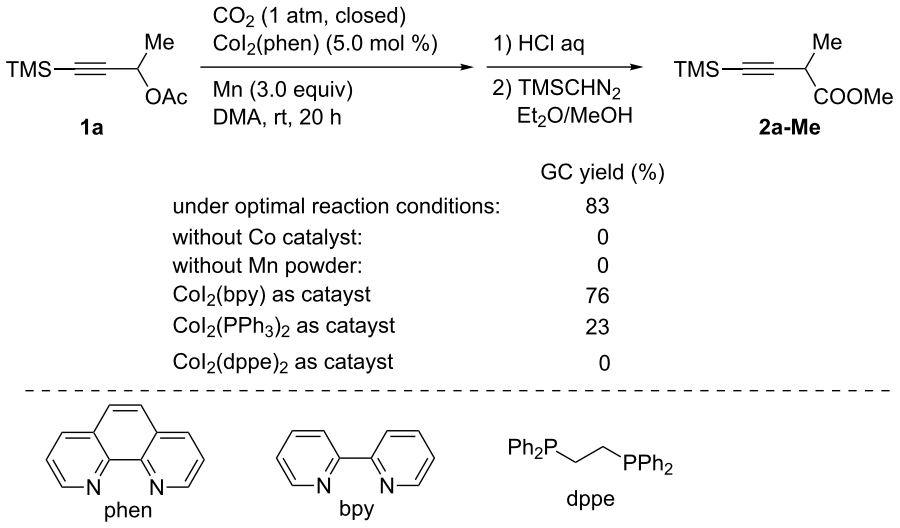

Scheme 1: Optimization of the Co-catalyzed carboxylation of **1a**.

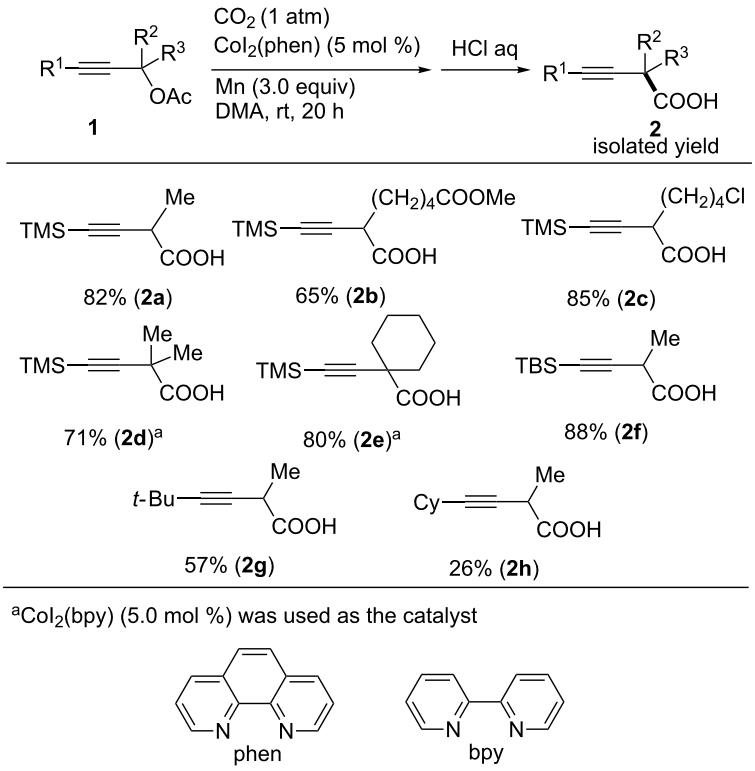

Scheme 2: Co-catalyzed carboxylation of propargyl acetates **1**.

Scheme 3 presents a plausible reaction mechanism for this transformation. Accordingly, a Co(I) catalytic species **A** is first generated by the reduction of Co(II) with Mn. Secondly, the oxidative addition of the C–O bond in **1** occurs, affording Co(III) intermediate **B** (step a) [30]. Next, the propargyl Co(III) species **B** is reduced by Mn, producing the corresponding propargyl Co(II) intermediate **C** (step b). Subsequently, the nucleophilic Co species **C** reacts with CO_2, which provides carboxylate

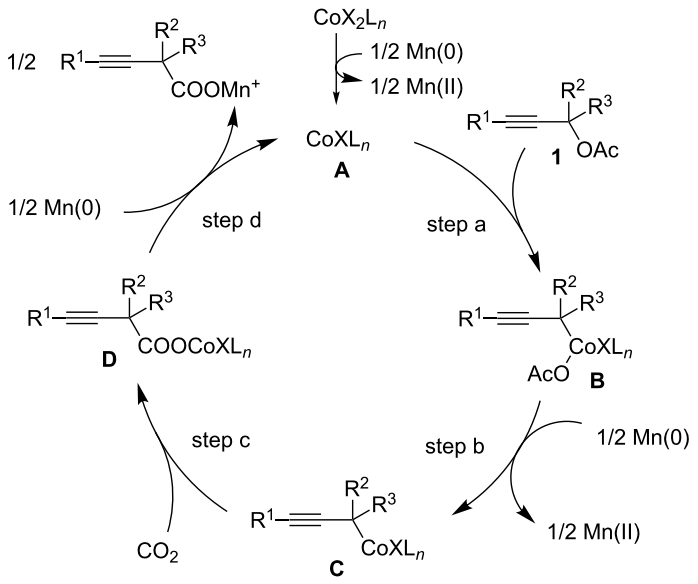

Scheme 3: Plausible reaction mechanism for the Co-catalyzed carboxylation of propargyl acetates **1**.

Co(II) intermediate **D** (step c). Finally, the reduction of **D** with Mn affords the corresponding carboxylate, regenerating the Co(I) catalytic species **A** (step d).

Carboxylation of alkenyl and aryl triflates

The catalytic carboxylation of aryl halides and pseudohalides using CO_2 is an important reaction to yield benzoic acid derivatives. In 2009, Martin reported the Pd-catalyzed carboxylation of aryl bromides using $ZnEt_2$ as the reductant [31]. In 2012, we first reported the Ni-catalyzed carboxylation of aryl chlorides and vinyl chlorides using Mn powder as the suitable reductant [32]. These reactions can be performed under mild conditions, i.e., an atmospheric pressure of CO_2 at room temperature.

We also reported the Co-catalyzed carboxylation of alkenyl and aryl trifluoromethanesulfonates (triflates) as substrates [33]. As a model reaction (Scheme 4), alkenyl triflate **3a** was selected as the substrate, and the carboxylation of **3a** was performed using Mn powder (1.5 equiv) as the reductant in DMA as the solvent under an atmospheric pressure of CO_2 at room temperature. Employing $CoI_2(Me_2phen)$ (Me_2phen = 2,9-dimethyl-1,10-phenanthroline) as the catalyst, **4a-Me** was obtained in 86% yield after esterification. Other bidentate ligands such as bpy, phen, and dppe were not suitable for this reaction. Control experiments revealed that both the Co catalyst and the Mn reductant were indispensable to the reaction.

The carboxylation of diverse alkenyl triflates was also examined. As a result, the desired carboxylic acids **4a**–**k** were obtained in good-to-high yields, as shown in Scheme 5. Notably, the ester and *p*-toluenesulfonate functionalities in **4c** and **4d**, respectively, were tolerated. An indole-functionalized substrate **3f** was converted into its corresponding carboxylic acid **4f**. Conjugated alkenyl triflates **3g–i** were also subjected to the reaction, and the desired carboxylic acids **4g–i** were obtained in moderate-to-high yields. Furthermore, the seven-membered cyclic substrate **3j** that was derived from cycloheptanone afforded its corresponding conjugated carboxylic acid **4j** in 75% yield. The alkenyl triflate **3k** prepared from the corresponding aldehyde was also carboxylated, and its corresponding product **4k** was obtained in moderate yield.

The catalyst $CoI_2(Me_2phen)$ was also effective with sterically hindered aryl triflates: the carboxylation of mesityl triflate (**5**) at 40 °C proceeded successfully, affording **6** in 77% yield (Scheme 6)

Carboxylation of α,β-unsaturated nitriles and esters

α,β-Unsaturated carbonyl compounds are good substrates for conjugate additions that use a catalytic amount of a metal complex and a stoichiometric amount of reductant, as exemplified by the reductive aldol reaction of α,β-unsaturated nitriles catalyzed by cobalt using phenylsilane as the reductant [34].

Yamada found that the reductive carboxylation of α,β-unsaturated compounds with CO_2 proceeded in the presence of Co catalysts and reductants (Scheme 7) [35,36]. When the reaction of 5-phenylpent-2-enenitrile (**7a**) was performed in the pres-

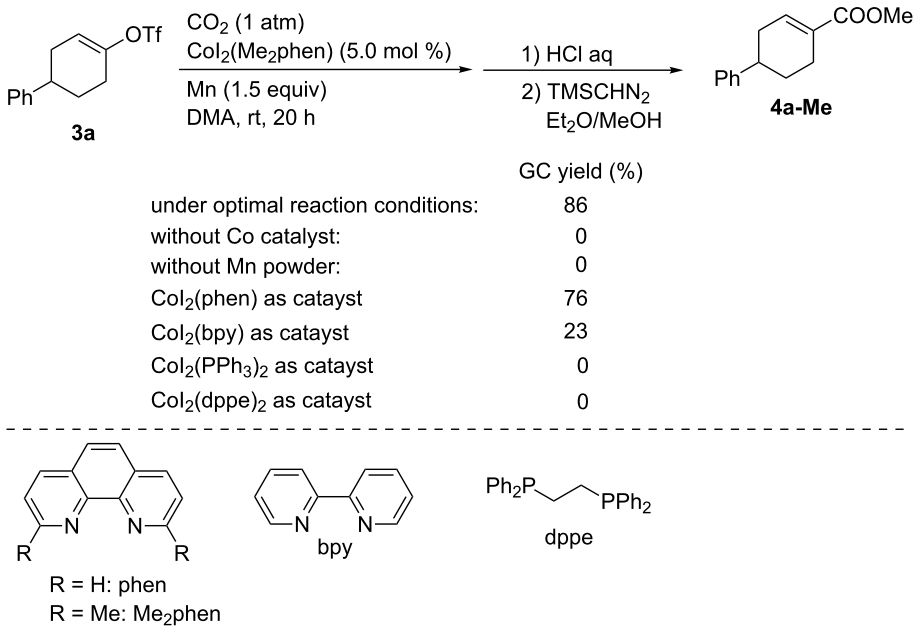

Scheme 4: Optimization of the Co-catalyzed carboxylation of **3a**.

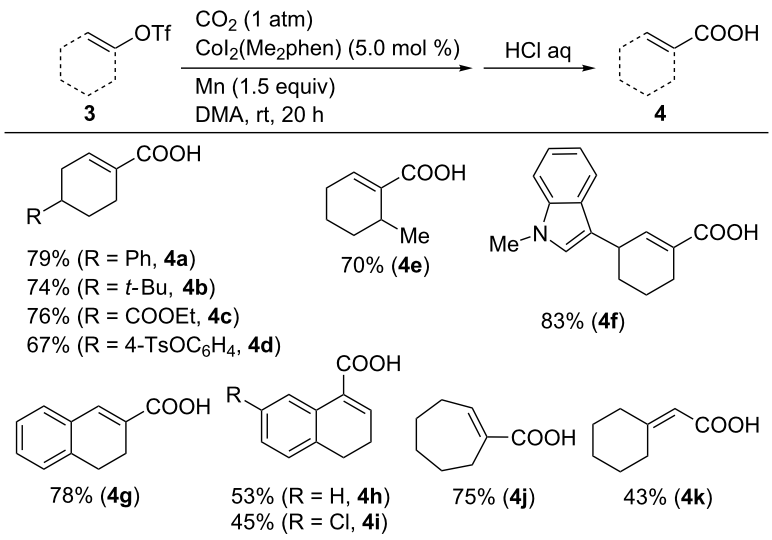

Scheme 5: Co-catalyzed carboxylation of vinyl triflates **3**.

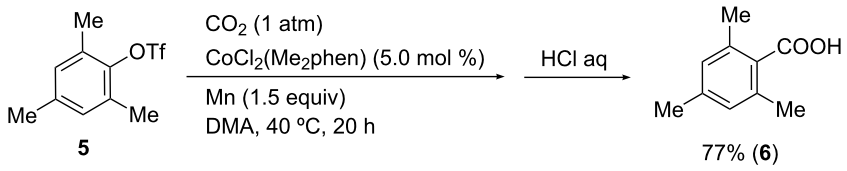

Scheme 6: Co-catalyzed carboxylation of a sterically hindered aryl triflate **5**.

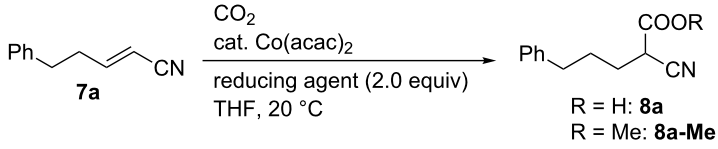

reducing agent	amount of $Co(acac)_2$ (mol %)	CO_2 pressure (MPa)	yield (%)
Et_2Zn	5	0.1	99 (**8a-Me**)
Et_2Zn	5	1.0	87 (**8a-Me**)
Et_2Zn	100	1.3	62 (**8a**)
Et_2AlCl	100	1.3	26 (**8a**)
Et_3B	100	1.0	10 (**8a**)

Scheme 7: Optimization of the Co-catalyzed carboxylation of **7a**.

ence of catalytic $Co(acac)_2$ and with Et_2Zn as the reductant, the carboxylation proceeded to yield **8a-Me** after its derivatization to the corresponding methyl ester. In these reactions, the selection of the reductant is crucial: other reductants such as Et_2AlCl and Et_3B yielded the corresponding product in low yields even after using a stoichiometric amount of $Co(acac)_2$ at high pressure.

Under the optimal reaction conditions with the $Co(acac)_2/Et_2Zn$ system, various α,β-unsaturated nitriles were carboxylated to the corresponding products, which were isolated as methyl esters (Scheme 8). Thus, compound **7** bearing alkyl, ether, ester, and halide substituents exhibited good reactivity. Cinnamonitrile afforded **8f-Me** in 81% yield using 10 mol % of catalyst. α-Phenyl-substituted α,β-unsaturated nitrile also reacted with

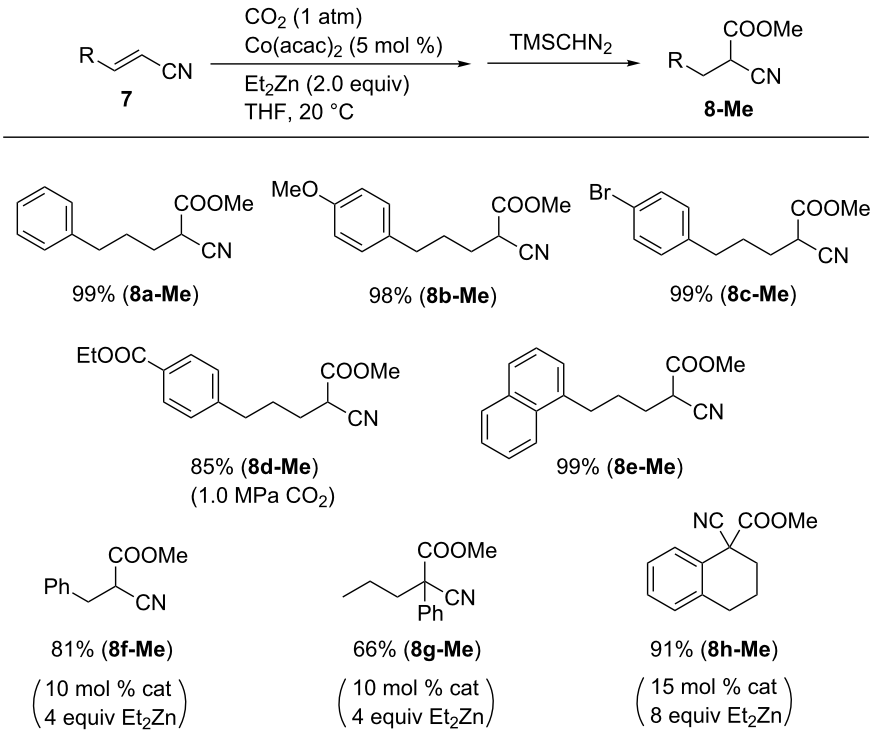

Scheme 8: Scope of the reductive carboxylation of α,β-unsaturated nitriles **7**.

CO_2, affording the carboxylated product **8g-Me** in good yield. In addition, compound **8h-Me** was obtained from the reaction of α-cyano-substituted dihydronaphthalene **7h** with CO_2 in the presence of 15 mol % of catalyst and 8 equiv of Et_2Zn.

The $Co(acac)_2/Et_2Zn$ system can also be applied to carboxylate α,β-unsaturated carboxamides **9** (Scheme 9). By using 10 mol % of $Co(acac)_2$ and 4 equiv of Et_2Zn, *N*-methylanilide derivatives **9a**–**f** were smoothly converted into the corresponding products **10a**–**f** in high yields. Trifluoromethyl and chloro substituents were tolerated in these reactions, judging by the formation of products **10c-Me** and **10d-Me**. With regard to other amide groups, morpholides **9g–i** could be used and benzylmethylamide- and diethylamide-bearing substrates, which afforded the corresponding products **10j-Me** and **10k-Me**, albeit with moderate yields.

Allylic C(sp^3)–H bond carboxylation

The development of methods for the catalytic carboxylation of less reactive C–H bonds with CO_2 is crucial regarding both C–H activation and CO_2 fixation processes. Mita and Sato reported a cobalt-catalyzed allylic C–H carboxylation of allylarenes (Scheme 10), in which 1-allyl-4-phenylbenzene (**11a**) was reacted with CO_2 (1 atm) in the presence of $AlMe_3$ (3 equiv) using catalytic amounts of a Co precursor and ligands [37]. The catalytic system comprising $Co(acac)_2$ and Xantphos (4,5-bis(diphenylphosphino)-9,9-dimethylxanthene) afforded the corresponding carboxylated product **12a-Me** in an NMR yield of 71% after CH_2N_2 treatment. In the reaction mixture, olefin isomers were also generated in 20% yield. The ligands were found to have a strong influence in yields and selectivity. Thus, the use of DPEphos (2,2′-bis(diphenylphosphino)diphenyl ether), dppf (1,1′-bis(diphenylphosphino)ferrocene), dppp (1,3-bis(diphenylphosphino)propane), and bpy as ligands afforded the olefin isomerization product as the major product. Further screening of the reaction conditions revealed that the amount of $AlMe_3$ was critical: the product yield increased with decreasing $AlMe_3$ to 1.5 equiv. The concentration of **11a** also affected the efficiency of the reaction, and the isomerization of olefins could be suppressed at lower concentrations of **11a**, affording the desired **12a-Me** in 58% yield. With the addition of 1 equiv of CsF, the carboxylation was further accelerated to give **12a-Me** in 71% yield.

Using optimized reaction conditions, the substrate scope was examined (Scheme 11). Allylbenzene was converted into its corresponding carboxylated product **12a** in an isolated 68% yield, and various functionalized allylarenes bearing trifluoromethyl (**11b**) and alkoxy (**11c**,**d**) substituents were tolerated. The selectivity of the reaction was demonstrated with

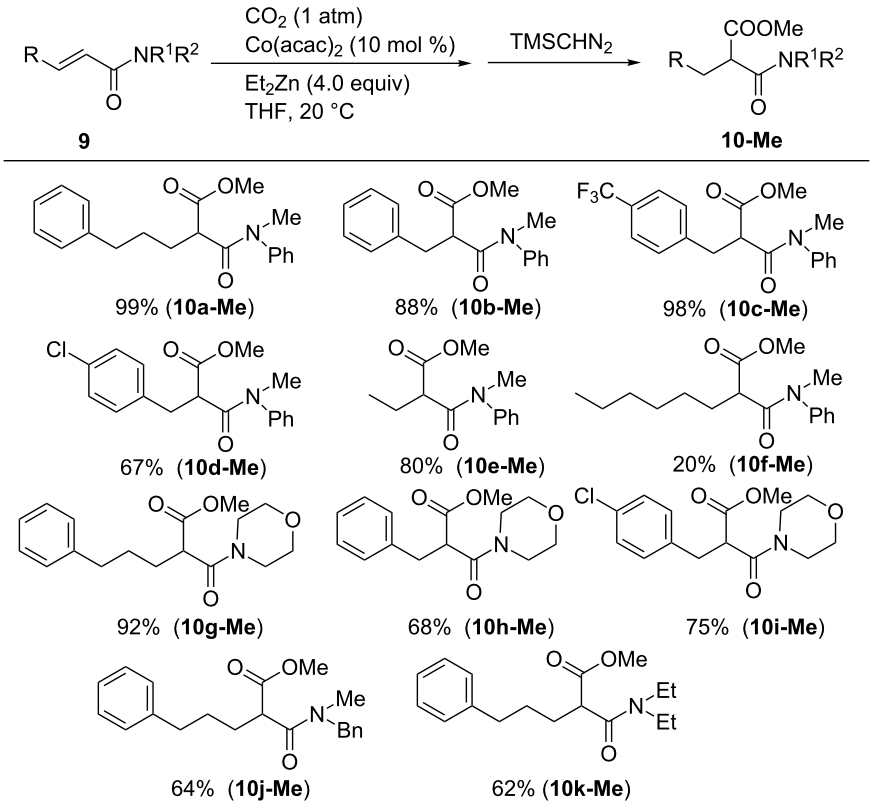

Scheme 9: Scope of the carboxylation of α,β-unsaturated carboxamides **9**.

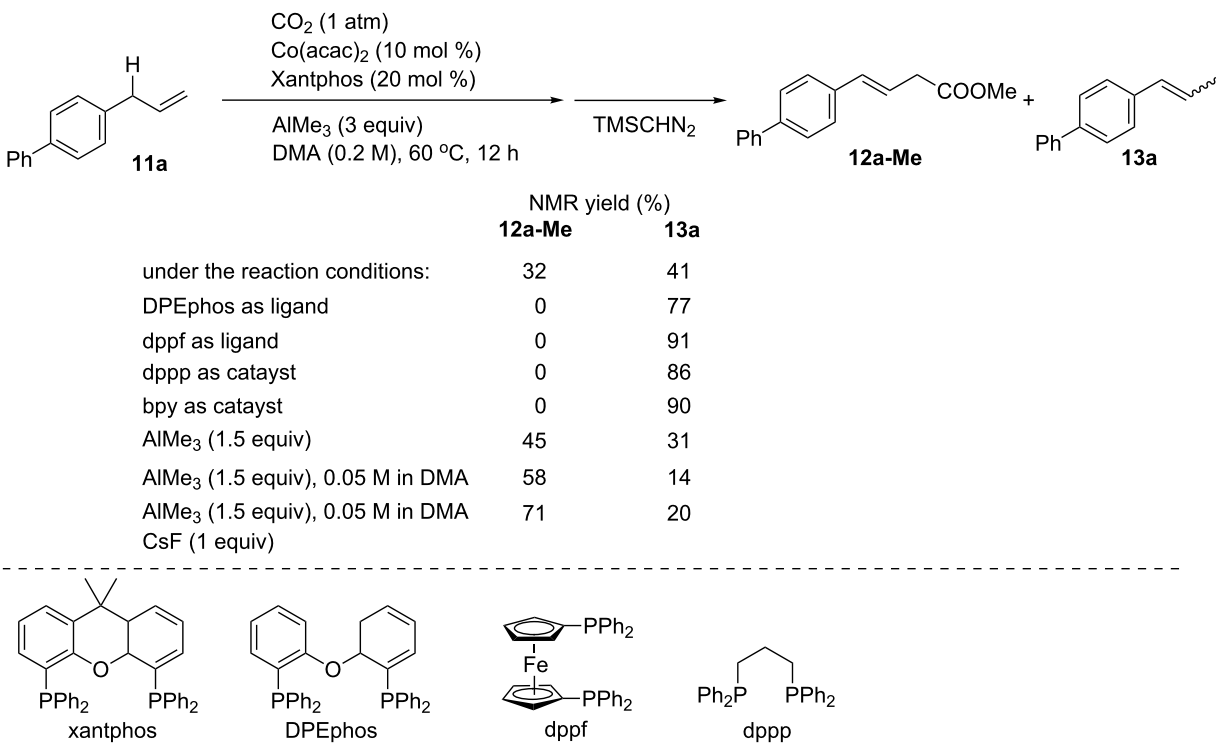

	NMR yield (%) 12a-Me	13a
under the reaction conditions:	32	41
DPEphos as ligand	0	77
dppf as ligand	0	91
dppp as catayst	0	86
bpy as catayst	0	90
$AlMe_3$ (1.5 equiv)	45	31
$AlMe_3$ (1.5 equiv), 0.05 M in DMA	58	14
$AlMe_3$ (1.5 equiv), 0.05 M in DMA CsF (1 equiv)	71	20

Scheme 10: Optimization of the Co-catalyzed carboxylation of **11a**.

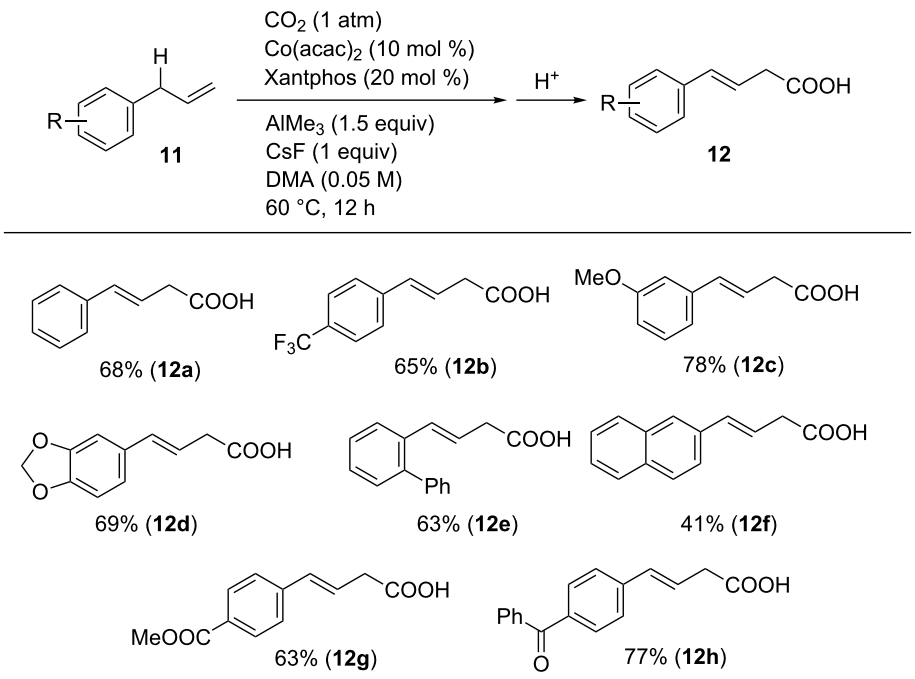

Scheme 11: Scope of the carboxylation of allylarenes **11**.

substrates **11g** and **11h** containing ester and ketone moieties, respectively, which are generally more reactive toward nucleophiles than CO_2.

Notably, the Co-catalyst system was found to be applicable for the carboxylation of 1,3-diene derivatives **14** with CO_2 (Scheme 12), which afforded various hexa-3,5-dienoic acid derivatives. Diene **14a** was converted into the corresponding carboxylic acid **15a** in good yield. In addition, 1,4-dienes having cyclohexenyl and geminal diphenyl substituents (**14b** and **14c**) produced their corresponding linear carboxylic acids **15b** and **15c** in 78% and 57% yields, respectively. Substrate **14e**

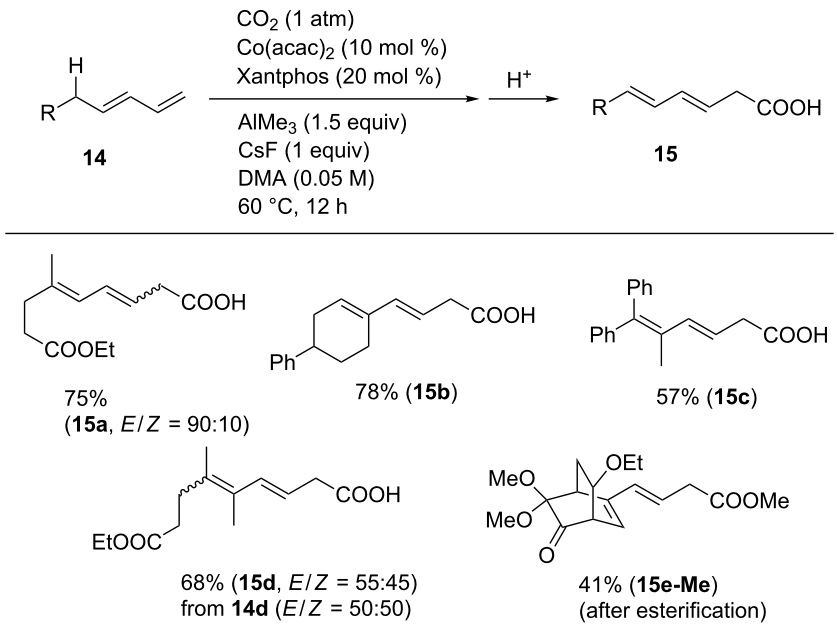

Scheme 12: Scope of the carboxylation of 1,4-diene derivatives **14**.

containing a bicyclo[2.2.2]octane framework with ketone and dimethyl ketal moieties was also converted and the corresponding product was isolated as the methyl ester **15e-Me** after esterification.

For the Co-catalyzed C(sp^3)–H carboxylation of allylarenes, a mechanism shown in Scheme 13 can be envisaged. The process starts with the generation of a low-valent methyl-Co(I) species **A** by the reaction of the Co(II) complex with $AlMe_3$. The C–C double bond of the substrate then coordinates to the metal, and the subsequent cleavage of the adjacent allylic C–H bond affords η^3-allyl-Co(III) species **B** (step a). Subsequently, the reductive elimination of methane from **B** yields the low-valent allyl-Co(I) species **C** (step b). Then, C–C bond formation at the γ-position occurs via a reaction with CO_2, affording the carboxylate Co species **D** (step c). Finally, a linear carboxylated product is obtained by the transmetalation between **D** and $AlMe_3$, with the concomitant regeneration of methyl-Co(I) **A** (step d).

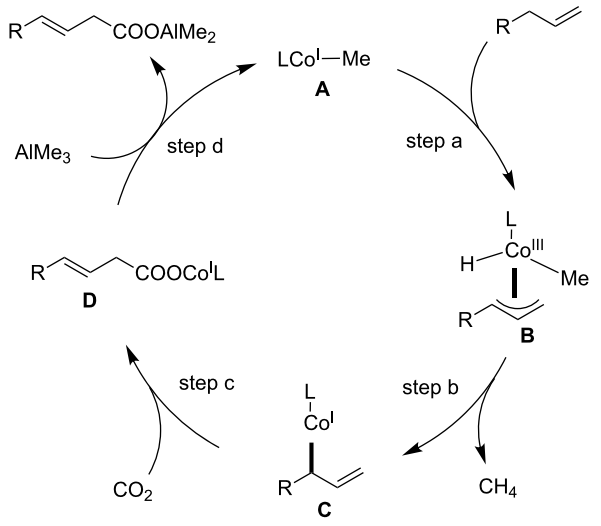

Scheme 13: Plausible reaction mechanism for the Co-catalyzed C(sp^3)–H carboxylation of allylarenes.

Carboxyzincation of alkynes

The good reactivity and high functional-group compatibility of organozinc compounds render them as important reagents in organic synthesis [38,39]. For their preparation, direct and useful methods such as the transition-metal-catalyzed carbozincation of alkynes that affords stereodefined alkenylzinc compounds have been developed. To date, a variety of organozinc reagents (RZnX and R_2Zn: R = aryl, alkyl, alkenyl, alkynyl, allyl, and benzyl groups) have been used in these reactions, and the corresponding alkenylzinc compounds can be prepared.

In this context, we reported the first carboxyzincation of alkynes using CO_2 and Zn metal powder in the presence of a cobalt complex as the catalyst (Scheme 14) [40]. 5-Decyne (**16a**) was treated with Zn powder (1.5 equiv) in the presence of CoI_2(dppf) (10 mol %), $Zn(OAc)_2$ (10 mol %), and Et_4NI (10 mol %) in a mixture of CH_3CN and DMF (v/v = 10:1) under an atmospheric pressure of CO_2 at 40 °C. When the reaction mixture was quenched with D_2O (>99% D), deuterated **17a-D** was obtained in a ^1H NMR yield of 80% with excellent deuterium incorporation ratio (94%) at the β-position. Al-

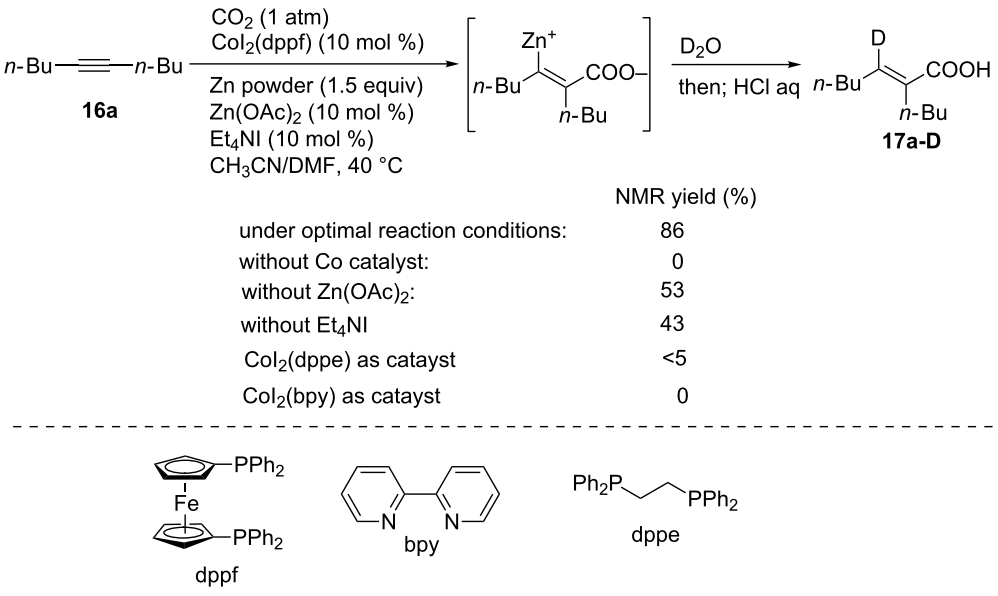

Scheme 14: Optimization of the Co-catalyzed carboxyzincation of **16a**.

though $Zn(OAc)_2$ and Et_4NI were not indispensable for the reaction to proceed, these two additives caused an increased product yield. In contrast, the reaction did not occur in the absence of the catalyst. The use of the dppf ligand also proved to be essential, because other ligands such as dppe and bpy were not effective in the reaction.

After the reaction with 4-octyne (**17b**) under the aforementioned conditions, the reactions with I_2 and $(PhSe)_2$ produced **17b-I** and **17b-Se** in good yields (Scheme 15). Notably, **16b** was successfully subjected to the Pd-catalyzed Negishi coupling with aryl bromide, affording the corresponding sterically congested alkene **17b-Ar** in 56% yield after two steps. The Negishi coupling with benzyl chloride and the Cu-catalyzed allylation of allyl bromide also afforded the corresponding products **17b-Bn** and **17b-Allyl**, respectively, in good yields.

The reaction successfully proceeded even with unsymmetrical internal alkynes. For instance, 1-(1-naphthyl)-1-hexyne (**16c**) afforded **17c-D** in 82% yield with excellent regioselectivity (Scheme 16). Thienyl-substituted alkynes such as **16d** and **16e** selectively furnished **17d-D**, **17d-Allyl**, and **17e-D**. Unsymmetrical internal alkynes bearing 4-$Me_2NC_6H_4$ and 4-$MeOC_6H_4$ moieties (**16f** and **16g**) afforded **17f-D**, **17g-D**, and **17g-Ar** regioselectively after treatment with D_2O or aryl iodide/Pd catalyst.

A possible reaction mechanism for the carboxyzincation reaction is displayed in Scheme 17. First, the Co(II) precursor is reduced to Co(I) (**A**) in the presence of metallic Zn. The oxidative cyclization of **A** with alkyne **16** and CO_2 affords cobaltacycle **B** (step a). Next, the transmetalation between **B** and the Zn(II) species occurs, which affords the alkenylzinc intermediate **C** (step b) [41], which is then reduced with Zn powder, thereby giving the carboxyzincated product and regenerating Co(I) species **A** (step c).

We also achieved the four-component coupling of alkynes **16**, acrylates **18**, CO_2, and Zn metal, as depicted in Scheme 18 [40]. As a model reaction, the reaction using diphenylacetylene (**16h**), butyl acrylate (**18a**), CO_2, and Zn was performed. After treatment with H_2O and allyl bromide, the corresponding products **19a-H** and **19a-Allyl** were obtained in high yields. Chloro and trifluoromethyl functionalities were well tolerated under the reaction conditions, and **19b-Me** and **19c-Me** were obtained in 55% and 57% yields, respectively. The reaction of unsymmetrical 1-phenyl-1-hexyne with **18a** afforded **19d-H** and **19d-Et** regioselectively. In addition, an alkyne with a thiophene ring regioselectively produced the desired product **19e-Me** after methylation with MeI. It is noteworthy that an alkynoate was also converted into the corresponding product **19f-Me** in good yield. Methyl, ethyl, and *tert*-butyl acrylates **18b**, **18c**, and **18d**, respectively, also afforded the corresponding products. The product of the reaction with acrylamide **18e** was also obtained.

Scheme 19 shows a plausible reaction mechanism for this four-component coupling reaction. In a similar manner to that described for the carboxyzincation, the reduction of the Co(II)

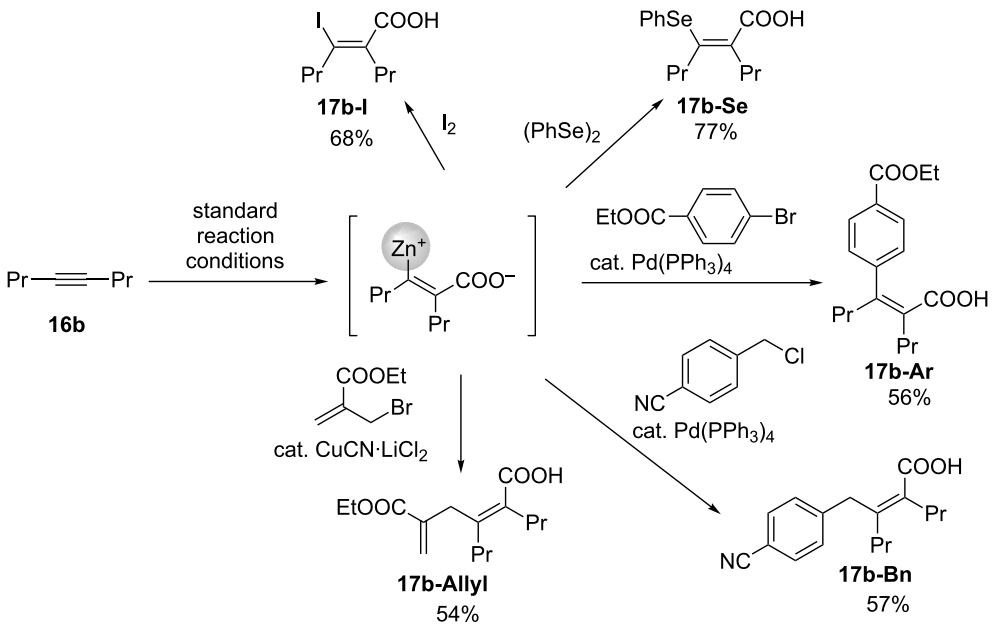

Scheme 15: Derivatization of the carboxyzincated product.

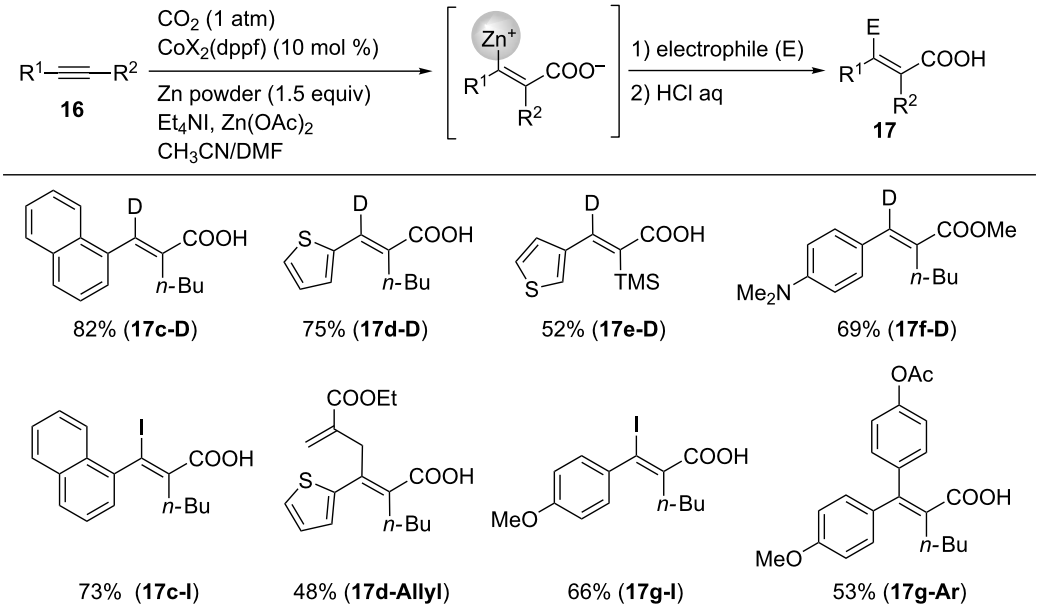

Scheme 16: Co-catalyzed carboxyzincation of alkynes **16**.

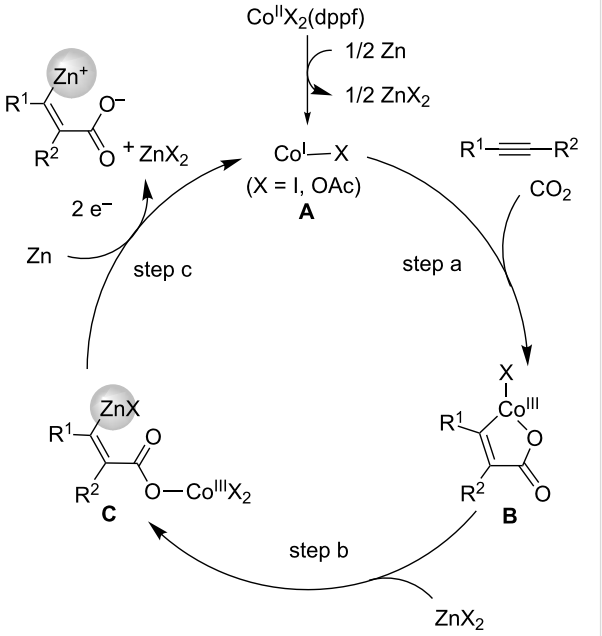

Scheme 17: Plausible reaction mechanism for the Co-catalyzed carboxyzincation of alkynes **16**.

precursor to Co(I) species **A** in the presence of Zn metal activates the catalytic cycle. Next, the oxidative cyclization of **A**, alkyne **16**, and acrylate **18** proceeds regioselectively, and cobaltacycle **B** is formed (step a) [42]. Then, the insertion of CO_2 into the Co–C(sp^3) bond occurs, and the seven-membered Co intermediate **C** is obtained (step b). The transmetalation of **C** with the Zn(II) species proceeds then to afford the alkenylzinc species **D** (step c). The subsequent two-electron reduction of **D** with Zn metal occurs, and the alkenylzinc intermediate **E** is subsequently obtained, along with the regeneration of Co(I) species **A** (step d). After 1,4-migration of zinc in **E**, product **19** is obtained (step e).

Visible-light-driven hydrocarboxylation of alkynes

The Use of photoenergy to organic synthesis is of importance, since the highly reactive intermediate can be generated by photochemical reaction such as electron transfer and energy transfer [43-45]. Among them, light-energy-driven CO_2 fixation reactions via C–C bond formation are promising in terms of mimicking photosynthesis. In 2015, Murakami et al. found the direct carboxylation reaction with CO_2 under photo-irradiation reaction conditions [46]. Jamison et al. also reported the synthesis of α-amino acid derivatives using amine and CO_2 [47]. Iwasawa disclosed the Pd-catalyzed carboxylation of aryl halides using CO_2 in the presence of an Ir photo-redox catalyst under visible-light irradiation conditions [48].

Zhao and Wu reported the visible-light-driven hydrocarboxylation of alkynes in the presence of a Co catalyst [49]. The reaction of alkynes was carried out using $CoBr_2$/dcype (dcype = bis(dicyclohexylphosphino)ethane) as catalysts in the presence of [Ir(ppy)(dtbpy)](PF_6) and iPr_2NEt as photoredox catalyst and a sacrificial reagent, respectively, in acetonitrile under an atmospheric pressure of CO_2 (Scheme 20). 1-Phenyl-1-propyne (**16n**) afforded hydrocarboxylated products as a mixture of

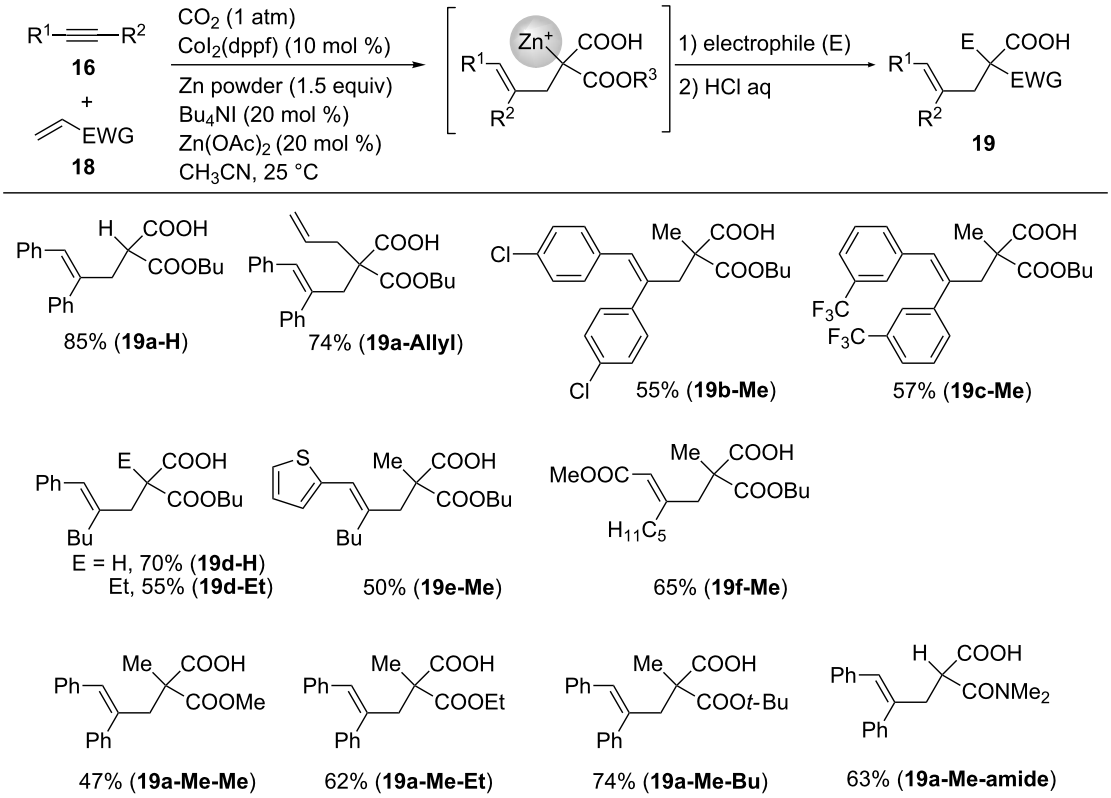

Scheme 18: Co-catalyzed four-component coupling of alkynes **16**, acrylates **18**, CO_2, and zinc.

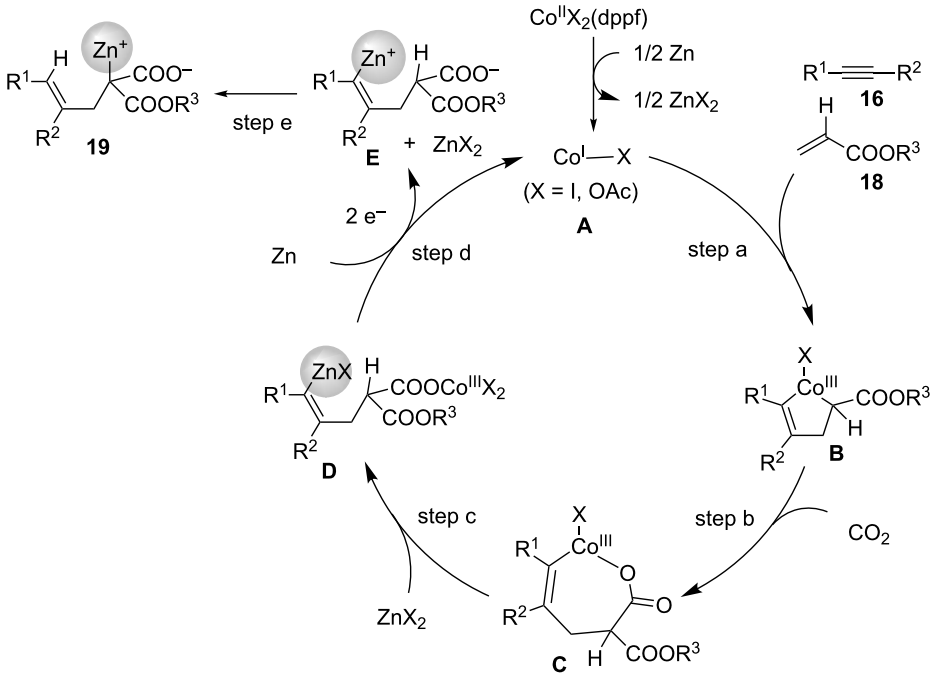

Scheme 19: Proposed reaction mechanism for the Co-catalyzed four-component coupling.

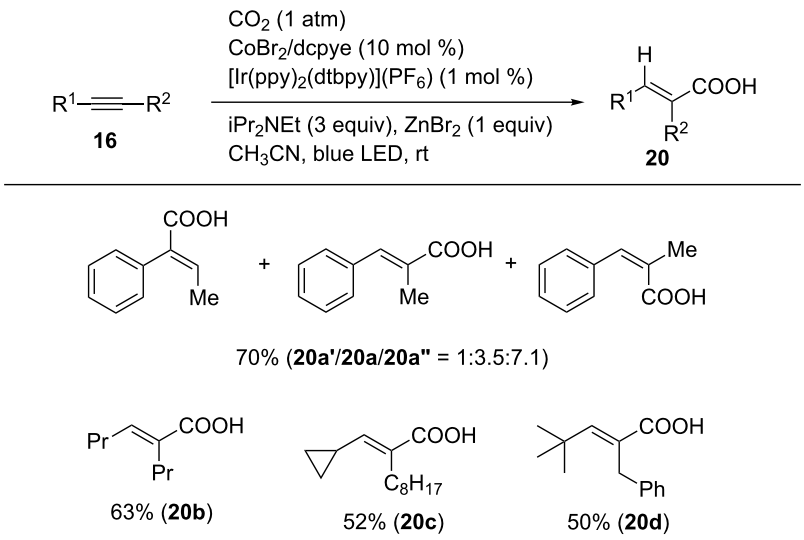

Scheme 20: Visible-light-driven hydrocarboxylation of alkynes.

regio- and stereoisomers. 4-Octyne (**16b**) afforded the product **20b** in good yield. Other unsymmetrical internal alkynes were converted to the corresponding products regioselectively.

The same protocol could be expanded to the synthesis of γ-hydroxybutenolides by using arylalkynes bearing *ortho*-esters of the aromatic ring (Scheme 21) [49]. Various alkynes **21** were

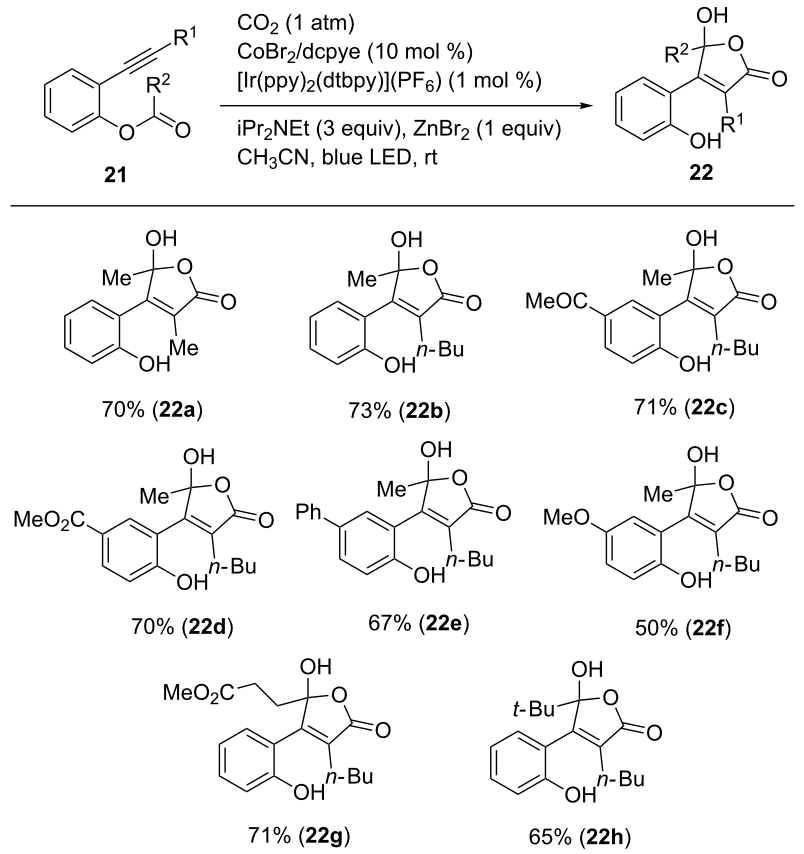

Scheme 21: Visible-light-driven synthesis of γ-hydroxybutenolides from *ortho*-ester-substituted aryl alkynes.

converted to the corresponding products in moderate-to-good yields. Notably, ketone (**22c**) and ester (**22d**,**g**) functionalities were tolerated in the reaction. A bulky ester moiety took part in the reaction and the corresponding product **22h** was obtained in good yield.

Furthermore, the same group discovered the one-pot synthesis of coumarin derivatives via hydrocarboxylation/alkene isomerization/cyclization reactions (Scheme 22) [49]. A key of the sequential reactions is a use of aromatic alkynes bearing a momo-protected hydroxy group at the *ortho* position on the aromatic ring (**23**). The corresponding coumarin derivatives were obtained in moderate-to-good yields. Notably, ketone (**24e**), ester (**24d**) moieties were tolerated in the reaction. In addition, 2-quinolones (**24f** and **24g**) were obtained using alkynes bearing a Boc protected carbamate in place of the MOM protected ether.

Scheme 23 shows a plausible reaction mechanism for these reactions. First, the Co(II) precursor is reduced to Co(I) **A** by the aid of an Ir photoredox catalyst and an amine under irradiation. The oxidative cyclization of **A** with **23** and CO_2 affords cobaltacycle **B** (step a). Next, the protonation of **B** affords an intermediate **C** (step b). Finally, two-electron reduction of Co(III) in **C** occurs and Co(I) species **A** regenerates (step c). $ZnBr_2$ may facilitate the step. Under the irradiation conditions, an *E*-isomer with aryl moiety can undergo a reversible isomerization to form the corresponding Z-isomer. Acid-mediated cyclization affords a coumarin derivative.

Rhodium catalysts

Carboxylation of aryl and alkenylboronic esters

Aryl and alkenylboronic acids or their esters are of interest in organic synthesis because they are commonly used for C–C bond-forming reactions such as Pd-catalyzed Suzuki–Miyaura coupling reactions [50-53].

Iwasawa et al. reported the Rh-catalyzed carboxylation of arylboronic esters using CO_2 (Scheme 24) [54]. The reaction of **25a** was performed using a catalytic amount of $[Rh(OH)(cod)]_2$ and 1,3-bis(diphenylphosphino)propane (dppp) in the presence of CsF as a base in 1,4-dioxane at 60 °C. Under these reaction conditions, the desired carboxylated product **26a** was obtained in 75% yield. A variety of arylboronic esters (**25b**–**i**) were converted into the corresponding carboxylic acids **26b**–**i** in good-to-high yields. It is noteworthy that ketone, ester, and nitrile functionalities in **26d**, **26e**, and **26f**, respectively, were tolerated in the reaction. Sterically hindered substrates could be subjected to the reaction, and **26g** was obtained from **25g**. Moreover, a substrate having a heteroaromatic ring (**25i**) was converted into its corresponding carboxylic acid **26i**.

Alkenylboronic esters **27** were also converted into the corresponding α,β-unsaturated carboxylic acids **28** using $[RhCl(nbd)]_2$ (nbd = norbornadiene) as a catalytic precursor (Scheme 25) [54]. When an alkyl-substituted substrate was examined, the *p*-methoxy-substituted dppp derivative was found to be the suitable ligand.

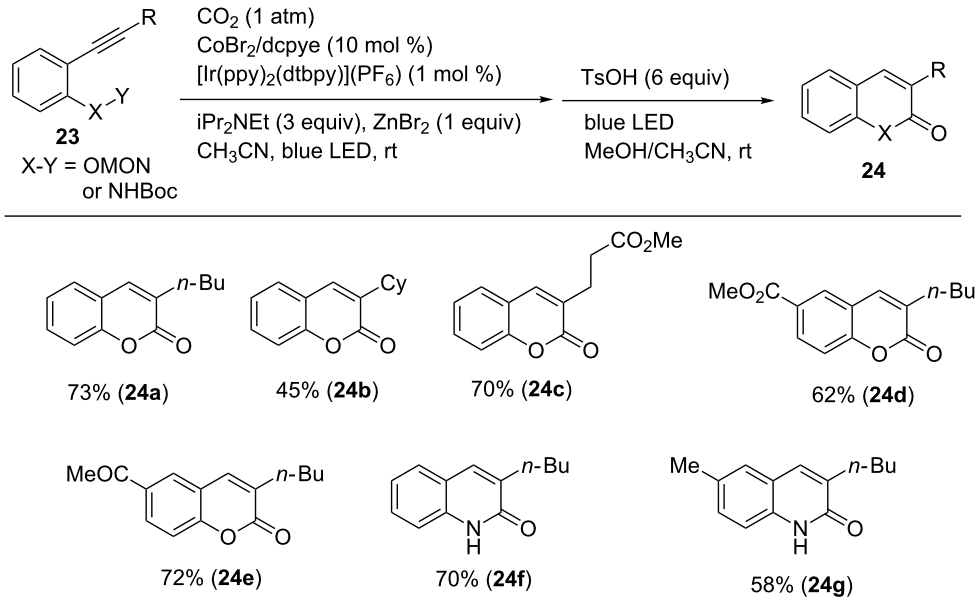

Scheme 22: One-pot synthesis of coumarines and 2-quinolones via hydrocarboxylation/alkyne isomerization/cyclization.

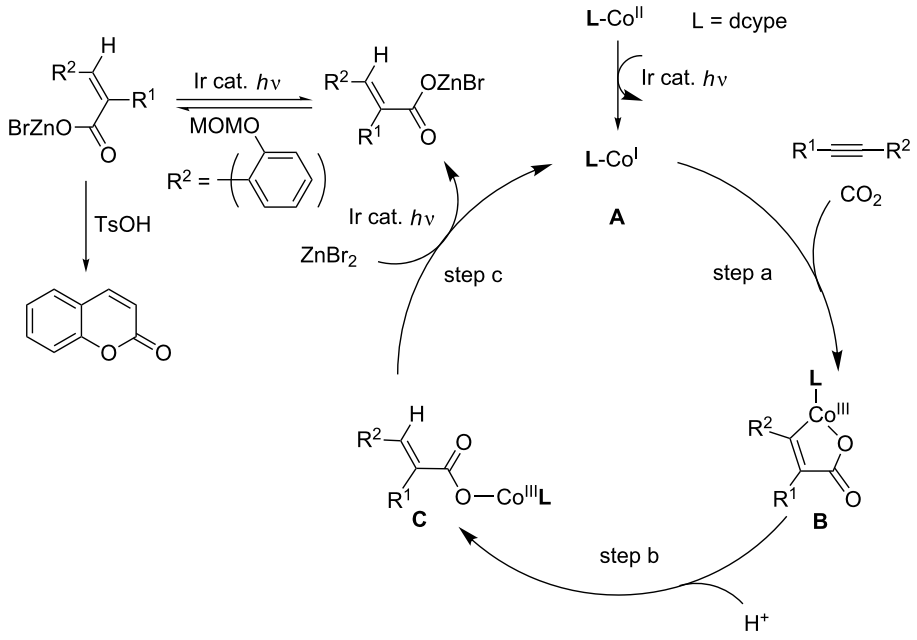

Scheme 23: Proposed reaction mechanism for the Co-catalyzed carboxylative cyclization of *ortho*-substituted aromatic alkynes.

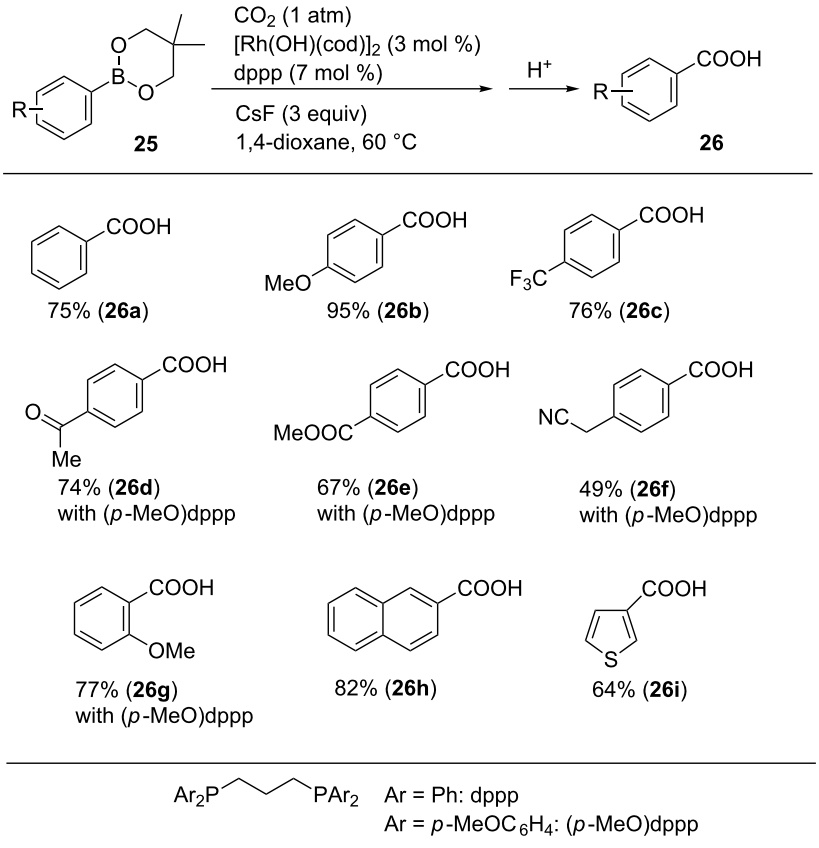

Scheme 24: Rh-catalyzed carboxylation of arylboronic esters **25**.

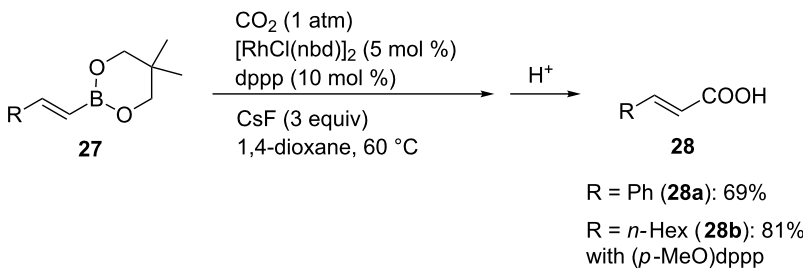

Scheme 25: Rh-catalyzed carboxylation of alkenylboronic esters **27**.

For this transformation, the reaction mechanism depicted in Scheme 26 was proposed. The catalytic cycle is activated by the generation of aryl-Rh intermediate **A** from the reaction of the Rh(I) species with the corresponding arylboronic ester. Next, the reaction of **A** with CO_2 proceeds with the concomitant generation of the corresponding carboxylate Rh species **B** (step a). Finally, transmetalation between **B** and the arylboronic ester affords the product, along with the aryl-Rh intermediate **A** (step b)

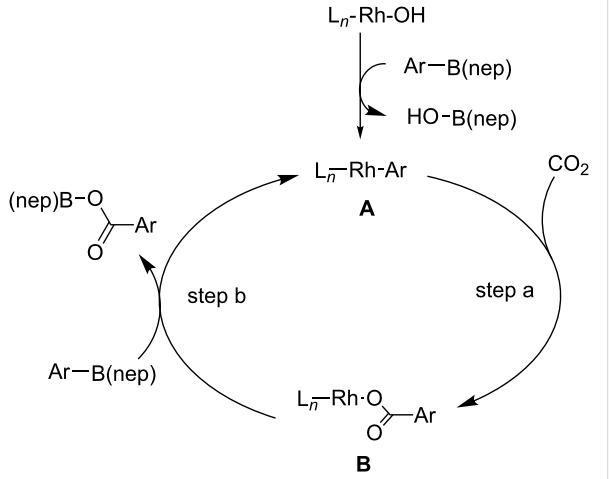

Scheme 26: Plausible reaction mechanism for the Rh-catalyzed carboxylation of arylboronic esters **25**.

After this contribution, the Cu-catalyzed carboxylation of aryl and alkenylboronic esters was independently reported by the groups of Iwasawa and How [55,56].

Direct C(sp^2)–H bond carboxylation

As described above, C–H carboxylations with CO_2, particularly C(sp^2)–H carboxylation reactions, have attracted much research interest. As a consequence, Nolan [57] and Hou [58] independently reported Cu-catalyzed carboxylations using heteroarenes as substrates, which occur at the relatively acidic C–H bond.

Regarding Rh as the catalyst, Iwasawa et al. first reported a rhodium-catalyzed chelation-assisted C(sp^2)–H carboxylation using methylaluminum as a reducing reagent (Scheme 27) [59]. Subsequently, the reaction of 2-phenylpyridine (**29a**) was performed using $AlMe_2(OMe)$ in DMA at 70 °C. Employing $[RhCl(coe)]_2$ (coe = cyclooctene) and $P(Mes)_3$ ($(P(Mes)_3$ = tris(2,4,6-trimethylphenyl)phosphine) as the catalyst, the carboxylated product **30a** was obtained in 67% yield, along with the formation of a methylated byproduct **31a**. Other phosphine ligands such as PPh_3, P(*t*-Bu)$_3$, and PCy_3 afforded the product in low-to-good yields.

Under the optimal reaction conditions using PCy_3 as the ligand, various 2-pyridylarenes **29** were converted into the corresponding products **30** (Scheme 28). Substrates bearing either electron-donating or electron-withdrawing substituents at the aryl ring afforded the corresponding products. Interestingly, a terminal alkenyl group remained intact after the reaction (**30d**). Furthermore, substrates bearing naphthyl or furyl rings were carboxylated, and the corresponding products, **30e** and **30f**, respectively, were obtained in good yields.

A plausible reaction mechanism for this Rh-catalyzed chelation-assisted C(sp^2)–H bond carboxylation is shown in Scheme 29. First, a low-valent methyl–Rh(I) species **A** is generated by transmetalation. Secondly, a pyridine ring in the substrate coordinates to the Rh center, which prompts the cleavage of the adjacent C–H bond, affording Rh(III) species **B** (step a). Subsequently, the reductive elimination of methane from **B** affords the low-valent Rh(I) species **C**. Then, C–C bond formation with CO_2 proceeds, and Rh carboxylate **D** is formed. Finally, the carboxylated product is obtained by the transmetalation between **D** and $AlMe_2(OMe)$, and methyl–Rh(I) **A** is regenerated.

Later, Iwasawa et al. achieved the Rh-catalyzed direct carboxylation of arenes without any directing group (Scheme 30) [60,61]. The reactions proceeded using a catalytic amount of Rh complex bearing dcype (dcype = 1,2-bis(dicyclohexylphosphino)ethane) as the ligand and $AlMe_2(OEt)$ as a reducing agent

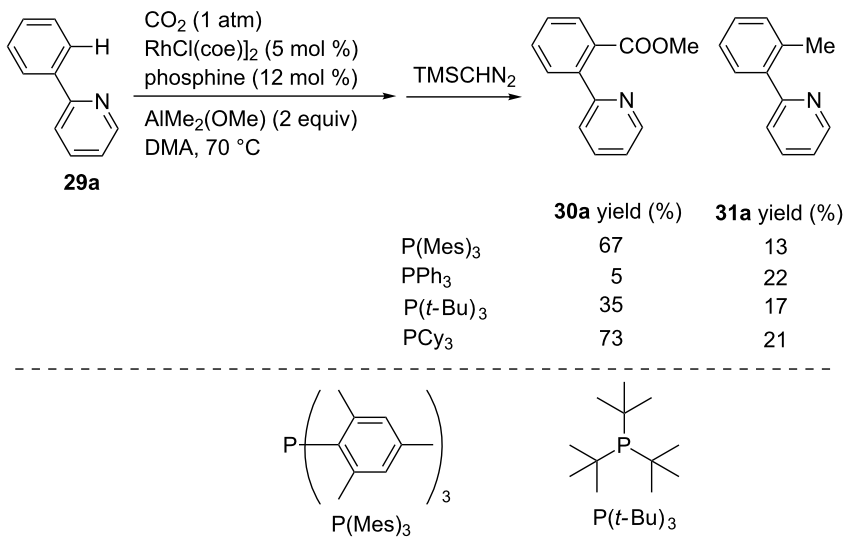

Scheme 27: Ligand effect on the Rh-catalyzed carboxylation of 2-phenylpyridine **29a**.

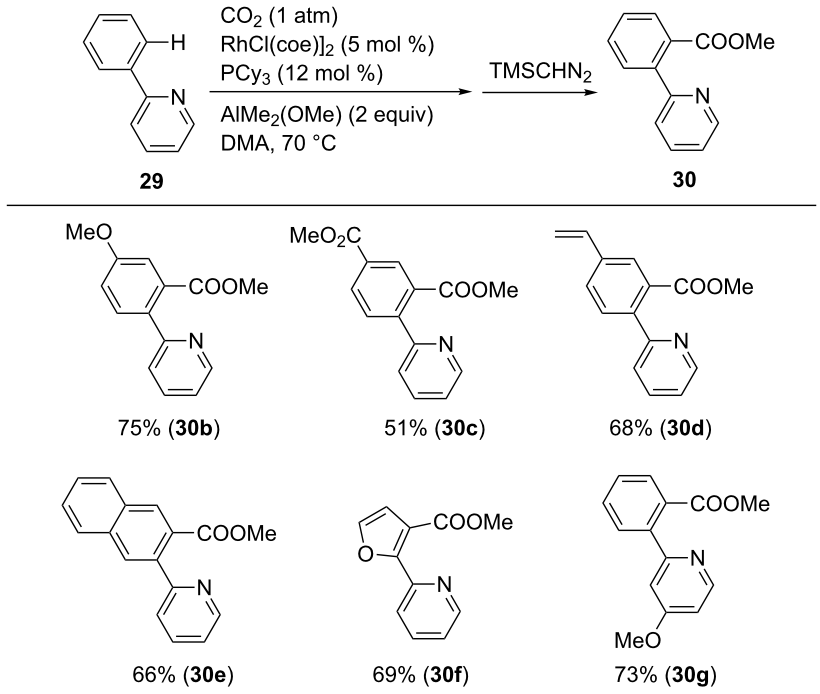

Scheme 28: Rh-catalyzed chelation-assisted C(sp^2)–H bond carboxylation with CO_2.

in a mixture of DMA and 1,1,3,3-tetramethylurea (TMU) as a solvent. Under the reaction conditions, benzene (**32a**) was converted into benzoic acid (**33a**, TON: 37) at 85 °C. The monosubstituted arenes such as toluene (**32b**), fluorobenzene (**32c**), and trifluoromethylbenzene (**32d**) afforded the corresponding carboxylic acids **33b, 33c**, and **33d** in good TON. *o*-Xylene yielded its corresponding mixture of carboxylic acids **33e**. When 1,3-bis(trifluoromethyl)benzene (**32f**) was used as the substrate at 145 °C, the corresponding carboxylic acid **33f** was site-selectively obtained in good TON. Benzofuran (**32h**) and indole (**32i**) also gave the carboxylic acids, which were isolated as their methyl esters.

Li and co-workers reported the Rh-catalyzed site-selective C(sp^2)–H carboxylation reaction using 2-arylphenols as the substrates (Scheme 31) [62]. The desired reactions proceeded using

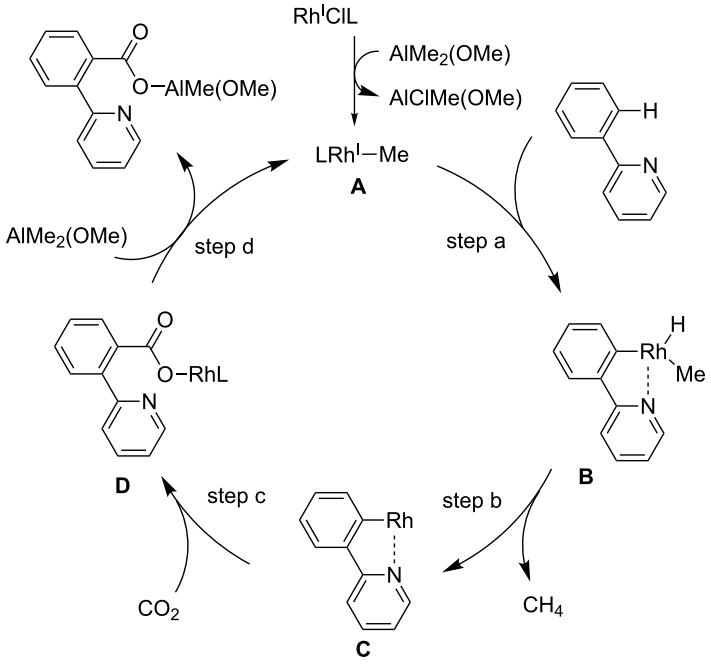

Scheme 29: Reaction mechanism for the Rh-catalyzed C(sp^2)–H carboxylation of 2-pyridylarenes **29**.

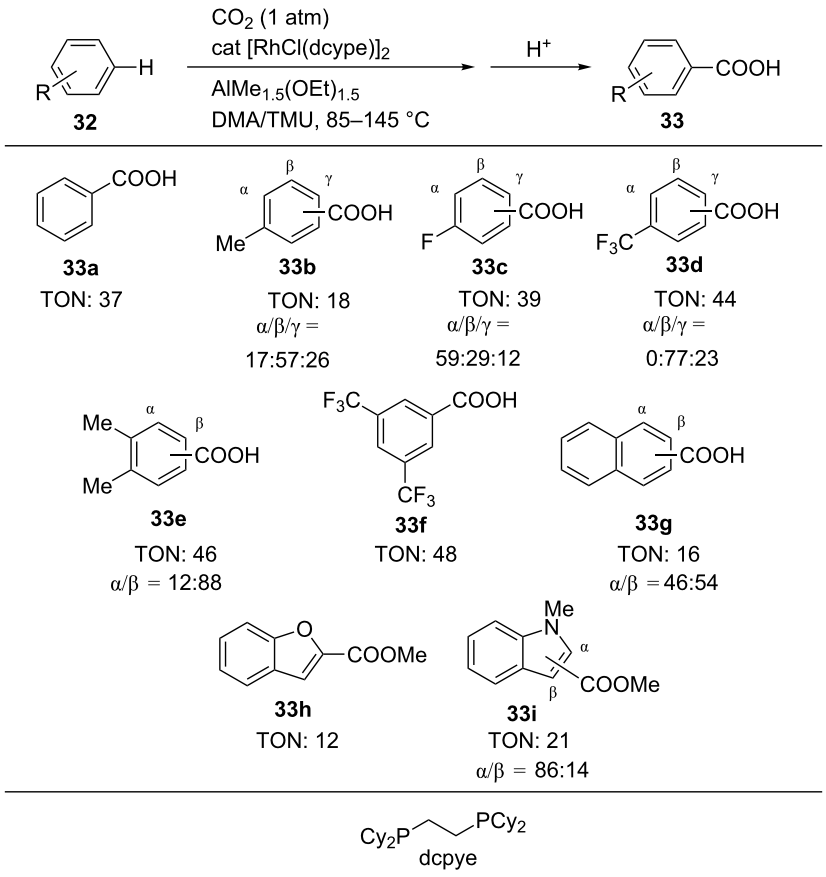

Scheme 30: Carboxylation of C(sp^2)–H bond with CO_2.

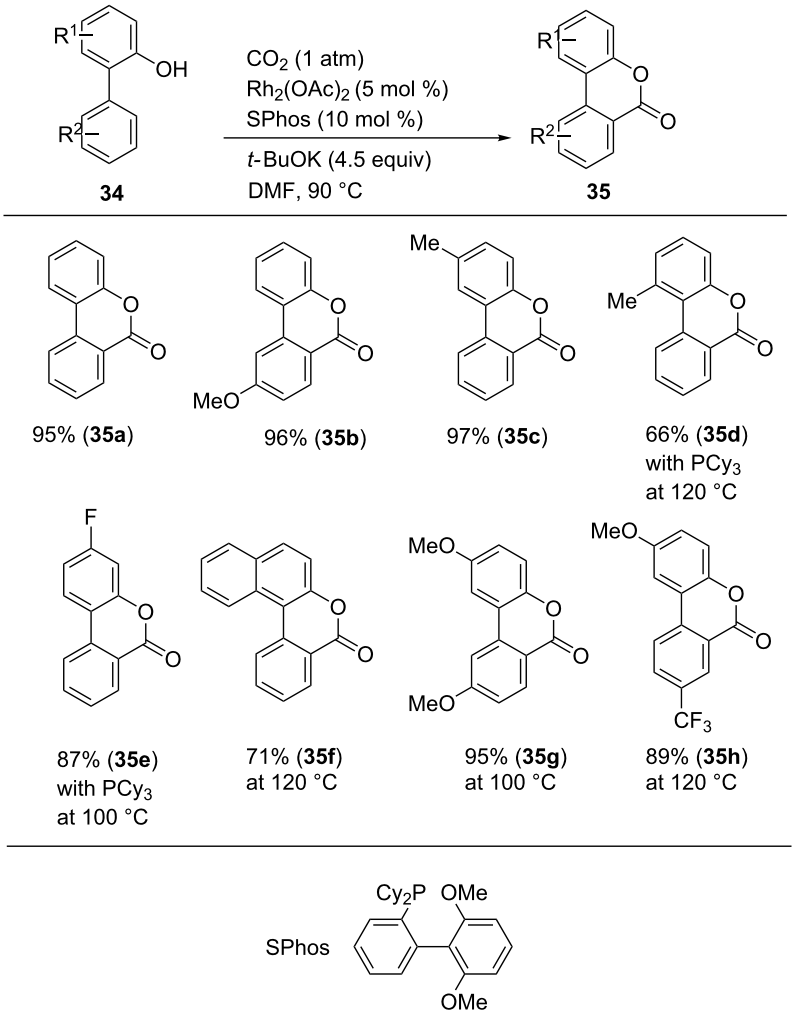

Scheme 31: Carboxylation of C(sp^2)–H bond with CO_2.

a $Rh_2(OAc)_4$/SPhos catalyst system and *t*-BuOK as a base in DMF. Under the optimal reaction conditions, the reaction with 2-phenylphenol (**34a**) afforded dibenzopyranone (**35a**) in 95% yield. Other substituted 2-arylphenol derivatives (**34b–h**) were converted to the corresponding dibenzopyranones (**35b–h**) in good-to-high yields. Notably, sterically hindered substrates (**34d** and **34f**) were allowed by elevating the reaction temperature.

A plausible reaction mechanism is shown in Scheme 32. First, a phenoxide **34'** generated by the reaction of 2-arylphenol with *t*-BuOK reacts with a Rh complex **A** to generate a Rh complex **B** (step a). Then, chelation-assisted C–H bond activation proceeds to generate a rhodacycle **C** (step b). The reaction of **C** with CO_2 affords an eight-membered rhodacycle intermediate **D** (step c). Next, **D** is converted to the corresponding rhodium complex **E** by ligand exchange with KOAc (step d). Possibly another ligand exchange between **E** and KOAc regenerates the Rh complex **A** (step e). The desired product (**35**) is obtained after lactonization.

Hydrocarboxylation of arylalkenes

Hydrocarboxylation is an essential carboxylation reaction. To date, transition-metal-catalyzed hydrocarboxylation reactions using alkynes [63-66], alkenes [67,68], allenes [69-71] and 1,3-dienes [72,73] have been reported. In this regard, Mikami et al. reported the Rh-catalyzed hydrocarboxylation of styrene derivatives depicted in Scheme 33 [74]. The desired reaction proceeded using $[RhCl(cod)]_2$ as a catalyst and Et_2Zn as a reducing agent in DMF at 0 °C. As a result, diverse styrene derivatives **36a–f** bearing an electron-withdrawing group were converted into their corresponding carboxylic acids **37a–f** in moderate-to-high yields. Notably, the ester, ketone, and amide functionalities of **37a**, **37c**, and **37d**, respectively, were toler-

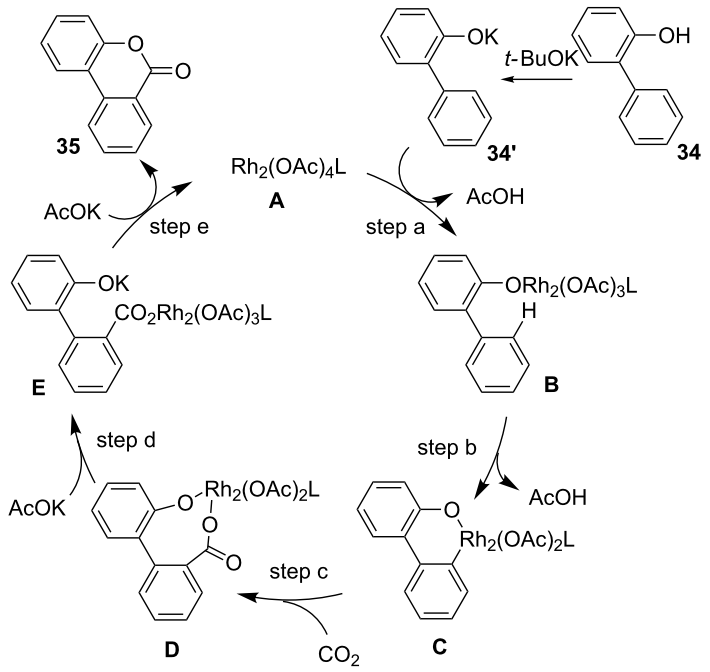

Scheme 32: Reaction mechanism for the Rh-catalyzed C(sp^2)–H carboxylation of 2-arylphenols **34**.

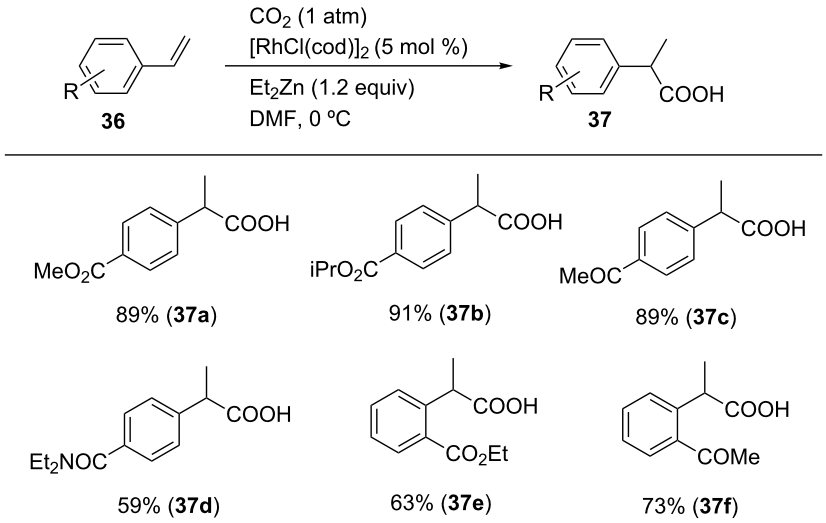

Scheme 33: Hydrocarboxylation of styrene derivatives with CO_2.

ated in the reaction. However, substrates such as 4-methoxystyrene or styrene did not yield the desired products.

The same Rh-catalytic system proved to be applicable to the carboxylation of α,β-unsaturated esters **38** (Scheme 34). A variety of substrates **38a**–**f**, including those containing an electron-donating substituent or benzyl-substituted esters, were converted into their corresponding products **39a**–**f** in good-to-high yields.

Notably, the asymmetric hydrocarboxylation was archived by using a chiral bisphosphine as a ligand (Scheme 35).

Scheme 36 illustrates a plausible reaction mechanism for this transformation. First, transmetalation between the Rh(I) and Zn reagents generates ethyl–Rh(I) species **A**, from which β-hydrogen elimination occurs to yield the hydride-Rh intermediate **B** (step a). Subsequently, the hydrorhodation of the C–C double bond occurs, affording an

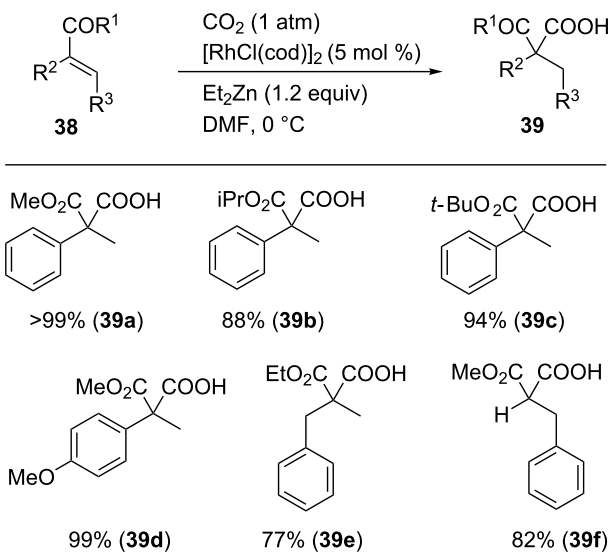

Scheme 34: Hydrocarboxylation of α,β-unsaturated esters with CO_2.

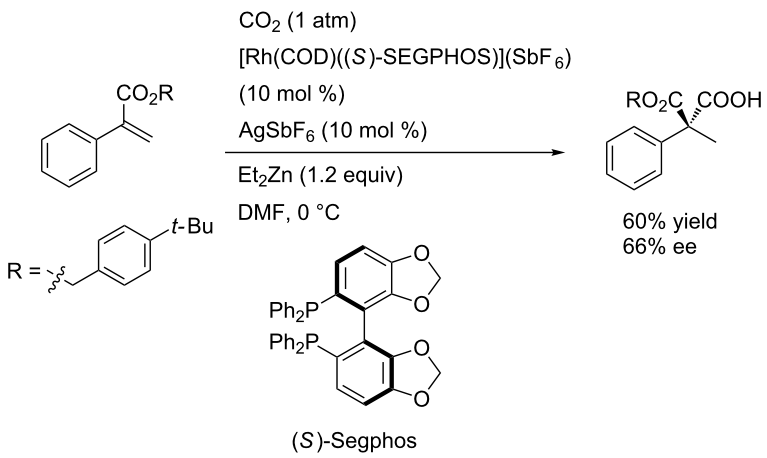

Scheme 35: Asymmetric hydrocarboxylation of α,β-unsaturated esters with CO_2.

alkyl-Rh(I) species **C** (step b). Then, C–C bond formation with CO_2 proceeds to give Rh carboxylate **D** (step c) Finally, the carboxylated product is obtained by the transmetalation between **D** and Et_2Zn, with the concomitant regeneration of ethyl–Rh(I) **A** (step d).

Visible light-driven hydrocarboxylation of alkenes

Iwasawa et al. reported the Rh-catalyzed hydrocarboxylation of alkenes driven by visible-light irradiation conditions in the presence of a photoredox catalyst (Scheme 37) [75]. A model reaction using 4-cyanostyrene (**40a**) was carried out using $iPrNEt_2$ as a sacrificial electron donor in the presence of $[Ru(bpy)_3](PF_6)_2$ as a photoredox catalyst under visible-light irradiation (425 nm). Employing $Rh(PPh_3)_3H$ as a catalyst, the desired hydrocarboxylated product **41a** was obtained in 33% yield along with the formation of reduced product **42a**. $Rh(PPh_3)_3Cl$ and $[Rh(PPh_3)_2Cl]_2$ were not efficient while a use of $[Rh(P(4\text{-}CF_3C_6H_4)_3)_2Cl]_2$ afforded **41a** in 54% yield. Finally, an addition of Cs_2CO_3 dramatically reduced the by-product and **41a** was obtained in 67% yield.

Under the optimal reaction conditions, several substrates were examined and the corresponding hydrocarboxylated products were obtained in moderate yields (Scheme 38).

[2 + 2 + 2] Cycloaddition of diynes with CO_2

The [2 + 2 + 2] cycloaddition of diynes with CO_2 is an important reaction in the field of CO_2 fixation. In these reactions,

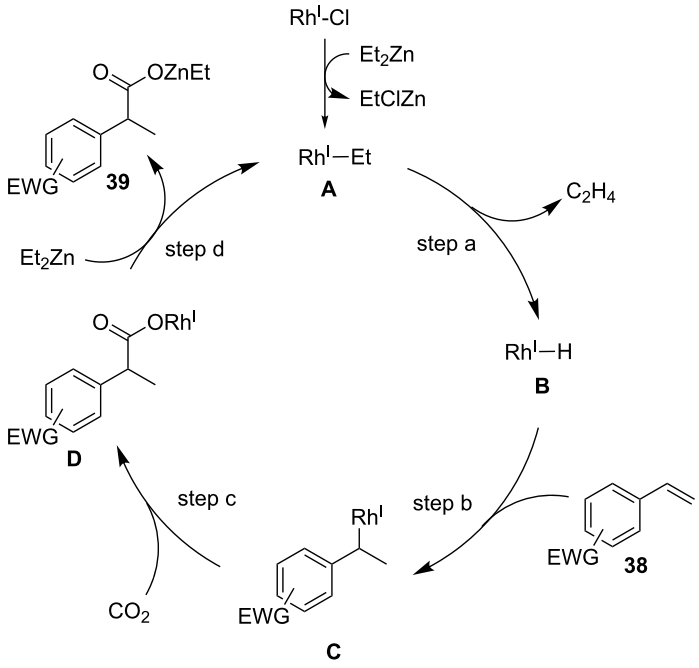

Scheme 36: Proposed reaction mechanism for the Rh-catalyzed hydrocarboxylation of C–C double bonds with CO_2.

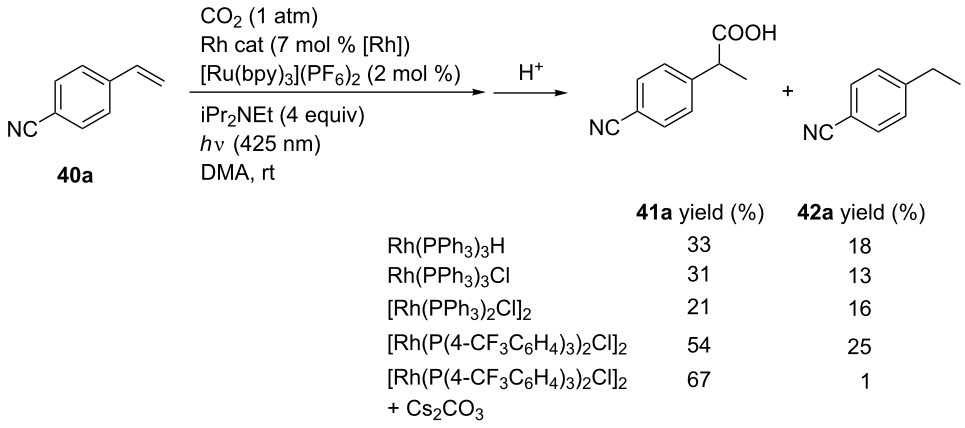

	41a yield (%)	**42a** yield (%)
$Rh(PPh_3)_3H$	33	18
$Rh(PPh_3)_3Cl$	31	13
$[Rh(PPh_3)_2Cl]_2$	21	16
$[Rh(P(4\text{-}CF_3C_6H_4)_3)_2Cl]_2$	54	25
$[Rh(P(4\text{-}CF_3C_6H_4)_3)_2Cl]_2$ + Cs_2CO_3	67	1

Scheme 37: Visible-light-driven hydrocarboxylation with CO_2.

cyclic esters such as pyrones can be obtained, which are classically catalyzed by Ni complexes [76-78]. Tanaka et al. reported that a Rh complex with a suitable bidentate ligand was an efficient catalyst for the [2 + 2 + 2] cycloaddition reaction (Scheme 39) [79]. The reaction of **43a** was performed using 20 mol % $[Rh(cod)_2]BF_4$ and a bidentate phosphine in 1,2-dichloroethane at room temperature. Prior to the addition of **43a**, the mixture of $[Rh(cod)_2]BF_4$ and phosphine was stirred for 30 min. Then, **43a** was added dropwise to the mixture over 10 min, and the resulting reaction mixture was further stirred for 16 h. As ligands, SEGPHOS, BIPHEP, and DPPF were ineffective, but BINAP and H_8-BINAP afforded the product **44a** in moderate yields. Notably, the addition of **43a** over 120 min improved the yield even at low catalyst loadings (5 mol %). A high (94%) yield was eventually obtained by reducing the prestirring time to 5 min.

A variety of diynes having different tether units (**43a**–**g**) were converted into the corresponding pyrones **44a**–**g** in good-to-high yields within 1 h (Scheme 40). Ester, ketone, and hydroxy groups were tolerated in the reaction. In the case of an unsymmetrical diyne bearing methyl and isopropyl groups (**43g**), a mixture of regioisomers **44g** + **44g′** was obtained in high yield with high regioselectivity.

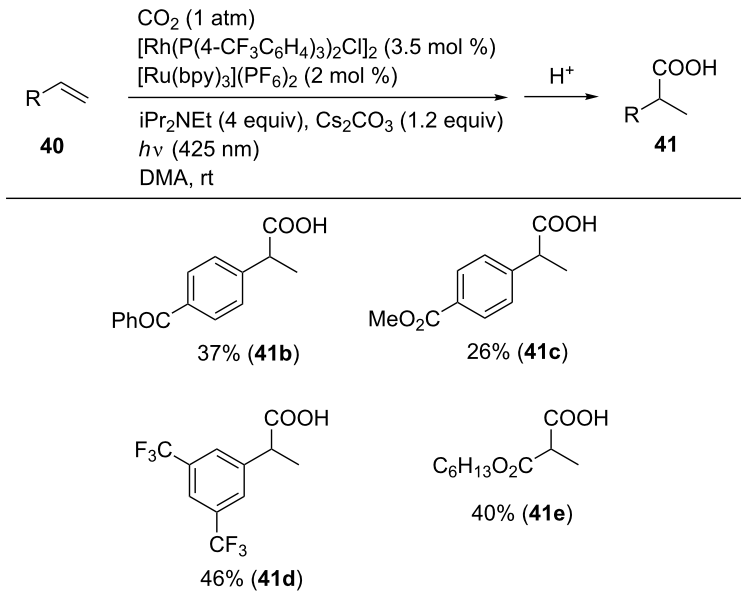

Scheme 38: Visible-light-driven Rh-catalyzed hydrocarboxylation of C–C double bonds with CO_2.

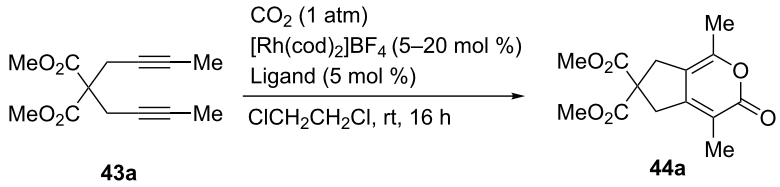

ligand	loading (mol %)	prestirring time (min)	addition time (min)	yield (%)
SEGPHOS	20	30	10	19
BIPHEP	20	30	10	9
DPPF	20	30	10	25
BINAP	20	30	10	41
H_8-BINAP	20	30	10	48
H_8-BINAP	5	30	10	18
H_8-BINAP	5	30	120	78
H_8-BINAP	5	5	120	94

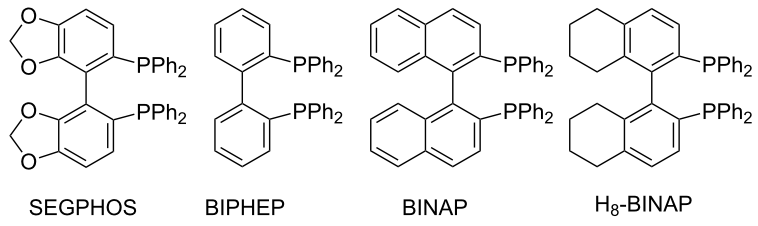

Scheme 39: Optimization of reaction conditions on the Rh-catalyzed [2 + 2 + 2] cycloaddition of diyne **42a** and CO_2.

For this transformation, the reaction pathways depicted in Scheme 41 can be envisaged. The Rh(I) species **A** reacts with a diyne to afford rhodacycle **B** (step a). Then, the reaction of **B** with CO_2 produces the seven-membered rhodium intermediate **C** (step b), from which reductive elimination occurs to yield its corresponding pyrone and the Rh(I) species **A** (step c). Alternatively, the oxidative cyclization of **A** proceeds as one of the C–C triple bonds of the diyne and CO_2 react regioselectively,

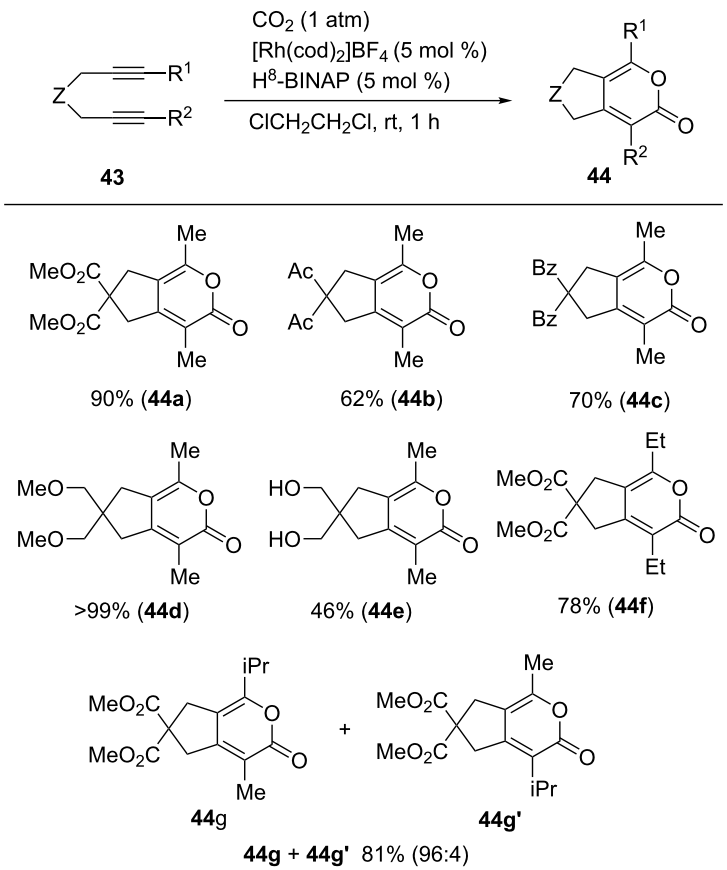

Scheme 40: [2 + 2 + 2] Cycloaddition of diyne and CO_2.

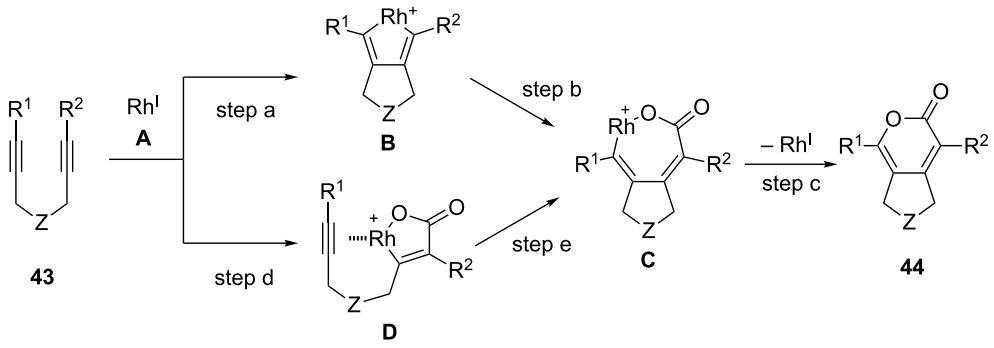

Scheme 41: Proposed reaction pathways for the Rh-catalyzed [2 + 2 + 2] cycloaddition of diyne and CO_2.

and rhodacycle **D** is subsequently formed (step d). Then, the insertion of the alkyne into the Rh–C bond occurs to give rhodacycle **C** (step e).

Conclusion

In this review, the Co- and Rh-catalyzed transformation of CO_2 via carbon–carbon bond-forming reactions is summarized. Co complexes can catalyze the carboxylation of propargyl acetates and alkenyl triflates. The cobalt-catalyzed reductive carboxylation of α,β-unsaturated nitriles and carboxyamides proceeds using Et_2Zn. In addition, a cobalt complex proved to be an efficient catalyst in the allylic $C(sp^3)$–H carboxylation. In the presence of zinc as the reagent, carboxyzincation and the four-component coupling reaction between alkyne, acrylates, CO_2, and zinc occur efficiently. Rh complexes also catalyze the carboxylation of aryl and vinylboronic esters, the $C(sp^2)$–H carboxyla-

tion of aromatic compounds, and the hydrocarboxylation of styrene derivatives. The Rh-catalyzed [2 + 2 + 2] cycloaddition of diynes and CO_2 proceeds to afford pyrenes. Combinations of metals (cobalt or rhodium), substrates, and reducing agents can realize efficient carboxylation reactions using CO_2 under mild reaction conditions. Furthermore, the development of novel carboxylation reactions using clean reducing agents such as non-metallic organic reductants such as amine, water, or hydrogen gas can be envisaged in the near future.

ORCID® iDs

Tetsuaki Fujihara - https://orcid.org/0000-0002-6687-2528

References

1. Suib, S. L., Ed. *New and Future Developments in Catalysis, Activation of Carbon Dioxide;* Elsevier: Amsterdam, 2013.
2. Aresta, M., Ed. *Carbon Dioxides as Chemical Feedstock;* Wiley-VHC: Weinheim, 2010. doi:10.1002/9783527629916
3. Artz, J.; Mueller, T. E.; Thenert, K.; Kleinekorte, J.; Meys, R. I.; Sternberg, A.; Bardow, A.; Leitner, W. *Chem. Rev.* **2018,** *118,* 434–504. doi:10.1021/acs.chemrev.7b00435
4. Aresta, M.; Dibenedetto, A.; Angelini, A. *Chem. Rev.* **2014,** *114,* 1709–1742. doi:10.1021/cr4002758
5. Luan, Y.-X.; Ye, M. *Tetrahedron Lett.* **2018,** *59,* 853–861. doi:10.1016/j.tetlet.2018.01.035
6. Hazari, N.; Heimann, J. E. *Inorg. Chem.* **2017,** *56,* 13655–13678. doi:10.1021/acs.inorgchem.7b02315
7. Wu, X.-F.; Zheng, F. *Top. Curr. Chem.* **2017,** *375,* No. 4. doi:10.1007/s41061-016-0091-6
8. Börjesson, M.; Moragas, T.; Gallego, D.; Martin, R. *ACS Catal.* **2016,** *6,* 6739–6749. doi:10.1021/acscatal.6b02124
9. Juliá-Hernández, F.; Gaydou, M.; Serrano, E.; van Gemmeren, M.; Martin, R. *Top. Curr. Chem.* **2016,** *374,* No. 45. doi:10.1007/s41061-016-0045-z
10. Sekine, K.; Yamada, T. *Chem. Soc. Rev.* **2016,** *45,* 4524–4532. doi:10.1039/C5CS00895F
11. Wang, S.; Du, G.; Xi, C. *Org. Biomol. Chem.* **2016,** *14,* 3666–3676. doi:10.1039/C6OB00199H
12. Yu, D.; Teong, S. P.; Zhang, Y. *Coord. Chem. Rev.* **2015,** *293–294,* 279–291. doi:10.1016/j.ccr.2014.09.002
13. Yeung, C. S.; Dong, V. M. *Top. Catal.* **2014,** *57,* 1342–1350. doi:10.1007/s11244-014-0301-9
14. Cai, X.; Xie, B. *Synthesis* **2013,** *45,* 3305–3324. doi:10.1055/s-0033-1340061
15. Zhang, L.; Hou, Z. *Chem. Sci.* **2013,** *4,* 3395–3403. doi:10.1039/c3sc51070k
16. Tsuji, Y.; Fujihara, T. *Chem. Commun.* **2012,** *48,* 9956–9964. doi:10.1039/c2cc33848c
17. Manjolinho, F.; Arndt, M.; Gooßen, K.; Gooßen, L. J. *ACS Catal.* **2012,** *2,* 2014–2021. doi:10.1021/cs300448v
18. Huang, K.; Sun, C.-L.; Shi, Z.-J. *Chem. Soc. Rev.* **2011,** *40,* 2435–2452. doi:10.1039/c0cs00129e
19. Cokoja, M.; Bruckmeier, C.; Rieger, B.; Herrmann, W. A.; Kühn, F. E. *Angew. Chem., Int. Ed.* **2011,** *50,* 8510–8537. doi:10.1002/anie.201102010
20. Riduan, S. N.; Zhang, Y. *Dalton Trans.* **2010,** *39,* 3347–3357. doi:10.1039/b920163g
21. Tsuji, J. *Palladium Reagents and Catalysts;* Wiley: Chichester, UK, 2004. doi:10.1002/0470021209
22. Trost, B. M. *Acc. Chem. Res.* **1996,** *29,* 355–364. doi:10.1021/ar9501129
23. Trost, B. M. *Acc. Chem. Res.* **1980,** *13,* 385–393. doi:10.1021/ar50155a001
24. Torii, S.; Tanaka, H.; Hamatani, T.; Morisaki, K.; Jutand, A.; Peluger, F.; Fauvarque, J.-F. *Chem. Lett.* **1986,** *15,* 169–172. doi:10.1246/cl.1986.169
25. Medeiros, M. J.; Pintaric, C.; Olivero, S.; Dunach, E. *Electrochim. Acta* **2011,** *56,* 4384–4389. doi:10.1016/j.electacta.2010.12.066
26. Moragas, T.; Cornella, J.; Martin, R. *J. Am. Chem. Soc.* **2014,** *136,* 17702–17705. doi:10.1021/ja509077a
27. Mita, T.; Higuchi, Y.; Sato, Y. *Chem. – Eur. J.* **2015,** *21,* 16391–16394. doi:10.1002/chem.201503359
28. León, T.; Correa, A.; Martin, R. *J. Am. Chem. Soc.* **2013,** *135,* 1221–1224. doi:10.1021/ja311045f
29. Nogi, K.; Fujihara, T.; Terao, J.; Tsuji, Y. *Chem. Commun.* **2014,** *50,* 13052–13055. doi:10.1039/C4CC03644A
30. Qian, X.; Auffrant, A.; Felouat, A.; Gosmini, C. *Angew. Chem., Int. Ed.* **2011,** *50,* 10402–10405. doi:10.1002/anie.201104390
31. Correa, A.; Martín, R. *J. Am. Chem. Soc.* **2009,** *131,* 15974–15975. doi:10.1021/ja905264a
32. Fujihara, T.; Nogi, K.; Xu, T.; Terao, J.; Tsuji, Y. *J. Am. Chem. Soc.* **2012,** *134,* 9106–9109. doi:10.1021/ja303514b
33. Nogi, K.; Fujihara, T.; Terao, J.; Tsuji, Y. *J. Org. Chem.* **2015,** *80,* 11618–11623. doi:10.1021/acs.joc.5b02307
34. Isayama, S.; Mukaiyama, T. *Chem. Lett.* **1989,** *18,* 2005–2008. doi:10.1246/cl.1989.2005
35. Hayashi, C.; Hayashi, T.; Kikuchi, S.; Yamada, T. *Chem. Lett.* **2014,** *43,* 565–567. doi:10.1246/cl.131163
36. Hayashi, C.; Hayashi, T.; Yamada, T. *Bull. Chem. Soc. Jpn.* **2015,** *88,* 862–870. doi:10.1246/bcsj.20150043
37. Michigami, K.; Mita, T.; Sato, Y. *J. Am. Chem. Soc.* **2017,** *139,* 6094–6097. doi:10.1021/jacs.7b02775
38. Knochel, P.; Leuser, H.; Gong, L.-Z.; Perrone, S.; Kneisel, F. F. Polyfunctional Zinc Organometallics for Organic Synthesis. *Handbook of Functionalized Organometallics;* Wiley-VCH: Weinheim, 2005; Vol. 1, pp 251–346. doi:10.1002/9783527619467.ch7
39. Knochel, P.; Singer, R. D. *Chem. Rev.* **1993,** *93,* 2117–2188. doi:10.1021/cr00022a008
40. Nogi, K.; Fujihara, T.; Terao, J.; Tsuji, Y. *J. Am. Chem. Soc.* **2016,** *138,* 5547–5550. doi:10.1021/jacs.6b02961
41. Fillon, H.; Gosmini, C.; Périchon, J. *J. Am. Chem. Soc.* **2003,** *125,* 3867–3870. doi:10.1021/ja0289494
42. Wang, C.-C.; Lin, P.-S.; Cheng, C.-H. *J. Am. Chem. Soc.* **2002,** *124,* 9696–9697. doi:10.1021/ja026543l
43. Skubi, K. L.; Blum, T. R.; Yoon, T. P. *Chem. Rev.* **2016,** *116,* 10035–10074. doi:10.1021/acs.chemrev.6b00018
44. Romero, N. A.; Nicewicz, D. A. *Chem. Rev.* **2016,** *116,* 10075–10166. doi:10.1021/acs.chemrev.6b00057
45. Prier, C. K.; Rankic, D. A.; MacMillan, D. W. C. *Chem. Rev.* **2013,** *113,* 5322–5363. doi:10.1021/cr300503r
46. Masuda, Y.; Ishida, N.; Murakami, M. *J. Am. Chem. Soc.* **2015,** *137,* 14063–14066. doi:10.1021/jacs.5b10032
47. Seo, H.; Katcher, M. H.; Jamison, T. F. *Nat. Chem.* **2017,** *9,* 453–456. doi:10.1038/nchem.2690
48. Shimomaki, K.; Murata, K.; Martin, R.; Iwasawa, N. *J. Am. Chem. Soc.* **2017,** *139,* 9467–9470. doi:10.1021/jacs.7b04838

49. Hou, J.; Ee, A.; Feng, W.; Xu, J.-H.; Zhao, Y.; Wu, J. *J. Am. Chem. Soc.* **2018,** *140,* 5257–5263. doi:10.1021/jacs.8b01561
50. Miyaura, N.; Suzuki, A. *Chem. Rev.* **1995,** *95,* 2457–2483. doi:10.1021/cr00039a007
51. Suzuki, A.; Brown, H. C. *Suzuki Coupling. Organic Syntheses via Boranes;* Aldrich: Milwaukee, 2003; Vol. 3.
52. Hayashi, T.; Yamasaki, K. *Chem. Rev.* **2003,** *103,* 2829–2844. doi:10.1021/cr020022z
53. Miyaura, N. *Bull. Chem. Soc. Jpn.* **2008,** *81,* 1535–1553. doi:10.1246/bcsj.81.1535
54. Ukai, K.; Aoki, M.; Takaya, J.; Iwasawa, N. *J. Am. Chem. Soc.* **2006,** *128,* 8706–8707. doi:10.1021/ja061232m
55. Takaya, J.; Tadami, S.; Ukai, K.; Iwasawa, N. *Org. Lett.* **2008,** *10,* 2697–2700. doi:10.1021/ol800829q
56. Ohishi, T.; Nishiura, M.; Hou, Z. *Angew. Chem., Int. Ed.* **2008,** *47,* 5792–5795. doi:10.1002/anie.200801857
57. Boogaerts, I. I. F.; Fortman, G. C.; Furst, M. R. L.; Cazin, C. S. J.; Nolan, S. P. *Angew. Chem., Int. Ed.* **2010,** *49,* 8674–8677. doi:10.1002/anie.201004153
58. Zang, L.; Cheng, J.; Ohishi, T.; Hou, Z. *Angew. Chem., Int. Ed.* **2010,** *49,* 8670–8673. doi:10.1002/anie.201003995
59. Mizuno, H.; Takaya, J.; Iwasawa, N. *J. Am. Chem. Soc.* **2011,** *133,* 1251–1253. doi:10.1021/ja109097z
60. Suga, T.; Mizuno, H.; Takaya, J.; Iwasawa, N. *Chem. Commun.* **2014,** *50,* 14360–14363. doi:10.1039/C4CC06188H
61. Suga, T.; Saitou, T.; Takaya, J.; Iwasawa, N. *Chem. Sci.* **2017,** *8,* 1454–1462. doi:10.1039/C6SC03838G
62. Fu, L.; Li, S.; Cai, Z.; Ding, Y.; Guo, Z.-Q.; Zhou, L.-P.; Yuan, D.; Sun, Q.-F.; Li, G. *Nat. Catal.* **2018,** *1,* 469–478. doi:10.1038/s41929-018-0080-y
63. Fujihara, T.; Xu, T.; Semba, K.; Terao, J.; Tsuji, Y. *Angew. Chem., Int. Ed.* **2011,** *50,* 523–527. doi:10.1002/anie.201006292
64. Li, S.; Yuan, W.; Ma, S. *Angew. Chem., Int. Ed.* **2011,** *50,* 2578–2582. doi:10.1002/anie.201007128
65. Miao, B.; Zheng, Y.; Wu, P.; Li, S.; Ma, S. *Adv. Synth. Catal.* **2017,** *359,* 1691–1707. doi:10.1002/adsc.201700086
66. Wang, X.; Nakajima, M.; Martin, R. *J. Am. Chem. Soc.* **2015,** *137,* 8924–8927. doi:10.1021/jacs.5b05513
67. Williams, C. M.; Johnson, J. B.; Rovis, T. *J. Am. Chem. Soc.* **2008,** *130,* 14936–14937. doi:10.1021/ja8062925
68. Takaya, J.; Miyama, K.; Zhu, C.; Iwasawa, N. *Chem. Commun.* **2017,** *53,* 3982–3985. doi:10.1039/C7CC01377A
69. Takaya, J.; Iwasawa, N. *J. Am. Chem. Soc.* **2008,** *130,* 15254–15255. doi:10.1021/ja806677w
70. Zhu, C.; Takaya, J.; Iwasawa, N. *Org. Lett.* **2015,** *17,* 1814–1817. doi:10.1021/acs.orglett.5b00692
71. Tani, Y.; Kuga, K.; Fujihara, T.; Terao, J.; Tsuji, Y. *Chem. Commun.* **2015,** *51,* 13020–13023. doi:10.1039/C5CC03932K
72. Takaya, J.; Sasano, K.; Iwasawa, N. *Org. Lett.* **2011,** *13,* 1698–1701. doi:10.1021/ol2002094
73. Gui, Y.-Y.; Hu, N.; Chen, X.-W.; Liao, L.-L.; Ju, T.; Ye, J.-H.; Zhang, Z.; Li, J.; Yu, D.-G. *J. Am. Chem. Soc.* **2017,** *139,* 17011–17014. doi:10.1021/jacs.7b10149
74. Kawashima, S.; Aikawa, K.; Mikami, K. *Eur. J. Org. Chem.* **2016,** 3166–3170. doi:10.1002/ejoc.201600338
75. Murata, K.; Numasawa, N.; Shimomaki, K.; Takaya, J.; Iwasawa, N. *Chem. Commun.* **2017,** *53,* 3098–3101. doi:10.1039/C7CC00678K
76. Louie, J.; Gibby, J. E.; Farnworth, M. V.; Tekavec, T. N. *J. Am. Chem. Soc.* **2002,** *124,* 15188–15189. doi:10.1021/ja027438e
77. Tsuda, T.; Morikawa, S.; Sumiya, R.; Saegusa, T. *J. Org. Chem.* **1988,** *53,* 3140–3145. doi:10.1021/jo00249a003
78. Inoue, Y.; Itoh, Y.; Hashimoto, H. *Chem. Lett.* **1978,** *7,* 633–634. doi:10.1246/cl.1978.633
79. Ishii, M.; Mori, F.; Tanaka, K. *Chem. – Eur. J.* **2014,** *20,* 2169–2174. doi:10.1002/chem.201304623

License and Terms

BEILSTEIN JOURNAL OF ORGANIC CHEMISTRY

Learning from B_{12} enzymes: biomimetic and bioinspired catalysts for eco-friendly organic synthesis

Keishiro Tahara[1], Ling Pan[2], Toshikazu Ono[3,4,5] and Yoshio Hisaeda*[3,4]

Review

Open Access

Address:
[1]Department of Material Science, Graduate School of Material Science, University of Hyogo, 3-2-1, Kouto, Kamigori, Ako 678-1297, Japan, [2]Department of Chemistry, Northeast Normal University, Changchun 130024, P. R. China, [3]Department of Chemistry and Biochemistry, Graduate School of Engineering, Kyushu University, 744 Motooka, Nishi-ku, Fukuoka 819-0395, Japan, [4]Center for Molecular Systems (CMS), Kyushu University, Fukuoka 819-0395, Japan and [5]PRESTO, Japan Science and Technology Agency (JST), 4-1-8 Honcho, Kawaguchi, Saitama 332-0012, Japan

Email:
Yoshio Hisaeda* - yhisatcm@mail.cstm.kyushu-u.ac.jp

* Corresponding author

Keywords:
dehalogenation; electrolysis; green chemistry; heptamethyl cobyrinate; methyl transfer; 1,2-migration; photosensitizer; vitamin B_{12}

Beilstein J. Org. Chem. **2018,** *14,* 2553–2567.
doi:10.3762/bjoc.14.232

Received: 02 June 2018
Accepted: 13 September 2018
Published: 02 October 2018

This article is part of the thematic issue "Cobalt catalysis".

Guest Editor: S. Matsunaga

Abstract

Cobalamins (B_{12}) play various important roles in vivo. Most B_{12}-dependent enzymes are divided into three main subfamilies: adenosylcobalamin-dependent isomerases, methylcobalamin-dependent methyltransferases, and dehalogenases. Mimicking these B_{12} enzyme functions under non-enzymatic conditions offers good understanding of their elaborate reaction mechanisms. Furthermore, bio-inspiration offers a new approach to catalytic design for green and eco-friendly molecular transformations. As part of a study based on vitamin B_{12} derivatives including heptamethyl cobyrinate perchlorate, we describe biomimetic and bioinspired catalytic reactions with B_{12} enzyme functions. The reactions are classified according to the corresponding three B_{12} enzyme subfamilies, with a focus on our recent development on electrochemical and photochemical catalytic systems. Other important reactions are also described, with a focus on radical-involved reactions in terms of organic synthesis.

Review

1. Introduction

1-1. Redox and coordination chemistry of B_{12}

Cobalamins (B_{12}) are naturally occurring cobalt complexes with unique structures that play various important roles in vivo [1-5]. In B_{12}, the cobalt center is coordinated by four equatorial pyrroles of the corrin ring and 2,3-dimethylbenzimidazole as a lower axial ligand (Figure 1a) [6-8]. The cobalamin with an upper ligand is termed vitamin B_{12} (a cyanide group), methylcobalamin (a methyl group), and adenosylcobalamin (an adenosyl group), respectively. The oxidation state of cobalt ions

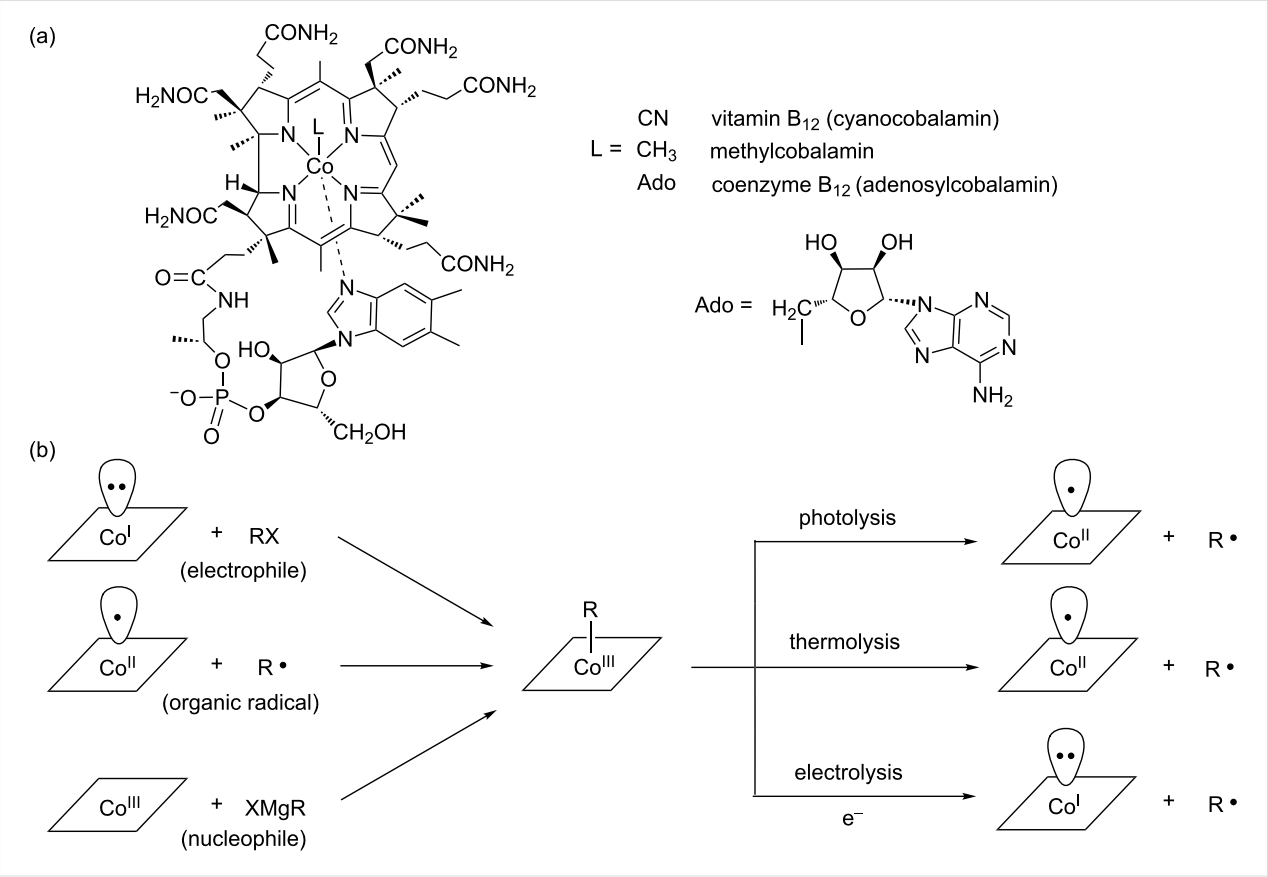

Figure 1: (a) Structure and (b) reactivity of B_{12}.

in B_{12} ranges from +1 to +3. Each oxidation state of cobalamins exhibits quite different ligand-accepting abilities and reactivities. Cob(III)alamins strongly favor 6-coordination with 2,3-dimethylbenzimidazole in homogeneous solutions at physiological pH (denoted as base-on form). In particular, cob(III)alamins with upper alkyl ligands are quite interesting because of their structural relevance to methylcobalamin and adenosylcobalamin (coenzyme B_{12}) that serve as organometallic cofactors in B_{12}-dependent enzymes. The photolysis (thermolysis) of alkylcob(III)alamins leads to the formation of the corresponding alkyl radical and cob(II)alamin with homolytic Co(III)–C bond cleavage (Figure 1b). This high lability is attributed to a relatively weak Co(III)–C bond, as exemplified by its bond dissociation energies of 30 kcal/mol in coenzyme B_{12} and 37 kcal/mol in methylcobalamin in base-on forms [9]. Cob(II)alamin favors 5-coordination in the homogeneous solutions at physiological pH [10]. It is paramagnetic and has an unpaired electron in the axial dz^2 orbital. It acts as a high efficient "radical trap" and reacts with alkyl radicals to yield alkylcob(III)alamin (Figure 1b). Four-coordinated cob(I)alamin has a paired electron in the axial dz^2 orbital, resulting in high nucleophilicity with a Pearson constant of 14 [11]. It is slightly basic, with a pK_a lower than 1 for the Co–H complex [12]. The "supernucleophilic" cob(I)alamin is found in many enzymes such as methionine synthetases, adenosyltransferases, and reductive dehalogenases. In addition, the reactivity of cob(I)alamin has been investigated using various electrophiles such as alkyl halides [13], vinyl halides [14-16], aryl halides [17,18] and epoxides [19,20] in homogeneous solutions (Figure 1b).

1-2. Design of biomimetic and bioinspired B_{12} catalytic systems

Schematic representations of B_{12} enzymes and enzyme-involving systems are shown in Figure 2a. The remarkable in vivo and in vitro characters of B_{12} are summarized as follows:

1. B_{12} shows good accessibility to Co(I) species with a redox potential (the Co(II)/Co(I) couple in the base-off form) of −500 mV vs the standard hydrogen electrode [21], because of the monoanionic corrin ligand.
2. B_{12} is reduced to Co(I) species in the active center by reductases in sustainable processes.
3. The partially π-conjugated system of the corrin ring is less easy to be adducted by free radicals than those of porphyrins.

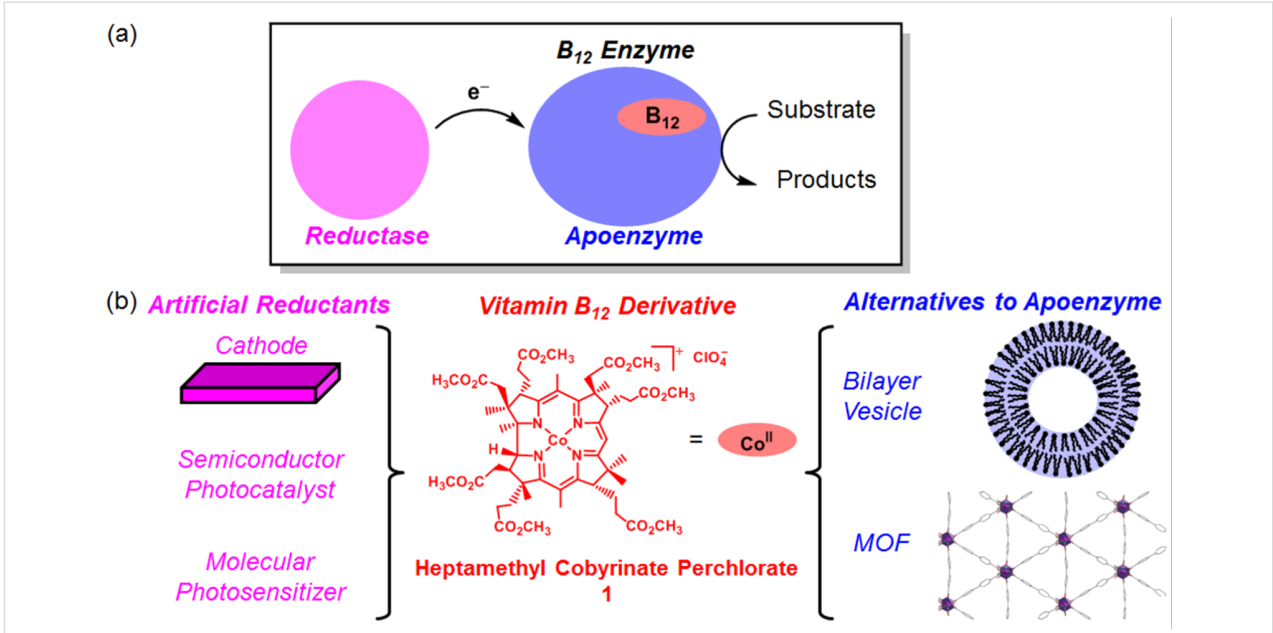

Figure 2: (a) Schematic representation of B_{12} enzyme-involving systems. (b) Construction of biomimetic and bioinspired catalytic systems by combining functional equivalents of B_{12} enzyme-involving systems as components.

4. B_{12} is bound to a number of proteins and acts as a module.
5. Different chemical functions of B_{12} are exploited by bound apoenzymes.
6. B_{12} is recycled or reactivated in vivo as observed in methyonine synthetases.

Understanding the mechanisms of B_{12} enzyme reactions and the role of B_{12} is very important from the viewpoint of bioinorganic and organometallic chemistry, organic syntheses, and catalysts. Despite extensive research, reproducing B_{12} enzyme reactions in vitro had been difficult in homogenous solutions.

Construction of sustainable catalytic systems inspired by B_{12} enzymes is another important issue that must be addressed for green chemistry. Due to the above-mentioned unique redox and coordination chemistry, vitamin B_{12} and its derivatives [22] are used as effective homogenous catalysts in various organic reactions [23-25], although an excess of chemical reductants are often used to activate B_{12} to the Co(I) species. Green catalytic systems capable of activating B_{12} have not been reported in the literature, with the exception of electrocatalytic systems [26,27].

To achieve functional simulations of B_{12} enzymes under non-enzymatic conditions, our strategy is to fabricate the artificial enzymes by combining a functional equivalent of B_{12} and that of an apoenzyme (Figure 2b). We have been exploring the utility of hydrophobic B_{12} model complexes, such as heptamethyl cobyrinate perchlorate **1**, that possess ester groups in place of the peripheral seven-amide moieties [28,29]. **1** was developed by Eschenmoser et al. as a model complex for the total synthesis of vitamin B_{12} [30]. Indeed, in the crystal structure, **1** maintained the same corrin framework as natural B_{12} [31]. We combined the hydrophobic B_{12} derivatives with bilayer vesicles [32,33], a protein [34], organic polymers [35-40], and metal organic frameworks (MOFs) [41]. Furthermore, to construct green catalytic systems inspired by B_{12} enzymes, we combined the hydrophobic B_{12} derivatives with a functional equivalent of reductases. In the resultant catalytic systems, the Co(I) species was generated through electron transfers from the cathodes [42,43], semiconductors [44], or molecular photosensitizers [45] to the B_{12}. In this review, we summarize the biomimetic and bioinspired catalytic reactions with B_{12} enzyme functions, with a focus on our recent work on electrochemical and photochemical systems.

2. 1,2-Migrations of functional groups

Enzymes using radical species are models of good catalysts for chemists because they efficiently mediate difficult organic reactions under mild conditions [46-51]. In some catalysis mediated by B_{12} enzymes, the high reactivity of the adenosyl radical is exploited for isomerization. The microenvironments provided by the apoenzymes activate and cleave the Co(III)–C bond of the B_{12} coenzyme B_{12} in a homolytic fashion to produce an adenosyl radical [52,53]. In methylmalonyl-CoA mutase (MMCM), the conversion from *R*-methylmalonyl-CoA to succinyl-CoA (Scheme 1a) starts with hydrogen abstraction by the adenosyl radical.

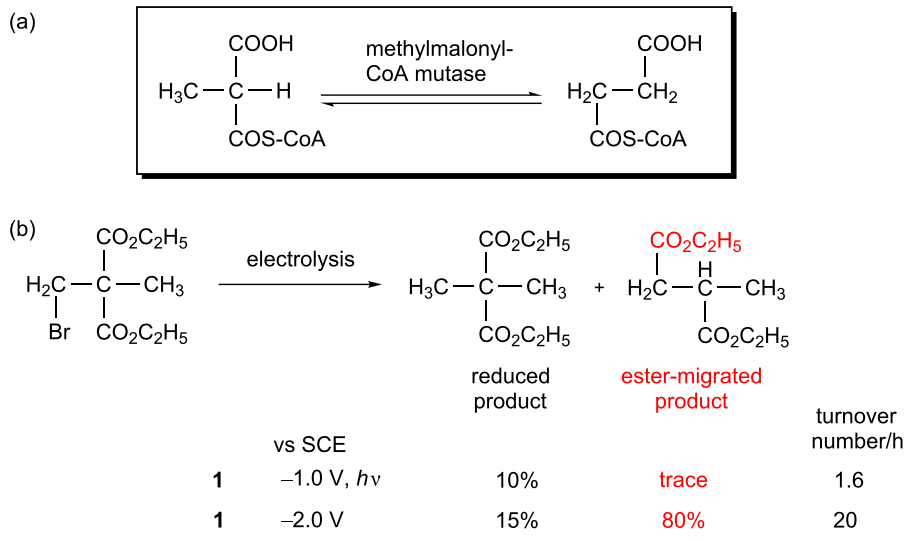

Scheme 1: (a) Carbon-skeleton rearrangement mediated by a coenzyme B_{12}-depenedent enzyme. (b) Electrochemical carbon-skeleton rearrangement mediated by **1**.

2-1. Electrochemical catalytic reactions

We deeply investigated the electrochemical catalytic reactions mediated by **1** and related complexes and succeeded in the functional simulations of MMCM-type 1,2-migration reactions [42]. For example, when 2,2-bis(ethoxycarbonyl)-1-bromopropane was selected as a model substrate, the 1,2-migration of carboylic ester (80%) and some simple reduction product (20%) were obtained under controlled-potential electrolysis at −2.0 V vs SCE in the presence of catalyst **1** in DMF (Scheme 1b) [54]. There were different ratios for the simple reduced product and the ester-migrated product, depending on the reaction conditions. Mechanistic investigations revealed that the formation of the two-electron-reduced species of Co(III)-monoalkylated complex of **1** was vital for carbon-skeleton rearrangement reactions. It was also discovered that the 1,2-migration of the carboxylic ester group proceeded via an anionic intermediate. To clarify the migratory aptitude of the functional groups, several kinds of substrates with an electron-withdrawing group were utilized. The yields of the migrated products increased in the order of CN < CO_2R < COR [54]. For alkyl halides with two carboxylic ester groups that differ in their bulkiness, the yields of the migrated products are higher for the smaller ester group [55].

Furthermore, we succeeded in tuning selectivity in the 1,2-migration of a functional group mediated by **1** by controlling the electrolysis potential (Scheme 2) [56]. The electrolysis of diethyl 2-bromomethyl-2-phenylmalonate at −2.0 V vs

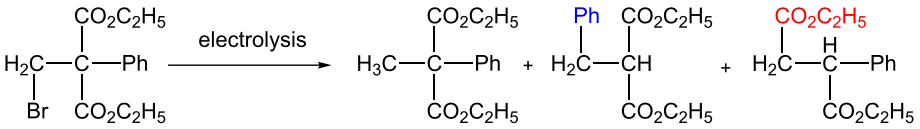

Scheme 2: Electrochemical carbon-skeleton arrangements mediated by B_{12} model complexes.

Ag/AgCl yielded carboxylic ester migrated product as the major product. Conversely, the electrolysis of the substrate at −1.0 V vs Ag/AgCl through light irradiation, as well as at −1.5 V vs Ag/AgCl in the dark, yielded the simple reduced product and the phenyl migrated product. The cathodic reactivity of the monoalkylated complex of **1** was found to be critical to the selectivity of the migrating group.

Interestingly, the electrochemical carbon-skeleton rearrangement reactions were successfully mediated by simple B_{12} model complexes **2** (Figure 3). The imine/oxime-type square planar ligands of cobalt complexes **2** are superior to porphyrin ligands in terms of the model for the corrin framework of B_{12}; both the imine/oxime-type and corrin ligands are monoanionic [57-60]. The imine/oxime-type cobalt complex **2** can be isolated in both the monoalkylated and dialkylated forms [59,60]. This is in contrast to **1**; **1** cannot be dialkylated because of steric hindrances [42]. The Co(III)-monoalkylated complex can be electrochemically reduced to form Co(I) species and a Co(III)-dialkylated complex through disproportionation. The resulting Co(III)-dialkylated complex shows different electrochemical reactivity. It can be electrochemically oxidized to form the Co(III)-monoalkylated complex. These electrochemical reactivities are exemplified by those of the Co(III)–CH_3 and Co(III)–$(CH_3)_2$ complexes of compound **2a** in Figure 3. In the electrolysis, the reduction of the Co(III)-monoalkylated complex and the oxidation of the Co(III)-dialkylated complex proceeded at the cathode and anode, respectively [61]. These processes were coupled to achieve the 1,2-migration of functional groups. Further investigations with diethyl 2-bromomethyl-2-phenylmalonate as a substrate confirmed that the carboxylic ester-migrated product was formed via not a radical, but a cationic intermediate that was generated by the fragmentation to the monoalkylated complex at the anode (Scheme 2).

2-2. Artificial enzyme-mediated reactions

A vesicle-type B_{12} artificial enzyme was constructed by combining bilayer vesicles composed of synthetic lipids and alkylated complexes of heptapropyl cobyrinate (Scheme 3) [32,33]. The alkylated B_{12} model complexes were introduced into the vesicle in aqueous solutions through non-covalent hydrophobic interactions and irradiated with a 500 W tungsten lamp to result in the homolytic cleavage of the Co(III)–C bonds. The carbon-skeleton rearrangements were achieved in the vesicle due to cage effects in the apoenzyme model. Conversely, such reactions hardly proceeded in homogenous solutions. The yields of the migration products increased in order of CN ~ $CO_2C_2H_5$ < $COCH_3$. A cyclophane-type B_{12} artificial enzyme also mediated similar carbon-skeleton rearrangements [32].

We developed another artificial enzyme composed of human serum albumin (HSA) and heptapropyl cobyrinate [34]. It is known that HSA acts as a carrier for in vivo hydrophobic molecules. Hydrophobic B_{12} model complexes were successfully incorporated into the HSA. The incorporated amounts increased as the hydrophobicity of the B_{12} model complexes increased. The hydrophobicity can be varied through chemical modification of the peripheral ester groups placed at the peripheral sites of the corrin skeleton. The HSA microenvironments increased the yield of the acetyl-migrated product compared with the homogenous conditions of the methanol or benzene solutions

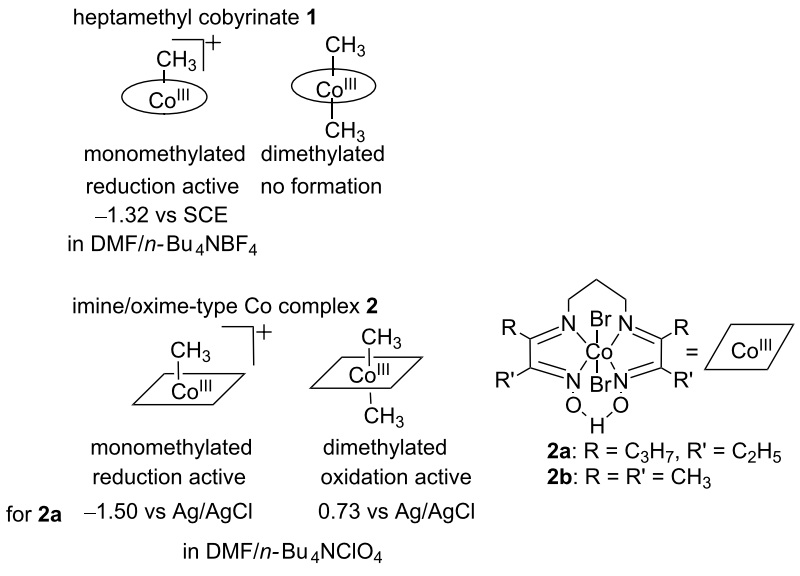

Figure 3: Key electrochemical reactivity of **1** and **2** in methylated forms.

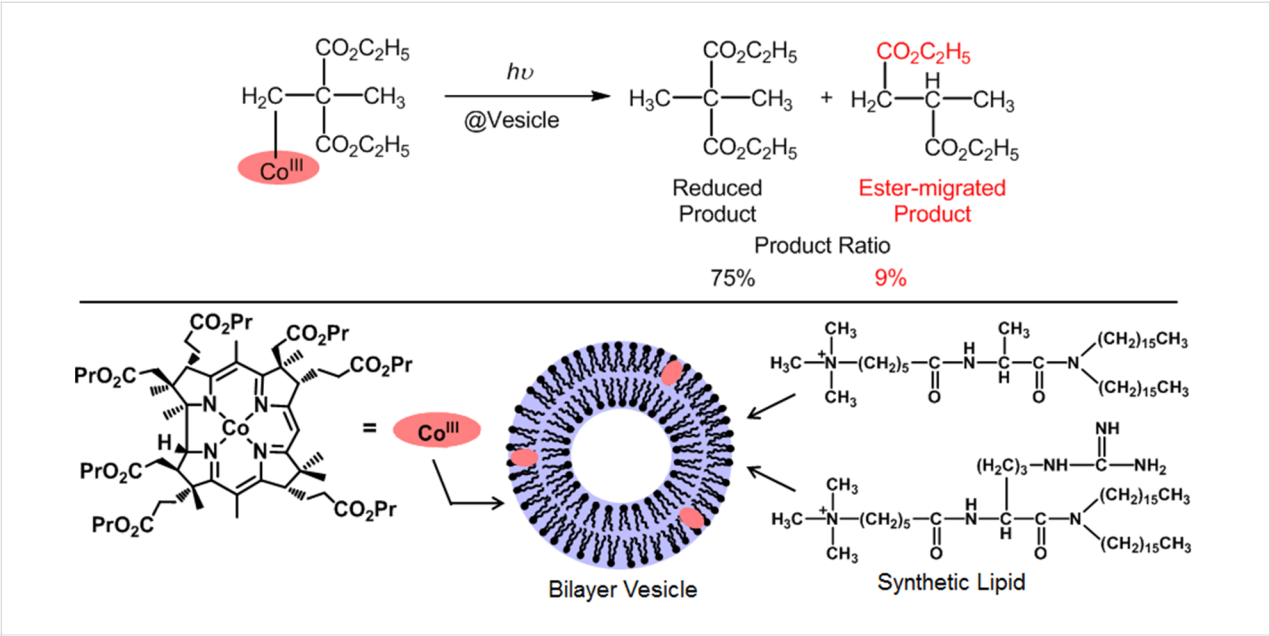

Scheme 3: Carbon-skeleton arrangements mediated by B_{12}-vesicle artificial enzymes.

(Scheme 4). This increase resulted from the effects of suppression of molecular motion and the desolvation of the B_{12} model complex in HSA.

MOFs are a class of crystalline materials constructed from metal connecting nodes and molecular building blocks [62-64]. To explore the utilities of the microenvironments provided by MOFs for B_{12} catalytic reactions, a new MOF $\{Zn_4Ru_2(bpdc)_4 \cdot 4NH_2(CH_3)_2 \cdot 9DMF\}_n$ (H_2bpdc = 4,4′-biphenyldicarboxylic acid) was prepared by the reaction of H_2bpdc, $Ru(bpy)_2Cl_2$, and a zinc source under solvothermal conditions (bpy = 2,2′-bipyridine, Scheme 5) [41]. The molecular photosensitizer $[Ru(bpy)_3]^{2+}$ was incorporated into the MOF through adsorption to form Ru@MOF, accompanied by a color change. Furthermore, **1** was effectively immobilized on Ru@MOF, as was confirmed through ESR measurements. The resultant heterogeneous hybrid catalyst B_{12}-Ru@MOF successfully mediated the photochemical carbon-skeleton arrangement. Previous studies had demonstrated that the hemolytic cleavage of the Co(III)–C bond of the alkylated complex of **1** generated Co(II) species and an alkyl radical intermediate A [54]. The prolonged lifetime of the radical intermediate A could be provided by the channel of MOF, enabling conversion to the acetyl-migrated radical B. The radicals A and B may abstract hydrogen radicals to form the reduced product and the acetyl-migrated product, respectively. It was noticeable that the catalytic cycle for 1,2-migration was constructed for the B_{12}-Ru@MOF system. This stands in contrast to the stoichiometric reactions in the previous B_{12} artificial enzymes. Furthermore, the catalytic process of the B_{12}-Ru@MOF system is visible-light-driven through the use of $[Ru(bpy)_3]^{2+}$ as an alternative to reductases. This serves as a simplified analogy for the B_{12} en-

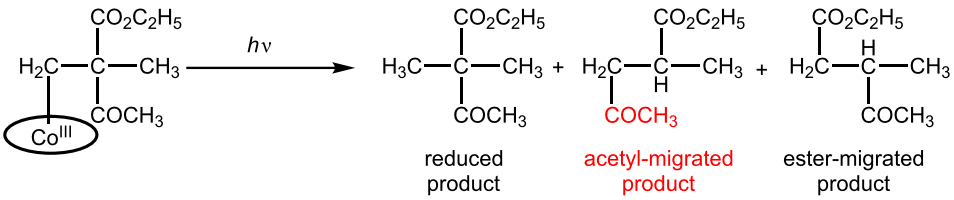

methanol	90%	10%	trace
benzene	87%	13%	trace
HSA	32%	68%	trace

Scheme 4: Carbon-skeleton arrangements mediated by B_{12}-HSA artificial enzymes.

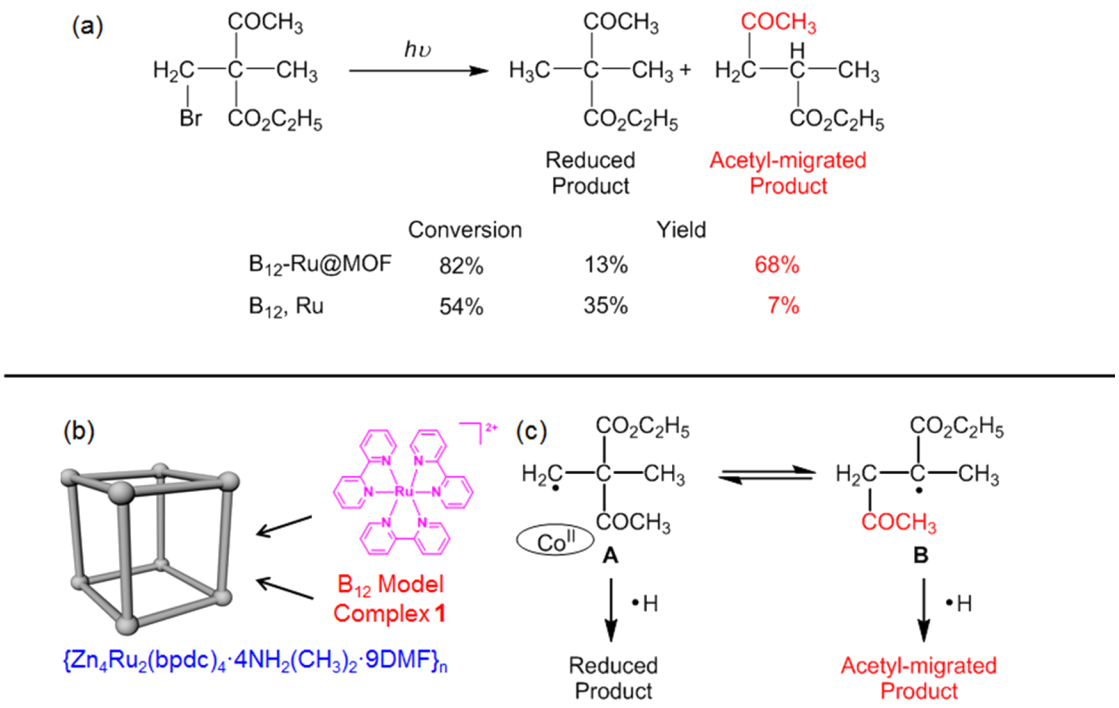

Scheme 5: Photochemical carbon-skeleton arrangements mediated by B_{12}-Ru@MOF.

zyme-involving system (Figure 2a). The B_{12}-Ru@MOF is the best system for the functional simulation of MMCM among our B_{12} artificial enzymatic systems.

3. Methyl transfer reactions

The B_{12}-dependent methionine synthase catalyzes the methyl transfer reaction as shown in Scheme 6a. In the active center of the enzyme, cob(I)alamin accepts the methyl group from methyltetrahydrofolate (CH_3-H4-folate) and the resultant methylcobalamin donates it to homocysteine [65,66]. Constructing the methyl transfer cycle under non-enzymatic conditions is a challenging issue for chemists. Here, we describe model studies of the methylation of B_{12} derivatives and methyl transfer from methylated B_{12} derivatives. Zn^{2+} ions were considered as the essential cofactors in the enzymatic reactions reported by many researchers [67-69].

3-1. Methyl transfer to thiols

Chemical reductants such as $NaBH_4$ or electrochemical reduction could provide Co(I) species, so that α-methylated and β-methylated B_{12} could be formed by the oxidative addition reaction with a methyl donor. The supernucleophile Co(I) species readily react with various methyl halides such as methyl iodide to form a methyl–cobalt complex. Moreover, methanol could also serve as a methyl donor after the activation of the OH group by a Lewis acid such as Zn^{2+} [70,71]. Thiols could also mediate the methylation of **1** with methyl iodide or methyl tosylate ($TsOCH_3$) as the methyl donor [72]. Kräutler et al. found an equilibrium methyl transfer between methylcobalamin and the methylated complex of **1** resulting in cob(II)alamin and β-methyl heptamethyl cob(III)yrinate. Such a thermal equilibration takes 16 days at room temperature [73].

Keese et al. successfully constructed a complete methyl transfer cycle from methylamines to 1-hexanethiol as an excellent bioinspired system. The use of Zn and $ZnCl_2$ in refluxing ethanol was vital for the bioinspired methyl transfer [74]. Recently, we developed a catalytic methyl transfer system for the first time through electrolysis under non-enzymatic conditions. The methyl transfer from $TsOCH_3$ to 1-octanethiol was mediated by controlled-potential electrolysis at −1.0 V vs Ag/AgCl in the presence of **1** at 50 °C (Scheme 6b) [75]. The Zn plate was used as a sacrificial anode and the resultant Zn^{2+} ions was vital for the activation of 1-octanethiol [76]. A similar reaction was successfully mediated by the imine/oxime-type cobalt complex **2a** using zinc powder [77].

3-2. Methyl transfer to inorganic arsenic for the detoxification of arsenic

The wide utilization of inorganic arsenics causes large-scale environmental pollution, resulting in very chronic diseases [78].

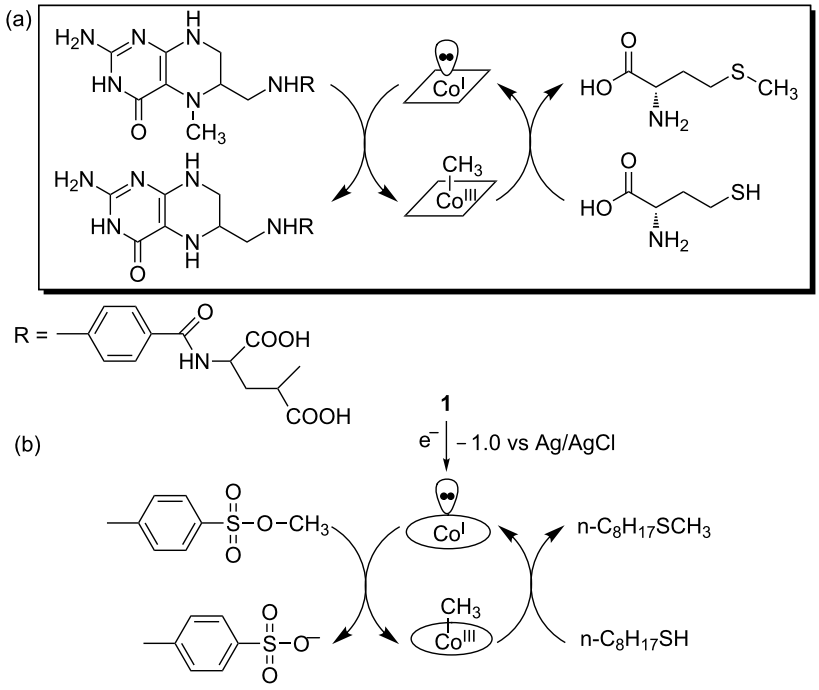

Scheme 6: (a) Methyl transfer reaction mediated by B_{12}-dependent methionine synthase. (b) Methyl transfer reaction from $TsOCH_3$ to 1-octanthiol mediated by **1**.

However, it was known that the toxicity of organic arsenics is generally much lower than inorganic ones. For example, the acute toxicity of arsenobetaine (AB) is about one three-hundredth that of arsenic trioxide [79]; trimethylarsine oxide (TMAO) that is an intermediate in the synthesis of AB also has lower toxicity than inorganic arsenics. Moreover, inorganic arsenics could be converted to methylated arsenics via human or animal metabolism involving a methyltransferase and a reductase [80-82]. Thus, biomimetic transformation from inorganic arsenics to organic arsenics via methyl transfer could be an eco-friendly methodology for the detoxification of arsenic. The B_{12}-mimetic methyl transfer reaction for the detoxification of inorganic arsenics has recently been developed. The highly toxic As_2O_3 was transformed to AB via TMAO under mild conditions, as shown in Scheme 7 [83,84]. High efficiency transformation of As_2O_3 to TMAO was newly achieved with methylated complex of **1** as a methyl donor and GSH as a reductase model.

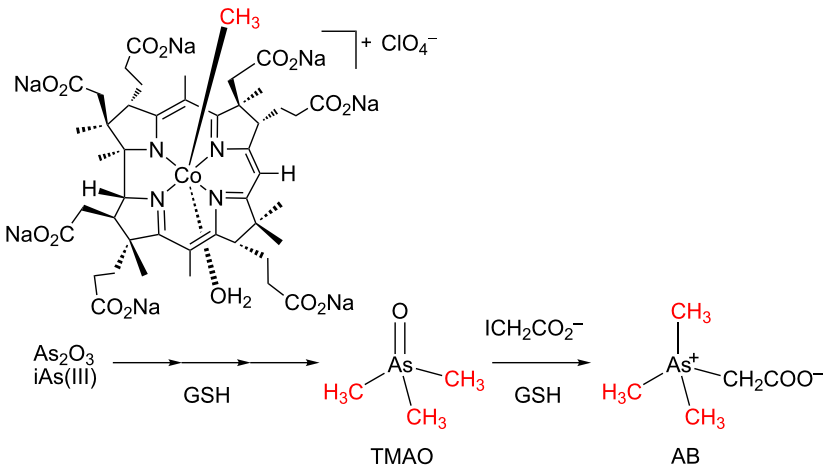

Scheme 7: Methyl transfer reaction for the detoxification of inorganic arsenics.

The methyl transfer reaction to As_2O_3 was first examined at 37 °C in Tris–HCl buffer for 24 h. A methylated complex of **1** was proved to be more efficient than the naturally occurring methylcobalamin [84]. More than 95% of As_2O_3 was converted into methylarsonic acid (MMA, 67.8%), dimethylarsonic acid (DMA, 27.2%), and TMAO (0.1%) in the reaction of **1**, whereas only 20% conversion of As_2O_3 was observed in the reaction of methylcobalamin with lower methylated MMA (17.2%) and DMA (2.8%) as products. When the reaction of the methylated complex of **1** was performed at 100 °C in Tris–HCl buffer for 2 h, As_2O_3 was methylated to TMAO with much as 99% yield [83]. Combined with the nearly quantitative conversion of TMAO to AB in the presence of GSH and iodoacetic acid in phosphoric acid–citric acid buffer at 37 °C, a safe and eco-friendly detoxification of inorganic arsenics was developed via methyl transfer reactions mediated by biomimetic vitamin B_{12}.

4. Dehalogenation reactions

"Dehalorespiration" is also a model of good catalysts for chemists because the anaerobic metabolism of microbes couples the dehalogenation of organic halides with energy conservation [85]. In some electron transport chains, reductive dehalogenases contain B_{12} derivatives as cofactors [86]. The reductive dehalogenase originating from the anaerobic bacteria, *Sulfurospiririllum multivorans*, uses 1,1,2,2-tetrarchloroethene as a terminal electron acceptor to be reduced to trichloroethene (Scheme 8a) [87]. In electron transport chains, reductases reduce the Co(II) species of the B_{12} cofactor to the Co(I) species in the active site of reductive dehalogenases [88]. The Co(I) species is a key form for electron transfer to a substrate.

4-1. Choice of alternatives to reductases

Although anaerobic microbes can be applied to remediation technologies, the dehalogenation abilities of microbes are equal to the intrinsic abilities of nature in principle. Chemical methods are considered as efficient techniques to directly degrade halogenated pollutants. Completely mimicking the complicated dehalorespiration systems requires tedious efforts. The concept of bioinspired chemistry would be an effective methodology to design sustainable systems. To construct good

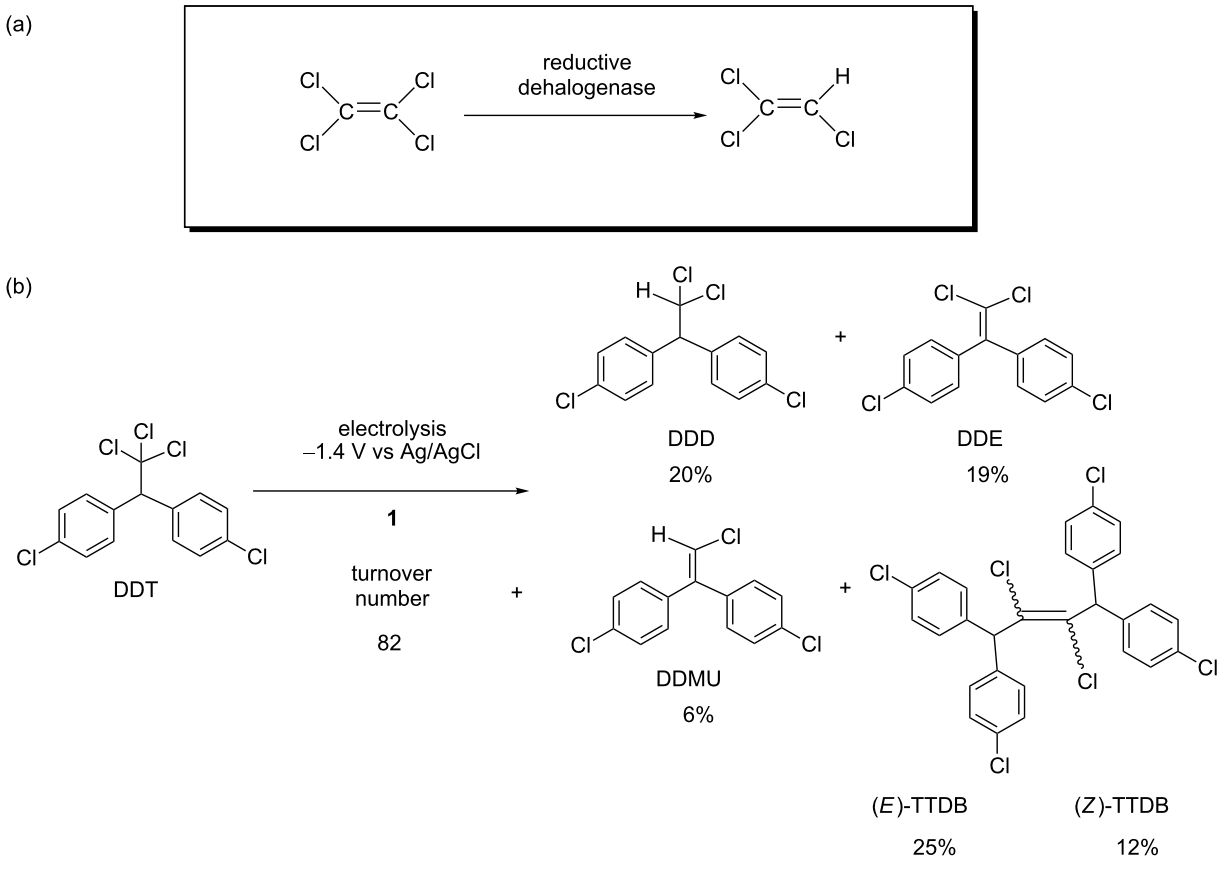

Scheme 8: (a) Dechlorination of 1,1,2,2-tetrarchloroethene mediated by a reductive dehalogenase. (b) Electrochemical dechlorination of DDT mediated by **1**.

catalytic dehalogenation systems, the key process is the reduction of Co(II) species of B_{12} derivatives to the Co(I) species in sustainable processes.

Electroorganic synthesis is considered an eco-friendly method for synthetic organic chemistry [89-91]. Clean redox events between electrodes and substrates can be achieved without any chemical redox reagents. The use of mediators enables energy savings with mild applied potentials or small amounts of electricity. We constructed electrochemical catalytic systems for dehalogenation of alkyl halides using **1**. The electron transfer from reductases to B_{12} was replaced with that from the cathodes to B_{12} derivatives [43].

Light-driven organic transformations attract great attention due to their relevance to photosynthesis in nature as an ideal sustainable system [92-94]. In this context, we constructed light-driven catalytic systems using **1** by replacing reductases with semiconductor photosensitizers and molecular photosensitizers. For example, we reported an ultraviolet-light-driven system using titanium dioxide (TiO_2) semiconductor [95-101]. The conductive band electron of TiO_2 (E_{red} = −0.5 V vs NHE in neutral water) could reduce **1** to form Co(I) species upon irradiation with ultraviolet (UV) light. We also reported a visible-light-driven system with a molecular photosensitizer such as $Ru(bpy)_3^{2+}$ [39,40,102,103], cyclometalated iridium(III) complexes [104], and organic red dyes [105-107].

4-2. Dechlorination of DDT and related compounds

We developed an electrochemical catalytic system for the dechlorination of 1,1-bis(4-chlorophenyl)-2,2,2-trichloroethane (DDT) that is one of the most problematic persistent organic pollutants (POPs) [108]. The controlled-potential electrolysis of DDT was performed at −1.4 V vs Ag/AgCl in the presence of **1** in DMF/*n*-Bu_4NClO_4. The DDT was converted to 1,1-bis(4-chlorophenyl)-2,2-dichloroethane (DDD), 1,1-bis(4-chlorophenyl)-2,2-dichloroethylene (DDE), 1-chloro-2,2-bis(4-chlorophenyl)ethylene (DDMU), and 1,1,4,4-tetrakis(4-chlorophenyl)-2,3-dichloro-2-butene (TTDB, *E*/*Z*) through dechlorination (Scheme 8b) [109]. A turnover number of 82 based on **1** was achieved. Mechanistic investigation revealed that the electrochemically generated Co(I) species of **1** participated in the dechlorination. To recycle the catalyst, ionic liquids are promising solvents due to their excellent electronic conductivity and nonvolatility. Thus, 1-butyl-3-methylimidazolium tetrafluoroborate ([bmim][BF_4]) was utilized as the solvent in the dechlorination of DDT [110]. During the extraction process, the product and **1** were separated in the organic solvent and ionic liquid layers, respectively. The ionic liquid layer could be recycled for further reactions. More interestingly, the catalytic ability of **1** increased nearly four times the reaction using DMF as solvent. This was consistent with the Hughes–Ingold prediction of solvent polarity effects on reaction rates [111].

We also developed a visible-light-driven catalytic system for the dechlorination of DDT using **1** as catalyst and $[Ru(bpy)_3]Cl_2$ as photosensitizer [102]. The redox potential of $[Ru(bpy)_3]Cl_2$ for Ru(II)/Ru(I) couple is −1.35 V vs SCE in CH_3CN. Thus, **1** was reduced to the Co(I) species by the photosensitizer in the presence of triethanolamine (TEOA) as sacrificial reductant on irradiation with a 500 W tungsten lamp in ethanol. DDT was successfully converted to DDD, DDE, and TTDB (*E*/*Z*). The recycled use of **1** and $[Ru(bpy)_3]Cl_2$ was also achieved using an ionic liquid as the reaction medium [103]. Recently, we have found that cyclometalated iridium(III) complexes such as Irdfppy [112] are superior to $[Ru(bpy)_3]Cl_2$ in terms of their photosensitization abilities in visible-light-driven B_{12} catalytic systems (Scheme 9) [104]. This was probably due to the gradual decomposition of $[Ru(bpy)_3]Cl_2$ under visible light irradiation. This is consistent with the report by Yoon et al. in which light irradiation to $Ru(bpy)_3^{2+}$ resulted in rapid decomposition during the photocatalytic reaction [113]. It was remarkable that a significantly high turnover number based on **1** (10,880) was obtained in the prolonged reaction with Irdfppy. Quenching experiments with time-resolved photoluminescence spectroscopy revealed that the oxidative quenching of the excited state of Irdfppy favorably proceeds over the reductive quenching mechanism. The combination of **1** and Irdfppy offers the best choice for the dechlorination of DDT among our light-driven systems in terms of both catalytic activity and visible-light harvesting.

In relation to the reactivity of **1** with DDT, interesting reactions of trichlorinated organic compounds have recently been investigated [100,114]. The B_{12}-TiO_2 hybrid catalyst converted trichlorinated organic compounds into esters and amides by UV light irradiation in the presence of oxygen, whereas dichlorostilbenes (*E* and *Z* forms) were formed under nitrogen atmosphere from benzotrichloride [100]. It was noticeable that an oxygen switch in dechlorination was successfully demonstrated. A benzoyl chloride was identified as an intermediate of the esters and amides. The aerobic electrolysis of trichlorinated organic compounds was also mediated by **1** to yield esters and amides [114]. These reactions are important in terms of fine chemical production from trichlorinated organic compounds through easy operations (i.e., in air at room temperature).

5. Radical-involved organic synthesis

B_{12} derivatives can mediate various molecular transformations in addition to the above three-type catalytic reactions. In particular, alkylated complexes can generate radicals through the cleavage of the Co(III)–C bonds upon light irradiation, heating,

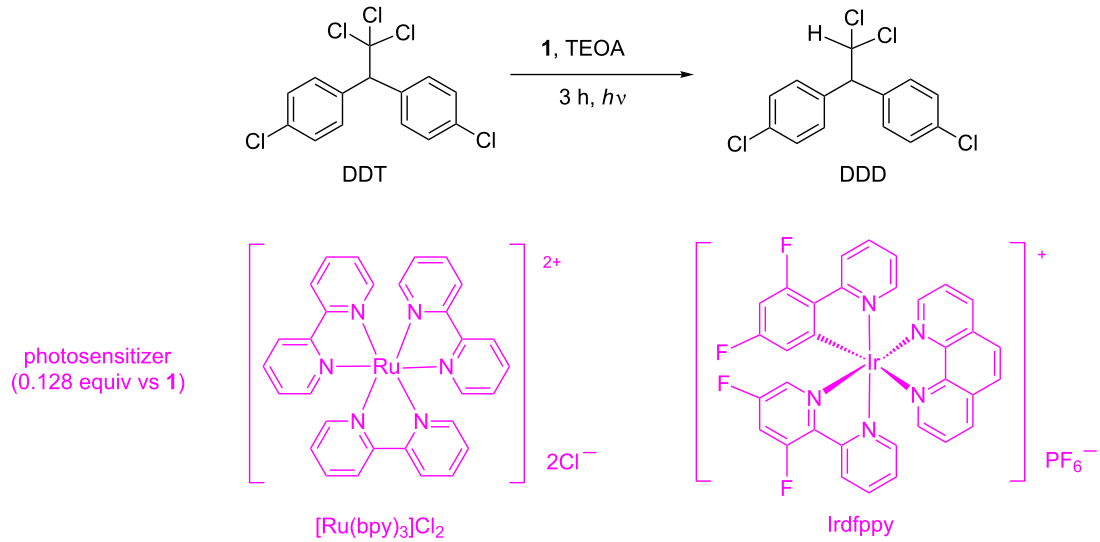

	[Ru(bpy)$_3$]Cl$_2$	Irdfppy
conversion	28%	100%
yield	26%	93%
turnover number based on **1**	78	279

Scheme 9: Visible-light-driven dechlorination of DDT using **1** in the presence of photosensitizers.

or electrochemical reduction. In addition, the corrin-ring of the B_{12} derivatives is tolerant to free radicals, as described above. Thus, alkylated complexes have been used for radical-mediated organic synthesis such as halide coupling, alkene coupling, and addition to double bonds [7,26,27]. In particular, the Co(III) form of **1** has recently been found to catalyze atom transfer radical addition of alkyl halides to olefins (phenyl vinyl sulfone and acrylates) in the presence of $NaBH_4$ [115]. In addition, a new light-driven method for generating acyl radicals from 2-*S*-pyridyl thioesters was developed through the use of vitamin B_{12} [116]. Furthermore, cobalester, an amphiphilic vitamin B_{12} derivative with six ester groups and a nucleotide loop, has recently been developed to show good catalytic activity for C–C bond forming reactions [117,118].

The above-mentioned visible-light-driven system composed of **1**, and Irdfppy system was used for radical-mediated isomerization reactions. Visible-light irradiation of diethyl 2-bromomethyl-2-phenylmalonate produced the phenyl-migrated product (Scheme 10) [104]. The product distribution highly depended on the solvents. The yield of phenyl-migrated products relative to those of simple reduced products significantly increased in PhCN, a poor hydrogen radical donor solvent, compared with those in EtOH and CH_3CN. Similar phe-

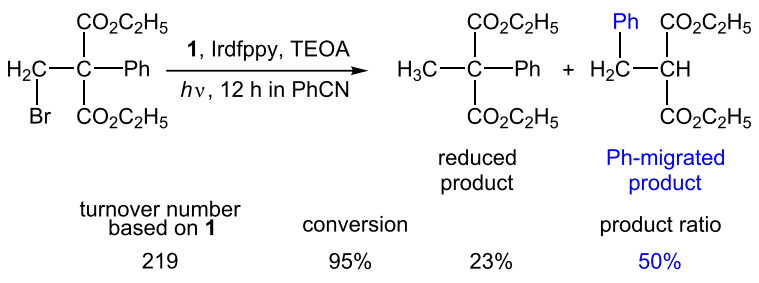

turnover number based on **1**	conversion	reduced product	Ph-migrated product
			product ratio
219	95%	23%	50%

Scheme 10: 1,2-Migration of a phenyl group mediated by the visible-light-driven catalytic system composed of **1** and Irdfppy.

nyl migration was achieved in the UV-light-driven system of the B_{12}-TiO_2 hybrid catalyst [96-98]. The involvement of a radical species was confirmed by the spin-trapping technique followed by the ESR measurements.

The B_{12}-TiO_2 hybrid catalyst also mediated the ring-expansion reactions of alicyclic ketones with carboxylic ester and bromomethyl groups (Scheme 11) [96,98]. The products involving six-, seven-, and eight-membered rings were obtained through isomerization with 1,2-migration of the ester groups. The B_{12}-TiO_2 hybrid catalyst can be regarded as a good alternative for conventional radical-involved organic syntheses using tin compounds.

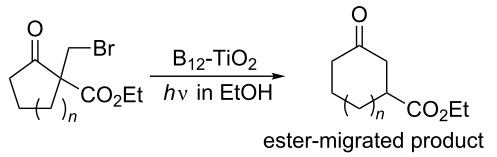

		yield	turnover number based on B_{12}
n = 1	10 h	80%	198
n = 2	12 h	77%	191
n = 3	13 h	80%	198

Scheme 11: Ring-expansion reactions mediated by the B_{12}-TiO_2 hybrid catalyst with UV-light irradiation.

Recently, we discovered that the B_{12} derivative **1** can mediate trifluoromethylation and perfluoroalkylation of aromatic and heteoaromatic compounds by means of electrolysis [119,120]. Introducing trifluoromethyl and perfluoroalkyl groups (R_F) into organic compounds is an important target in organic synthesis because the corresponding fluoroalkylated molecules have received significant interest because of their metabolic stability and superior electron-withdrawing and lipophilic properties [121]. The controlled-potential electrolysis of cost-effective fluoroalkylating reagents with carbon–iodine bonds R_FI (R_F = CF_3, n-C_3F_7, n-C_4F_9, n-C_8F_{17}, and n-$C_{10}F_{21}$) was carried out at −0.80 V vs Ag/AgCl in the presence of **1** in methanol/n-Bu_4NClO_4 to form Co(III)–R_F complexes with deiodination. These complexes released R_F radicals on the Co(III)-bond cleavage through visible-light irradiation. The resultant radicals reacted with aromatic reagents to form the target products through direct C–H functionalization (Scheme 12).

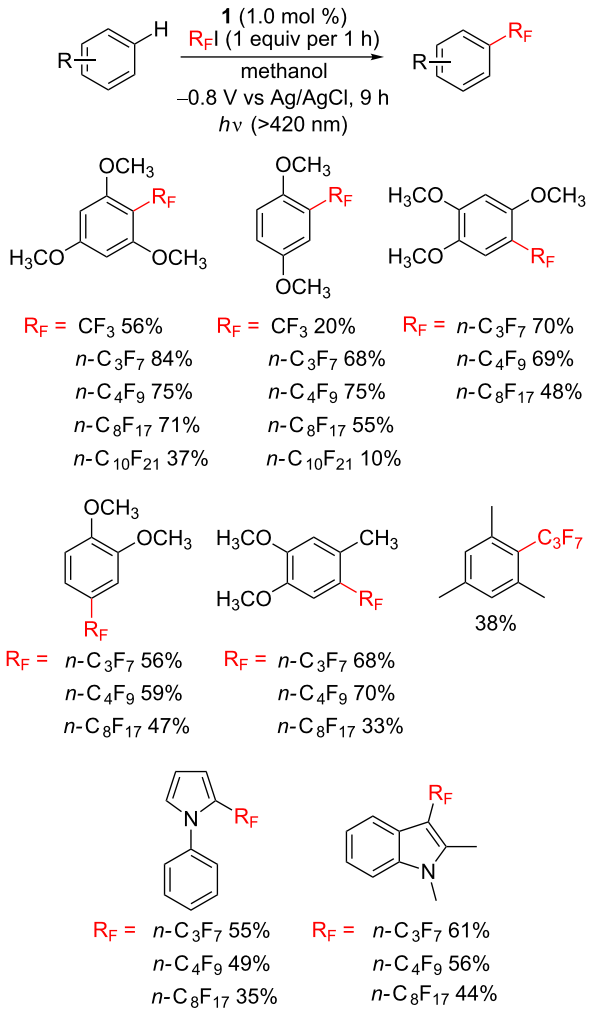

Scheme 12: Trifluoromethylation and perfluoroalkylation of aromatic compounds achieved through electrolysis with catalyst **1**.

Conclusion

In this review, we described biomimetic and bioinspired catalytic reactions with B_{12} enzyme functions, with a classification into the corresponding three enzyme subfamilies. A variety of B_{12} enzymes mediate various molecular transformations, in conjunction with other enzymes. Bound apoenzymes maximize the potential ability of B_{12} as a molecular catalyst. We conceptually broke up natural systems involving B_{12} enzymes into pieces and artificially assembled them again in a unique fashion. The resultant biomimetic and bioinspired systems provide new insights into designing catalytic systems in terms of green and eco-friendly reactions.

Acknowledgements

This work was partially supported by JSPS KAKENHI Grant Number JP18H04265 in Precisely Designed Catalysts with Customized Scaffolding and Grant Number JP16H04119. The authors would like to thank Enago (http://www.enago.jp) for the English language review.

ORCID® iDs

Yoshio Hisaeda - https://orcid.org/0000-0001-9196-8006

References

1. Kräutler, B. In *Vitamin B_{12} and B_{12}-Proteins;* Kräutler, B.; Arigoni, D.; Golding, B. T., Eds.; Wiley-VCH: Weinheim, 1998. doi:10.1002/9783527612192
2. Wohlfarth, G.; Diekert, G. In *Chemistry and Biochemistry of B_{12};* Banerjee, R., Ed.; Wiley-Interscience: New York, 1999.
3. Banerjee, R.; Ragsdale, S. W. *Annu. Rev. Biochem.* **2003,** *72,* 209–247. doi:10.1146/annurev.biochem.72.121801.161828
4. Kräutler, B. *Biochem. Soc. Trans.* **2005,** *33,* 806–810. doi:10.1042/BST0330806
5. Gruber, K.; Puffer, B.; Kräutler, B. *Chem. Soc. Rev.* **2011,** *40,* 4346–4363. doi:10.1039/c1cs15118e
6. Brown, K. L. *Chem. Rev.* **2005,** *105,* 2075–2150. doi:10.1021/cr030720z
7. Giedyk, M.; Goliszewska, K.; Gryko, D. *Chem. Soc. Rev.* **2015,** *44,* 3391–3404. doi:10.1039/C5CS00165J
8. Dereven'kov, I. A.; Salnikov, D. S.; Silaghi-Dumitrescu, R.; Makarov, S. V.; Koifman, O. I. *Coord. Chem. Rev.* **2016,** *309,* 68–83. doi:10.1016/j.ccr.2015.11.001
9. Waddington, M. D.; Finke, R. G. *J. Am. Chem. Soc.* **1993,** *115,* 4629–4640. doi:10.1021/ja00064a026
10. Kräutler, B.; Keller, W.; Kratky, C. *J. Am. Chem. Soc.* **1989,** *111,* 8936–8938. doi:10.1021/ja00206a037
11. Schrauzer, G. N.; Deutsch, E.; Windgassen, R. J. *J. Am. Chem. Soc.* **1968,** *90,* 2441–2442. doi:10.1021/ja01011a054
12. Tackett, S. L.; Collat, J. W.; Abbott, J. C. *Biochemistry* **1963,** *2,* 919–923. doi:10.1021/bi00905a004
13. Hill, H. A. O.; Pratt, J. M.; O'Riordan, M. P.; Williams, F. R.; Williams, R. J. P. *J. Chem. Soc. A* **1971,** 1859–1862. doi:10.1039/j19710001859
14. Burris, D. R.; Delcomyn, C. A.; Smith, M. H.; Roberts, A. L. *Environ. Sci. Technol.* **1996,** *30,* 3047–3052. doi:10.1021/es960116o
15. Glod, G.; Angst, W.; Holliger, C.; Schwarzenbach, R. P. *Environ. Sci. Technol.* **1997,** *31,* 253–260. doi:10.1021/es9603867
16. McCauley, K. M.; Pratt, D. A.; Wilson, S. R.; Shey, J.; Burkey, T. J.; van der Donk, W. A. *J. Am. Chem. Soc.* **2005,** *127,* 1126–1136. doi:10.1021/ja048573p
17. Gantzer, C. J.; Wackett, L. P. *Environ. Sci. Technol.* **1991,** *25,* 715–722. doi:10.1021/es00016a017
18. Krone, U. E.; Thauer, R. K.; Hogenkamp, H. P. C.; Steinbach, K. *Biochemistry* **1991,** *30,* 2713–2719. doi:10.1021/bi00224a020
19. Fischli, A. *Helv. Chim. Acta* **1982,** *65,* 1167–1190. doi:10.1002/hlca.19820650406
20. Motwani, H. V.; Fred, C.; Haglund, J.; Golding, B. T.; Törnqvist, M. *Chem. Res. Toxicol.* **2009,** *22,* 1509–1516. doi:10.1021/tx900088w
21. Lexa, D.; Saveant, J. M. *Acc. Chem. Res.* **1983,** *16,* 235–243. doi:10.1021/ar00091a001
22. ó Proinsias, K.; Giedyk, M.; Gryko, D. *Chem. Soc. Rev.* **2013,** *42,* 6605–6619. doi:10.1039/c3cs60062a
23. Njue, C. K.; Nuthakki, B.; Vaze, A.; Bobbitt, J. M.; Rusling, J. F. *Electrochem. Commun.* **2001,** *3,* 733–736. doi:10.1016/S1388-2481(01)00255-7
24. Shey, J.; McGinley, C. M.; McCauley, K. M.; Dearth, A. S.; Young, B. T.; van der Donk, W. A. *J. Org. Chem.* **2002,** *67,* 837–846. doi:10.1021/jo0160470
25. Sun, F.; Darbre, T. *Org. Biomol. Chem.* **2003,** *1,* 3154–3159. doi:10.1039/b305782h
26. Scheffold, R.; Rytz, G.; Walder, L. *Mod. Synth. Methods* **1983,** *3,* 355–439.
27. Scheffold, R.; Abrecht, S.; Orlinski, R.; Ruf, H.-R.; Stamouli, P.; Tinembart, O.; Walder, L.; Weymuth, C. *Pure Appl. Chem.* **1987,** *59,* 363–372. doi:10.1351/pac198759030363
28. Murakami, Y.; Hisaeda, Y.; Kajihara, A. *Bull. Chem. Soc. Jpn.* **1989,** *56,* 3642–3646. doi:10.1246/bcsj.56.3642
29. Hisaeda, Y.; Shimakoshi, H. In *Handbook of Porphyrin Science;* Kadish, K. M.; Smith, K. M.; Guilard, R., Eds.; World Scientific: Singapore, 2010; Vol. 10, pp 313–370.
30. Werthemann, L. *Dissertation, ETH Zürich (Nr. 4097);* Juris Druck and Verlag: Zürich, 1968.
31. Kräutler, B.; Keller, W.; Hughes, M.; Caderas, C.; Kratky, C. *J. Chem. Soc., Chem. Commun.* **1987,** 1678–1680. doi:10.1039/C39870001678
32. Murakami, Y.; Kikuchi, J.-i.; Hisaeda, Y.; Hayashida, O. *Chem. Rev.* **1996,** *96,* 721–758. doi:10.1021/cr9403704
33. Qiao, Y.; Tahara, K.; Zhang, Q.; Song, X.-M.; Hisaeda, Y.; Kikuchi, J.-i. *Chem. Lett.* **2014,** *43,* 684–686. doi:10.1246/cl.140025
34. Hisaeda, Y.; Masuko, T.; Hanashima, E.; Hayashi, T. *Sci. Technol. Adv. Mater.* **2006,** *7,* 655–661. doi:10.1016/j.stam.2006.08.003
35. Tahara, T.; Shimakoshi, H.; Tanaka, A.; Hisaeda, Y. *Tetrahedron Lett.* **2007,** *48,* 5065–5068. doi:10.1016/j.tetlet.2007.05.092
36. Tahara, K.; Shimakoshi, H.; Tanaka, A.; Hisaeda, Y. *Dalton Trans.* **2010,** *39,* 3035–3042. doi:10.1039/b923924c
37. Tahara, K.; Shimakoshi, H.; Tanaka, A.; Hisaeda, Y. *Bull. Chem. Soc. Jpn.* **2010,** *83,* 1439–1446. doi:10.1246/bcsj.20100221
38. Shimakoshi, H.; Nishi, M.; Tanaka, A.; Chikama, K.; Hisaeda, Y. *Chem. Lett.* **2010,** *39,* 22–23. doi:10.1246/cl.2010.22
39. Shimakoshi, H.; Nishi, M.; Tanaka, A.; Chikama, K.; Hisaeda, Y. *Chem. Commun.* **2011,** *47,* 6548–6550. doi:10.1039/c1cc11970b
40. Zhang, W.; Shimakoshi, H.; Houfuku, N.; Song, X.-M.; Hisaeda, Y. *Dalton Trans.* **2014,** *43,* 13972–13978. doi:10.1039/C4DT01360C
41. Xu, J.; Shimakoshi, H.; Hisaeda, Y. *J. Organomet. Chem.* **2015,** *782,* 89–95. doi:10.1016/j.jorganchem.2014.11.015
42. Hisaeda, Y.; Nishioka, T.; Inoue, Y.; Asada, K.; Hayashi, T. *Coord. Chem. Rev.* **2000,** *198,* 21–37. doi:10.1016/S0010-8545(99)00222-2
43. Shimakoshi, H.; Hisaeda, Y. *Curr. Opin. Electrochem.* **2018,** *8,* 24–30. doi:10.1016/j.coelec.2017.12.001
44. Shimakoshi, H.; Hisaeda, Y. *ChemPlusChem* **2017,** *82,* 18–29. doi:10.1002/cplu.201600303
45. Hisaeda, Y.; Tahara, K.; Shimakoshi, H.; Masuko, T. *Pure Appl. Chem.* **2013,** *85,* 1415–1426. doi:10.1351/PAC-CON-12-10-05
46. Frey, P. A. *Chem. Rev.* **1990,** *90,* 1343–1357. doi:10.1021/cr00105a014
47. Frey, P. A. *Annu. Rev. Biochem.* **2001,** *70,* 121–148. doi:10.1146/annurev.biochem.70.1.121
48. Stubbe, J. *Annu. Rev. Biochem.* **1989,** *58,* 257–285. doi:10.1146/annurev.bi.58.070189.001353
49. Stubbe, J.; van der Donk, W. A. *Chem. Rev.* **1998,** *98,* 705–762. doi:10.1021/cr9400875
50. Jordan, A.; Reichard, P. *Annu. Rev. Biochem.* **1998,** *67,* 71–98. doi:10.1146/annurev.biochem.67.1.71

51. Sawers, G.; Watson, G. *Mol. Microbiol.* **1998,** *29,* 945–954. doi:10.1046/j.1365-2958.1998.00941.x
52. Toraya, T. *Chem. Rev.* **2003,** *103,* 2095–2128. doi:10.1021/cr020428b
53. Buckel, W.; Golding, B. T. *Chem. Soc. Rev.* **1996,** *25,* 329–337. doi:10.1039/cs9962500329
54. Murakami, Y.; Hisaeda, Y.; Ozaki, T.; Tashiro, T.; Ohno, T.; Tani, Y.; Matsuda, Y. *Bull. Chem. Soc. Jpn.* **1987,** *60,* 311–324. doi:10.1246/bcsj.60.311
55. Murakami, Y.; Hisaeda, Y.; Ozaki, T. *J. Coord. Chem.* **1991,** *23,* 77–89. doi:10.1080/00958979109408244
56. Tahara, K.; Pan, L.; Yamaguchi, R.; Shimakoshi, H.; Abe, M.; Hisaeda, Y. *J. Inorg. Biochem.* **2017,** *175,* 239–243. doi:10.1016/j.jinorgbio.2017.07.021
57. Tamblyn, W. H.; Klingler, R. J.; Hwang, W. S.; Kochi, J. K. *J. Am. Chem. Soc.* **1981,** *103,* 3161–3172. doi:10.1021/ja00401a038
58. Elliot, C. M.; Hershenhart, E.; Finke, R. G.; Smith, B. L. *J. Am. Chem. Soc.* **1981,** *103,* 5558–5566. doi:10.1021/ja00408a047
59. Murakami, Y.; Hisaeda, Y.; Fan, S.-D.; Mastuda, Y. *Chem. Lett.* **1988,** *17,* 835–838. doi:10.1246/cl.1988.835
60. Murakami, Y.; Hisaeda, Y.; Fan, S.-D.; Mastuda, Y. *Bull. Chem. Soc. Jpn.* **1989,** *62,* 2219–2228. doi:10.1246/bcsj.62.2219
61. Tahara, K.; Chen, Y.; Pan, L.; Masuko, T.; Shimakoshi, H.; Hisaeda, Y. *Chem. Lett.* **2011,** *40,* 177–179. doi:10.1246/cl.2011.177
62. Deng, H.; Grunder, S.; Cordova, K. E.; Valente, C.; Furukawa, H.; Hmadeh, M.; Gándara, F.; Whalley, A. C.; Liu, Z.; Asahina, S.; Kazumori, H.; O'Keeffe, M.; Terasaki, O.; Stoddart, J. F.; Yaghi, O. M. *Science* **2012,** *336,* 1018–1023. doi:10.1126/science.1220131
63. Deshmukh, M. M.; Ohba, M.; Kitagawa, S.; Sakaki, S. *J. Am. Chem. Soc.* **2013,** *135,* 4840–4849. doi:10.1021/ja400537f
64. Yanai, N.; Uemura, T.; Inoue, M.; Matsuda, R.; Fukushima, T.; Tsujimoto, M.; Isoda, S.; Kitagawa, S. *J. Am. Chem. Soc.* **2012,** *134,* 4501–4504. doi:10.1021/ja2115713
65. Banerjee, R. V.; Frasca, V.; Ballou, D. P.; Matthews, R. G. *Biochemistry* **1990,** *29,* 11101–11109. doi:10.1021/bi00502a013
66. Matthews, R. G. *Acc. Chem. Res.* **2001,** *34,* 681–689. doi:10.1021/ar0000051
67. Gonzáles, J. C.; Peariso, K.; Penner-Hahn, J. E.; Matthews, R. G. *Biochemistry* **1996,** *35,* 12228–12234. doi:10.1021/bi9615452
68. Peariso, K.; Goulding, C. W.; Huang, S.; Matthews, R. G.; Penner-Hahn, J. E. *J. Am. Chem. Soc.* **1998,** *120,* 8410–8416. doi:10.1021/ja980581g
69. Zhou, Z. S.; Peariso, K.; Penner-Hahn, J. E.; Matthews, R. G. *Biochemistry* **1999,** *38,* 15915–15926. doi:10.1021/bi992062b
70. Schnyder, A.; Darbre, T.; Keese, R. *Angew. Chem., Int. Ed.* **1998,** *37,* 1283–1285. doi:10.1002/(SICI)1521-3773(19980518)37:9<1283::AID-ANIE1283>3.0.CO;2-N
71. Zheng, D.; Darbre, T.; Keese, R. *J. Inorg. Biochem.* **1999,** *73,* 273–275. doi:10.1016/S0162-0134(99)00028-8
72. Wedemeyer-Exl, C.; Darbre, T.; Keese, R. *Org. Biomol. Chem.* **2007,** *5,* 2119–2128. doi:10.1039/b703421k
73. Kräutler, B.; Hughes, M.; Caderas, C. *Helv. Chim. Acta* **1986,** *69,* 1571–1575. doi:10.1002/hlca.19860690708
74. Wedemeyer-Exl, C.; Darbre, T.; Keese, R. *Helv. Chim. Acta* **1999,** *82,* 1173–1184. doi:10.1002/(SICI)1522-2675(19990804)82:8<1173::AID-HLCA1173>3.0.CO;2-2
75. Pan, L.; Shimakoshi, H.; Hisaeda, Y. *Chem. Lett.* **2009,** *38,* 26–27. doi:10.1246/cl.2009.26
76. Pan, L.; Shimakoshi, H.; Masuko, T.; Hisaeda, Y. *Dalton Trans.* **2009,** 9898–9905. doi:10.1039/b909163g
77. Pan, L.; Tahara, K.; Masuko, T.; Hisaeda, Y. *Inorg. Chim. Acta* **2011,** *368,* 194–199. doi:10.1016/j.ica.2011.01.004
78. Yamauchi, H.; Aminaka, Y.; Yoshida, K.; Sun, G.; Pi, J.; Waalkes, M. P. *Toxicol. Appl. Pharmacol.* **2004,** *198,* 291–296. doi:10.1016/j.taap.2003.10.021
79. Kaise, T.; Watanabe, S.; Ito, K. *Chemosphere* **1985,** *14,* 1327–1332. doi:10.1016/0045-6535(85)90153-5
80. Edmonds, J. S.; Francesconi, K. A. *Experientia* **1987,** *43,* 553–557. doi:10.1007/BF02143584
81. Edmonds, J. S. *Bioorg. Med. Chem. Lett.* **2000,** *10,* 1105–1108. doi:10.1016/S0960-894X(00)00176-1
82. Thomas, D. J.; Waters, S. B.; Styblo, M. *Toxicol. Appl. Pharmacol.* **2004,** *198,* 319–326. doi:10.1016/j.taap.2003.10.020
83. Nakamura, K.; Hisaeda, Y.; Pan, L.; Yamauchi, H. *Chem. Commun.* **2008,** 5122–5124. doi:10.1039/b808937j
84. Nakamura, K.; Hisaeda, Y.; Pan, L.; Yamauchi, H. *J. Organomet. Chem.* **2009,** *694,* 916–921. doi:10.1016/j.jorganchem.2008.12.002
85. Holliger, C.; Wohlfarth, G.; Diekert, G. *FEMS Microbiol. Rev.* **1999,** *22,* 383–398. doi:10.1111/j.1574-6976.1998.tb00377.x
86. Kräutler, B.; Fieber, W.; Ostermann, S.; Fasching, M.; Ongania, K.-H.; Gruber, K.; Kratky, C.; Mikl, C.; Siebert, A.; Diekert, G. *Helv. Chim. Acta* **2003,** *86,* 3698–3716. doi:10.1002/hlca.200390313
87. Bommer, M.; Kunze, C.; Fesseler, J.; Schubert, T.; Diekert, G.; Dobbek, H. *Science* **2014,** *346,* 455–458. doi:10.1126/science.1258118
88. Payne, K. A. P.; Quezada, C. P.; Fisher, K.; Dunstan, M. S.; Collins, F. A.; Sjuts, H.; Levy, C.; Hay, S.; Rigby, S. E. J.; Leys, D. *Nature* **2015,** *517,* 513–516. doi:10.1038/nature13901
89. Francke, R.; Little, R. D. *Chem. Soc. Rev.* **2014,** *43,* 2492–2521. doi:10.1039/c3cs60464k
90. Yoshida, J.-i.; Kataoka, K.; Horcajada, R.; Nagaki, A. *Chem. Rev.* **2008,** *108,* 2265–2299. doi:10.1021/cr0680843
91. Savéant, J.-M. *Chem. Rev.* **2008,** *108,* 2348–2378. doi:10.1021/cr068079z
92. Albini, A.; Fagnoni, M. *Green Chem.* **2004,** *6,* 1–6. doi:10.1039/b309592d
93. Palmisano, G.; Augugliaro, V.; Pagliaro, M.; Palmisano, L. *Chem. Commun.* **2007,** 3425–3437. doi:10.1039/b700395c
94. Fagnoni, M.; Dondi, D.; Ravelli, D.; Albini, A. *Chem. Rev.* **2007,** *107,* 2725–2756. doi:10.1021/cr068352x
95. Shimakoshi, H.; Sakumori, E.; Kaneko, K.; Hisaeda, Y. *Chem. Lett.* **2009,** *38,* 468–469. doi:10.1246/cl.2009.468
96. Shimakoshi, H.; Abiru, M.; Izumi, S.-i.; Hisaeda, Y. *Chem. Commun.* **2009,** 6427–6429. doi:10.1039/b913255d
97. Shimakoshi, H.; Abiru, M.; Kuroiwa, K.; Kimizuka, N.; Watanabe, M.; Hisaeda, Y. *Bull. Chem. Soc. Jpn.* **2010,** *83,* 170–172. doi:10.1246/bcsj.20090234
98. Izumi, S.-i.; Shimakoshi, H.; Abe, M.; Hisaeda, Y. *Dalton Trans.* **2010,** *39,* 3302–3307. doi:10.1039/b921802e
99. Shimakoshi, H.; Hisaeda, Y. *ChemPlusChem* **2014,** *79,* 1250–1253. doi:10.1002/cplu.201402081
100. Shimakoshi, H.; Hisaeda, Y. *Angew. Chem., Int. Ed.* **2015,** *54,* 15439–15443. doi:10.1002/anie.201507782
101. Tian, H.; Shimakoshi, H.; Imamura, K.; Shiota, Y.; Yoshizawa, K.; Hisaeda, Y. *Chem. Commun.* **2017,** *53,* 9478–9481. doi:10.1039/C7CC04377E

102. Shimakoshi, H.; Tokunaga, M.; Baba, T.; Hisaeda, Y. *Chem. Commun.* **2004,** 1806–1807. doi:10.1039/b406400c
103. Shimakoshi, H.; Kudo, S.; Hisaeda, Y. *Chem. Lett.* **2005,** *34,* 1096–1097. doi:10.1246/cl.2005.1096
104. Tian, H.; Shimakoshi, H.; Park, G.; Kim, S.; You, Y.; Hisaeda, Y. *Dalton Trans.* **2018,** *47,* 675–683. doi:10.1039/C7DT03742B
105. Tahara, K.; Hisaeda, Y. *Green Chem.* **2011,** *13,* 558–561. doi:10.1039/c0gc00478b
106. Tahara, K.; Mikuriya, K.; Masuko, T.; Kikuchi, J.-i.; Hisaeda, Y. *J. Porphyrins Phthalocyanines* **2013,** *17,* 135–141. doi:10.1142/S1088424612501398
107. Tahara, K.; Mikuriya, K.; Masuko, T.; Kikuchi, J.-i.; Hisaeda, Y. *Supramol. Chem.* **2016,** *28,* 141–150. doi:10.1080/10610278.2015.1103373
108. Hitchman, M. L.; Spackman, R. A.; Ross, N. C.; Agra, C. *Chem. Soc. Rev.* **1995,** *24,* 423–430. doi:10.1039/cs9952400423
109. Shimakoshi, H.; Tokunaga, M.; Hisaeda, Y. *Dalton Trans.* **2004,** 878–882. doi:10.1039/b315170k
110. Jabbar, M. A.; Shimakoshi, H.; Hisaeda, Y. *Chem. Commun.* **2007,** 1653–1655. doi:10.1039/b700725f
111. Cooper, K. A.; Dhar, M. L.; Hughes, E. D.; Ingold, C. K.; MacNulty, B. J.; Woolf, L. I. *J. Chem. Soc.* **1948,** 2043–2049. doi:10.1039/jr9480002043
112. You, Y.; Nam, W. *Chem. Soc. Rev.* **2012,** *41,* 7061–7084. doi:10.1039/c2cs35171d
113. Akhtar, U. S.; Tae, E. L.; Chun, Y. S.; Hwang, I. C.; Yoon, K. B. *ACS Catal.* **2016,** *6,* 8361–8369. doi:10.1021/acscatal.6b02595
114. Shimakoshi, H.; Luo, Z.; Inaba, T.; Hisaeda, Y. *Dalton Trans.* **2016,** *45,* 10173–10180. doi:10.1039/C6DT00556J
115. Proinsias, K. ó; Jackowska, A.; Radzewicz, K.; Giedyk, M.; Gryko, D. *Org. Lett.* **2018,** *20,* 296–299. doi:10.1021/acs.orglett.7b03699
116. Ociepa, M.; Baka, O.; Narodowiec, J.; Gryko, D. *Adv. Synth. Catal.* **2017,** *359,* 3560–3565. doi:10.1002/adsc.201700913
117. Giedyk, M.; Fedosov, S. N.; Gryko, D. *Chem. Commun.* **2014,** *50,* 4674–4676. doi:10.1039/C4CC01064G
118. Giedyk, M.; Shimakoshi, H.; Goliszewska, K.; Gryko, D.; Hisaeda, Y. *Dalton Trans.* **2016,** *45,* 8340–8346. doi:10.1039/C6DT00355A
119. Hossain, M. J.; Ono, T.; Wakiya, K.; Hisaeda, Y. *Chem. Commun.* **2017,** *53,* 10878–10881. doi:10.1039/C7CC06221D
120. Ono, T.; Wakiya, K.; Hossain, M. J.; Shimakoshi, H.; Hisaeda, Y. *Chem. Lett.* **2018,** *47,* 979–981. doi:10.1246/cl.180355
121. Alonso, C.; Martínez de Marigorta, E.; Rubiales, G.; Palacios, F. *Chem. Rev.* **2015,** *115,* 1847–1935. doi:10.1021/cr500368h

License and Terms

BEILSTEIN JOURNAL OF ORGANIC CHEMISTRY

Copolymerization of epoxides with cyclic anhydrides catalyzed by dinuclear cobalt complexes

Yo Hiranoi and Koji Nakano*

Full Research Paper

Open Access

Address:
Department of Organic and Polymer Materials Chemistry, Tokyo University of Agriculture and Technology, 2-24-16 Naka-cho, Koganei, Tokyo 184-8588, Japan

Email:
Koji Nakano* - k_nakano@cc.tuat.ac.jp

* Corresponding author

Keywords:
cobalt; copolymerization; cyclic anhydrides; epoxides; polyesters

Beilstein J. Org. Chem. **2018,** *14,* 2779–2788.
doi:10.3762/bjoc.14.255

Received: 16 August 2018
Accepted: 16 October 2018
Published: 05 November 2018

This article is part of the thematic issue "Cobalt catalysis".

Guest Editor: S. Matsunaga

Abstract

The alternating copolymerization of epoxides with cyclic anhydrides (CAs) is a highly diverse synthetic method for polyesters as the polymers' architectures and properties can be easily controlled depending on the combination of two monomers. Thus, a variety of catalyst designs has been reported to prepare the desired copolymers efficiently. We herein report dinuclear cobalt–salen complexes with a benzene ring as a linker and their activities in copolymerization reactions. The dinuclear cobalt complexes showed a higher catalytic activity for the copolymerization of propylene oxide with phthalic anhydride than the corresponding mononuclear cobalt–salen complex and achieved one of the highest turnover frequencies ever reported. A variety of epoxides and CAs were also found to be copolymerized successfully by the dinuclear cobalt complex with a high catalytic activity.

Introduction

Aliphatic polyesters have received significant attention owing to their good biocompatibility and biodegradability [1-4]. These attractive features allow them to be applied in medical and ecological materials as well as in commodity materials. The conventional way of synthesizing polyesters is the step-growth polymerization of diacids (or diacid derivatives) with diols. The ready availability of structurally diverse diacids and diols provides access to a wide range of polyesters. In this method, an extremely high conversion of the carboxy and hydroxy groups should be achieved for synthesizing high molecular weight polyesters. However, there are some burdensome requisites, such as a precise stoichiometric balance between the carboxy and hydroxy groups and an efficient removal of small molecule byproducts, for the high conversion. Another conventional method for polyester synthesis is the chain-growth ring-opening polymerization (ROP) of lactones and cyclic diesters [5-10]. In contrast to the step-growth polymerization, the ROP does not give any small molecule byproducts and proceeds under mild conditions. In addition, high molecular weight polyesters with narrow polydispersity can be prepared even at a low monomer

conversion. A variety of lactones and cyclic diesters, such as ε-caprolactone, β-propiolactone, lactic acid (LA), and glycolide have been used for the ROP. However, the employable monomers are rather limited, which restricts the range of polymer properties.

In view of the aforementioned, the alternating copolymerization of epoxides with cyclic anhydrides (CAs) is a promising alternative for polyester synthesis [11,12]. A broad range of epoxides and CAs are readily available and can be copolymerized through this method. Therefore, the polymer architectures and properties can be easily controlled depending on the combination of the two monomers used. This copolymerization method was first reported in 1960 where a tertiary amine was used as a catalyst [13]. Since then, a range of polymerization catalysts including alkyl metals and inorganic salts have been reported. However, the development of the epoxide/CA copolymerization was constricted until recently because of low catalytic activity and poor control over the main chain sequence (formation of ether linkages through consecutive epoxide enchainment) and molecular weight. In 2007, Coates and co-workers reported that β-diiminate zinc complexes exhibited a high catalytic activity for the epoxide/CA copolymerization [14]. The resulting polyesters were found to possess completely alternating structures with high molecular weight and relatively narrow polydispersity. Following this report, a range of highly active and/or selective catalysts has been developed based on well-defined metal complexes such as metalloporphyrins and metal–salen complexes [15-21]. In parallel to the development of catalysts, new polyester materials also were prepared by employing unprecedented monomers or by the combination with other polymerization methods [22-26].

Cooperative dinuclear metal catalysts have been considered as a promising design for high activity and/or selectivity in organic transformations including polymerizations [27-30]. This was found to be true for the epoxide/CA copolymerization. In 2013, Lu and co-workers reported that the dinuclear chromium–salan complex showed a much higher catalytic activity than the corresponding mononuclear chromium–salan complex in the copolymerization of epoxides with maleic anhydride (MA) [31]. Following this report, some dinuclear metal complexes have been reported to demonstrate high and/or unique catalytic performances in the epoxide/CA copolymerization [23,32-39]. Recently, we have reported the dinuclear cobalt–salen complexes as catalysts for the copolymerization of epoxides with carbon dioxide (CO_2), affording superior catalytic activity compared to the corresponding mononuclear cobalt–salen complexes [40]. During the course of our study, the dinuclear cobalt–salen complex (*R*,*R*,*S*,*S*)-**1** was found to exhibit a high catalytic activity for the alternating copolymerization of propylene oxide (PO) with phthalic anhydride (PA, Figure 1). The observed catalytic activity was much higher than that achieved by using the mononuclear cobalt–salen complex. Although mononuclear cobalt–salen complexes are known as one of the most active catalysts for the epoxide/CA copolymerization [15], there has been no report on the catalyst design based on dinuclear cobalt–salen complexes. This context prompted us to explore the catalyst performance of the dinuclear cobalt–salen complexes. Herein we report our further investigation on the epoxide/CA copolymerization by using dinuclear cobalt–salen complexes.

Results and Discussion

Synthesis of dinuclear cobalt–salen complexes

In our previous preliminary investigation, we used the heterochiral dinuclear cobalt–salen complex (*R*,*R*,*S*,*S*)-**1** with *tert*-butyl groups at the 5-positions of the salicylidene moieties and a pentafluorobenzoate group as an axial ligand [40]. Recently, the substituents at the 5-positions and the axial ligand of mononuclear cobalt–salen complexes were proven to have a great

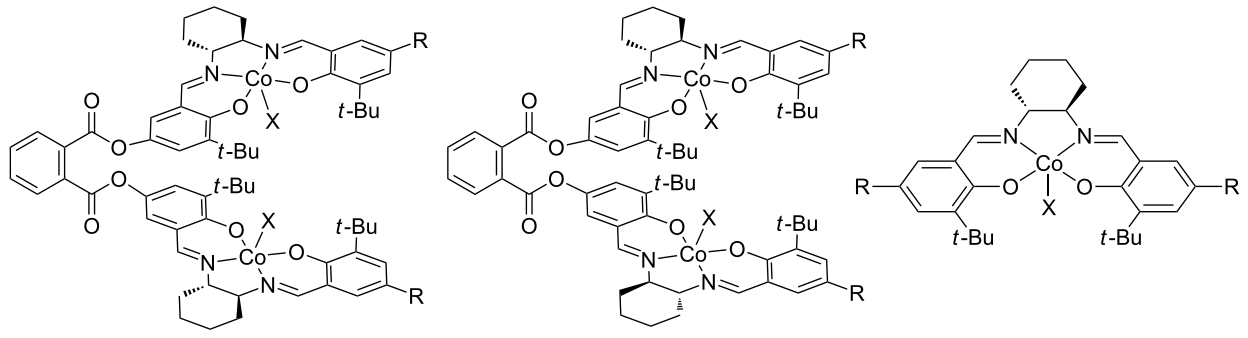

Figure 1: Structures of cobalt–salen complexes **1**–**4**.

impact on the catalytic activity [15]. The electron-withdrawing fluoro group at the 5-positions and a nitrate axial ligand gave the most active catalyst for the PO/MA copolymerization. Accordingly, we designed the heterochiral dinuclear cobalt–salen complex (*R*,*R*,*S*,*S*)-**2** as well as the homochiral complex (*R*,*R*,*R*,*R*)-**2** with fluoro groups at the 5-positions and nitrate axial ligands.

The heterochiral bis(salen) ligand precursor (*R*,*R*,*S*,*S*)-**8** was synthesized according to the procedure we have reported previously (Scheme 1) [40]. First, the reaction of bis(salicylaldehyde) **5** with (*R*,*R*)-half-salen **6**, which was prepared from (*R*,*R*)-1,2-cyclohexanediamine monohydrochloride and 3-*tert*-butyl-5-fluoro-2-hydroxybenzaldehyde, gave monosalen (*R*,*R*)-**7** in 39% yield. Then, the obtained mono(salen) (*R*,*R*)-**7** was converted into the heterochiral bis(salen) ligand precursor (*R*,*R*,*S*,*S*)-**8** in 52% yield through the condensation with (*S*,*S*)-half-salen **6**. In addition, the homochiral bis(salen) ligand precursor (*R*,*R*,*R*,*R*)-**8** was prepared by the reaction of bis(salicylaldehyde) **5** with two equivalents of (*R*,*R*)-half-salen **6** in 45% yield. Both, (*R*,*R*,*S*,*S*)-**8** and (*R*,*R*,*R*,*R*)-**8** were then treated with cobalt(II) nitrate and the following oxidation under air afforded the corresponding dinuclear cobalt–salen complexes (*R*,*R*,*S*,*S*)-**2** and (*R*,*R*,*R*,*R*)-**2**, respectively.

Copolymerization of propylene oxide with phthalic anhydride

The catalysts' performances were evaluated through the copolymerization of PO with PA (Table 1). For a convenient comparison of the different catalytic systems, the catalytic activity is expressed in terms of turnover frequency [TOF, (mol of PA incorporated in the copolymer)·(mol of Co center)$^{-1}$·h^{-1}]. First, the copolymerization was conducted in the presence of the homochiral dinuclear cobalt–salen complex (*R*,*R*,*R*,*R*)-**1** and [Ph_3P=N=PPh_3][$OCOC_6F_5$] ([PPN][$OCOC_6F_5$]) as the co-catalyst at 30 °C for 1 h (Table 1, entry 1, [PO]/[PA]/[Co] (= 2[(*R*,*R*,*R*,*R*)-**1**])/[co-catalyst] = 4,000:400:1:1). Since the solubility of PA in PO at 30 °C is limited, a large excess of PO over PA was used to maintain a homogeneous system. Under these conditions, a high catalytic activity with a TOF of 299 h^{-1} was accomplished. A decrease in the amount of co-catalyst resulted in a lower TOF (Table 1, entry 2) and the copolymerization did not proceed at all in the absence of co-catalyst (Table 1, entry 3). Thus, one equivalent of a co-catalyst is necessary for a high catalytic activity. A remarkably high TOF of 908 h^{-1} was achieved at the higher copolymerization temperature of 60 °C (Table 1, entry 4). This is one of the highest TOF values ever reported for the metal-catalyzed PO/PA copolymerization [41].

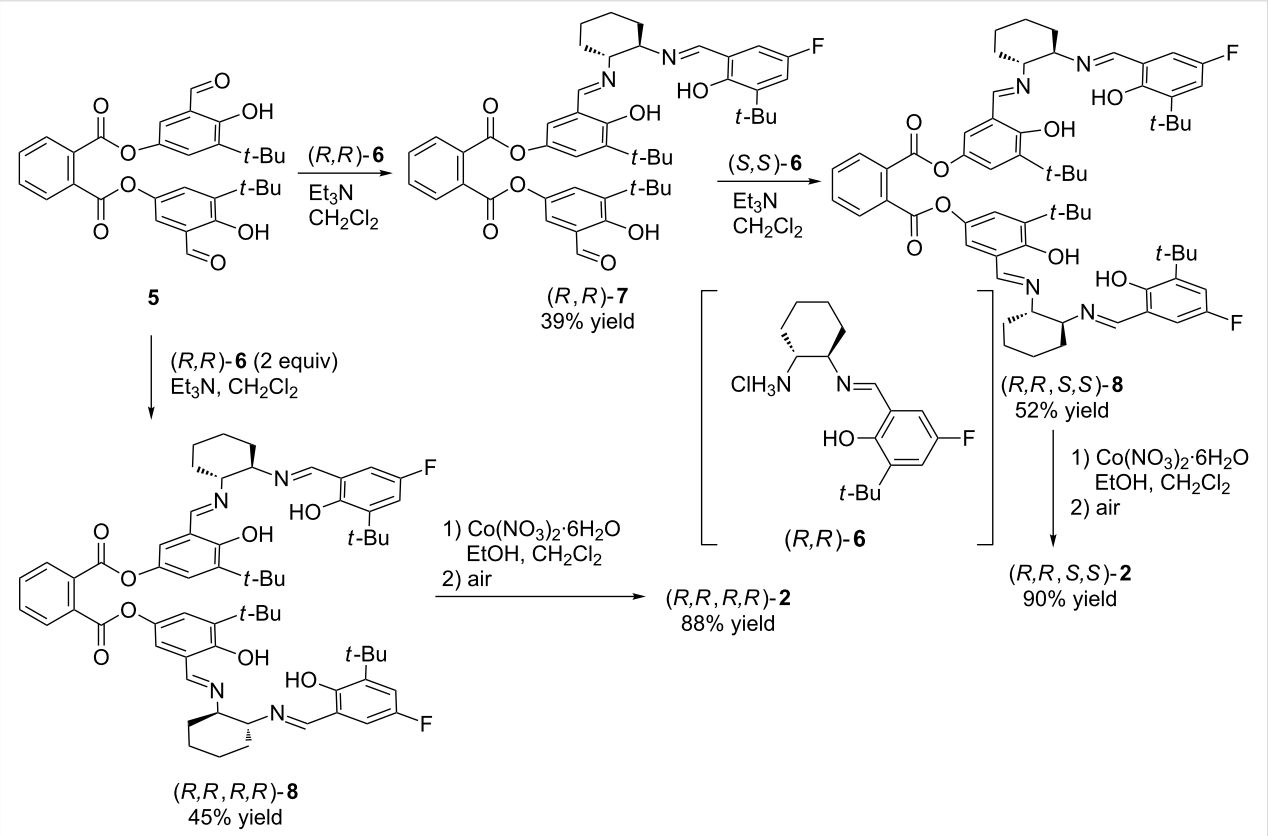

Scheme 1: Synthesis of dinuclear cobalt–salen complexes (*R*,*R*,*S*,*S*)-**2** and (*R*,*R*,*R*,*R*)-**2**.

Table 1: Copolymerization of propylene oxide (PO) with phthalic anhydride (PA) using cobalt–salen complexes.[a]

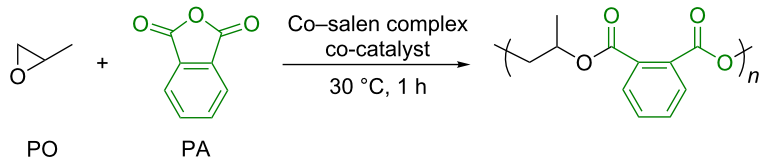

entry	Co–salen complex	co-catalyst	TOF[b] (h^{-1})	M_n[c]	M_w/M_n[c]
1	(*R*,*R*,*R*,*R*)-**1**	[PPN][$OCOC_6F_5$]	299	15,500	1.13
2[d]	(*R*,*R*,*R*,*R*)-**1**	[PPN][$OCOC_6F_5$]	132	7,800	1.13
3	(*R*,*R*,*R*,*R*)-**1**		0	–[e]	–[e]
4[f]	(*R*,*R*,*R*,*R*)-**1**	[PPN][$OCOC_6F_5$]	908	12,000	1.14
5[g]	(*R*,*R*,*R*,*R*)-**1**	[PPN][$OCOC_6F_5$]	149	7,700	1.18
6	(*R*,*R*,*S*,*S*)-**1**	[PPN][$OCOC_6F_5$]	237	13,700	1.14
7	(*R*,*R*)-**3**	[PPN][$OCOC_6F_5$]	203	11,400	1.14
8[g]	(*R*,*R*)-**3**	[PPN][$OCOC_6F_5$]	50	–[e]	–[e]
9	*rac*-**3**	[PPN][$OCOC_6F_5$]	207	13,600	1.16
10	(*R*,*R*,*R*,*R*)-**2**	[PPN][NO_3]	33	–[e]	–[e]
11	(*R*,*R*,*R*,*R*)-**2**	[PPN][$OCOC_6F_5$]	31	–[e]	–[e]
12	(*R*,*R*,*S*,*S*)-**2**	[PPN][NO_3]	12	–[e]	–[e]
13	*rac*-**4**	[PPN][NO_3]	107	5,400	1.25

[a]Copolymerization conditions: PO (20 mmol), PA (2.0 mmol), cobalt complex, and [PPN][$OCOC_6F_5$] as co-catalyst at 30 °C for 1 h. [PO]/[PA]/[Co]/[co-catalyst] = 4,000:400:1:1. [b]Turnover frequency (TOF) = (mol of PA incorporated in the copolymer)·(mol of Co center)$^{-1}$·h^{-1} calculated based on the ^{1}H NMR spectrum of the polymerization mixture using phenanthrene as an internal standard. [c]Estimated by size-exclusion-chromatography analysis using a polystyrene standard. [d][PO]/[PA]/[Co]/[co-catalyst] = 4,000:400:1:0.5. [e]Not determined because of no or low conversion of PA. [f]60 °C for 15 min. [g][PO]/[PA]/[Co]/[co-catalyst] = 4,000:400:0.25:0.25.

As there were no detectable signal for ether linkages in the ^{1}H NMR spectra of the obtained copolymers, the resulting copolymers possess a completely alternating structure. The regioselectivity in the ring-opening of PO was estimated by analyzing the stereochemistry of the copolymer prepared from enantiomerically pure (*S*)-PO. Because a ring opening at the methine carbon results in both a regioerror and the inversion of stereochemistry at the stereocenter, the enantiomeric excess (ee) of the repeating unit in the copolymer should reflect the regioregularity [15]. The ee of propylene glycol, which was obtained after hydrolysis of the copolymer obtained with (*S*)-PO and PA, was found to be 88%, indicating a high level of regioregularity. Molecular weight distributions are relatively narrow, while a bimodal distribution was observed in the SEC traces. The peak molecular weight of the higher molecular weight portion was twice as large as that of the lower molecular weight portion. Accordingly, trace amounts of diacid in PA and/or water contaminants would work as bifunctional chain-transfer agents and gave twice the molecular weight of the copolymer initiated by monofunctional pentafluorobenzoate from (*R*,*R*,*S*,*S*)-**1** and [PPN][$OCOC_6F_5$] [19]. The formation of the alternating copolymers initiated by monofunctional pentafluorobenzoate and the bifunctional chain-transfer agents was confirmed by matrix-assisted laser desorption/ionization time-of-flight mass spectrometry (MALDI–TOF MS, Figure 2). Several series of signals with a regular interval of 206.1 (repeating unit) were observed in the lower mass range. The *m*/*z* value of each signal of the major distribution corresponds with [166.0 (C_6F_5COO, initiating group) + 206.1*n* (repeating unit) + 59.1 ($CH_2CHMeOH$, terminal group) + 23.0 (Na^+ ion)]. Thus, the expected α-C_6F_5COO,ω-OH-terminated copolymer was obtained as a main product. As a minor distribution, the α-C_6F_5COO,ω-COOH-terminated copolymer was observed, while the cyclic polyester via intramolecular transesterification was not detected (Supporting Information File 1, Figure S14). In a higher mass range, a series of signals for the copolymer with hydroxy groups at both chain ends (the α-OH,ω-OH-terminated copolymer) was observed as the major distribution along with the α-OH,ω-COOH-terminated copolymer as the minor distribution.

Next, we investigated the effect of linking two cobalt–salen complexes on the catalytic activity. The heterochiral complex (*R*,*R*,*S*,*S*)-**1** demonstrated a much lower TOF of 237 h^{-1} than the homochiral one (*R*,*R*,*R*,*R*)-**1** (Table 1, entry 6). Thereby, a combination of the same absolute configuration of two salen

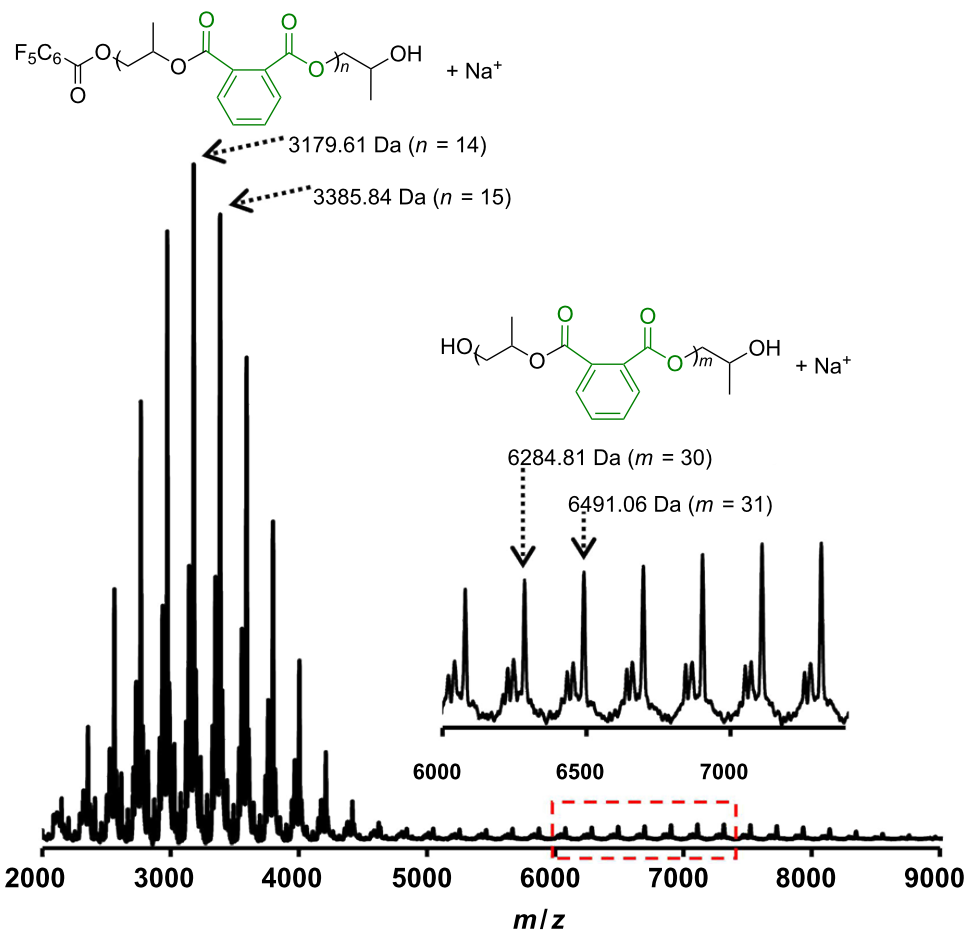

Figure 2: MALDI–TOF mass spectrum of the PO/PA copolymer. The low molecular weight copolymer for MS analysis was prepared by using (*R*,*R*,*R*,*R*)-**1** at 30 °C for 15 min.

moieties was found to be favorable for a high catalytic activity. Such dependence of the catalytic activity on the absolute configuration contrasts with our previous observation in the epoxide/CO_2 copolymerization where the heterochiral (*R*,*R*,*S*,*S*)-**1** showed a much higher catalytic activity than the corresponding homochiral complex (*R*,*R*,*R*,*R*)-**1** [40]. Both mononuclear complexes (*R*,*R*)-**3** and *rac*-**3** demonstrated similar and relatively high TOFs of 203 and 207 h^{-1}, respectively (Table 1 entries 7 and 9). However, these TOFs are lower than those obtained with the dinuclear complexes (*R*,*R*,*R*,*R*)-**1** and (*R*,*R*,*S*,*S*)-**1**. When the catalyst loading was reduced to one fourth, the TOFs of the dinuclear complex (*R*,*R*,*R*,*R*)-**1** and the mononuclear complex (*R*,*R*)-**3** fell to about one half and one quarter, respectively (Table 1, entries 5 and 8). Thus, the dinuclear complex (*R*,*R*,*R*,*R*)-**1** was found to be less affected by the catalyst loading. It is unclear whether the copolymerization proceeds via bimetallic propagation mechanism in the present catalyst systems. Nevertheless, these results indicated that the linking of two (or more) cobalt–salen complexes is a promising design for highly active catalysts.

The effect of substituents on the salen moieties and the axial ligands on the cobalt centers was also investigated. As mentioned above, fluoro substituents at 5-positions of the salicylidene moieties and a nitrate axial ligand on the cobalt center were reported to be an optimal combination for the PO/MA copolymerization with mononuclear cobalt–salen complexes [15]. Therefore, we expected that the dinuclear cobalt–salen complexes (*R*,*R*,*R*,*R*)-**2** and (*R*,*R*,*S*,*S*)-**2** would give higher catalytic activities than complexes **1**. The homochiral and heterochiral complexes **2** efficiently copolymerized PO with PA and showed TOFs of 33 and 12 h^{-1}, respectively, again demonstrating dependence of the catalytic activity on the absolute configuration (Table 1, entries 10 and 12). However, the TOFs unexpectedly are much lower than those obtained by using (*R*,*R*,*R*,*R*)-**1** and (*R*,*R*,*S*,*S*)-**1**. This trend was also observed for mononuclear complexes: the mononuclear complex *rac*-**4** with fluoro substituents at the 5-positions and a nitrate axial ligand gave a much lower TOF than *rac*-**3** (Table 1, entry 13). In addition, the TOF obtained with (*R*,*R*,*R*,*R*)-**2** and [PPN][$OCOC_6F_5$] was almost identical to that with [PPN][NO_3] (Table 1, entries

11 and 10). Therefore, *tert*-butyl substituents and a pentafluorobenzoate axial ligand were found to be more suitable for the PO/PA copolymerization. It should also be noted that the linking of two complexes has a negative impact on catalytic activity in the case of the cobalt–salen complex with a fluoro substituent and a nitrate axial ligand (Table 1, entries 10 and 13).

Monomer scope

In order to evaluate the copolymerization scope, the dinuclear cobalt–salen complex (*R*,*R*,*R*,*R*)-**1** and co-catalyst [PPN][$OCOC_6F_5$] were employed for the copolymerization of other epoxides with PA (Table 2). 1-Hexene oxide (HO), a terminal epoxide with an expanded alkyl chain, can be copolymerized at 30 °C to afford a completely alternating copolymer, while the TOF (61 h^{-1}) was much lower than that obtained for the PO/PA copolymerization (Table 2, entry 1). A higher polymerization temperature improved the TOF up to 399 h^{-1} and almost complete conversion of PA was achieved within 1 h (Table 2, entry 2). The copolymerization with cyclohexene oxide (CHO), a common alicyclic epoxide in epoxide/CA copolymerization, also gave the corresponding alternating copolymer (Table 2, entries 3 and 4). The TOF of 244 h^{-1} was achieved at 60 °C, which was the highest one ever reported for a CHO/PA copolymerization. The copolymerization of PO with other CAs was also tested to evaluate the scope. Cyclohexane dicarboxylic anhydride (CHDA) was successfully converted into the corresponding polyester with a TOF of 53 h^{-1} (Table 2, entry 5). The copolymerization with maleic anhydride (MA), a common CA in the epoxide/CA copolymerization, took place (Table 2, entries 6 and 7). However, the TOF was low even at a higher temperature. The mononuclear cobalt–salen complex with fluoro substituents at 5-positions of the salicylidene moieties and a nitrate axial ligand on the cobalt center was reported to be most active for PO/MA copolymerization [15]. Thus, we also applied complex (*R*,*R*,*R*,*R*)-**2** with [PPN][NO_3] as co-catalyst in the copolymerization. As a result, the complex was found to show a slightly higher activity compared with (*R*,*R*,*R*,*R*)-**1** although the TOF was much lower than that obtained with the mononuclear complex (Table 2, entry 8). Finally, we attempted the terpolymerization of PO, HO, and PA (Scheme 2). Although equimolar amounts of PO and HO were used, the obtained copolymer contained a larger amount of the PO-derived repeating unit, reflecting a higher reactivity of PO.

Conclusion

We reported the alternating copolymerization of epoxides with cyclic anhydrides using dinuclear cobalt–salen complexes with a benzene linker. The substituents on the salen moieties, an

Table 2: Copolymerization of various epoxides and cyclic anhydrides.[a]

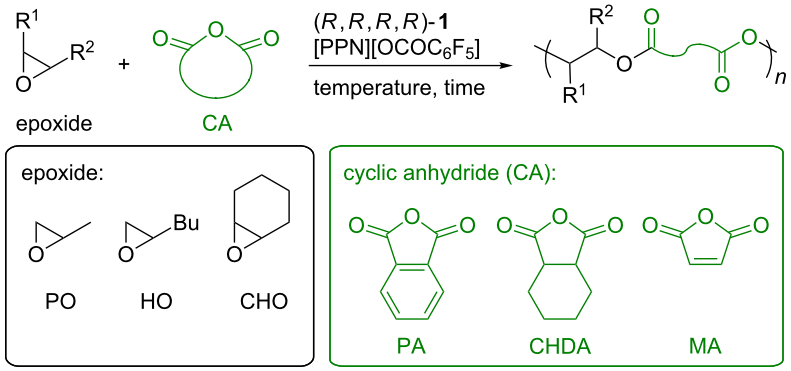

entry	monomer	*T* (°C)	time (h)	[epoxide]/[CA]/[Co]/[co-catalyst]	TOF[b] (h^{-1})	M_n[c]	M_w/M_n[c]
1	HO/PA	30	2	2,400:400:1:1	61	8,400	1.20
2	HO/PA	60	1	2,400:400:1:1	399	22,000	1.18
3	CHO/PA	30	2	2,800:400:1:1	20	500	1.97
4	CHO/PA	60	1	2,800:400:1:1	244	7,000	1.16
5	PO/CHDA	30	2	4,000:400:1:1	53	1,400	2.06
6	PO/MA	30	2	2,000:200:1:1	10	–[d]	–[d]
7	PO/MA	60	1.5	2,000:200:1:1	39	–[d]	–[d]
8[e]	PO/MA	30	2	2,000:200:1:1	22	–[d]	–[d]

[a]Copolymerization conditions: epoxide, CA (2.0 mmol for entries 1–5; 1.0 mmol for entries 6–8), cobalt complex, [PPN][$OCOC_6F_5$] as a co-catalyst. [b]Turnover frequency (TOF) = (mol of CA incorporated in the copolymer)·(mol of Co center)$^{-1}$·h^{-1} calculated based on the ^{1}H NMR spectrum of the polymerization mixture using phenanthrene as an internal standard. [c]Estimated by size-exclusion-chromatography analysis using a polystyrene standard. [d]Not determined because of low conversion of MA. [e](*R*,*R*,*R*,*R*)-**2** and [PPN][NO_3].

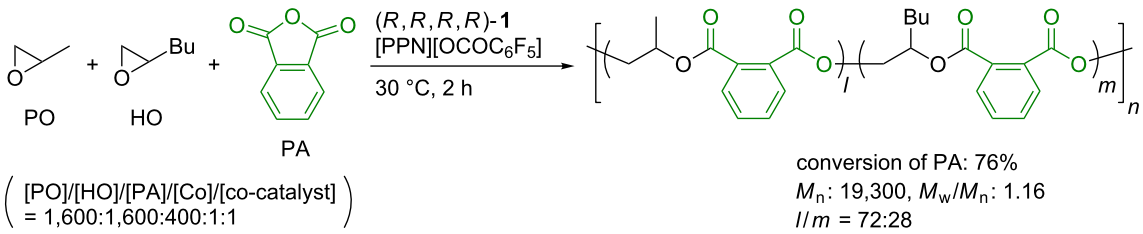

Scheme 2: Terpolymerization of PO, HO, and PA with (*R*,*R*,*R*,*R*)-**1**.

axial ligand on the cobalt center, and a combination of the absolute configuration of the two cobalt–salen moieties were found to have a great impact on the catalytic activity. Through these investigations, the homochiral dinuclear cobalt–salen complex having *tert*-butyl substituents and a pentafluorobenzoate axial ligand was developed as a highly active catalyst. Furthermore, the dinuclear cobalt–salen complex demonstrated a higher catalytic activity than the corresponding mononuclear cobalt–salen complex. These results indicate that the design based on di- or multinuclear metal complexes is a promising strategy for the development of highly active catalysts. Our future studies will focus on the optimization of linker structures as well as ligand structures for the epoxide/CA copolymerization to achieve higher activity and/or selectivity.

Experimental

General procedures: All manipulations involving air and/or moisture-sensitive compounds were carried out using standard Schlenk techniques under argon. Analytical thin-layer chromatography was performed on glass plates coated with 0.25 mm 230–400 mesh silica gel containing a fluorescence indicator. Column chromatography was performed on silica gel (spherical neutral, particle size: 63–210 μm). Most of the reagents were purchased from commercial suppliers, such as Sigma-Aldrich Co. LLC, Tokyo Chemical Industry Co., Ltd., and Kanto Chemical Co., Inc., and were used without further purification unless otherwise specified. Commercially available anhydrous solvents were used for air and/or moisture-sensitive reactions. Epoxides for the polymerizations were dried over CaH_2 and distilled under argon and cyclic anhydrides were purified by sublimation. (*R*,*R*,*S*,*S*)- and (*R*,*R*,*R*,*R*)-**1** [40], (*R*,*R*)- and *rac*-**3** [42], *rac*-**4** [15], **5** [40], [PPN][$OCOC_6F_5$] [42], and [PPN][NO_3] [15] were prepared according to the literature.

NMR spectra were recorded in $CDCl_3$ on a JEOL–ECX400 spectrometer (^{1}H NMR at 400 MHz; ^{13}C NMR at 101 MHz) or a JEOL–ECA500 spectrometer (^{19}F NMR at 471 MHz). Chemical shifts are reported in ppm relative to the internal standard signal (0 ppm for Me_4Si in $CDCl_3$) for ^{1}H NMR and the solvent signal (77.16 ppm for $CDCl_3$) for ^{13}C NMR. Data are presented as follows: chemical shift, multiplicity (s = singlet, d = doublet, dd = doublet of doublets, m = multiplet and/or multiple resonances), coupling constant in hertz (Hz), and signal area integration in natural numbers. High resolution mass spectra are taken with a Bruker Daltonics micrOTOF-QII mass spectrometer by atmospheric pressure chemical ionization–time-of-flight (APCI–TOF) method. Size-exclusion-chromatography (SEC) analyses for evaluating molecular weights were carried with two columns (Shodex KF-804L) using chloroform as an eluent at 40 °C at 1 mL/min. The molecular weight was calibrated against standard polystyrene samples. The recycling preparative HPLC was performed with YMC-GPC T-2000 and T-4000 columns (chloroform as an eluent). HPLC analysis for determining the ee was carried out using a DAICEL CHIRALCEL® IA-3 column (4.6 mm × 250 mm).

Synthesis of mono(salen) (*R*,*R*)-7: A Schlenk tube was charged with (*R*,*R*)-1,2-cyclohexanediamine monohydrochloride (0.14 g, 0.93 mmol), 3-*tert*-butyl-5-fluoro-2-hydroxybenzaldehyde (0.18 g, 0.93 mmol), molecular sieves 4Å, and dry MeOH (1.5 mL) under argon. After stirring at room temperature for 50 min, the resulting solution was slowly transferred to another Schlenk tube containing bis(salicylaldehyde) **5** (0.72 g, 1.4 mmol), Et_3N (0.47 mL, 3.4 mmol) and dichloromethane (7 mL). The reaction mixture was stirred at room temperature for 18 h and the resulting suspension was filtered off with dichloromethane. The filtrate was concentrated under reduced pressure and the crude residue was purified by silica-gel column chromatography (AcOEt/hexane/Et_3N 1:5:0.12 as an eluent, R_f 0.30] to provide (*R*,*R*)-**7** (0.36 g, 39% yield) as yellow solid: ^{1}H NMR (400 MHz, $CDCl_3$) δ 11.73 (s, 1H), 9.75 (s, 1H), 8.24 (s, 1H), 8.19 (s, 1H), 7.99–7.92 (m, 2H), 7.71–7.67 (m, 2H), 7.29 (s, 2H), 7.04 (d, J = 2.7 Hz, 1H), 6.98 (dd, J = 11.0, 3.2 Hz, 1H), 6.90 (d, J = 2.7 Hz, 1H), 6.70 (dd, J = 7.8, 3.2Hz, 1H), 3.40–3.28 (m, 2H), 2.00–1.88 (m, 4H), 1.76–1.68 (m, 2H), 1.52–1.45 (m, 2H), 1.36 (s, 9H), 1.32 (s, 18H); ^{13}C NMR (101 MHz, $CDCl_3$) δ 196.5, 166.5, 166.3, 164.7, 159.3, 158.6, 156.5, 155.0 (d, $J_{C–F}$ = 234.8 Hz), 142.6, 141.7, 140.4, 139.4 (d, $J_{C–F}$ = 4.8 Hz), 139.1, 132.0, 131.9, 131.8, 131.7, 129.8, 129.6, 128.1, 128.0, 123.4, 122.9, 121.3, 120.2, 118.3, 118.1 (d, $J_{C–F}$ = 7.7 Hz), 117.1 (d, $J_{C–F}$ = 24.9 Hz), 114.2 (d,

J_{C-F} = 22.0 Hz), 72.7, 72.1, 35.1, 35.0, 33.2, 33.0, 29.23, 29.15, 29.0, 24.34, 24.29; ^{19}F NMR (471 MHz, $CDCl_3$) δ −126.3; HRMS–APCI$^+$ (*m*/*z*): [M + H]$^+$ calcd for $C_{47}H_{54}FN_2O_8$, 793.3859; found, 793.3859.

Synthesis of bis(salen) (*R,R,S,S*)-8: The crude product was obtained from (*S,S*)-1,2-cyclohexanediamine monohydrochloride (28 mg, 0.19 mmol), 3-*tert*-butyl-5-fluoro-2-hydroxybenzaldehyde (37 mg, 0.19 mmol), (*R,R*)-**7** (0.13 g, 0.17 mmol), and Et_3N (0.11 mL, 0.79 mmol) according to the procedure described for the synthesis of (*R,R*)-**7**. Purification by silica gel column chromatography (AcOEt/hexane/Et_3N 1:5:0.12 as an eluent, R_f 0.38) gave (*R,R,S,S*)-**8** (95 mg, 52% yield) as yellow solid: ^{1}H NMR (400 MHz, $CDCl_3$) δ 8.24 (s, 2H), 8.17 (s, 2H), 7.93–7.89 (m, 2H), 7.67–7.62 (m, 2H), 7.01 (d, *J* = 2.7 Hz, 2H), 6.98 (dd, *J* = 11.0, 3.2 Hz, 1H), 6.88 (d, *J* = 2.7 Hz, 2H), 6.70 (dd, *J* = 7.8, 2.7 Hz, 2H), 3.38–3.28 (m, 4H), 2.00–1.88 (m, 8H), 1.79–1.66 (m, 4H), 1.52–1.45 (m, 4H), 1.37 (s, 9H), 1.36 (s, 9H), 1.27 (s, 18H); ^{13}C NMR (101 MHz, $CDCl_3$) δ 166.4, 164.8, 164.7 (d, J_{C-F} = 1.9 Hz), 158.5, 156.5, 155.0 (d, J_{C-F} = 234.8 Hz), 141.8, 139.4 (d, J_{C-F} = 5.8 Hz), 139.0, 131.9, 131.8, 129.6, 123.0, 121.4, 118.3, 118.1 (d, J_{C-F} = 7.7 Hz), 117.1 (d, J_{C-F} = 24.0 Hz), 114.2 (d, J_{C-F} = 22.0 Hz), 72.8, 72.0, 35.1, 35.0, 33.2, 33.0, 29.3, 29.1, 24.35, 24.29; ^{19}F NMR (471 MHz, $CDCl_3$) δ −126.3; HRMS–APCI$^+$ (*m*/*z*): [M + H]$^+$ calcd for $C_{64}H_{77}F_2N_4O_8^+$, 1067.5704; found, 1067.5697.

Synthesis of bis(salen) (*R,R,R,R*)-8: The crude product was obtained from (*R,R*)-1,2-cyclohexanediamine monohydrochloride (0.10 g, 0.66 mmol), 3-*tert*-butyl-5-fluoro-2-hydroxybenzaldehyde (0.13 g, 0.66 mmol), bis(salicylaldehyde) **5** (0.15 g, 0.30 mmol), and Et_3N (0.14 mL, 1.0 mmol) according to the procedure described for the synthesis of (*R,R*)-**7**. Purification by silica gel column chromatography (AcOEt/hexane/Et_3N 1:5:0.12 as an eluent, R_f 0.38) gave (*R,R,R,R*)-**8** (145 mg, 45% yield) as yellow solid: ^{1}H NMR (400 MHz, $CDCl_3$) δ 8.24 (s, 2H), 8.17 (s, 2H), 7.93–7.89 (m, 2H), 7.68–7.63 (m, 2H), 7.01 (d, *J* = 3,2 Hz, 2H), 6.98 (dd, *J* = 11.0, 2.7 Hz, 1H), 6.88 (d, *J* = 2.7 Hz, 2H), 6.70 (dd, *J* = 7.8, 3.2 Hz, 2H), 3.38–3.27 (m, 4H), 2.00–1.88 (m, 8H), 1.79–1.66 (m, 4H), 1.52–1.44 (m, 4H), 1.36 (s, 18H), 1.27 (s, 18H); ^{13}C NMR (101 MHz, $CDCl_3$) δ 166.5, 164.8, 164.7 (d, J_{C-F} = 2.9 Hz), 158.5, 156.5, 155.0 (d, J_{C-F} = 234.8 Hz), 141.8, 139.4 (d, J_{C-F} = 5.8 Hz), 139.0, 131.9, 131.8, 129.6, 123.0, 121.4, 118.3, 118.1 (d, J_{C-F} = 7.7 Hz), 117.1 (d, J_{C-F} = 24.0 Hz), 114.2 (d, J_{C-F} = 23.0 Hz), 72.8, 72.0, 35.1, 35.0, 33.2, 33.0, 29.2, 29.1, 24.34, 24.28; HRMS–APCI$^+$ (*m*/*z*): [M + H]$^+$ calcd for $C_{64}H_{77}F_2N_4O_8^+$, 1067.5704; found, 1067.5702.

Synthesis of dinuclear Co–salen complex (*R,R,S,S*)-2: A Schlenk tube was charged with $Co(NO_3)_2{\cdot}6H_2O$ (52 mg, 0.18 mmol). After stirring at 60 °C under reduced pressure for 1.5 h, EtOH (2.0 mL) was added. Another Schlenk tube was charged with (*R,R,S,S*)-**8** (88 mg, 80 μmol) and degassed CH_2Cl_2 (3.0 mL) added under argon. After the solution of $Co(NO_3)_2$ was slowly added to the ligand solution, the resulting mixture was stirred at room temperature for 1 h, and then opened to air. The reaction mixture was stirred at room temperature for 13 h, filtered, and concentrated under reduced pressure. The resulting residue was rinsed with pentane until the filtrate was clear, and then dried at 60 °C under reduced pressure to provide (*R,R,S,S*)-**2** (94 mg, 90% yield for two steps) as dark green powder: HRMS–APCI$^+$ (*m*/*z*): [M + H − 2(NO_3)]$^+$ calcd for $C_{64}H_{73}Co_2F_2N_4O_8^+$, 1181.4055; found, 1181.4054; anal. calcd for $C_{64}H_{72}Co_2F_2N_6O_{14}$ (%): C, 58.90; H, 5.56; N, 6.44; found: C, 55.84; H, 5.82; N, 5.33.

Synthesis of dinuclear Co–salen complex (*R,R,R,R*)-2: Complex (*R,R,R,R*)-**2** was obtained from $Co(NO_3)_2{\cdot}6H_2O$ (35 mg, 0.12 mmol), (*R,R,R,R*)-**8** (58 mg, 54 μmol) as dark green powder (62 mg, 88% yield for two steps) according to the procedure described for the synthesis of (*R,R,S,S*)-**2**: HRMS–APCI$^+$ (*m*/*z*): [M + H − 2(NO_3)]$^+$ calcd for $C_{64}H_{73}Co_2F_2N_4O_8^+$, 1181.4055; found, 1181.4055; anal. calcd for $C_{64}H_{72}Co_2F_2N_6O_{14}$ (%): C, 58.90; H, 5.56; N, 6.44; found: C, 59.23; H, 5.93; N, 5.06.

Representative procedure for the copolymerization of propylene oxide with phthalic anhydride (Table 1**):** A flame-dried Schlenk tube was charged with the propylene oxide (1.4 mL, 20 mmol), phthalic anhydride (296 mg, 2.0 mmol), cobalt complex (5.0 μmol of Co center), and co-catalyst (5.0 μmol [PO]/[PA]/[Co]/[co-catalyst] = 4,000:400:1:1) under argon. The reaction mixture was stirred at 30 °C for 1.0 h. The polymerization mixture was diluted with CH_2Cl_2, and quenched with several drops of MeOH/1 M HCl (50:50 vol %). Phenanthrene as an internal standard was dissolved in the resulting mixture, and a small aliquot of the mixture was taken out and concentrated under reduced pressure. Then, the residue was analyzed by ^{1}H NMR spectroscopy and SEC to determine the conversion of PA, TOF, molecular weight, and molecular weight distribution.

The ^{1}H NMR spectra of the obtained PO/PA [15], CHO/PA [33], PO/CHDA [21], and PO/MA [15] copolymers were identical to those in the literatures.

Evaluation of regioregularity: The copolymerization of (*S*)-PO and PA was carried out under standard conditions using (*R,R,R,R*)-**1**. The reaction mixture was diluted with CH_2Cl_2 and quenched with several drops of MeOH/1 M HCl (50:50 vol %). The resulting mixture was poured into an excess of MeOH to

precipitate the copolymer. After the precipitation was repeated two more times, the precipitate was collected and dried under deduced pressure.

The obtained copolymer (ca. 150 mg) was dissolved in a mixture of CH_2Cl_2 (2.5 mL) and MeOH (7.5 mL), and NaOH (100 mg) was added. After stirring at 60 °C for 25 h, the resulting suspension was neutralized with 4 M HCl (in cyclopentyl methyl ether). The solvents were removed under reduced pressure and Et_2O (5 mL) was added to the resulting powder. After stirring for 10 min, the slurry was filtrated off and the resulting filtrate was concentrated under reduced pressure to give propylene glycol.

A flame-dried flask was charged with the obtained propylene glycol (26 mg, 0.34 mmol), 4-(dimethylamino)pyridine (8 mg, 0.07 mmol), trimethylamine (70 μL, 0.7 mmol), and CH_2Cl_2 (3.4 mL). Benzoyl chloride (39 μL, 0.34 mmol) was added dropwise to the solution with stirring. After stirring at room temperature for 25 min, the reaction mixture was poured into water and extracted with CH_2Cl_2. The organic layer was washed with 1 M HCl and brine and concentrated under reduced pressure. The resulting crude product was purified by the recycling preparative HPLC to give 2-hydroxypropyl benzoate [43]. The ee of the benzoate was determined by HPLC analysis using a DAICEL CHIRALCEL® IA-3 column [t_R = 12.65 min for the (*S*)-isomer and 14.50 min for the (*R*)-isomer (flow rate: 1.0 mL; eluent: hexane/iPrOH 95:5)].

Supporting Information

Supporting Information File 1

NMR spectra of new compounds.
[https://www.beilstein-journals.org/bjoc/content/supplementary/1860-5397-14-255-S1.pdf]

Acknowledgements

This work was partially supported by MEXT KAKENHI Grant Number 16K05788.

ORCID® iDs

Koji Nakano - https://orcid.org/0000-0003-4166-7074

References

1. Hillmyer, M. A.; Tolman, W. B. *Acc. Chem. Res.* **2014,** *47,* 2390–2396. doi:10.1021/ar500121d
2. Coulembier, O.; Degée, P.; Hedrick, J. L.; Dubois, P. *Prog. Polym. Sci.* **2006,** *31,* 723–747. doi:10.1016/j.progpolymsci.2006.08.004
3. Gigli, M.; Fabbri, M.; Lotti, N.; Gamberini, R.; Rimini, B.; Munari, A. *Eur. Polym. J.* **2016,** *75,* 431–460. doi:10.1016/j.eurpolymj.2016.01.016
4. Albertsson, A.-C.; Varma, I. K. Aliphatic Polyesters: Synthesis, Properties and Applications. *Degradable Aliphatic Polyesters;* Springer: Berlin, Heidelberg, 2002; pp 1–40.
5. Albertsson, A.-C.; Varma, I. K. *Biomacromolecules* **2003,** *4,* 1466–1486. doi:10.1021/bm034247a
6. Dutta, S.; Hung, W.-C.; Huang, B.-H.; Lin, C.-C. Recent Developments in Metal-Catalyzed Ring-Opening Polymerization of Lactides and Glycolides: Preparation of Polylactides, Polyglycolide, and Poly(lactide-co-glycolide). In *Synthetic Biodegradable Polymers;* Rieger, B.; Künkel, A.; Coates, G. W.; Reichardt, R.; Dinjus, E.; Zevaco, T. A., Eds.; Springer: Berlin Heidelberg, 2012; pp 219–283.
7. Lecomte, P.; Jérôme, C. Recent Developments in Ring-Opening Polymerization of Lactones. In *Synthetic Biodegradable Polymers;* Rieger, B.; Künkel, A.; Coates, G. W.; Reichardt, R.; Dinjus, E.; Zevaco, T. A., Eds.; Springer: Berlin, Heidelberg, 2012; pp 173–217.
8. Lou, X.; Detrembleur, C.; Jérôme, R. *Macromol. Rapid Commun.* **2003,** *24,* 161–172. doi:10.1002/marc.200390029
9. Thomas, C. M. *Chem. Soc. Rev.* **2010,** *39,* 165–173. doi:10.1039/b810065a
10. Stridsberg, K. M.; Ryner, M.; Albertsson, A.-C. Controlled Ring-Opening Polymerization: Polymers with designed Macromolecular Architecture. *Degradable Aliphatic Polyesters;* Springer: Berlin, Heidelberg, 2002; pp 41–65.
11. Paul, S.; Zhu, Y.; Romain, C.; Brooks, R.; Saini, P. K.; Williams, C. K. *Chem. Commun.* **2015,** *51,* 6459–6479. doi:10.1039/c4cc10113h
12. Longo, J. M.; Sanford, M. J.; Coates, G. W. *Chem. Rev.* **2016,** *116,* 15167–15197. doi:10.1021/acs.chemrev.6b00553
13. Fischer, R. F. *J. Polym. Sci.* **1960,** *44,* 155–172. doi:10.1002/pol.1960.1204414314
14. Jeske, R. C.; DiCiccio, A. M.; Coates, G. W. *J. Am. Chem. Soc.* **2007,** *129,* 11330–11331. doi:10.1021/ja0737568
15. DiCiccio, A. M.; Longo, J. M.; Rodríguez-Calero, G. G.; Coates, G. W. *J. Am. Chem. Soc.* **2016,** *138,* 7107–7113. doi:10.1021/jacs.6b03113
16. Van Zee, N. J.; Sanford, M. J.; Coates, G. W. *J. Am. Chem. Soc.* **2016,** *138,* 2755–2761. doi:10.1021/jacs.5b12888
17. Robert, C.; de Montigny, F.; Thomas, C. M. *Nat. Commun.* **2011,** *2,* No. 586. doi:10.1038/ncomms1596
18. DiCiccio, A. M.; Coates, G. W. *J. Am. Chem. Soc.* **2011,** *133,* 10724–10727. doi:10.1021/ja203520p
19. Hosseini Nejad, E.; van Melis, C. G. W.; Vermeer, T. J.; Koning, C. E.; Duchateau, R. *Macromolecules* **2012,** *45,* 1770–1776. doi:10.1021/ma2025804
20. Jeon, J. Y.; Eo, S. C.; Varghese, J. K.; Lee, B. Y. *Beilstein J. Org. Chem.* **2014,** *10,* 1787–1795. doi:10.3762/bjoc.10.187
21. Darensbourg, D. J.; Poland, R. R.; Escobedo, C. *Macromolecules* **2012,** *45,* 2242–2248. doi:10.1021/ma2026385
22. Sanford, M. J.; Van Zee, N. J.; Coates, G. W. *Chem. Sci.* **2018,** *9,* 134–142. doi:10.1039/c7sc03643d
23. Winkler, M.; Romain, C.; Meier, M. A. R.; Williams, C. K. *Green Chem.* **2015,** *17,* 300–306. doi:10.1039/c4gc01353k
24. Van Zee, N. J.; Coates, G. W. *Angew. Chem., Int. Ed.* **2015,** *54,* 2665–2668. doi:10.1002/anie.201410641
25. Duan, Z.; Wang, X.; Gao, Q.; Zhang, L.; Liu, B.; Kim, I. *J. Polym. Sci., Part A: Polym. Chem.* **2014,** *52,* 789–795. doi:10.1002/pola.27057
26. Fournier, L.; Robert, C.; Pourchet, S.; Gonzalez, A.; Williams, L.; Prunet, J.; Thomas, C. M. *Polym. Chem.* **2016,** *7,* 3700–3704. doi:10.1039/c6py00664g
27. Matsunaga, S.; Shibasaki, M. *Chem. Commun.* **2014,** *50,* 1044–1057. doi:10.1039/c3cc47587e

28. Park, J.; Hong, S. *Chem. Soc. Rev.* **2012,** *41,* 6931–6943. doi:10.1039/c2cs35129c
29. Delferro, M.; Marks, T. J. *Chem. Rev.* **2011,** *111,* 2450–2485. doi:10.1021/cr1003634
30. Matsunaga, S.; Shibasaki, M. *Bull. Chem. Soc. Jpn.* **2008,** *81,* 60–75. doi:10.1246/bcsj.81.60
31. Liu, J.; Bao, Y.-Y.; Liu, Y.; Ren, W.-M.; Lu, X.-B. *Polym. Chem.* **2013,** *4,* 1439–1444. doi:10.1039/c2py20842c
32. Garden, J. A.; Saini, P. K.; Williams, C. K. *J. Am. Chem. Soc.* **2015,** *137,* 15078–15081. doi:10.1021/jacs.5b09913
33. Zhu, Y.; Romain, C.; Williams, C. K. *J. Am. Chem. Soc.* **2015,** *137,* 12179–12182. doi:10.1021/jacs.5b04541
34. Yu, C.-Y.; Chuang, H.-J.; Ko, B.-T. *Catal. Sci. Technol.* **2016,** *6,* 1779–1791. doi:10.1039/c5cy01290b
35. Wu, L.-y.; Fan, D.-d.; Lü, X.-q.; Lu, R. *Chin. J. Polym. Sci.* **2014,** *32,* 768–777. doi:10.1007/s10118-014-1425-x
36. Saini, P. K.; Romain, C.; Zhu, Y.; Williams, C. K. *Polym. Chem.* **2014,** *5,* 6068–6075. doi:10.1039/c4py00748d
37. Thevenon, A.; Garden, J. A.; White, A. J. P.; Williams, C. K. *Inorg. Chem.* **2015,** *54,* 11906–11915. doi:10.1021/acs.inorgchem.5b02233
38. Zhu, L.; Liu, D.; Wu, L.; Feng, W.; Zhang, X.; Wu, J.; Fan, D.; Lü, X.; Lu, R.; Shi, Q. *Inorg. Chem. Commun.* **2013,** *37,* 182–185. doi:10.1016/j.inoche.2013.09.059
39. Liu, D.-F.; Wu, L.-Y.; Feng, W.-X.; Zhang, X.-M.; Wu, J.; Zhu, L.-Q.; Fan, D.-D.; Lü, X.-Q.; Shi, Q. *J. Mol. Catal. A: Chem.* **2014,** *382,* 136–145. doi:10.1016/j.molcata.2013.11.002
40. Hiranoi, Y.; Hatanaka, M.; Nakano, K. *J. Polym. Sci., Part A: Polym. Chem.* **2017,** *55,* 2150–2159. doi:10.1002/pola.28590
41. Previously, Lee and co-workers have reported by far the highest TOF (≈ 1,900 h−1) for the PO/PA copolymerization by using the cobalt–salen complex with ammonium tethers [20].
42. Cohen, C. T.; Chu, T.; Coates, G. W. *J. Am. Chem. Soc.* **2005,** *127,* 10869–10878. doi:10.1021/ja051744l
43. Liu, H.-X.; Dang, Y.-Q.; Yuan, Y.-F.; Xu, Z.-F.; Qiu, S.-X.; Tan, H.-B. *Org. Lett.* **2016,** *18,* 5584–5587. doi:10.1021/acs.orglett.6b02818

License and Terms